The degradation of PHB and P(HB/HV) copolymers and their uses in drug delivery

Majid, Mohamed. Isa bin Abd

Award date:
1988

Awarding institution:
University of Bath

The degradation of PHB and P(HB/HV) copolymers and their uses in drug delivery

submitted by Mohamed Isa bin Abd. Majid , BPharm (USM , Malaysia)

for the degree of PhD

of the University of Bath

1988

Copyright

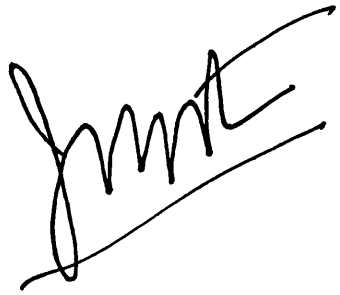

ProQuest LLC
789 East Eisenhower Parkway
P.O. Box 1346
Ann Arbor, MI 48106-1346

ACKNOWLEDGEMENTS

In the name of ALLAH , Most Gracious, Most Merciful.

In the course of this study, the author has drawn on the time and experience of many people.

The author deeply appreciates and would like to thank his academic supervisors, Dr. C. W. Pouton and Dr. L. J. Notarianni for their guidance, encouragement , critical discussion and understanding throughout the whole of this study.

The author would also like to thank Dr. P. H. Christie of the Computer Unit, University of Bath, for the advice regarding the preparation of this thesis. The assistance of Ms. Dominique Plumanns in the typing of this thesis is also acknowledged.

The author would also like to thank the assistance of numerous technical staff of the School of Pharmacy and Pharmacology, University of Bath.

Lastly, the author would like to thank Universiti Sains Malaysia, Penang, Malaysia and Public Services Department, Government of Malaysia for providing the financial assistance.

to my wife, Siti Khalijah

and my children,Siti Musmirah and Muhammad Amin

TABLE OF CONTENTS

SUMMARY

Non-aqueous size exclusion chromatography was used to determine Mark-Houwink constants and to characterize the molecular weight distribution of PHB. The SEC column was calibrated using an universal method and an iterative algorithm enabled the Mark-Houwink constants for PHB to be determined from polydisperse samples of polymer. The SEC assay was used to study the catalytic degradation of PHB in non-aqueous solution and the degradation of PHB films in the presence of aqueous solutions. Random chain scission of PHB occured in non-aqueous solution. Degradation of PHB and P(HB/HV) films in the presence of water occured by surface hydrolysis with no change in molecular weight or crystallinity of the bulk film. The rate of surface hydrolysis was influenced by pH, temperature and copolymer composition. Hydroxyl ions catalysed the degradation of all polymers studied.

Release of methyl red from cast films was characterised according to the theory of release by diffusion from matrices. Surface erosion of polymers played a minor part in influencing release of methyl red from polymer films. Release rate was influenced by loading of methyl red and by the composition of the polymer used.

PART I

GENERAL INTRODUCTION

Chapter 1

POLYMERIC MATERIALS AND DRUG DELIVERY

1.1 Introduction.

Polymeric materials have been used for many years in the formulation of medicines as suspending and emulsifying agents, flocculating agents, adhesives, packaging and coating materials. Many traditional materials have been of natural origin or have been *semi-synthetic* derivatives of natural products, such as cellulose derivatives. However, the availability of synthetic polymers and a desire to improve the control of drug release from medicines have led to a rapid expansion in the use of polymers in pharmacy. In early developments, drugs were coated with slowly dissolving barrier materials (such as shellac) permitting formulation as unit dosage forms with prolonged activity (Hawkins and Thompson, 1953). However, the release of drug from such systems was neither precisely nor completely controlled. For example, the rate of dissolution of the coating material varied according to the pH of gastrointestinal tract (Levy and Hollister, 1965). Various terms were used to describe the release of drugs from this generation of delayed release preparations, such as sustained release, prolonged action and repeat-action.

De Haan and Lerk (1984) have defined each products as follows:

- A **prolonged action** product provides a slow release of a drug at a rate sufficient to cause a therapeutic response over a period of time, measurable increased in length when compared to the usual single dose.

- A **sustained release** dosage form provides an amount of drug initially made available to the body to cause the desired therapeutic response, followed by a constant release of medication for maintenance of activity over a period of time.

- A **repeat-action** product is considered to provide a dose which is released immediately upon administration and a second dose which is released some time after administration. A **repeat-action** product is considered to have no therapeutic advantage over individually administered single doses since the drug profile of concentration in the blood against time is similar to those produced after repeated administration of conventional dosage forms (Figure 1.1).

Since these first generation systems for drug optimization were significantly influenced by the physiology and local mileau of the gastro intestinal tract, a second generation of products, often called **controlled release systems** have been developed. **Controlled release systems** have been defined as those which result in the delivery of an active agent from a device to a target site at a rate and for a duration that are controlled by the device itself (Mills and Davis, 1987). Such device-controlled delivery may offer several important advantages over conventional therapy. These advantages are rapidly becoming widely appreciated and accepted. They include:-

- maintenance of optimal drug concentrations in body tissues, resulting in greater efficacy of treatment.

- avoidance of *peaks* and *troughs* in drug concentration resulting in fewer side-effects and enhanced safety.

- ability to administer drugs with narrow therapeutic indices or

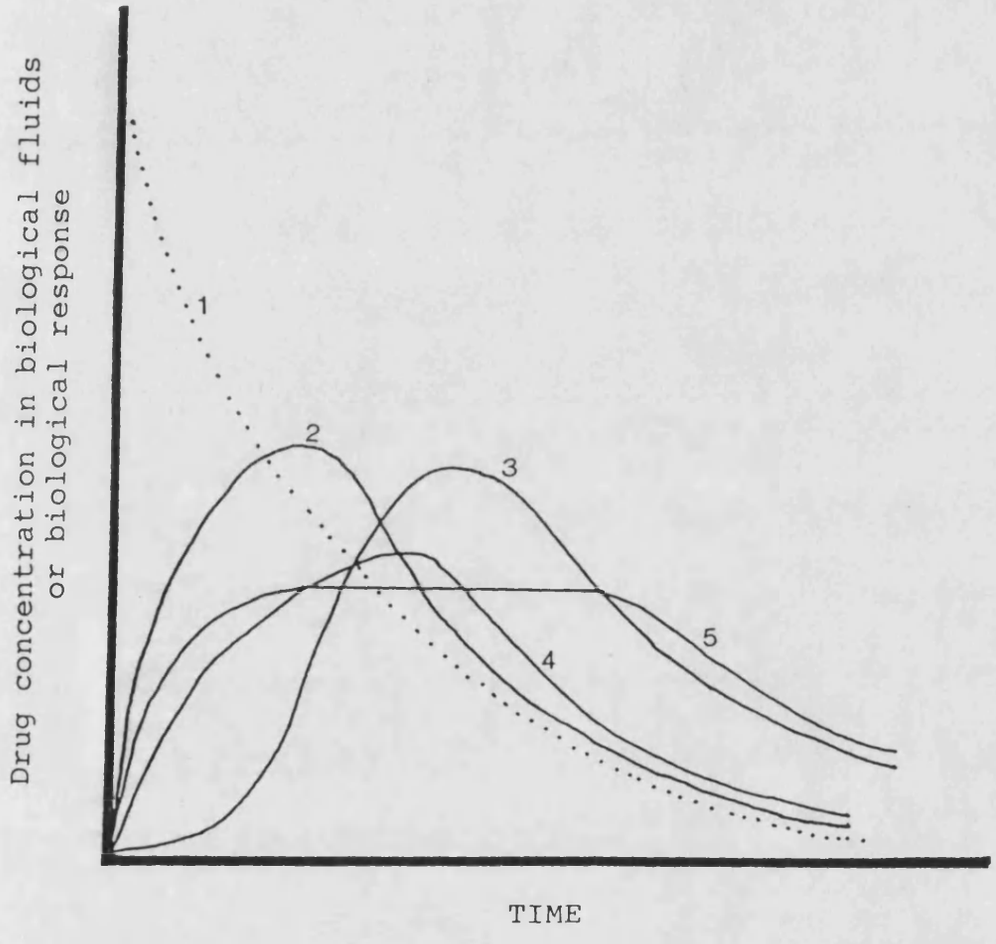

Figure 1.1:- Theoretical drug profiles in biological fluids assuming first order linear pharmacokinetics and assuming a linear correlation between drug concentration biological response, after extravascular administration of four types of drug delivery systems. IV administration is shown for comparison 1 - intravenous administration; 2 - conventional extravascular administration; 3 - delayed release form; 4 - sustained release dosage form; 5 - idealized controlled release dosage form.
(Reproduced from Rubinstein and Robinson, 1987).

short biological half-lives.

- greater patient convenience and compliance resulting from the use of fewer administrations per unit time.

The above considerations have motivated both academic and industrial scientists to study a wide variety of **controlled release delivery systems.** These take the form of transdermal systems and implants as well as systems for oral administration. However the term **controlled delivery** should be used with caution. Thus far there are few examples of delivery systems which allow modification of release rate *in vivo* , that is after the product has been administered. In the future, one expects a third generation of devices to develop with this extra dimension of control to provide a higher quality of drug therapy which will permit adjustment of dosage rate in response to the course of disease.

The development of drug delivery systems has depended on an understanding of diffusion in polymeric materials. This is considered in section 1.2. A brief review of the variety of different delivery systems (section 1.3) is followed by a summary of the scope of the present study (section 1.4).

1.2 Diffusion through polymeric materials.

Diffusion can be defined as the tendency for particles to move spontaneously from a region of higher concentration to a region of lower concentration until equilibrium occurs. The mechanism of release from controlled delivery systems often involves diffusion across polymeric membranes. Transport of drugs through membranes occurs by a process in which the solute first dissolves in the membrane and then diffuses through the membrane in a direction towards the lower solute

concentration. The diffusion process is described by an expression known as Fick's first law which states that the rate of diffusion across a plane perpendicular to the direction of diffusion is proportional to the concentration gradient across the plane (Crank, 1975). Mathematically Fick's first law is given by equation 1.1

$$\frac{dQ}{dt} \alpha \frac{dc}{dx} \quad \ldots\ldots (1.1)$$

where

Q is the mass of material diffusing,

t is the unit time.

Thus dQ/dt represents the rate of mass transfer and dc/dx represents the change in concentration per unit distance.

Using D as the proportionality constant, Fick's first law can be written as

$$\frac{dQ}{dt} = -D\frac{dc}{dx} \quad \ldots\ldots (1.2)$$

where D is defined as the diffusion coefficient (or diffusivity). The negative value of D indicates that diffusion occurs in a direction opposite to that of increasing concentration. Equation 1.2 implies unit area flux, that is dQ/dt must be divided by the surface area, A as follows:

$$\frac{dQ}{dt} = -D\,A\frac{dc}{dx} \quad \ldots\ldots (1.3)$$

When diffusion across a polymer membrane is of interest,

$$\frac{dc}{dx} = \frac{\Delta C}{l}$$

$$= \frac{C_R - C_D}{l}$$

Thus

$$\frac{dQ}{dt} = D\,A\left(\frac{C_D - C_R}{l}\right)$$

where C_R and C_D represent concentration of the drug on the receptor side and donor side of the membrane respectively.

Chien (1980) observed that the release rates of various steroids from silicone capsules were slower *in vitro* than they were *in vivo*.These results were attributed to the lack of sink conditions *in vitro* demonstrating the importance of their maintenance during *in vitro/in vivo* correlation experiments. Sink conditions are met by setting the concentration of drug in the bulk solution (receptor phase) very close to zero. When this condition is met, equation 1.3 can be approximated to

$$\frac{dQ}{dt} = \frac{D\,A\,C}{l} \quad \ldots\ldots \quad (1.4)$$

where C is the concentration of drug in the membrane at the donor surface.

When the concentration of drug on the donor side is maintained by a suspension of drug, as in many reservoir devices, then a saturated solution of drug will be present on the donor side of the membrane and C can be taken to the solubility of drug in the polymer membrane. When C is a constant, integration of equation 1.4 gives equation 1.5

$$Q = \frac{D\,A\,C_p}{l} t \quad \ldots\ldots \quad (1.5)$$

where C_p is the solubility of the drug in the membrane. In the special case represented by Equation 1.5, maintenance of the terms on the right hand side of the equation will generate a constant rate of drug release, that is $dQ/dt = K$, which is the aim of many reservoir-controlled delivery systems. By reference to equation 1.4, it can be seen that the rate of diffusion through a polymer membrane is governed by two factors: the diffusion coefficient (or diffusivity) of the drug and its solubility in the polymer, both of which will be influenced by the chemistry of the polymer and the drug. Smith and Lonsdale (1985) in their review have highlighted

factors that affected the diffusion coefficient:- the solute molecular weight, the glass transition temperature of the polymer and the crystallinity of the polymer. Figure 1.2 shows the empirical correlation between diffusion coefficient and solute molecular weight reported by the previous authors. Increase in solute molecular weight results in a lower diffusion coefficient.

The flexibility of the polymer also determines the diffusion coefficient. As indicated in Figure 1.2, polystyrene in the glassy state at 25°C was associated with the lowest diffusivities and greatest dependence on solute molecular weight. Two other polystyrenes, which were in a rubbery state, were associated with high diffusivities and less dependence on solute molecular weight. Smith and Lonsdale (1985) explain that rubbery polymers exhibit much greater chain flexibility than do glassy polymers and therefore permit higher diffusivities especially for large solute molecules. Diffusion of solutes in low molecular weight liquids, such as water, is very much more rapid than diffusion in polymers as indicated by Figure 1.2.

Polymer crystallinity also influences solute diffusivity. Crystalline or semi-crystalline bulk polymers contain crystallites which consists of regions of ordered, tight chain packing. Solute molecules cannot usually penetrate polymer crystallites (i.e. they have very low solubility in crystallites) and are therefore confined to diffuse in the amorphous regions between crystallites. Crystallinity thus reduces diffusivity in bulk polymers by causing diffusion to take place by way of irregular, tortuous pathways. This effect is demonstrated in Figure 1.2 . Solutes have a higher diffusivity in low density polyethylene, which is 50% crystalline, than they do in high density polyethylene, which is approximately 75% crystalline.

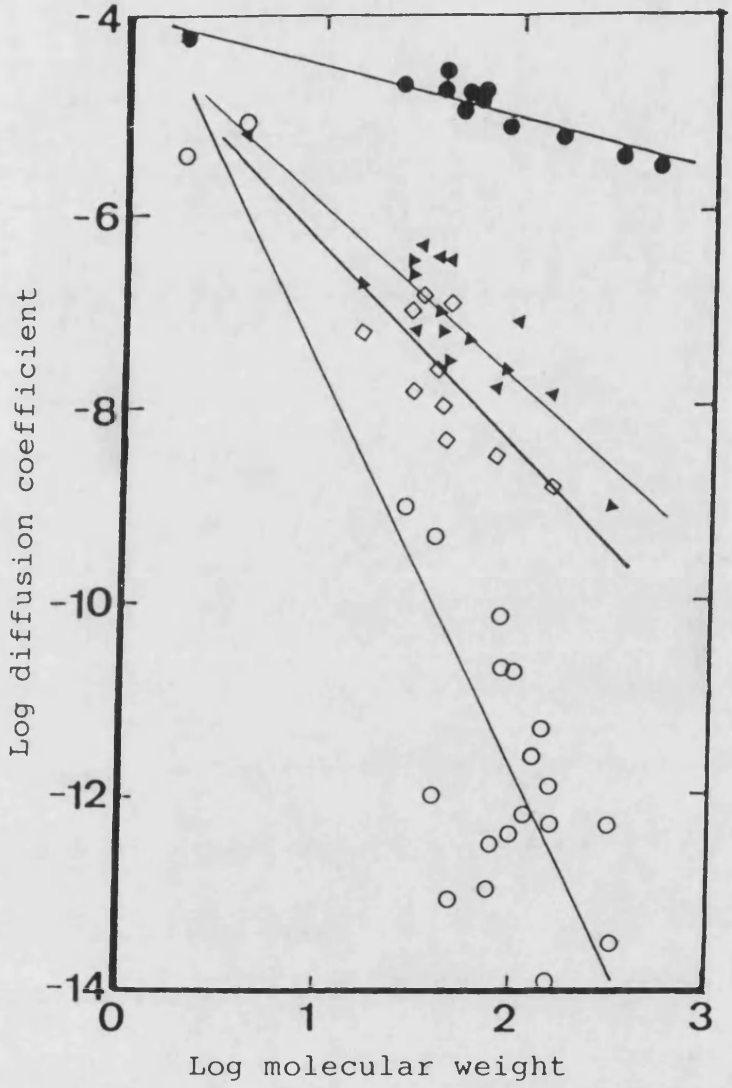

Figure 1.2:- Dependence of diffusion coefficient on solute molecular weight in water, (●); low-density polyethylene (LDPE), (▲); high-density polyethylene (HDPE) (□) and polystyrene, (O). Data at 25°C.
(Reproduced from Smith and Lonsdale, 1985).

An experimental study on diffusion from an aqueous solution through a polymer film has been reported by Pitt *et al.* (1979). In their diffusional study of poly (ϵ - caprolactone), poly (dl- lactate) and their copolymer films, the steady state diffusion coefficient was obtained by considering the presence of an aqueous boundary layer at the surface of the polymer film. The concentration of a drug in the polymer was taken as the product of the partition coefficient, K, and the aqueous solubility of the drug in the aqueous boundary layer. Thus the boundary layer may well play a significant part in the overall rate of mass transfer.

In some circumstances, drug is encapsulated within the bulk polymer itself which leads to a different mode of delivery. Devices of this type are usually referred to as matrix systems. Drug release from matrix systems is highly dependent on the efficiency of entrapment of the drug and the permeability of the polymer system to the surrounding medium. Release from reservoir systems and matrix devices are discussed separately in sections 1.3.1 and 1.3.2.

1.3 Drug delivery devices and mechanisms of drug release.

1.3.1. Reservoir systems.

Reservoir systems consist of a reservoir of an active ingredient enclosed by a polymeric membrane. Drug release is controlled by diffusion through the polymeric membrane and will be constant at steady state as predicted by Equation 1.5.

In practice, reservoir systems will not deliver drugs at a constant rate initially or towards the end of their working life due to two non-steady state conditions. During the initial period, the release rate can either be higher or lower than steady state release rate depending on the storage history of the device. For example, if the membrane device is stored for a long period of time, under conditions during which release

does not occur, then the membrane will become saturated with the drug and the initial release rate will be higher than the steady state release. This is often referred to as the burst effect (Hadgraft and Guy, 1987). If the device is used immediately after manufacture, there may be a slow release until the steady state is achieved after a lag time. If the drug concentration in the reservoir falls below saturation towards the end of its life, then, as drug release continues, the driving force for diffusion through the membrane decreases and the release rate decreases with time (Smith and Lonsdale, 1985).

Examples of commercially produced reservoir systems are Progestasert® and Ocusert® . Progestasert® was a uterine contraceptive system which was capable of delivering progesterone to the uterus for a duration of one year (Brenner *et al.* , 1975). The system consisted of a drug reservoir of progesterone in silicone oil together with barium sulphate being enclosed by ethylene/vinyl acetate copolymer membrane. Drug release from this device was reproducible but the device is no longer used due to problems associated with its presence in the uterus. The Ocusert® therapeutic system delivers pilocarpine to the eye for the treatment of glaucoma. The drug delivery device consists of an ethylene/vinyl acetate copolymer barrier membrane which encloses the drug dispersed in an alginic acid vehicle.

Heilman (1984) showed that the *in vivo* release rate of progesterone from Progestasert® was not constant but decreased with time. The release rate decreased by about 25% from its predicted rate over the course of a year. This decrease was due to a decrease in the volume of reservoir solution and the consequent decrease in membrane surface area contacted.

Chandrasekaran *et al.* (1978) showed that *in vitro* release rate of progesterone from the Progestasert® device was higher than the *in vivo* release rate. This was explained by the presence of a boundary - layer (hydrodynamic layer) around the device *in vivo* which was caused by an insufficient rate of drug removal from the membrane surface.

Since Equation 1.5 does not take into consideration the contribution of the hydrodynamic layer towards diffusion, Chien (1980) put forward a modified equation for diffusion which is shown below

$$Q=\frac{C_p K D_s D_p}{K D_s h_p + D_p h_d} t \quad \ldots\ldots \quad (1.6)$$

where

Q is the cumulative amount of drug released from a unit surface area of a capsule type delivery device

C_p is the solubility of drug in the polymeric membrane

K is the partition coefficient of drug between polymeric device and surrounding tissues fluid

D_s is the diffusion coefficient of drug in the surrounding tissues

D_p is the diffusion coefficient of drug in the polymeric membrane

h_p is the thickness of the polymeric membrane

h_d is the thickness of the hydrodynamic diffusion layer

When KD_sh_p is very much higher than D_ph_d , then Equation 1.6 is reduced to Equation 1.5 and the release of drug is controlled only by the membrane.

1.3.2 Matrix systems

Generally, the term matrix is used to describe drug delivery

systems in which the drug is dispersed, either molecularly or as solid drug particles, within a polymer network. The major advantages of matrix devices are the ease of manufacture and the fact that drug cannot be released rapidly by mechanical damage. Rapid release or *dumping* of the contents can be a serious problem upon rupture of a reservoir device. An example of a matrix drug delivery system is the transdermal Scopoderm® TTS which delivers scopolamine to treat kinetosis or motion sickness. Scopoderm® TTS is applied on the skin and provides 72 hour protection against dizziness, nausea and vomitting.

When a drug is trapped in a polymer which is impermeable to the surrounding medium the encapsulated drug particles cannot be released until they undergo the following process (Chien, 1980). The outermost surface layer of the drug must dissociate from the crystal lattice, dissolve into the surrounding polymer structure, diffuse through it and finally partition into the elution medium surrounding the delivery device. Following his studies on the release of various steroids from silicone polymers, Chien (1980) found that the rate limiting step was the solvation of drug and that this process was very dependent on the chemical structure of the steroid.

However, release of drug from matrix systems does not always occur by diffusion of the drug through the polymer. When the loading of drug is high, penetration of water can often take place by gradual dissolution of adjacent crystals of water-soluble drug (Siegel and Langer, 1984; Hsu and Langer, 1985), the rate of release is determined by diffusion through aqueous pores formed in the polymer matrix. This is the basis of sustained release from many dosage forms for oral delivery which are compacts of drug and polymer prepared by

tabletting. Such matrices usually contain more drug than polymer and drug release is designed to be comparatively rapid (less than 24 hours) (Korsatko *et al.*, 1983).

Systems for implantation are designed to release their drug content over a longer time period and usually contain a lower loading of drug. Release may be by aqueous pore diffusion or by diffusion through the polymer. The nature of the entrapment and loading of drug will affect crucially the mechanism of release. The cumulative release of drugs from matrix systems can often be represented by Higuchi's well-known equation (Higuchi, 1961).

$$Q=[(2A-C_p) C_p D_p t]^{1/2} \quad ..... \quad (1.7)$$

where

Q is the cumulative mass of drug released from a plane of unit area containing a homogenous dispersion of drug.

A is the initial amount of drug incorporated in a unit volume of the matrix device

C_p is the solubility of drug in the polymer phase

D_p is the diffusivity of drug in the polymer matrix structure.

Equation 1.7 was derived for a matrix with the geometry of a slab or film using the following assumptions. A region of depleted drug gradually forms at the surface and begins to penetrate the matrix. The rate of diffusion per unit area throughout this depleted region is independent of position. Equation 1.7 implies that the rate of drug release is dependent on the square root of time. In a subsequent paper, Higuchi (1963) considered the release of drug from spherical matrices. He found that the release of drug from these systems was also given by Equation 1.7 provided that the initial drug loading, A, was very much higher than the solubility of the drug in the

polymer (i.e. $A >> C_p$).

However, Brophy and Deasy (1987) observed that Higuchi's equation can only be used for drug release over a short duration. These authors modified Higuchi's equation by considering the extension of the depleted drug zone for a microparticulate system. Their modified equation is shown below

$$Q = B_1 t^{1/2} - B_2 t \quad \ldots\ldots \quad (1.8)$$

where

$B_1 = [(2 A - C_p) C_p D_p t]^{1/2}$ as in equation 1.7

$B_2 = 4/9 \, c \, C_p \, D_p (3A - 2C_p) (2A - C_p)^{-1}$

where c = 24 × the original length of a cube.

Brophy and Deasy (1987) used their model to study the release of sulphamethiazole from poly(β-hydroxybutyrate) microparticles. They observed that equation 1.8 modelled experimental results more completely than Higuchi's original equation. These authors recommend that Equation 1.8 can be used to represent drug release from matrices of any geometrical shape.

1.3.3 Degradable systems

There is much interest in the use of degradable polymers as the bases for implant devices largely because surgical removal of the device would not be required if the polymer were degraded and eliminated from the body. The release of drugs from matrices based on degradable polymers can be complicated by the degradation of the polymer (Wise *et al.* , 1979); indeed there is the possibility that the polymer degradation itself could be used to control drug delivery. Several polyesters are

already used as surgical sutures (Gilding, 1980) and recently many authors have suggested that these polymers could be used in sustained delivery of polypeptides (Wise *et al.* , 1987; Hutchinson and Furr, 1987). One such product, Zoladex® , entered the British market in 1987 (Pharmaceutical Journal, 1987). However the mechanisms controlling drug release from such systems are not well known and this is a major consideration of the current study (Part III). Hence the use of biodegradable systems is reviewed in detail in Chapter 5 of this thesis.

1.3.4. Particulate systems.

Current research trends in drug delivery involve the use of microparticles for delivery of drugs directly to their site of action. Particulate systems can be injected locally, for instance into joints for the treatment of arthritis (Ratcliffe *et al.* , 1984), or can be directed to certain organs after intravenous injection. The latter organ-specific delivery has been termed **passive targetting** (Tomlinson *et al.* 1984). Particulate systems themselves are varied in their design and manufacture and may release their content as a reservoir, as in the case of microencapsulated systems, or more commonly as matrices. Another advantage of particulate polymeric systems is that they can protect a labile drug, such as a polypeptide, from enzymatic degradation. Thus biodegradable particulate systems have great potential for controlled delivery of peptides (Wheatley and Langer, 1987). The advantage of a colloidal suspension is clear in that an injectable system could be formulated for intramuscular or subcutaneous use. This would obviate the need for a surgical implantation procedure. Particulate systems are best produced by emulsion polymerisation which leads to controlled size although this technique can only be used for certain polymers, such as acrylates (Douglas *et al.* , 1987; Louvreur *et al.* , 1986).

Most degradable particulate systems have been produced by solvent evaporation techniques (Bissery *et al.* ,1984) which are convenient on a laboratory scale but could not be used commercially. No commercial techniques are currently in use although spray drying of polymer solutions has potential (Deasy, 1984). A full review of the use of particulate systems is beyond the scope of this report although it is interesting to note that biodegradable polyesters increasingly are being used as particulate systems (Juni and Nakano, 1987b) and recently poly(β-hydroxybutyrate) (PHB) has been prepared as a particulate system (Brophy and Deasy 1986, 1987; Bissery *et al.*, 1984).

The size of the microparticles is important in determining their distribution after intravenous injection. This has been demonstrated by many authors with a variety of colloidal systems (Willmott *et al.* , 1984 ; Sjoholm and Edman, 1984; Couvreur *et al.* , 1986). Bissery *et al.* (1984) have injected microparticles of PHB of less than 15 μm intravenously. These particles were distributed to the fixed macrophages of the lung, liver and spleen in a similar manner to other particulate systems (Artursson, 1987). Thus PHB particles could be used for delivery of antiparasitic or macrophage stimulants to the reticulo-endothelial system.

1.3.5. Other polymeric drug delivery systems

As well as implant and oral drug delivery systems previously described in sections 1.3.1 and 1.3.2, in terms of their reservoir or matrix design, there are other specialised delivery systems in which polymers have a vital role to play. These delivery systems will be reviewed briefly in this section.

An important class of controlled delivery systems have used osmotic

pressure to facilitate zero order release. These are generally referred to as osmotic pumps (Eckenhoff and Yum, 1981; Fara, 1985). Osmotic pumps are used as implants for toxicological testing in animals and have been manufactured as tablets for oral administration. An elementary osmotic tablet consists of a core reservoir of drug and in most cases, an additional excipient to assist in creating osmotic pressure. The core is coated with a semipermeable membrane, permeable to water but not the drug, which is continuous but for a single hole drilled into the membrane using a laser.

The release of drug occurs as follows. Osmotic activity ensures that water from the gastrointestinal tract penetrates the system through the semipermeable membrane. The influx of water is constant and its rate is determined by the large mass of drug which maintains a saturated solution within the core. The influx of water forces the saturated solution out through the laser-drilled orifice at a constant rate. The uptake of water and thus the release of drug in a saturated solution remains constant as long as there is an excess of undissolved substance in the reservoir. When no more solid drug remains and the saturated drug solution becomes diluted by the continued influx of water, the rate of release steadily declines in a manner similar to that of a first order release.

The first commercial product of this type contained indomethacin for treating autoimmune diseases. However, due to the incidence of localised irritation to the mucosal surface which led to peptic ulceration and bleeding, the product was withdrawn (Heilmann, 1984). This was a major setback to the use of osmotic pumps although recently a salbutamol formulation of this type has been introduced (Pharmaceutical Journal, 1988).

Another delivery system in which polymers determine the rate of release is the transdermal therapeutic systems. A transdermal therapeutic system has the appearance of a plaster patch. Such systems deliver drugs at a controlled rate to the surface of the skin. As long as the drug is absorbed to a great enough extent through the skin, these systems can be used to deliver drugs at a zero-order rate to the systemic circulation (Shaw, 1985). The benefits of transdermal therapeutic systems can be summarized as follow:

- improved patient compliance especially in cases which would require relatively frequent oral administration.
- Avoidance of hepatic-first-pass metabolism.
- constant level of drug in biological fluids achieved at steady-state.

The main disadvantage of this type of drug delivery system is the significant barrier presented by the stratum corneum, the outermost layer of skin, which limits the number of drugs which can be administered by the route (Hadgraft, 1985).

There has been considerable interest in recent years in targetting of drugs by way of soluble polymeric carriers to which drugs are covalently linked. Macromolecular drug-carrier systems are able to modify the pharmacokinetic distribution of drugs such that the effects of drugs at a desired site of action are enhanced relative to their unwanted effects (Kopecek and Duncan, 1987). Detail examples of carriers to which drugs have been bound and their crosslinking agents were reviewed by Poznansky and Cleland (1980). These applications of polymers in drug delivery are likely to be of great importance in the future but are outside the scope of the current project.

1.4 Origins and scope of this study

Poly(β-hydroxybutyrate) is an optically active aliphatic polyester produced by a wide variety of bacteria (Dawes and Senior, 1973). Its biological function in these microorganisms is to serve as an energy and carbon storage product in much the same way as glycogen in mammalian tissue and starch in plants.

Recently this thermoplastic biopolymer has attracted industrial attention as a possible candidate for large scale biotechnological production since PHB has a high tensile strength, comparable to that of isotactic polypropylene and is said to degrade to a normal metabolite of the human body, d-β-hydroxybutyric acid (Holmes, 1985; Ratledge, 1986; Technical Insights, 1985). The polymer can be obtained in the pure state unlike other synthetically produced polymers which may contained catalyst or initiator residues.

Since PHB is related to a group of other biodegradable polyesters already in use, such as poly(lactate) and poly(glycolate), PHB has great potential for use in drug delivery systems. The present study aimed to examine the mode of *in vitro* hydrolytic degradation of PHB. Techniques have been used to allow distinction between two possible degradation mechanisms; random chain scission and surface hydrolysis. Central to the success of the project was the need to determine polymer molecular weight distribution on a routine basis. A size exclusion chromatographic method has been studied with this aim in mind. Developmental studies of this technique are reported in Part II of this thesis.

Copolymers of β-hydroxbutyrate with β-hydroxyvalerate are also available which may have advantages over the homopolymer. Thus degradation of various copolymers has been studied as a comparison with the homopolymer.

A third objective of this project has been to study the suitability of these polymers for controlling the release of drugs. Several workers have reported the use of PHB in sustained release systems. (Juni, *et al.*, 1986; Korsatko *et al.*, 1983; Gould *et al.*, 1987; Brophy and Deasy, 1986). The release of drug is expected to be a complex function of the morphology of the matrix and the physical properties of the drug. The scope of this study is limited in this respect. Studies have focused on a low molecular model compound, methyl red, which is soluble in the same solvents as the polymers themselves, making casting of films a simple process. The aim of the release studies reported here has been to establish the role of polymer degradation in release of low molecular weight drugs.

PART II

ASSAY OF POLYMER MOLECULAR WEIGHT DISTRIBUTION

Chapter 2

ASSAY OF POLYMER MOLECULAR WEIGHT DISTRIBUTION: AN INTRODUCTION

2.1 Introduction

Synthetic polymers and many naturally occuring macromolecules possess a range of molecular weights. It is therefore important to characterize both average molecular weights and the molecular weight distributions of polymers since they affect the physical properties of the polymers. For example, the strength and toughness of polyethylene film increases with an increase in the number-average molecular weight (Billmeyer, 1962). Also, the molecular weight of a polymer affects the release of drugs from polymeric drug delivery systems. The release of bovine serum albumin from different molecular weights of a copolymer, ethylene vinyl acetate (Evac), was studied by Hsu and Langer (1985). These authors found that molecular weight was a sensitive factor which affected the kinetics of drug release; the higher the molecular weight of the polymer carrier, the slower was the release of bovine serum albumin.

Commonly three parameters are used to characterize a polymer that is:

- Number-average molecular weight, M_n
- Weight-average molecular weight, M_w
- Degree of polydispersity, M_w/M_n

The number-average molecular weight, M_n , is defined as the mass of the sample in grams divided by the total number of molecules present. Mathematically, it can be represented as shown below:

$$M_n = \frac{\sum N_i M_i}{\sum N_i} = \frac{\sum W_i}{\sum \frac{W_i}{M_i}} \quad \ldots\ldots (2.1)$$

where

W_i , M_i and N_i are the total weight molecular weight and number of molecules respectively with molecular weight i.

i represents the incrementing index which covers the entire molecular weight distribution.

Experimentally, M_n is obtained by measurement of colligative properties.

The weight-average molecular weight, M_w is defined according to the equation shown below:

$$M_w = \frac{\sum N_i M_i^2}{\sum N_i M_i} = \frac{\sum W_i M_i}{\sum W_i} \quad \ldots\ldots (2.2)$$

From the two equations above, M_w is always larger than M_n except when these values are identical in the case of a monodisperse system. Thus the ratio of M_w/M_n is a measure of the breadth of the polymer molecular weight distribution being equal to unity for a monodisperse system.

2.2 Absolute molecular weight methods: Types, Advantages and Limitations.

Practical methods to determine the molecular weight of polymers may be either relative or absolute. Relative methods require calibration with samples of known molecular weights; these include viscometry and vapour-phase osmometry. Absolute methods are classified according to the type of average molecular weight obtained. For instance, absolute colligative techniques yield number-average, whereas, light scattering

and ultracentrifuge techniques yield weight-average (Cowie, 1973).

Determination of number-average molecular weight, M_n , involves use of end-group assay, thermodynamic or transport methods. The disadvantage of using these methods is that they are not sensitive to high molecular weight polymers. Such polymers can be characterised using the weight-average molecular weight methods. One of the requirements of M_w methods is that the polymer must be dissolved in a highly clarified solution. Therefore, these techniques are difficult and in addition, the light scattering methods of obtaining M_w is time consuming. With the practical limitations of absolute methods in mind, in this study, size exclusion chromatography was used to analyse the molecular weight distributions of polymers. The method requires small amounts of material for analysis and the results can be obtained within 15-20 minutes.

2.3 Size-Exclusion Chromatography.

2.3.1 Introduction.

Size-exclusion chromatography, or gel-permeation chromatography, is a technique that separates molecules according to their hydrodynamic radii in solution. The principal uses of the method have been for the characterization of the molecular weight distribution (MWD) of polymers and also in the analysis of oligomers and low molecular weight compounds (Cooper, 1982).

The origin of size-exclusion chromatography (SEC) is attributed to Porath and Flodin (1959) who analysed water soluble polymers using soft, cross-linked dextran gels. Modern high performance SEC has resulted from the development of small, more rigid, porous particles for column packings. The advance together with the introduction of high

quality instrumentation have reduced the time required for analysis.

2.3.2. Solute Retention in SEC.

In size-exclusion chromatography, polymeric solutes are partially excluded from the column packing and elute ahead of small molecules. As a solute band moves along with the solvent down the column and around the packing particles, the solute molecules continously diffuse in and out of the pores of the packing particles.

Size separation in SEC can be explained on the steric basis that large molecules can only partially permeate the pore volume of the column material. According to Yau *et al.* (1979), small molecules (such as the eluant) fully permeate the pores of the support/packing material and are eluted in a volume V_m , equivalent to the total volume of eluant on the column. Larger molecules which cannot enter any of the pores are totally excluded and are eluted in the extraparticle volume or void volume, V_o . Molecules of intermediate size are eluted between V_o and V_m . The degree of permeation of such intermediate molecules into the pore volume of the particles, V_p is denoted by K_{sec} and is termed as the exclusion coefficient. K_{sec} is related to the elution volume, V_r of any solute by an equation as shown below:

$$V_r=V_o+K_{sec}V_p \quad \ldots\ldots (2.3)$$

The pore volume is related to V_m and V_o by the equation as shown below:

$$V_m=V_o+V_p \quad \ldots\ldots (2.4)$$

The general relationship of the retention volume to solute molecular weight for each packing material is usually displayed as a plot of the logarithm of the molecular weight (MW) against the retention volume V_r and is called an **exclusion curve** or **SEC**

calibration curve. An example is shown in Figure 2.1. Various theories of separation by SEC have been proposed (see below). In practice, when the solutes are well dissolved in the eluant, separation is a function of hydrodynamic radius and various calibration methods can be employed (see section 2.4.).

2.3.3. Mechanism of SEC separation .

The mechanism of SEC separation has been modelled by two major theories (Cooper, 1982) namely:

- Equilibrium model (see 2.3.3.1)
- Steric exclusion model (see 2.3.3.2)

The equilibrium model explains the separation of solute molecules based on thermodynamic principles while the steric exclusion model explains the separation in terms of diameters of the solute molecules and the pore structures. Besides the two generally accepted theories of separation in SEC, other mechanisms have been put forward to explain SEC separation. These mechanisms failed to model the observed separation totally and were specific to certain processes only. I refer to the restricted diffusion mechanism (Ackers,1964) , separation by flow (DiMarzio and Guttmann, 1969) and the stochastic mechanism (Carmichael, 1968).

2.3.3.1 Equilibrium model.

Separation in SEC involves the migration of solute molecules between the moving and stationary phases. This process will continue until a thermodynamic equilibrium is achieved. The thermodynamic equilibrium of solute distribution is defined as the condition in which the chemical potential of each solute component is the same in the two

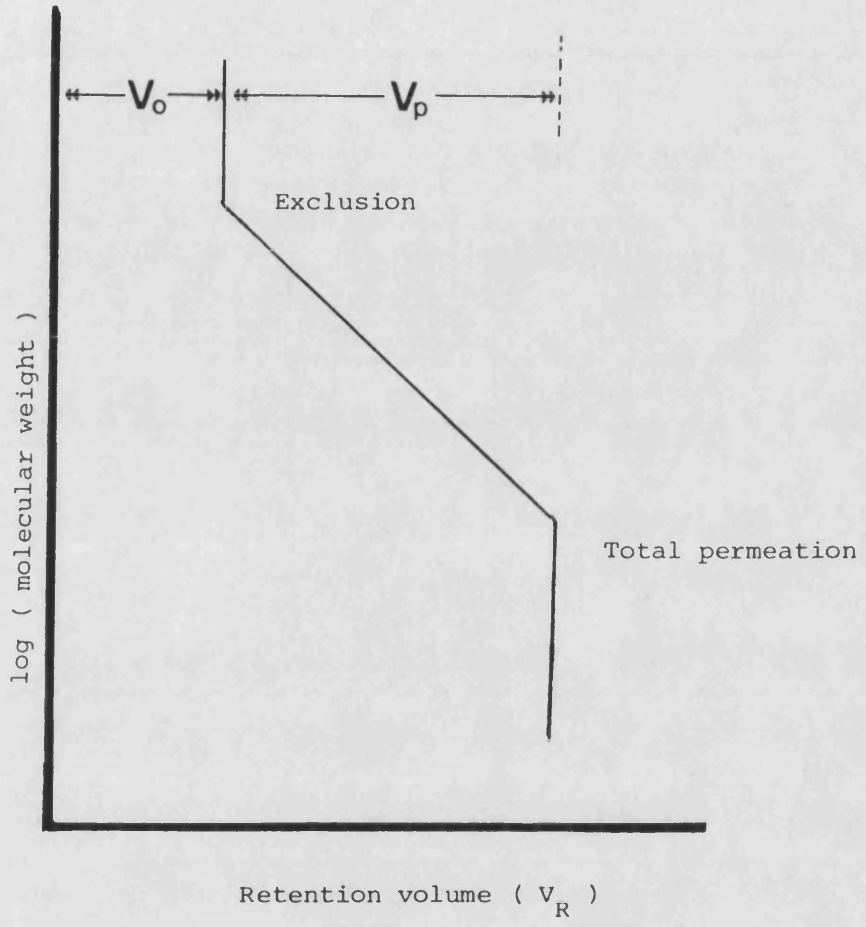

Figure 2.1 : A hypothetical SEC calibration curve

phases.

For dilute solutions at equilibrium, solute distribution can be related to the standard free energy change (ΔG^{o}) between the phases at constant temperature and pressure:

$$\Delta G^{o} = -R\,T\,\ln k \quad \ldots\ldots (2.5)$$

$$\Delta G^{o} = \Delta H^{o} - T\,\Delta S^{o} \quad \ldots\ldots (2.6)$$

where

k is the solute distribution coefficient,

R is the gas constant

T is the absolute temperature.

ΔH^{o} and ΔS^{o} are the standard enthalpy change and standard entropy change between the phases respectively.

Since SEC is governed mainly by the entropy change between the phases, K_{sec} can be derived as follow: (Dawkins, 1976).

$$K_{sec} = e^{\frac{\Delta S^{o}}{R}} \quad \ldots\ldots (2.7)$$

The equation above implies that there is no enthalpy change occuring in SEC and that the process is independent of temperature. In reality temperature changes have an effect on the hydrodynamic radii of polymeric solute molecules which in turn affect the value of ΔS^{o} . (Mori, 1984).

2.3.3.2. Steric Exclusion Models.

The steric exclusion model explains quantitatively the exclusion coefficient, K_{sec} , and the SEC calibration as a function of the size and the shape of the solute and the pores. There are various models representing the forms and structures of solute molecules and also the conformations

of the pore structures which can be used to explain the separation process in SEC.

Giddings *et al.* (1968) have obtained a theoretical relationship between the partition coefficient, K_{sec}, and parameters which characterise the solute and the stationary phase, assuming a uniform pore size and shape and a rigid solute molecule. Their statistical theory which showed the dependence of K_{sec} on the physical properties of solute molecules and the stationary phase was developed for solutes of spherical (example: serum albumin) to thin rod shape (example: DNA) and for pores which range in cross-sectional shape from circles to infinite slabs. An example of their theory, in this case modelling the separation of a spherical molecule by a circular pore, is shown in Figure 2.2:

The solute molecule has a radius of r and the pore is an infinite cylinder of radius R. Since the centre of the mass of the molecule cannot approach closer than a distance r from the wall of the pore, the part of the pore volume accessible to the centre of the mass is a cylinder of radius (R-r). Thus, the exclusion coefficient, K_{sec}, is equal to the fraction of the pore volume accessible to the molecule, as shown in the equations below:

$$K_{sec} = \left[1-\left(\frac{r}{R}\right)\right]^2 \cdots \text{for} \quad \left(\frac{r}{R}\right) < 1 \quad \ldots\ldots \quad (2.8)$$

$$K_{sec} = 0 \cdots \text{for} \quad \left(\frac{r}{R}\right) < 1 \quad \ldots\ldots \quad (2.9)$$

For a column with many pores the exclusion coefficient is equivalent to the ratio of the volume of pores accessible to the centre of the mass of the molecules (V_a) to the total volume of the pore (V_p) that is:

$$K_{sec} = \frac{V_a}{V_p} \quad \ldots\ldots \quad (2.10)$$

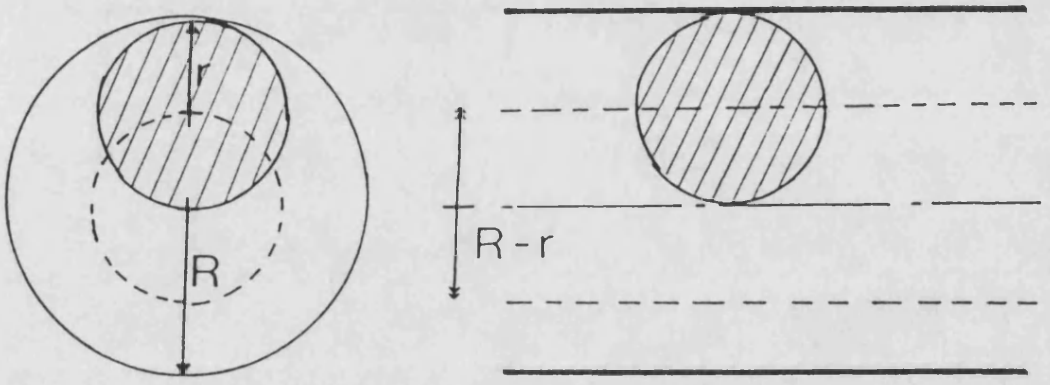

(a) END VIEW (b) SIDE VIEW

Figure 2.2:- Exclusion volume in SEC. The volume excluded by the macromolecule is a sphere of radius r, while exclusion due to the pore wall is the region outside the cylinder of radius R - r.

Besides proposing the above relationship for separation of spherical molecules by circular pores of infinite length, Giddings *et al.* (1968) have obtained equations for spherical molecules separated by various pore geometries and for thin rods separated by various pore geometries. However their equations do not take into consideration the polydispersity of pore size distribution within the stationary phase.

Van Kreveld and Van den Hoed (1973) attempted to overcome the problem of pore size distribution by proposing the random sphere model. The random sphere model gives a more realistic representation of the separation process by comparing the pore shapes inside SEC packing particles to the voids between randomly arranged microspheres. The above authors correlated K_{sec} values obtained experimentally with those calculated theoretically and arrived at a good agreement. They proceeded from these experimental findings to an examination of the microstructure of porous silica by electron microscopy. The particles of silica apparently consisted of agglomerates of microparticles of spherical shape, which justified their theoretical proposals.

The theory developed by Van Kreveld and Van den Hoed (1973) was based on uniform size spheres. Knox and Scott (1984) have developed the random sphere model further by accounting for the presence of polydisperse spheres. They correlated K_{sec} values obtained experimentally with those calculated theoretically and were able to improve on the agreement achieved by Van Kreveld and Van den Hoed (1973).

Since the conformation of a flexible polymer chain in a good solvent is random coil, Casassa (1971) has modelled the separation of randomly coiled solute molecules by SEC. The starting point of Casassa's theory is

random flight statistics which describe the conformation of a flexible polymer chain with one end fixed inside the cavity centre. This author derived the theoretical value of K_{sec} for different geometrical pore shapes as a function of the stationary pore geometry and molecular size. Good agreement between theoretical and observed results was obtained.

2.4. Calibration of SEC columns.

The raw data obtained from SEC experiment is actually the detector output, which represents the concentration of each molecular weight in the eluant. Retention can be determined as retention time or retention volume. Generally the retention time is used assuming the pump is capable of pumping at a constant rate.

The shape of the chromatogram will be determined by the pore size distribution within the porous packing and the sizes of the polymer molecules in solution. Usually in order to determine the molecular weight distribution (MWD) from the raw data, a calibration of the column is required.

SEC can be considered as an absolute method for the direct determination of molecular weight provided that the molecular weight of the polymer can be measured as it elutes in the solvent. This requires a system equipped with dual detectors for determining both the concentration and the molecular weight of the eluting polymer. An example of such a system is the low angle laser light scattering method as used by Grinshpun *et al.* (1984).

Traditionally SEC columns have been calibrated by determining retention times of polymer fractions of known molecular weight. Because separate experiments are required, first to establish the calibration curve and secondly to obtain the chromatogram for an

unknown polymer fraction, the chromatographic conditions such as the flow rate and the composition of the solvent and temperature must remain constant. The methods for establishing the calibration curve can be divided into 3 categories, namely: (Gilding *et al.*, 1981)

- Primary method
- Empirical method
- Universal method

The primary and empirical methods, relate to calibration with known fractions of the same polymer which is to be characterized. The primary and empirical methods make use of known samples with narrow molecular weight distributions (MWD) and broad MWD respectively. These two methods will be discussed together in the following section.

2.4.1. Primary and empirical methods.

The primary method involves use of reference standards with low polydispersities which cover a wide molecular weight range. Reference standards having low polydispersities ($M_w/M_n < 1.1$) have become available for various polymers, for example, polymethylmethacrylate, polyisoprene, polytetrahydrofuran, polystyrene, poly α - methylstyrene and polyethylene oxide. (Polymer Laboratories, 1985).

For other homopolymers, when reference standards are not freely available, polymer fractionation techniques may be considered but the experimental work involved is time consuming and another method of molecular weight determination would need to be employed. The calibration curve that results from using narrow distribution reference standards often appears like the curve shown in Figure 2.3.

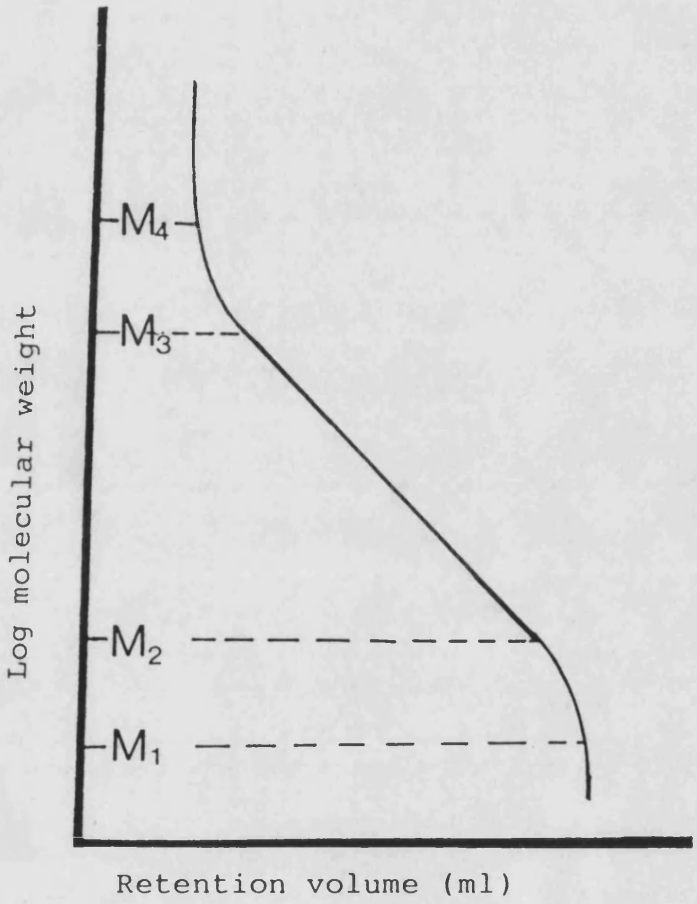

Figure 2.3:- Molecular weight calibration curve.

Since reference standards have a polydispersity, (M_w/M_n), less than 1.1, the retention time corresponding to each molecular weight is assumed to be the retention time of the peak of concentration as the polymer elutes, that is,

$$M_{peak} = M_n = M_w = M_v$$

As shown in figure 2.3, there is usually a region, between M_2 and M_3, which is linear and thus the calibration curve is given by the equation below:

$$\log_{10} M = C_1 - C_2 V \quad ..... \quad (2.11)$$

where C_1 and C_2 are constants.

The whole range of the calibration curve, between M_4 and M_1, can be represented by a polynomial curve which gives the best polynomial fit to the experimental data points as shown below:

$$\log_{10} M = A + B V + C V^2 + D V^3 + \cdots \quad ..... \quad (2.12)$$

where A,B,C,D..... are the coefficients of the polynomials. These coefficients can be determined by a least squares fit of the polynomial to the experimental calibration data points. An example of the polynomial fit to the calibration curve has been reported by Van Dijk *et al.* (1983).

The pore size of the column affect the linearity of the calibration and the molecular weight separation range. This observation was made by Yau *et al.* (1978) using porous inorganic silica as the column packing material. Their results are shown in Figure 2.4 and Figure 2.5. These authors observed that the linear portion of the calibration curve holds over 4-5 decades of molecular weight for a combination of two porous silicas each having a different pore size. Each packing material when tested alone produced a much narrower linear region. The expanded

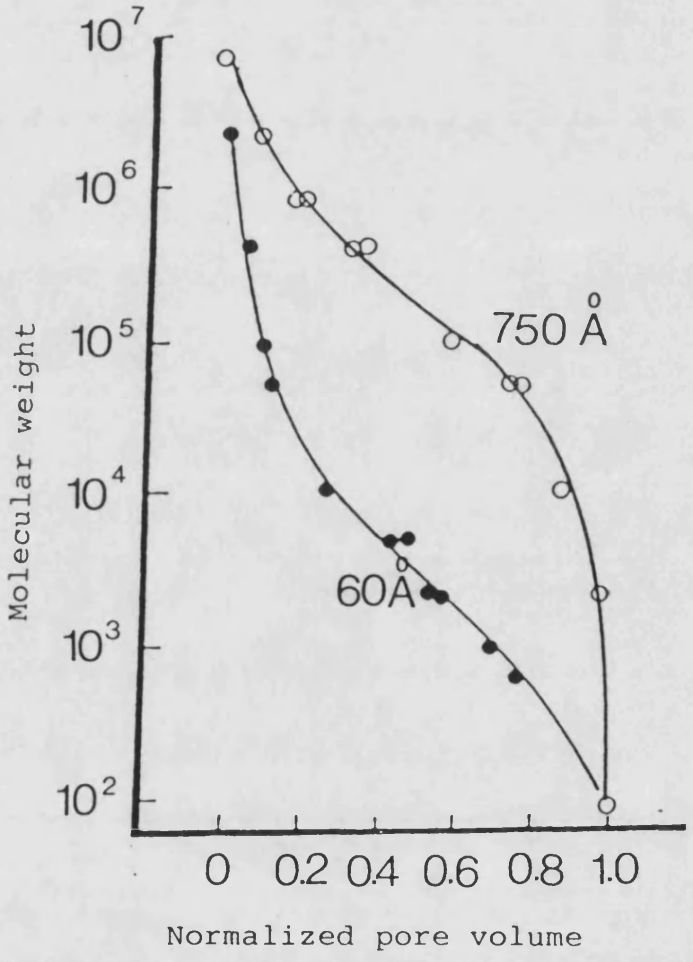

Figure 2.4:- Molecular weight fractionation ranges for polystyrene for two porous silicas with pore size distributions differing by about one decade (●), silica PSM 60Å; (O), silica PSM 750Å.
(Reproduced from Yau et al., 1978).

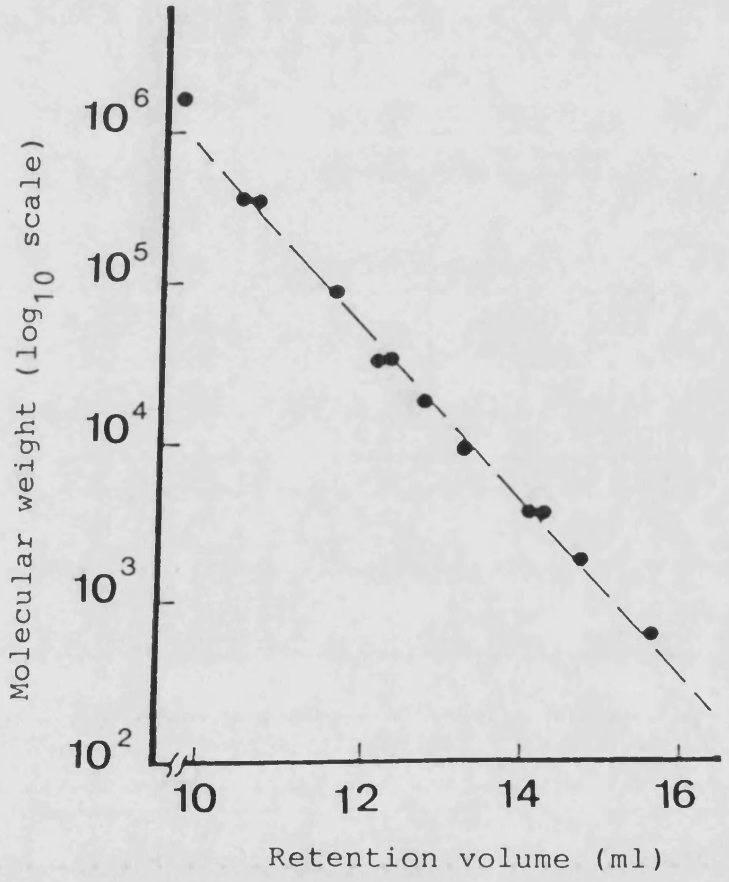

Figure 2.5:- Molecular weight calibration curve for polystyrene for bimodal column system assembled with porous silicas having calibration in Figure 2.4. (Reproduced from Yau et al., 1978).

linear portion of the calibration curve for the mixed silicas corresponded to the entire range covered by the separate columns.

The column material used in this study was spherical, semirigid, highly crosslinked, styrene/divinylbenzene copolymer beads about 5μm in diameter. Seven different pore sizes were contained in the same column making use of the same phenomenon as that observed by Yau *et al.* (1978) that is to expand the linear portion of the calibration curve so that one column can be used for a wide range of molecular weight analysis. The separate calibration curves obtained from each pore size by the manufacturer shown in Figure 2.6(a) and the calibration curve obtained from a combination of the seven pore sizes are shown as in Figure 2.6(b).

When the empirical calibration method is used, errors are introduced because the condition

$$M_{peak} = M_n = M_w = M_v$$

no longer holds. Unless the polydisperse samples are well characterised, the empirical method is undesirable.

2.4.2 Universal method.

In the absence of well-characterized reference materials of the same polymer which is later to be analysed, a calibration curve can be obtained using the assumption that the hydrodynamic volume is the parameter which determines retention on the column. This is the basis for the universal method.

From studies of the dilute solution viscosity of synthetic polymers, Flory (1953) introduced the concept of the equivalent hydrodynamic sphere to represent the polymer molecule in solution. Flory made

(a)

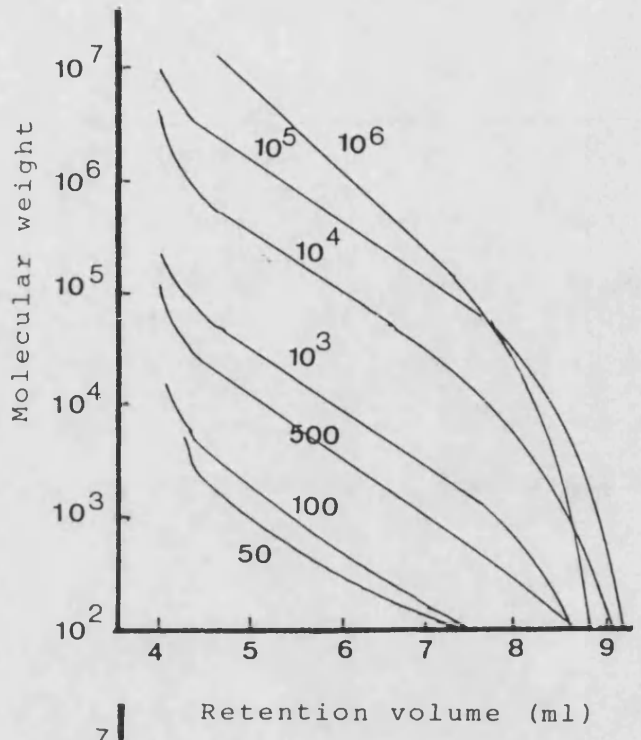

(b)

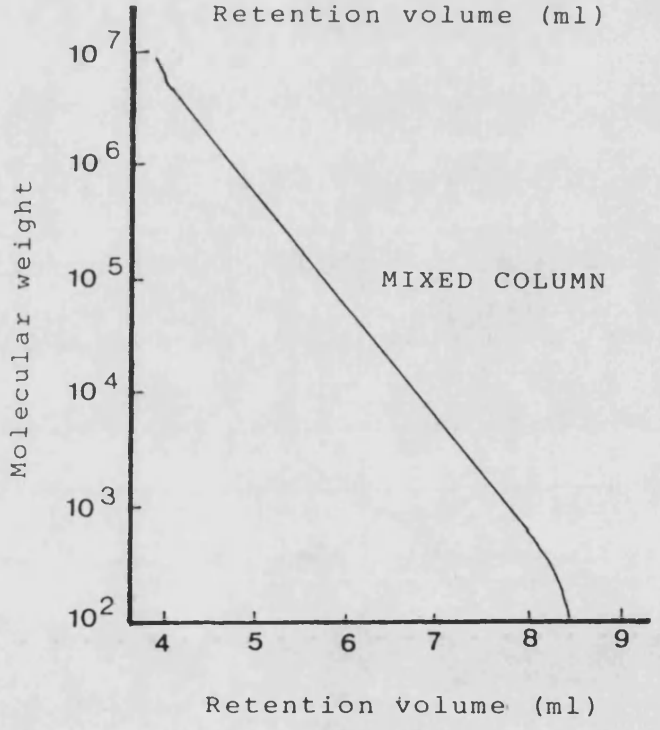

Figure 2.6 (a) : Calibration curves of polystyrene standards obtained from seven different pore sizes.(Each pore size is in A)

(b) : Calibration curve of the same polystyrene standards obtained from a mixed column containing seven different pore sizes as above. (from Polymer Laboratories,1985)

use of the Einstein's viscosity equation:

$$[\eta]M = 0.025 N_A V_h \quad \ldots\ldots \quad (2.13)$$

where

$[\eta]$ is the intrinsic viscosity,

M is the molecular weight,

N_A is the Avogadro's number

V_h is the hydrodynamic volume of the equivalent sphere.

Equation 2.13, as shown above, shows that the product of $[\eta]M$ is a direct measure of the hydrodynamic volume of the particles. Thus, if the hydrodynamic volume controls the separation in SEC, a plot of $[\eta]M$ versus retention time will be the same for all polymers. An experimental examination of the nature of the plot of $[\eta]M$ versus retention time was given by Grubisic *et al.* (1967). In their study, homopolymers and copolymers having various chemical and geometrical structures were used to test the universal method. Since all the polymers fitted on a single curve of log $[\eta]M$ versus retention time, this observation proved that the hydrodynamic volume determines the retention in SEC.

Since equation 2.13 represents spherical particles, Flory (1953) modified the equation to take into consideration the dimensions of flexibly coiled polymers. The modified equation is shown below.

$$[\eta]M = \Phi_0 \left(\langle r^2 \rangle \right)^{\frac{3}{2}} = \Phi'_0 \left(\langle s^2 \rangle \right)^{\frac{3}{2}} \quad \ldots\ldots \quad (2.14)$$

where

$\langle r^2 \rangle^{1/2}$ is the root-mean-squre end-to-end distance

$\langle s^2 \rangle^{1/2}$ is the root-mean-square radius of gyration

Φ_0 and Φ'_0 are universal constants.

Thus these molecular parameters can be used as measures of hydrodynamic volume. As an example, Cantow *et al.* (1967) have used the average end-to-end distance as a measure of hydrodynamic volume for the calibration curves of polystyrene and polyisobutylene in 1,2,4-trichlorobenzene.

Coll and Gilding (1970) instead have used another parameter to represent the hydrodynamic volume. They represented the hydrodynamic volume by the equation proposed by Ptitsyn and Eizner (1960) for the mean-square end-to- end distance as shown below:

$$\left\langle r^2 \right\rangle^{\frac{3}{2}} = \frac{[\eta]M}{\phi(\epsilon)} \quad \ldots\ldots \quad (2.15)$$

where

$$\phi(\epsilon) = \Phi_0 \left(1 - 2.63\epsilon + 2.86\epsilon^2\right)$$

where Φ is a constant as in equation 2.14. The function ϵ is a parameter which depends on polymer-solvent interaction and is related to α in the Mark-Houwink equation, $[\eta] = K M^{\alpha}$, by the equation shown below:

$$\epsilon = \frac{(2\alpha - 1)}{3} \quad \ldots\ldots \quad (2.16)$$

Finally, it can be said that the universal method proposed by Grubisic *et al.* (1967) was well supported by the various size parameters discussed previously.

Thus at a given retention time, the relationship shown below will apply.

$$\log[\eta]_p M_p = \log[\eta]_{ps} M_{ps} \quad \ldots\ldots \quad (2.17)$$

where p refers to the polymer requiring analysis and ps refers to the standard polymer .

With knowledge of the Mark-Houwink parameters for test and standard polymer, the universal method can be used. Moreover, the theory can be extended to allow determination of Mark-Houwink parameters. These concepts are dealt with in the following three sections (2.4.2.1, 2.4.2.2 and 2.4.2.3).

2.4.2.1. Evaluation of intrinsic viscosity.

From equation 2.17, the relationship between intrinsic viscosity and molecular weight must be known or determined in order to make use of the universal method. This section will discuss the determination of the intrinsic viscosity. The viscosity of a polymer solution can be calculated from an equation of the form

$$\eta=\alpha\rho(t-\frac{\beta}{\alpha t}) \quad \ldots\ldots \quad (2.18)$$

where

ρ is the density of solvent (or solution)

α and β are calibration constants, the latter which takes account of the small correction for kinetic energy.

In this study, the viscosities of dilute polymer solutions were measured using a suspended level dilution viscometer. The measurements of solution viscosity were made by comparing efflux time, t, the time required for a specified volume of polymer solution to pass through a capillary tube, with the corresponding efflux time, t_0, for the solvent. In such studies one is concerned with the increase in the viscosity of the solution caused by the polymeric solute. This is expressed as the relative viscosity, η_{rel}, where,

$$\eta_{rel}=\frac{t}{t_0} \quad \ldots\ldots (2.19)$$

Equation 2.19 is obtained by assuming that the correction factor for kinetic energy is small and, for a dilute solution, the densities of the solvent and the solution are the same.

The specific viscosity $\eta_{sp} = \eta_r - 1$, is a measure of the incremental increase in viscosity attributed to the polymeric solute. The ratio η_{sp}/c , where c is the polymer concentration, is a measure of the specific capacity of the polymer to increase the relative viscosity. The limiting value of this ratio at infinite dilution is called the intrinsic viscosity, which is designated by $[\eta]$

$$[\eta]=\lim_{c\to 0}\left(\frac{\eta_{sp}}{c}\right) \quad \ldots\ldots (2.20)$$

The intrinsic viscosity is usually calculated using the Huggins' equation as shown below:-

$$\frac{\eta_{sp}}{c}=[\eta] + k'[\eta]^2 c \quad \ldots\ldots (2.21)$$

where k' is a constant for a given polymer at a given temperature in a given solvent.

2.4.2.2 Intrinsic viscosity - molecular weight relationship

When the logarithms of the intrinsic viscosities for a series of fractionated linear polymer homologues are plotted against the logarithms of their molecular weights, a linear relationship usually exists which can be expressed by the Mark-Houwink equation;

$$[\eta]= K M^{\alpha} \quad \ldots\ldots (2.22)$$

where K and α are constants determined respectively by the intercept and the slope of the above plot. For randomly coiled polymers, the exponent α varies from 0.5 in theta solvents to a maximum of about

1.0. For many systems in good solvents, α lies between 0.6 and 0.8.

2.4.2.3. Calibration procedures by universal method.

It follows from equation 2.17 that at a given retention volume/time, the relationship below will apply.

$$\log[\eta]_p M_p = \log[\eta]_{ps} M_{ps}$$

Here subscript P refers to a polymer requiring analysis and subscript PS to a polymer standard.

In the absence of polymer fractions of narrow molecular distributions and known Mark-Houwink constants it is possible to use an iterative procedure described by Van Dijk *et al.* (1983) which allows determination of Mark-Houwink constants from polydisperse samples of polymer. Van Dijk *et al.* (1983) were able to use this method to obtain SEC calibration curve for poly (dl-lactate). The steps taken by Van Dijk *et al.* (1983) are outlined below.

According to the universal calibration method the product of the molecular weight M and the intrinsic viscosity is a universal function of the elution volume,V, or time,t, for various polymers ie:

$$M[\eta] = \mu(v) \quad \ldots\ldots \quad (2.23)$$

The method of Van Dijk *et al.* (1983) proceeds as follows. Intrinsic viscosities of monodisperse fractions of the standard polymer and polydisperse fractions of the test polymer are determined by classical viscometry. Values of μ (the universal function; Eqn 2.23) are calculated for the standard polymer. These can then be plotted against elution times to give a universal plot of log μ against V. Estimates of μ for the test polymer fractions are obtained from the universal plot using the peak of the chromatograms at the corresponding elution times. Using

the estimates of μ for the test polymer, initial estimates of Mark-Houwink constants for the test polymer (ie α and K) are obtained by plotting log [η] against log μ for the test polymer in accordance with

$$\log[\eta]=\frac{\alpha}{1+\alpha}\log\mu+\frac{1}{1+\alpha}\log K \quad \ldots\ldots \quad (2.24)$$

The slope of the plot enables estimation of the constant α and the intercept yields an estimate the value of K.

The estimates of α and K for the test polymer can then be used to calibrate the SEC column for the unknown polymer by correcting for the differences between the Mark-Houwink constants of test and standard polymer in accordance with equation 2.25 shown below:

$$\log M_1=\frac{1}{1+\alpha_1}\log\frac{K_2}{K_1}+\frac{1+\alpha_2}{1+\alpha_1}\log M_2 \quad \ldots\ldots \quad (2.25)$$

where the subscripts refer to two polymers labelled 1 and 2.

Since the values of K and α for the test polymer have been estimated using polydisperse fractions of the test polymer, the next step is to carry out an iteration process which enables calculation of the true Mark-Houwink constants for the test polymer. The iteration process involves inserting the initial values of K and α into equation 2.25 and, after performing a SEC experiment, using the calibration curve to obtain the viscosity-average molecular weight for test polymer fractions. The Mark-Houwink relationship is then replotted using the intrinsic viscosities, [η] and the above-obtained values of M_v , producing new values of α and K. Again these values are inserted into equation 2.25 and a second SEC experiment is performed, resulting in third estimates of α and K. The iterative process is performed in this way until constant values of α and K are obtained.

Chapter 3

ASSAY OF POLYMER MOLECULAR WEIGHT DISTRIBUTION:MATERIALS AND METHODS

3.1. Materials.

3.1.1. Chloroform.

Chloroform for size exclusion chromatography and viscometry was obtained from Fison (UK). The grade used for the size exclusion chromatography was high performance liquid chromatography (HPLC) standard. For viscometry, analytical grade (AR) was used.

3.1.2. Polystyrene standards.

A series of polystyrene samples with different molecular weights was obtained from Polymer Laboratories Ltd (UK). The polystyrene standards were prepared by anionic polymerization and have been reported by the manufacturer to be chemically stable. Characterization of the polystyrene standards was performed by Polymer Laboratories Ltd. Specifications of these polymers used for size exclusion chromatography are shown in Table 3.1.

3.1.3. Poly(β -hydroxybutyrate) (PHB)

PHB was obtained from Marlborough Biopolymers Ltd (UK). Samples of two batches with different mean molecular weights were obtained. Both samples were of high purity grade; the batch numbers used were as follows:-

- High molecular weight PHB. Batch number:- Bx IC 83/2
- Low molecular weight PHB. Batch number:- Bx IC 83/1-4B

Table 3.1 : Specification of polystyrene standards used for SEC

Peak molecular weight for SEC (M_n)	Degree of polydispersity $\frac{M_w}{M_n}$
1200	1.10
3770	1.10
10200	1.04
28000	1.05
68000	1.05
195000	1.05
490000	1.06
1080000	1.06
1750000	1.06
2750000	1.06

3.1.4. Other materials.

Methanol (analytical grade) was obtained from Fisons (UK). p-Toluene sulphonic acid, obtained from Fisons (UK) was a laboratory grade agent. Water was freshly distilled from an all glass apparatus.

3.2. Chromatographic equipment.

Figure 3.1 is a schematic diagram of the chromatographic equipment used for the determination of polymer molecular weight distribution.

3.2.1. Column and precolumn.

The SEC column packing consisted of 5 μm beads of a cross-linked styrene/divinyl benzene copolymer with mixed pore volumes (PL gel 5 μm MIXED), 0.3 x 30cm, from Polymer Laboratories Ltd (UK). A precolumn was used to guard the main column from impurities. This was a 10cm column of mixed PL gel 5 μm also obtained from Polymer Laboratories Ltd (UK).

3.2.2. Pumping system.

A single head reciprocating pump fitted with a pulse dampener was used. (Gilson model 303 fitted with a 10S pump head; obtained from Anachem Ltd (UK)).

3.2.3. Valve.

A Rheodyne syringe - loading injector valve (model 7125) fitted with a 20 μl injection loop was used throughout. Both valve and loop were obtained form Anachem Ltd. (UK).

3.2.4. Detector and Detector cell.

Polymers were detected by way of a Perkin Elmer Infrared spectrophotometer (model 782). A sodium chloride cell with 1.0mm path length was converted for use as a flow - cell and fitted to the

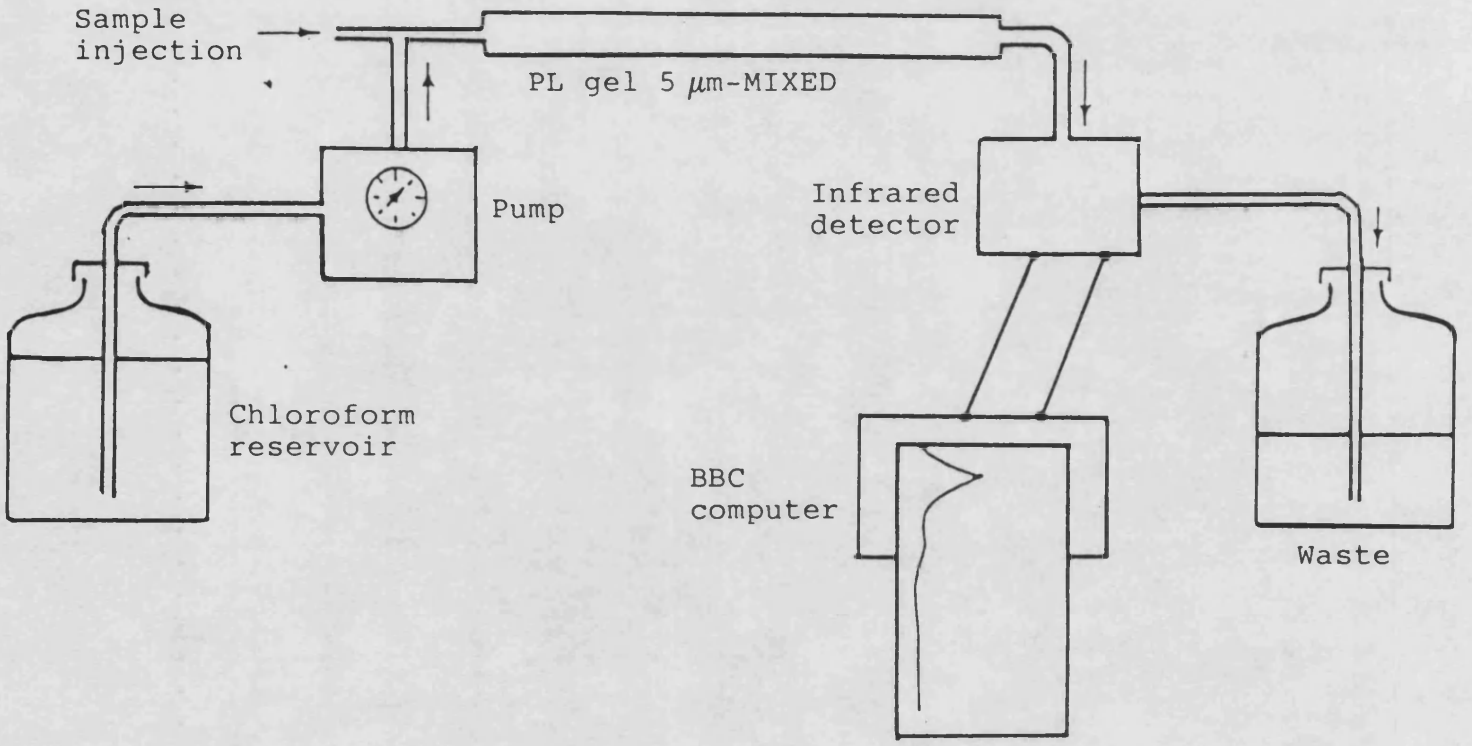

Figure 3.1:- Schematic diagram of size exclusion chromatography.

spectrophotometer.

3.2.5. Computer.

A BBC model B microcomputer was connected to the infrared spectrophotometer via a 15 pin D connector obtained from RS Ltd (UK). The internal analogue - to - digital converter provided with the BBC computer was used to digitise the 1 V analogue output from the spectrophotometer. Programs were written in BBC BASIC to

- sample the output from the infrared spectrophotometer and
- normalise the chromatogram and calculate the molecular weight distribution of a polymer.

3.3. Viscometric Equipment.

3.3.1. Constant temperature viscometer bath.

A constant temperature viscometer bath obtained from Laboratory Thermal Equipment Ltd (UK) was used at 25 ± 0.1°C.

3.3.2. Viscometer.

A suspended level dilution viscometer (type BS/IP/SL, size 2) was used throughout. This was obtained from Poulten Selfe Lee (PSL) Ltd (UK).

3.4. Methods.

3.4.1. The degradation of PHB to obtain samples of different molecular weight distributions.

The degradation of PHB was performed according to the method of Araki and Hayase (1979). These authors degraded poly-β-esters by using either of two catalysts:- p-toluene sulphonic acid (pTSA) or imidazole. Catalysts and polymers were usually dissolved in a mixture of

chloroform and methanol. In this study, 12.5 g of PHB was refluxed in a 500ml of a mixture of chloroform and methanol (2:3 by volume) for about 15 minutes. The dissolved PHB was cooled to room temperature and the required amount of catalyst (pTSA) was then added to the polymer solution. PHB was refluxed for an appropriate time with a variety of concentrations of catalyst to obtain ten batches of degraded polymer. The conditions of degradation are summarised in Table 3.2.

After refluxing for the appropriate time, the dissolved PHB was precipitated by pouring the solution into a mixture of methanol: distilled water (4:1 by volume), in which the pTSA was soluble. The degraded sample was then collected by filtering the sample through a Whatman No. 52 filter paper. The filtrate was washed with excess methanol to dissolve any traces of pTSA left on the surface of the filtrate. The degraded samples were then dried under vacuum at 40°C for 24 hours.

3.4.2. Viscosity measurement.

Prior to viscosity measurement, all glassware used was soaked overnight in chromic acid. The glassware was then rinsed with plenty of freshly obtained distilled water. Viscometers were then rinsed with acetone and dried using a filtered compressed air line. Viscometers, stock solutions of the degraded PHB samples and filtered chloroform were equilibrated in a water bath at 25°C.

Subsequently 15 mls of chloroform was pipetted into the viscometer through its wide-mouthed tube. The pipette was allowed to drain for 2 minutes and was removed from the viscometer with care to avoid contact with the sides of the viscometer. The flow time for passage of chloroform between the two marks on the viscometer was measured until three consecutive results within 0.2% were obtained. The mean of these three flow times was used in subsequent calculations.

Table 3.2 : Duration of reflux and concentration of pTSA used to obtain ten degraded samples of PHB

Sample code as used in Chapter 4	Duration of reflux with pTSA (minutes)	Concentration of pTSA (% w/v)
1	15	0.03
2	15	0.10
3	23	0.10
4	30	0.50
5	60	0.09
6	240	0.01
9	30	0.10
10	15	0.09
11	30	0.22
12	15	0.05

5mls of the stock solution of PHB was added and the solution mixed by blowing carefully down the side arm. After appropriate mixing, the flow time for the PHB solution was determined. Chloroform was then added successively to dilute the PHB solution in the viscometer, the flow times being determined for 6 to 7 different concentrations of the PHB.

Intrinsic viscosity was determined by linear regression of the Huggins plot. The viscometric experiment was replicated for each degraded sample of PHB and a statistical t-test (Bartlett test) was performed on the values of intrinsic viscosity to validate the data. When no significant difference was evident, a mean value of intrinsic viscosity was taken to be the representative of each particular sample of PHB.

3.4.3. Infrared analysis of PHB, polystyrene and chloroform.

A high molecular weight sample of PHB was dissolved in chloroform and poured onto a clean glass plate to form a thin film. The film was removed and then analysed using a scanning infrared spectrophotometer. Spectra for polystyrene and chloroform were obtained from the literature (Sadtler Research Laboratories,1962).

The three spectra were compared to allow selection of suitable wavenumbers for the analysis of PHB and polystyrene in chloroform. Both polystyrene and chloroform absorbed strongly at 2930 cm^{-1} , the C-H stretching region. Although polystyrene also absorbed at 1500 cm^{-1}, it was felt that 2930cm^{-1} was the preferred wavenumber for detection because the absorption coefficient ($E^{1\%}$ in 0.2mm cell) was much greater at 2930 cm^{-1} ($E^{1\%}$ = 0.60) than at 1500cm^{-1} ($E^{1\%}$ = 0.55).

Figure 3.2 shows the infrared spectrum of polystyrene dissolved in chloroform at a concentration of 1% w/v. The infrared spectrum of poly (β-hydroxybutyrate) (PHB) as a thin film is shown in Figure 3.3. The wavenumber chosen for detection of PHB was 1760cm^{-1} . This corresponded to absorption due to stretching of the carbonyl bond.

3.4.3.1. Beer-Lambert plots for polystyrene in chloroform

Figures 3.4 and 3.5 show the Beer Lambert plots at 2930cm^{-1} of the lowest molecular weight polystyrene (M_p = 1200) and the highest molecular weight polystyrene (M_p = 2750000) respectively. The plots were linear up to polymer concentrations of at least 1 %w/v and the slopes of both curves were identical.

These data validated the use of the infrared detector for molecular weight analysis of polystyrene in accordance with the criteria suggested by Pokorny (1984). According to the latter author, the response of the detector should be proportional to the concentration of the eluting polymer. In other words, there should be a linear dependence of the response on concentration. The second requirement is that the response should be independent of molecular weight. Both criteria were satisfied for polystyrene in chloroform at 2930cm^{-1}.

3.4.3.2. Beer-Lambert plots for PHB in chloroform.

Figure 3.6 and 3.7 show the Beer Lambert plots of the lowest molecular weight of PHB and the highest molecular weight of PHB respectively. Again both plots were linear with identical slopes. For PHB, the concentration required to produce an absorbance of 0.5 units was approximately 0.1% w/v.

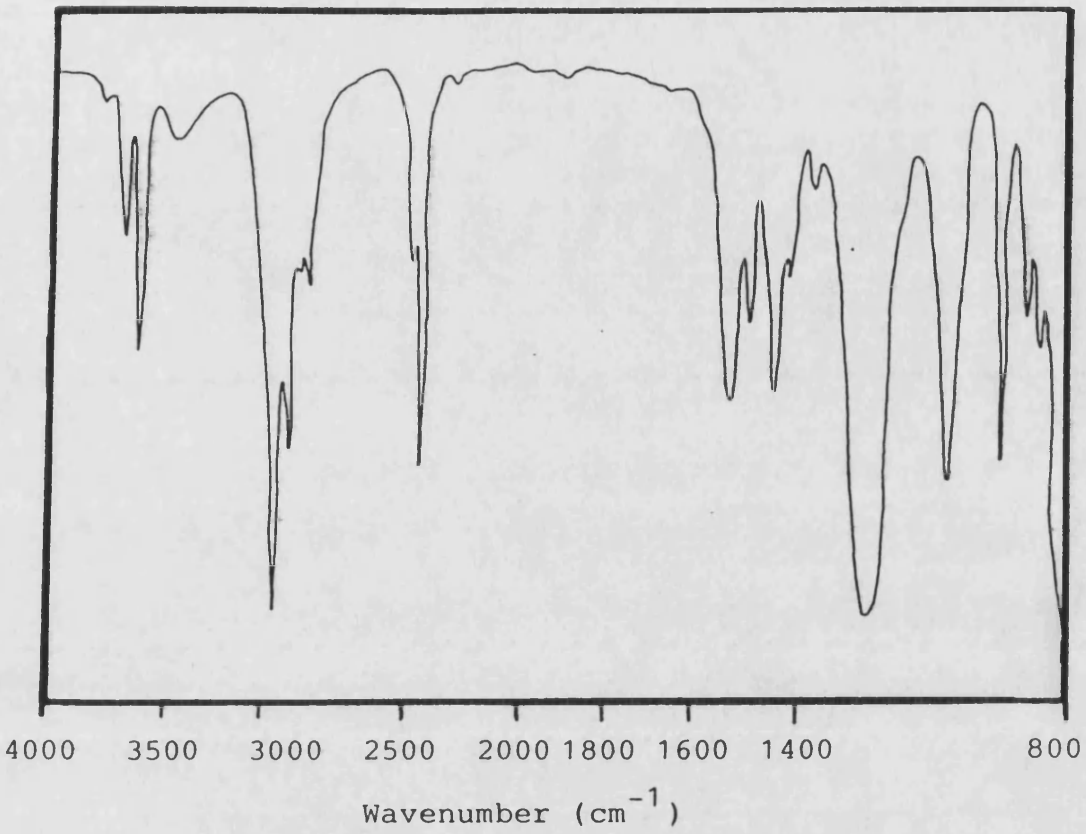

Figure 3.2:- Infrared spectrum of polystyrene dissolved in chloroform (1% $w/_v$)

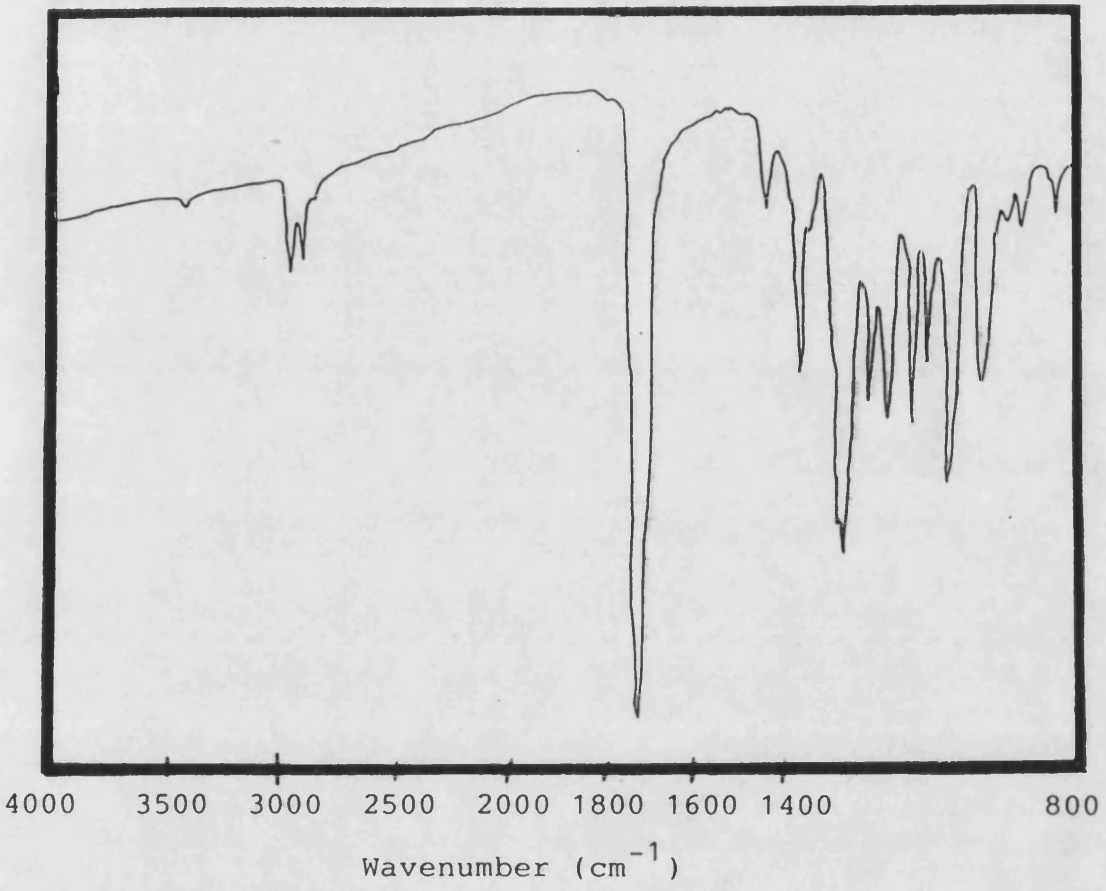

Figure 3.3:- Infrared spectrum of poly (β-hydroxybutyrate) as a thin film.

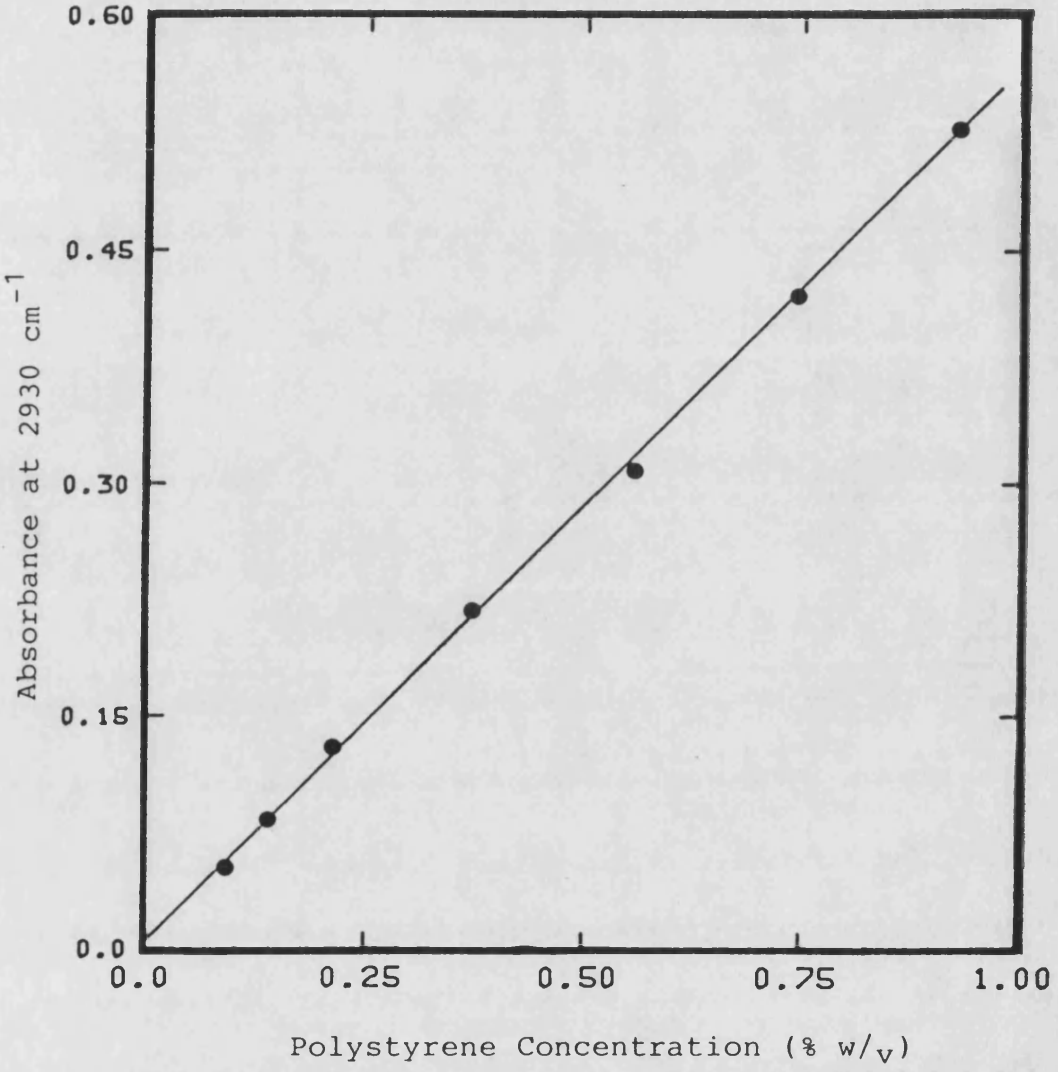

Figure 3.4:- Beer Lambert plot for the lowest molecular weight polystyrene in chloroform (Mp = 1200)

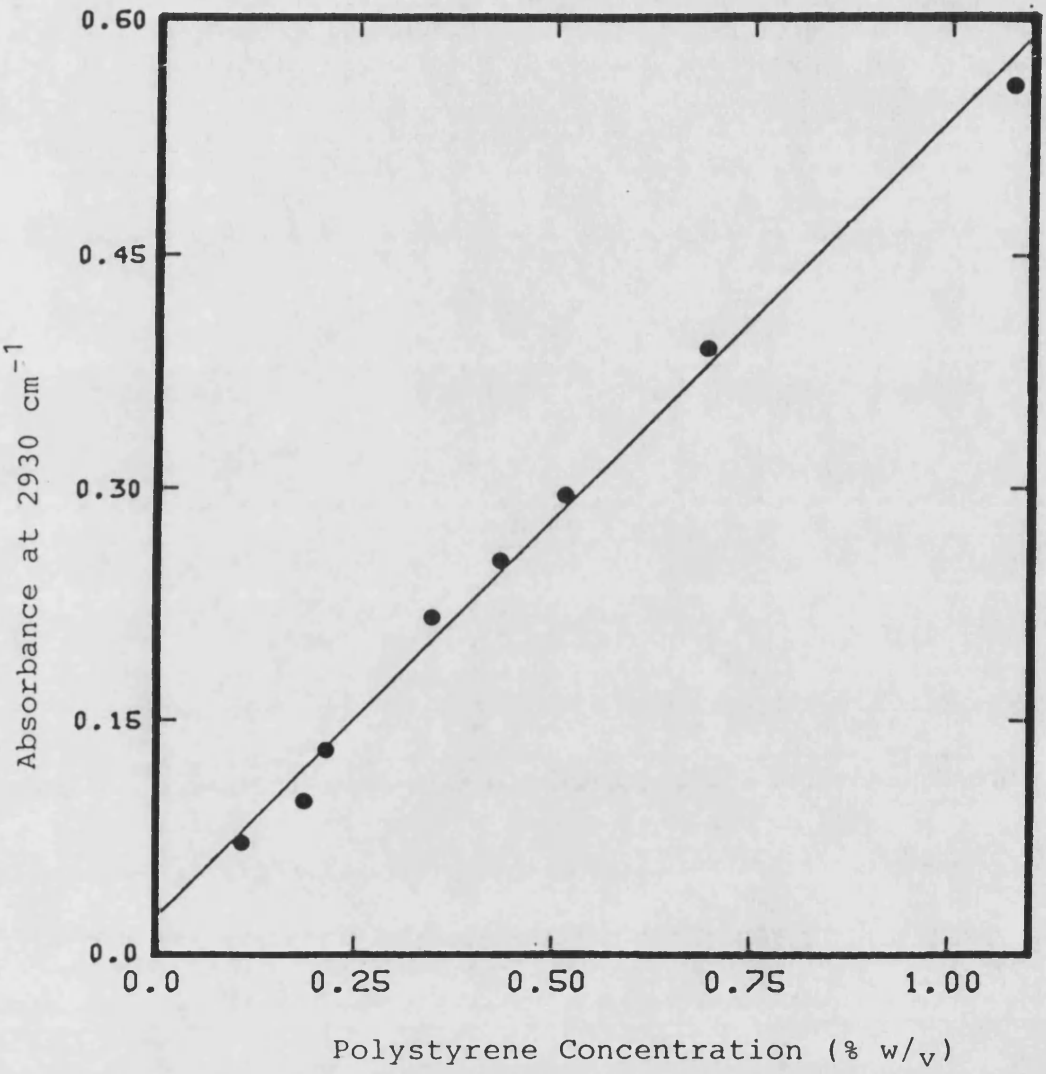

Figure 3.5:- Beer Lambert plot for the highest molecular weight polystyrene in chloroform (Mp = 2750000)

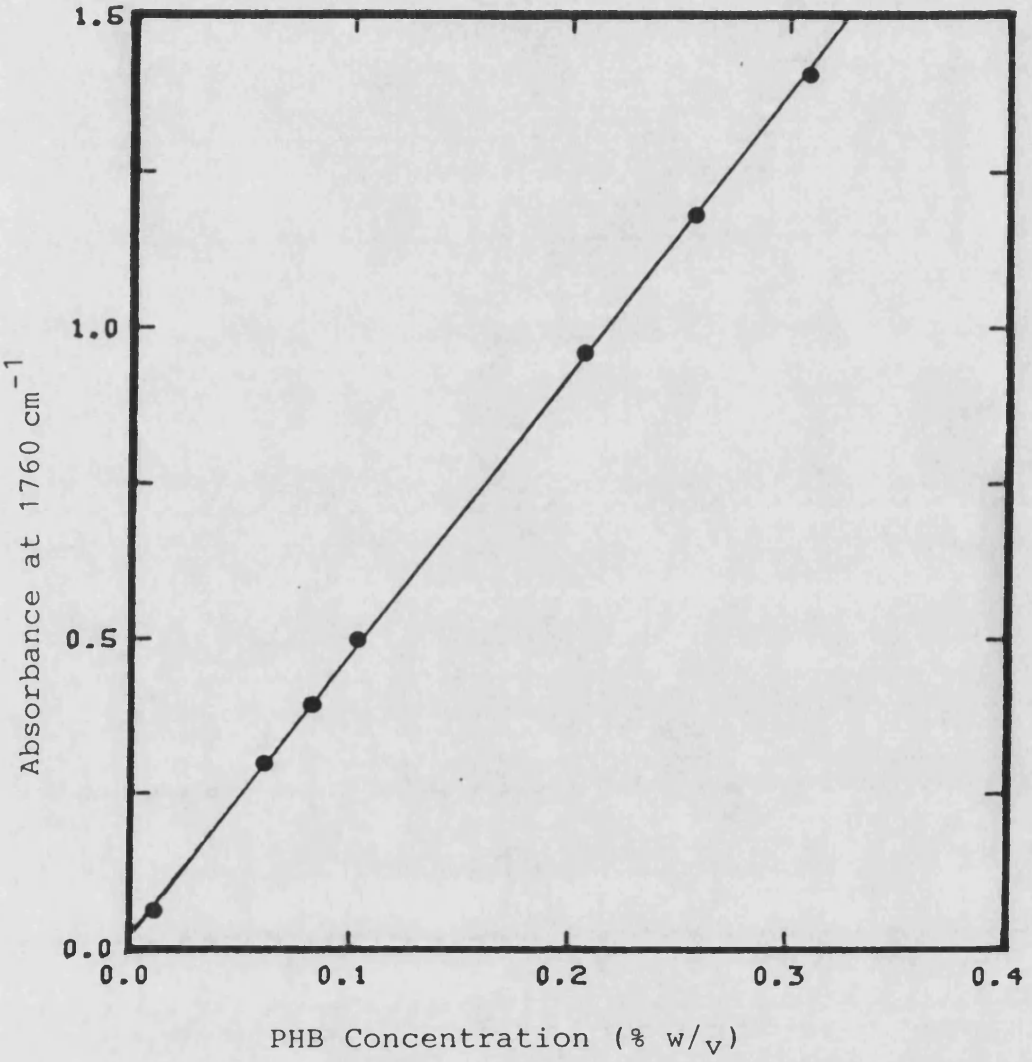

Figure 3.6:- Beer Lambert plot for the lowest molecular weight PHB in chloroform (Mw =19000)

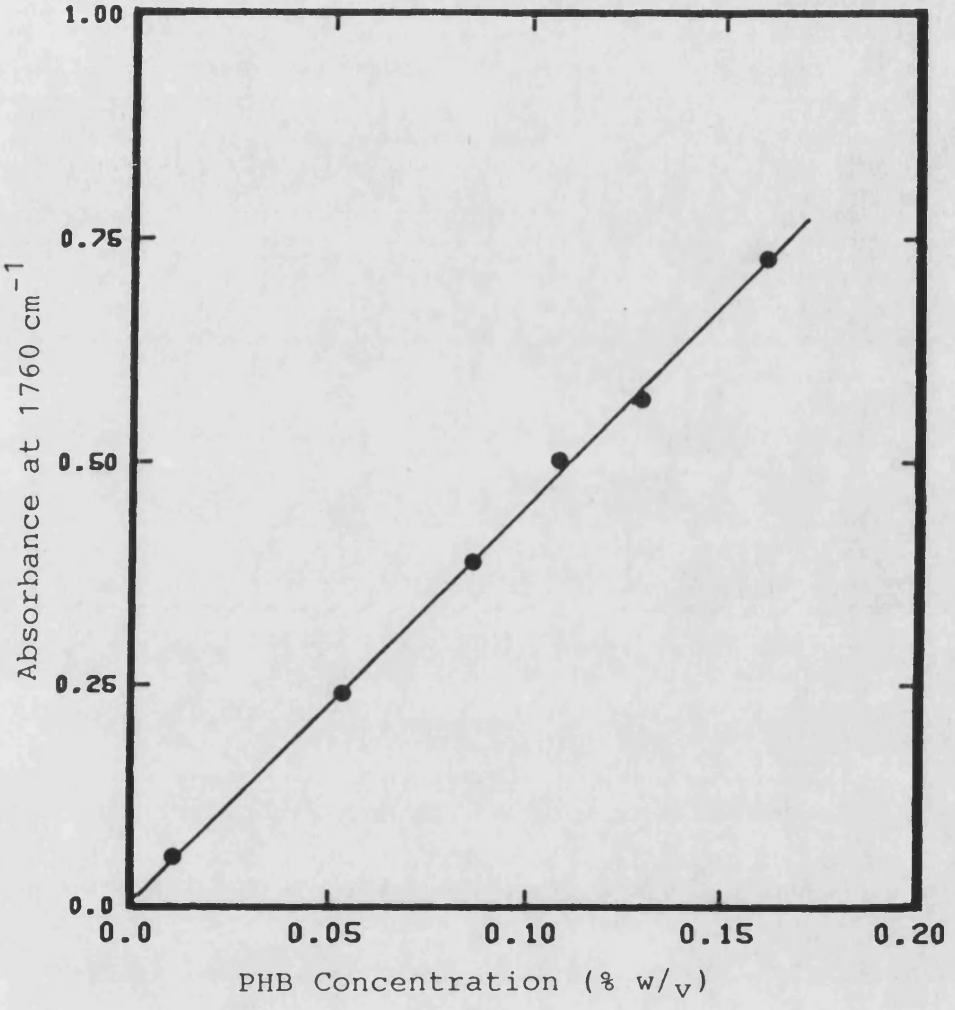

Figure 3.7:- Beer Lambert plot for the highest molecular weight PHB in chloroform (Mw = 868000)

3.4.4. Size Exclusion Chromatography (SEC)

The absorbance of the two polymers as determined by the Beer-Lambert plots were considered and standard concentrations were chosen for molecular weight analysis. All SEC experiments were performed at concentration of 1% w/v for polystyrene and 0.1% w/v for PHB. The conditions used for all SEC experiments were as follows. Injected sample volume was 20μl; temperature was controlled at 25 ± 0.5°C by placing the solvent reservoir in a water bath; the flow rate of the mobile phase was 0.74 ml/min.

Chapter 4

ASSAY OF POLYMER MOLECULAR WEIGHT DISTRIBUTION : RESULTS AND DISCUSSION

4.1 Viscometry.

In any viscosity determination, the general principle involves measuring the time for a reproducible volume of the liquid to flow through the capillary of a viscometer under an accurately reproducible head and at a closely controlled temperature.

In this study, the flow times have been determined for various molecular weight fractions of PHB at a variety of concentrations of polymer. The raw data is tabulated in Appendix 1.

From these values of flow times the value of intrinsic viscosity, [η], was determined in duplicate for each polymer sample using the Huggins' equation shown below:-

$$\frac{\eta_{sp}}{c} = [\eta] + k'[\eta]^2 c \quad \ldots\ldots \quad (4.1)$$

where

c is the concentration of the polymer solution in g/dl

k' is the Huggins' constant.

An example of Huggins plot is shown in Figure 4.1. This plot represents a sample of PHB having a weight-average molecular weight of 868K . Reproducibility of the values of intrinsic viscosity was analysed using a student's t-test. It was found that there were no significant differences (at the 95% level of significance) between the replicates reported in Table 4.1.

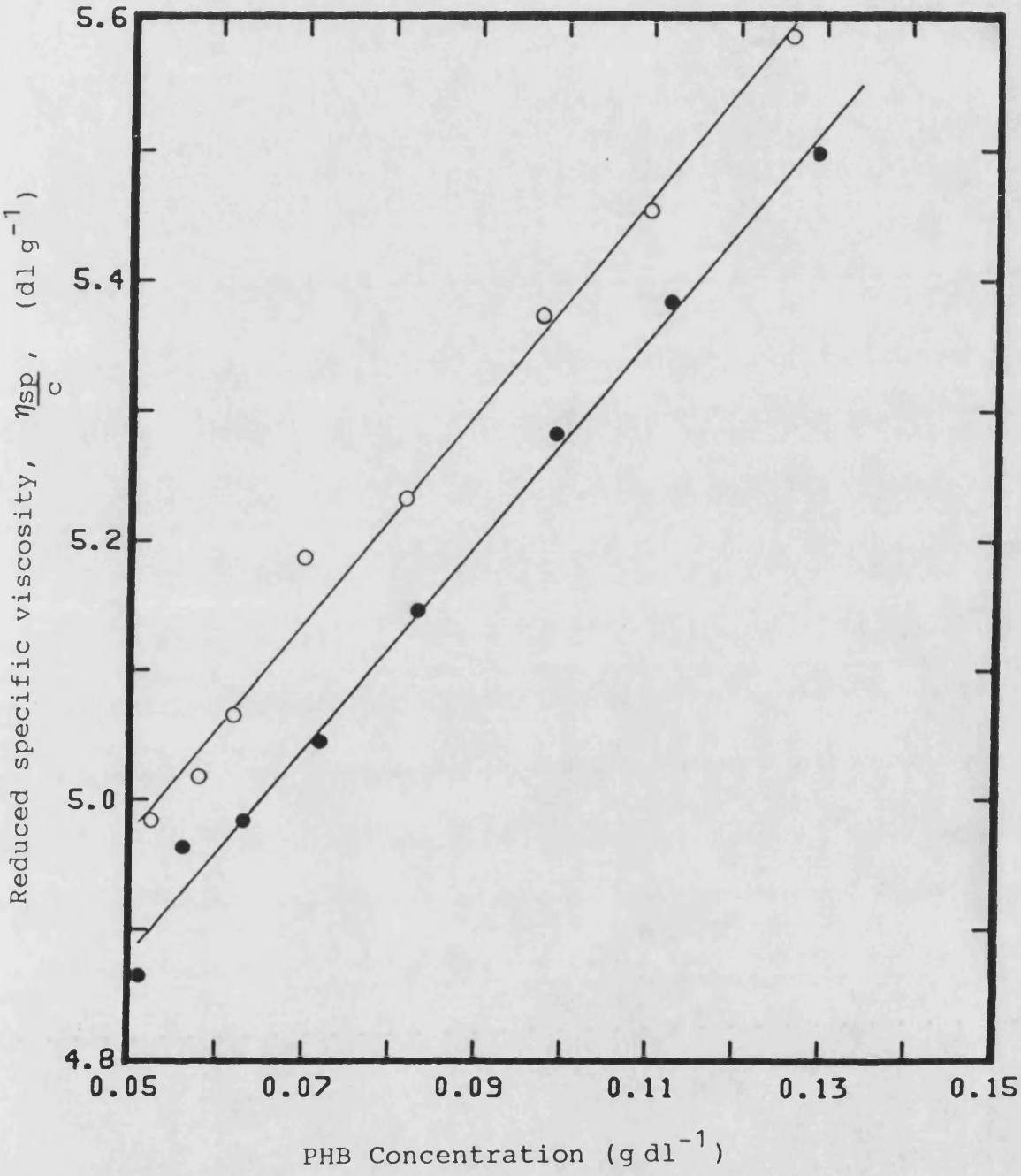

Figure 4.1:- Replicate Huggins plots for the PHB sample with the highest molecular weight (sample 7)

Table 4.1 : Intrinsic viscosities ± percent standard deviation for different molecular weight fractions of PHB (dl/d)

Sample code (see Chapter 3)	Intrinsic viscosity $[\eta]$, $\frac{dl}{g}$		Average intrinsic viscosity $[\eta]$, $\frac{dl}{g}$
	1	2	
1	0.396 (± 0.5)	0.399 (± 0.2)	0.398
2	2.357 (± 0.7)	2.339 (± 0.3)	2.348
3	0.786 (± 0.3)	0.789 (± 0.3)	0.788
4	1.243 (± 0.3)	1.246 (± 0.6)	1.245
5	3.835 (± 0.8)	3.896 (± 0.4)	3.866
6	1.836 (± 0.5)	1.828 (± 0.4)	1.832
7*	4.485 (± 0.5)	4.566 (± 0.6)	4.526
8#	0.239 (± 0.4)	0.240 (± 0.4)	0.240

* - represent the highest molecular weight PHB as received. # - represent the lowest molecular weight PHB as received.

The mean of the replicate intrinsic viscosity values was taken to represent a given molecular weight. The Huggins' constant, k' , gives an indication of the shape of the polymeric solute at a given temperature in a given solvent. Huggins (1942) has shown that the value of k' is constant for a given polymer in the same solvent at a given temperature; ie. it is independent of the length of the polymer chain or the molecular weight. The value of k' is usually in the range of $0.3 < k' < 0.4$ for a random coil. Solid spherical particles would have k' = 2.0 whereas, a rod like shape would give k' = 0.8.

Table 4.2 shows the values of k' from two determination for each PHB fraction. The value of k' varied from 0.2 to 0.4. This was thought to be due to the wide polydispersities of fractions studied. In this study the polydispersity indexes (M_w/M_n) of PHB samples were within the range 2.7 to 4.8. With such wide polydispersities, sampling problems may have accounted for the variation in the values of the Huggins' constants, which are highly dependent on the precision of the determination of intrinsic viscosity. The mean value of k' for all samples was 0.31 ± 0.05. This implies that in dilute solution in chloroform PHB has a random coil configuration. This is in agreement with the work of Akita *et al.* (1976) who studied PHB in chloroform at 30°C. However, Marchessault *et al.* (1970) reported that PHB exists as a rigid rod in chloroform at 30°C. Their conclusion was based on a study of optical rotary dispersion.

Table 4.3 shows intrinsic viscosities of four other fractions of PHB. This table shows the data for PHB fractions which failed the statistical t-test for the replication of the two determinations of intrinsic viscosity i.e. the replicates were significantly different (at 95% level). The raw data for fractions 9-12 are tabulated in Appendix 2.

Table 4.2 : Values of k' for PHB fractions

Sample code	Values of k'	
	1st determination	2nd determination
1	0.33	0.32
2	0.27	0.28
3	0.33	0.27
4	0.20	0.30
5	0.29	0.35
6	0.29	0.31
7	0.40	0.39
8	0.32	0.32

The Huggins plot for each determination were linear ; an example pair is shown in Figure 4.2. There was a statistical difference in the slope of the two determinations, hence in Figure 4.2 it can be seen that the two curves were antiparallel. The data suggest that it was not possible to replicate the stock solutions for these fractions either due to sampling problems or difficulties in dissolving high molecular weight molecules. In view of this sampling problem, only the first group of PHB fractions (Table 4.1) were used for determination of Mark-Houwink constants.

Since the molecular weight of each PHB fraction was unknown, size exclusion chromatography (SEC) was used to estimate their molecular weight in accordance with the methods described in Chapter Two. Molecular weight was routinely determined using the universal calibration method, that is with reference to a standard material, in this case, polystyrene. The universal calibration method requires knowledge of the Mark-Houwink constants for the reference material. Therefore the intrinsic viscosities of various polystyrene standards were determined.

Figure 4.3 shows the replicate Huggins plots for determination of the intrinsic viscosity of a polystyrene sample of molecular weight, M_p = 68000. A t-test was performed to compare the two values of intrinsic viscosities for each sample and there were no significant differences between them. Table 4.4 shows the replicate intrinsic viscosities for each polystyrene sample. A mean value was taken to represent a given molecular weight. Table 4.5 shows the values of the Huggins' constant, k' , for each polystyrene fraction. The values of k' were not very reproducible even though the values of intrinsic viscosity were within 0.5% of each other suggesting that variation in k' is normal. The k' values for PHB (Table 4.2) were no more variable than the mean

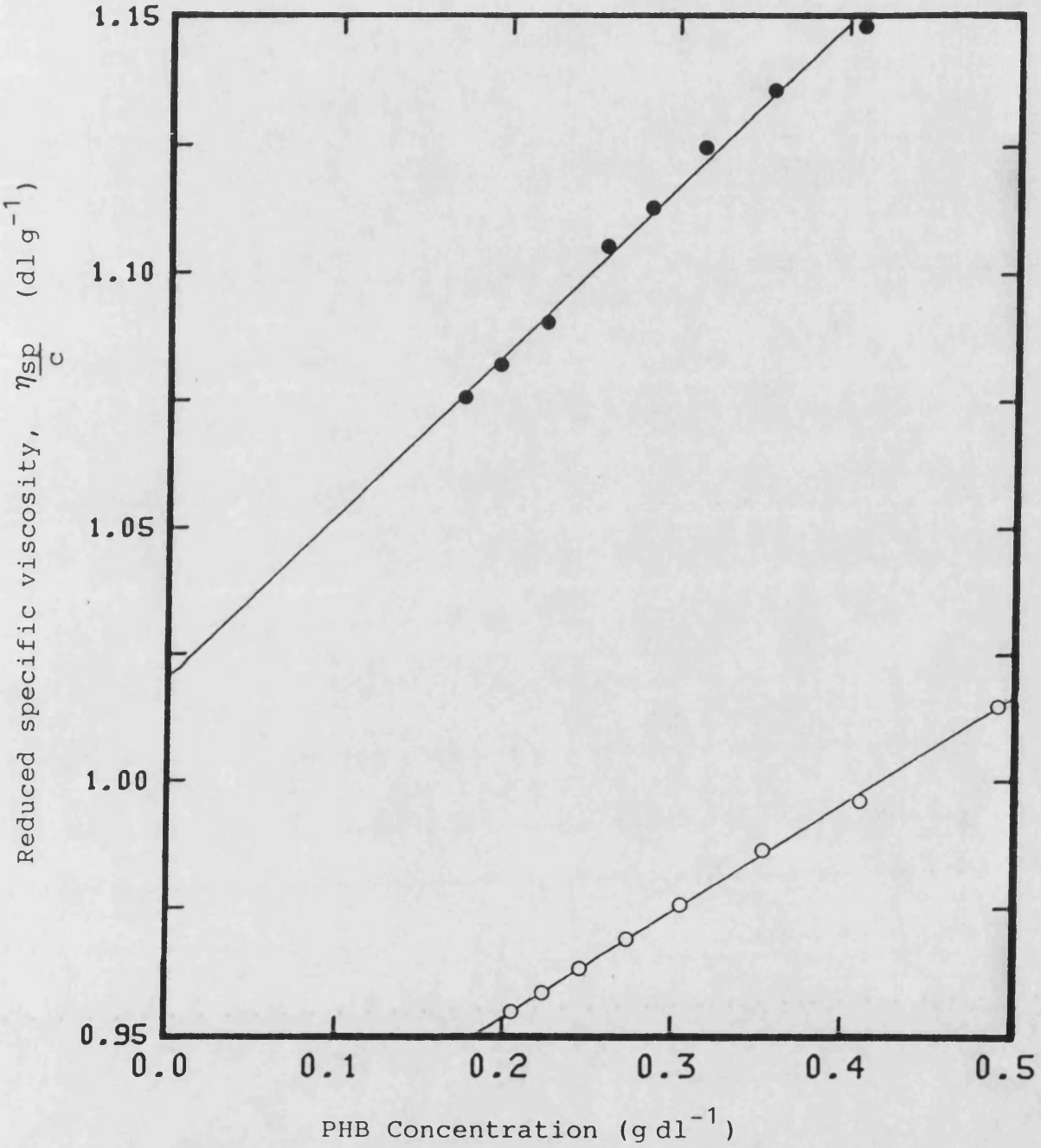

Figure 4.2:- Replicate Huggins plots for a degraded sample of PHB (sample 9). This pair of replicates were significantly different (see text).

Table 4.3 : Intrinsic viscosities (± percent standard deviation) for which replicates were significantly different.

Sample code (see Chapter 3)	Intrinsic viscosity $[\eta]$, $\frac{dl}{g}$		Average intrinsic viscosity $[\eta]$, $\frac{dl}{g}$
	1	2	
9	0.912 (± 0.1)	1.021 (± 0.3)	0.967 (± 8.0)
10	1.056 (± 0.7)	1.124 (± 0.4)	1.090 (± 4.4)
11	2.758 (± 0.2)	2.727 (± 0.2)	2.743 (± 0.8)
12	2.338 (± 0.3)	2.442 (± 0.2)	2.390 (± 3.1)

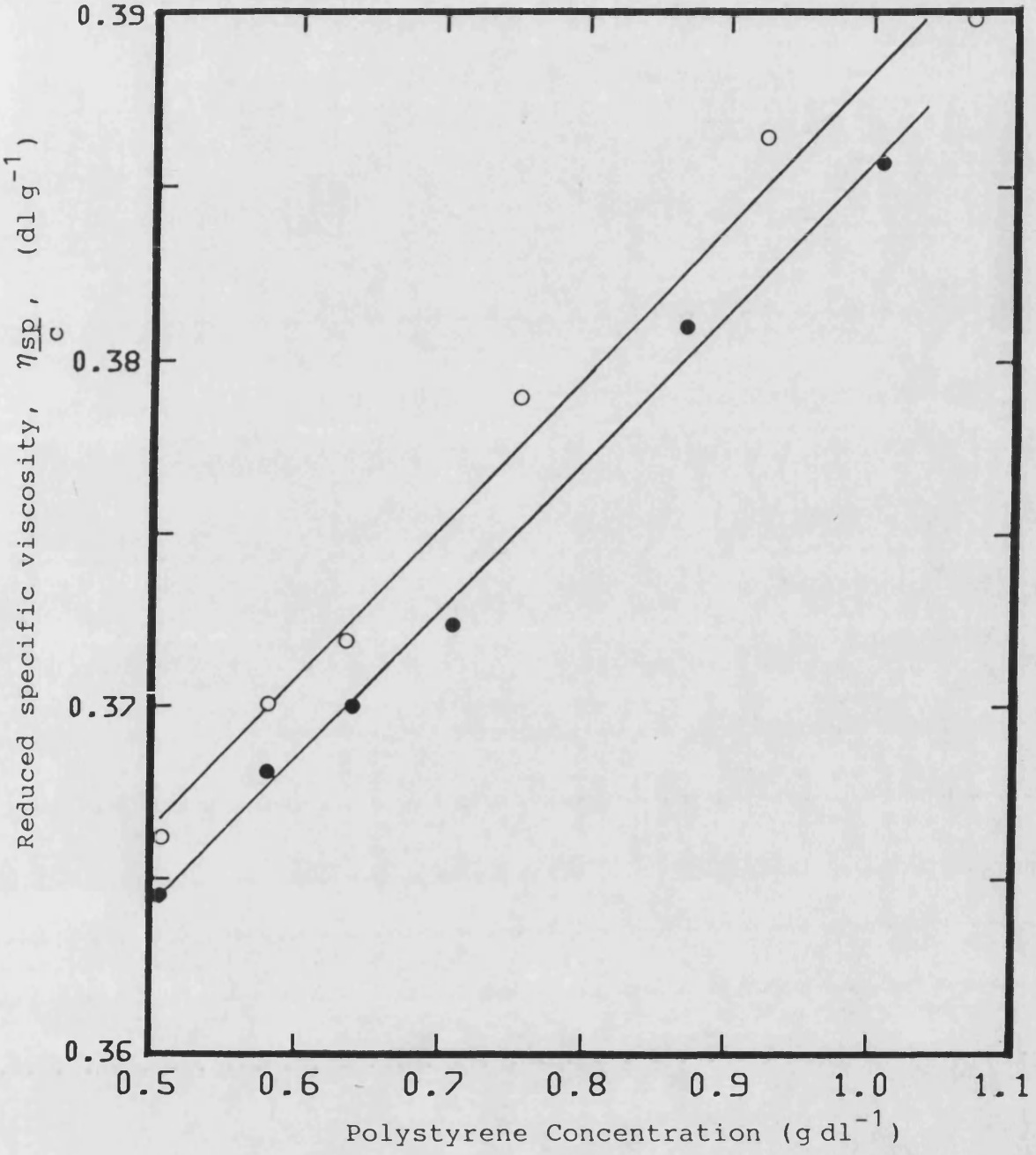

Figure 4.3:- Replicate Huggins plots for a polystyrene sample of molecular weight Mp = 68,000

Table 4.4 : Intrinsic viscosities (± standard deviation) for different molecular weight of polystyrene ($\frac{dl}{g}$)

Peak molecular weight	Intrinsic viscosity $[\eta]$,($\frac{dl}{g}$)		Average intrinsic viscosity $[\eta]$, ($\frac{dl}{g}$)
	1	2	
1080000	2.580 (± 0.2)	2.574 (± 0.5)	2.577
490000	1.467 (± 0.1)	1.463 (± 0.3)	1.465
195000	0.779 (± 0.3)	0.779 (± 0.1)	0.779
68000	0.343 (± 0.3)	0.344 (± 0.4)	0.343
28000	0.185 (± 0.2)	0.180 (± 0.3)	0.183

Table 4.5 : Values of k' for different molecular weights of polystyrene

Peak molecular weight	Value of k'	
	Determination 1	Determination 2
1080000	0.21	0.26
490000	0.23	0.32
195000	0.32	0.19
68000	0.37	0.38
28000	0.32	0.40

Table 4.6 : Mark Houwink constants for polystyrene in chloroform

K $\frac{ml}{mg}$	α	Temperature (°C)	References
0.011	0.73	25	present work
0.007	0.76	25	Oth and Desreux (1954)
0.011	0.73	25	Bawn *et al.* (1950)
0.005	0.79	30	Endo and Takeda (1962)
0.026	0.73	30	Endo and Takeda (1962)

value of k' for polystyrene, was 0.31 ± 0.07 indicating that polystyrene, like PHB, exists as a random coil in chloroform.

Since the molecular weight of each polystyrene sample had been determined by the manufacturer, it was possible to plot the relationship between molecular weight and intrinsic viscosity for polystyrene. This relationship is described by the empirical Mark-Houwink equation as follows:-

$$[\eta] = K M^{\alpha} \quad ..... \quad (4.2)$$

where

K and α are constants, known as the Mark-Houwink constants

M is the molecular weight of the polymer.

Figure 4.4 shows a plot of log [η] against log M for polystyrene. The value of α was obtained from the slope of this plot and the value of K was obtained from the intercept. Using least squares linear regression analysis, α was determined as 0.730 and K as 1.10×10^{-4} dl/g.

Besides its usefulness in the determination of molecular weight, the Mark-Houwink relationship also provides an assessment on the influence of solvent on the configuration of the polymer chain. Flory (1953) has shown that in the theta condition, a condition at which polymer molecules are on the verge of precipitation from the solution (that is unpertubed dimensions), the value of α is 0.5. In good solvents, polymer molecules will expand and the value of α will be greater than 0.5 up to a maximum value of 0.8. Based on this concept, it can be assumed that chloroform is a good solvent for polystyrene.

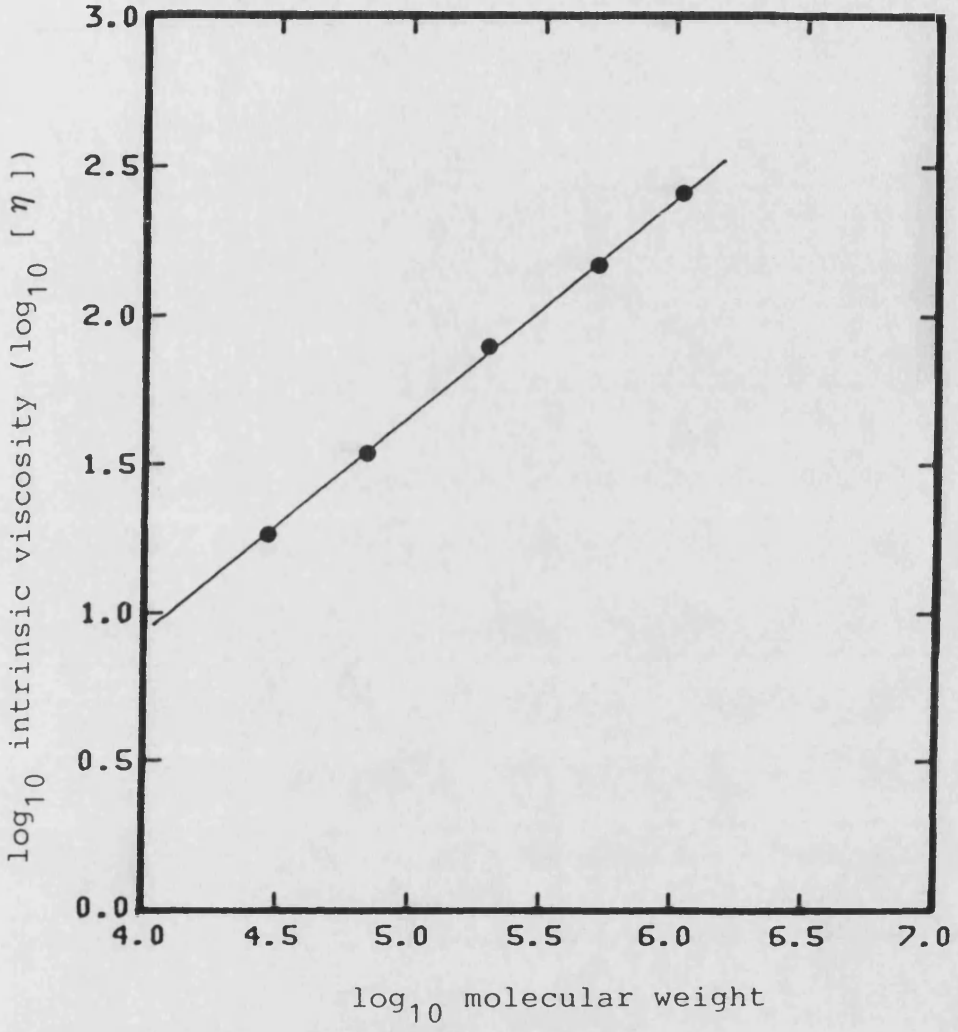

Figure 4.4:- Mark - Houwink plot of polystyrene in chloroform at 25°C.

Table 4.6. shows values of Mark-Houwink constants for polystyrene in chloroform determined at 25°C. The Mark-Houwink constants obtained in this study were in good agreement with those reported by previous authors. Table 4.6 also shows that the values of Mark-Houwink constants are dependent on temperature. Therefore when the universal SEC calibration is used, Mark-Houwink constants are required at the operating temperature for both standard and test polymers.

4.2. Size-exclusion chromatography.

The conditions used for SEC of polystyrene and PHB solutions were chosen on the basis of the infrared studies described in section 3.4.3. Using an injection volume of 20 μl, the concentrations of polystyrene and PHB used were 1% w/v and 0.1% w/v respectively.

It was considered important to use the same concentration for each molecular weight analysis. Chiantore and Guarta (1986) highlighted the importance of this factor by showing that sample concentration of polystyrene in tetrahydrofuran affected the molecular weight peak retention time. They found that the peak retention time of polystyrene increased with increasing concentration of the injected solution. The shift was more pronounced for polymers with higher molecular weights. This change was thought to be due to a decrease in the diversion of flexibly coiled polymers as the polymer concentration is increased.

Table 4.7. shows the retention times obtained for molecular weights standards of polystyrene. Since each polystyrene sample had a low value polydispersity index ($M_w/M_n < 1.1$), M_n, M_w and M_v were considered equivalent. Thus polymer molecular weight was represented by the chromatographic peak molecular weight. Table 4.7 represents the variation in the calibration curve of polystyrene over a period of

Table 4.7 : Calibration curves for polystyrene

Peak molecular weight	Retention times (minutes)						Average retention times ± std. deviation
	1	2	3	4	5	6	
1200	12.70	12.70	12.70	12.60	12.60	0	12.66 ± 0.05
3770	11.90	12.00	12.00	12.00	12.00	12.00	11.98 ± 0.04
10200	11.30	11.30	11.30	11.20	11.20	11.20	11.25 ± 0.05
28000	10.70	10.80	10.70	10.70	10.70	10.70	10.72 ± 0.04
68000	10.20	10.20	10.30	10.20	1030	10.10	10.22 ± 0.08
195000	9.40	9.40	9.40	9.30	9.40	0	9.38 ± 0.04
490000	9.00	9.00	9.00	9.00	9.00	9.00	9.00 ± 0
1080000	8.50	8.50	8.50	8.40	8.50	8.60	8.50 ± 0.06
1750000	8.30	8.40	8.30	8.30	8.30	8.30	8.32 ± 0.04
2750000	8.10	8.10	8.10	8.10	8.00	8.00	8.07 ± 0.05

one year. A comparison of these six calibration curves using a statistical t-test indicated no significant differences between them.

Figure 4.5 shows the average calibration curve of polystyrene obtained from six different calibration curves. There exists a good correlation with the first order of the polynomial equation, hence the curve was represented by a straight line equation for the range of molecular weights used. Since the assay was so dependable, it was possible during the later stages of the project to refer to previous calibration curves. The performance of the column was tested on a more routine basis, before each days work, by testing the retention times of four to five polystyrene standards injected simultaneously. These were always superimposed on the calibration curve.

A calibration curve for PHB was obtained using the universal calibration method. The basis for this method has been explained in Chapter Two. The method is based on the assumption that separation in SEC is controlled by the hydrodynamic size of the polymer molecule. Hence, at a given retention time, all polymer molecules will have the same hydrodynamic size, that is,

$$M[\eta]=\mu\ (\ v \text{ or } t\ ) \quad \ldots\ldots \quad (4.3)$$

where

M is the molecular weight

$[\ \eta\ ]$ is the intrinsic viscosity

μ is a universal function of the retention time, t , or elution volume ,v.

$$\log[\eta]_{PHB}=\frac{\alpha_{PHB}}{1+\alpha_{PHB}}\log\mu+\frac{1}{1+\alpha_{PHB}}\log K_{PHB} \quad \ldots\ldots \quad (4.4)$$

where

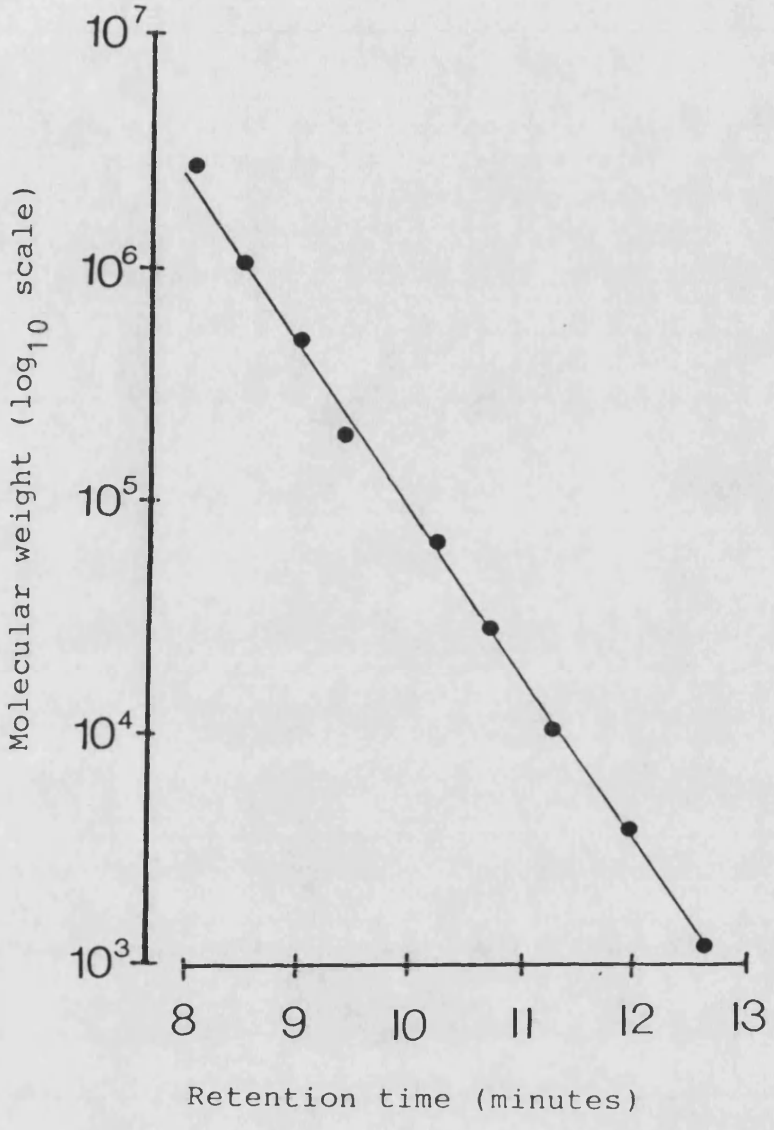

Figure 4.5:- SEC calibration curve for polystyrene.

$[\eta]_{PHB}$ is the intrinsic viscosity of PHB

α_{PHB} , K_{PHB} are the Mark-Houwink constants for PHB

μ is the universal constant given by Equation 4.3

Values of μ for the polystyrene standards were calculated using the Mark-Houwink constants determined previously. The logarithm of μ was plotted against the retention time, t, to produce a universal curve (Figure 4.6).

The unknown PHB samples were then injected onto the SEC column and their retention times were estimated using the retention time corresponding to the top of the chromatographic peak. By reference to the universal curve (Figure 4.6), values of μ were assigned to each of eight polydisperse samples of PHB (Table 4.8). The intrinsic viscosities of these samples had been determined previously (see section 4.1). This allowed calculation of initial estimates of the Mark-Houwink constants for PHB in accordance with equation 4.4. A plot of log μ against log $[\eta]$ was linear (Figure 4.7) allowing the initial estimates of the Mark-Houwink constants to be calculated by least squares linear regression analysis (α = 1.00, K = 0.1 x 10^{-4} dl/g).

Thus an initial calibration curve for PHB was obtained allowing the molecular weight distributions of the eight PHB samples to be estimated. This initial calibration curve of PHB was obtained by using equation 4.5 as shown below:-

$$\log M_{PHB} = \frac{1}{1+\alpha_{PHB}} \log \frac{K_{PS}}{K_{PHB}} + \frac{1+\alpha_{PS}}{1+\alpha_{PHB}} \log M_{PS} \quad \ldots\ldots \quad (4.5)$$

As all the parameters above were known, the calibration curve of PHB was obtained as follows :

$$\log M_{PHB} = -0.63\, t + 11.09 \quad \ldots\ldots \quad (4.6)$$

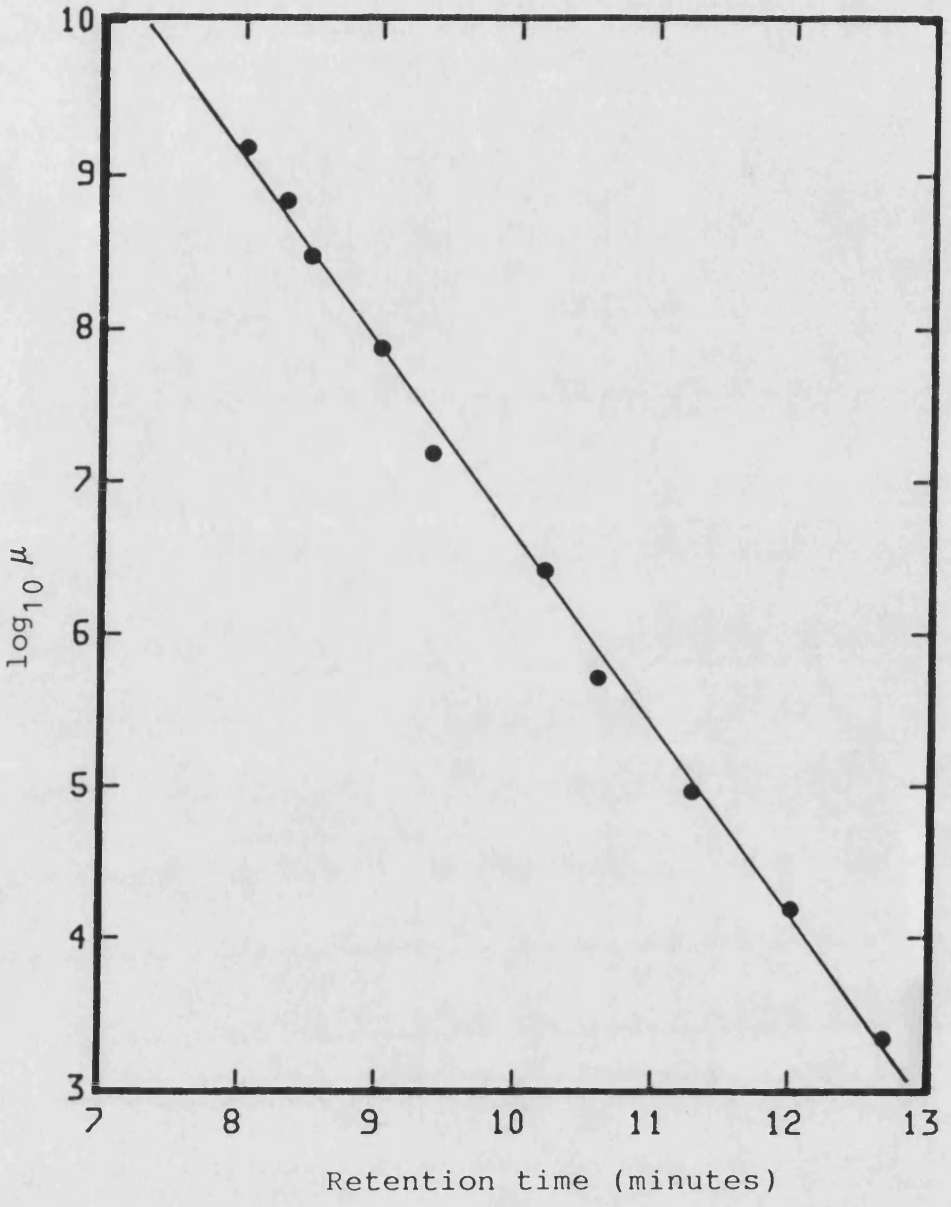

Figure 4.6:- Universal SEC calibration curve (log μ plotted against retention time)

Table 4.8 : The estimation of log μ for PHB fractions

Sample code	log μ		Mean	Standard deviation
	Determination 1	Determination 2		
1	6.24	6.11	6.17	0.09
2	7.63	7.70	7.66	0.05
3	6.79	6.92	6.85	0.09
4	7.01	7.11	7.06	0.07
5	8.00	8.10	8.05	0.07
6	7.53	7.55	7.54	0.01
7	8.39	8.43	8.41	0.03
8	5.74	5.75	5.75	0.01

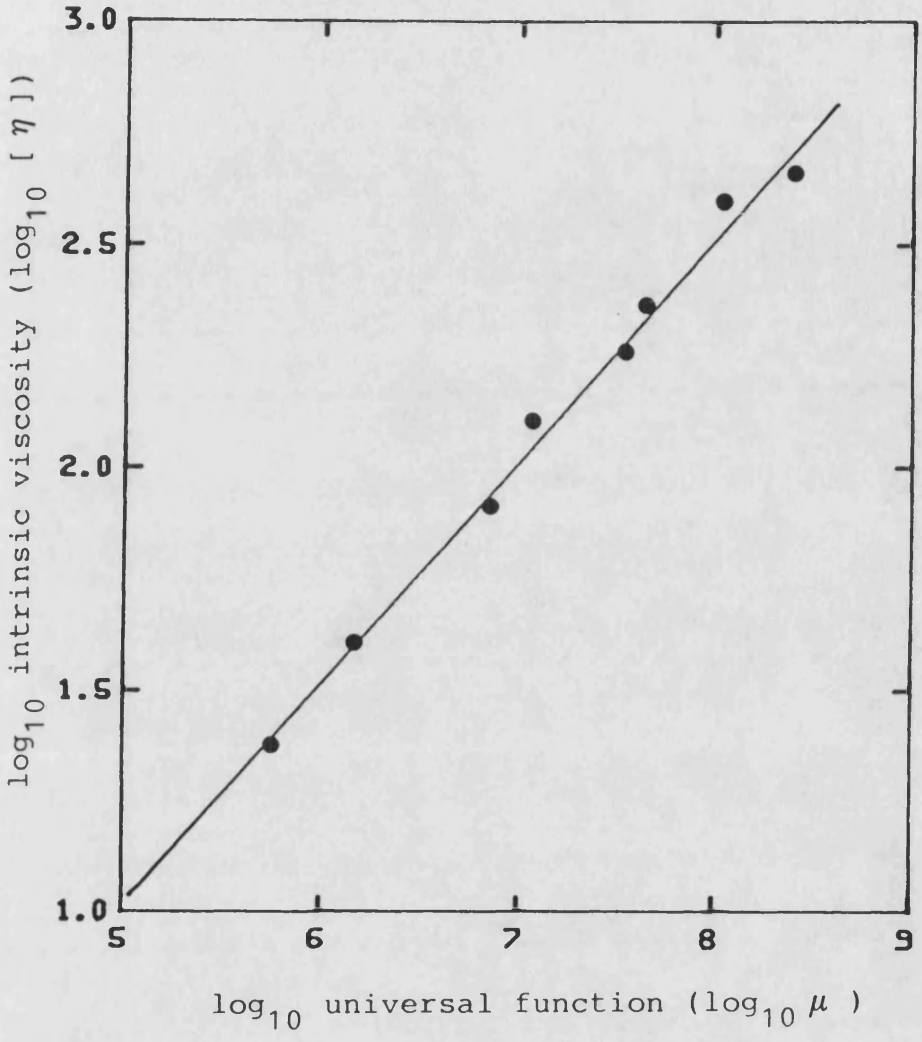

Figure 4.7:- $\log_{10}[\eta]$ against $\log_{10}\mu$ for polydisperse samples of PHB (samples 1-8)

Since the initial estimates of Mark-Houwink constants for PHB were obtained from polydisperse fractions, improvement of these values was achieved by an iteration process. The iteration process involved obtaining the viscosity-average molecular weights from PHB fractions by size exclusion chromatography and then re-calculating the Mark-Houwink constants by plotting the logarithm of viscosity-average molecular weight for each fraction against log [η]. These new values of the Mark-Houwink constants were then used to re-determine M_v by SEC, leading to another estimate of Mark-Houwink constants. This iteration was repeated until there were no significant differences between new estimates of the Mark- Houwink parameters.

Figure 4.8 shows the Mark-Houwink plot obtained after the first iteration. New values of the Mark-Houwink constants were obtained from the slope and intercept of such plots . The values of the Mark-Houwink constants after each iteration are shown in Table 4.9 . Figures 4.8 to 4.15 show the Mark-Houwink plots after iterations 1 to 8 respectively. A comparison of the values of α using a statistical t-test showed that there were no significant differences from iteration 3 onwards. Hence the average value of α was taken as the mean of the values generated by iterations 3 to 8. Figures 4.16 and 4.17, respectively, show the variation in α and K after each iteration. It can be seen that the values of α and K reached a constant level after the third iteration.

Finally, Table 4.10 compares the Mark-Houwink constants determined during the present work with those determined by other authors. There was good agreement between data obtained in the present study and that obtained by Akita *et al.* (1976) but the value of α obtained by Marchessault *et al.* (1970) was higher at 0.82. All three

Table 4.9 : Values of Mark-Houwink constants at each iteration

Iteration	α	$K\ (\frac{ml}{mg} \times 10^2)$
Initial estimate	1.00	0.1
Iteration 1	0.87 ± 0.04	0.6
Iteration 2	0.79 ± 0.03	1.1
Iteration 3	0.76 ± 0.03	1.6
Iteration 4	0.75 ± 0.02	1.6
Iteration 5	0.76 ± 0.02	1.4
Iteration 6	0.75 ± 0.02	1.9
Iteration 7	0.77 ± 0.02	1.4
Iteration 8	0.75 ± 0.02	1.6

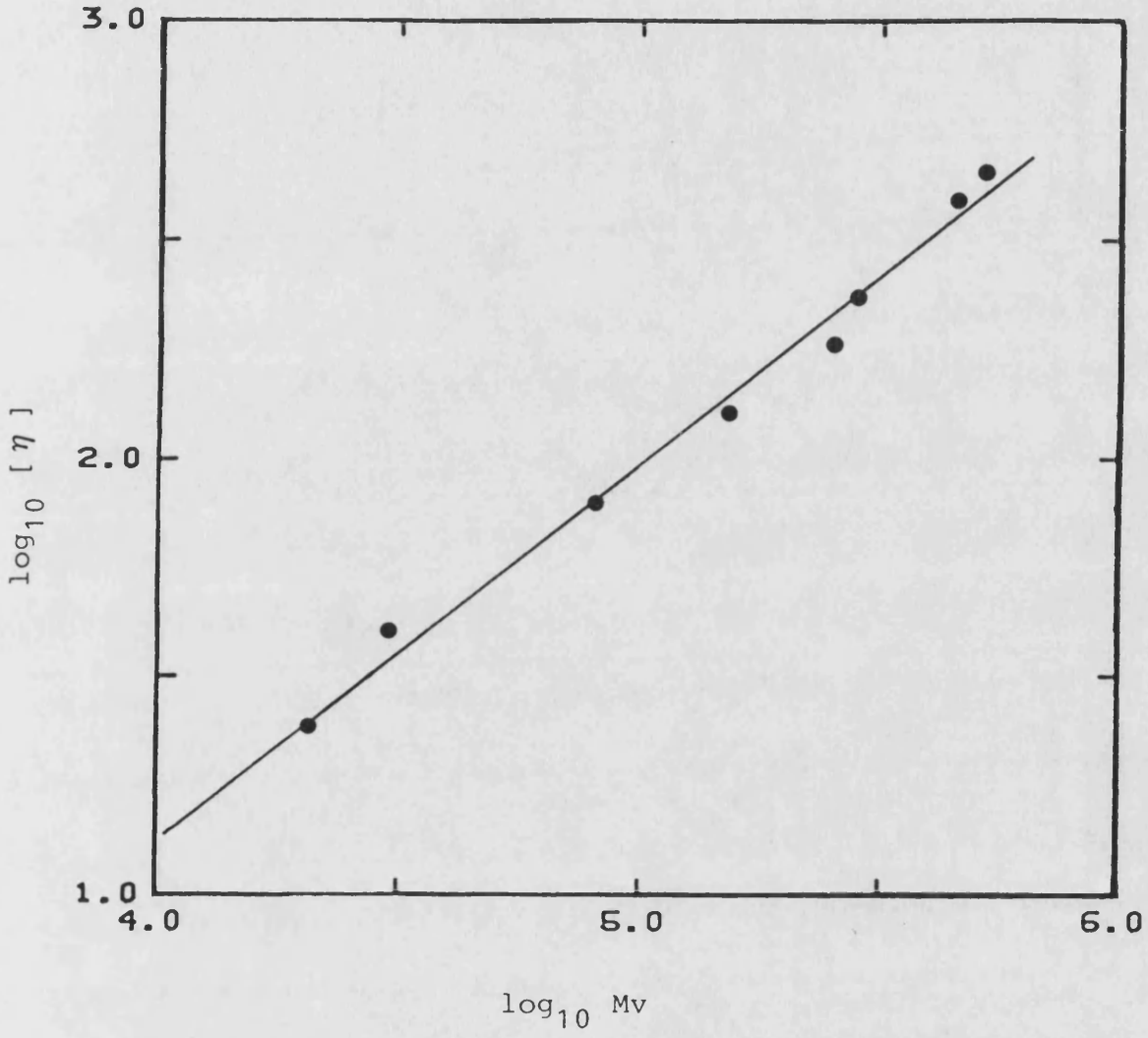

Figure 4.8:- Mark - Houwink plot of PHB after first iteration

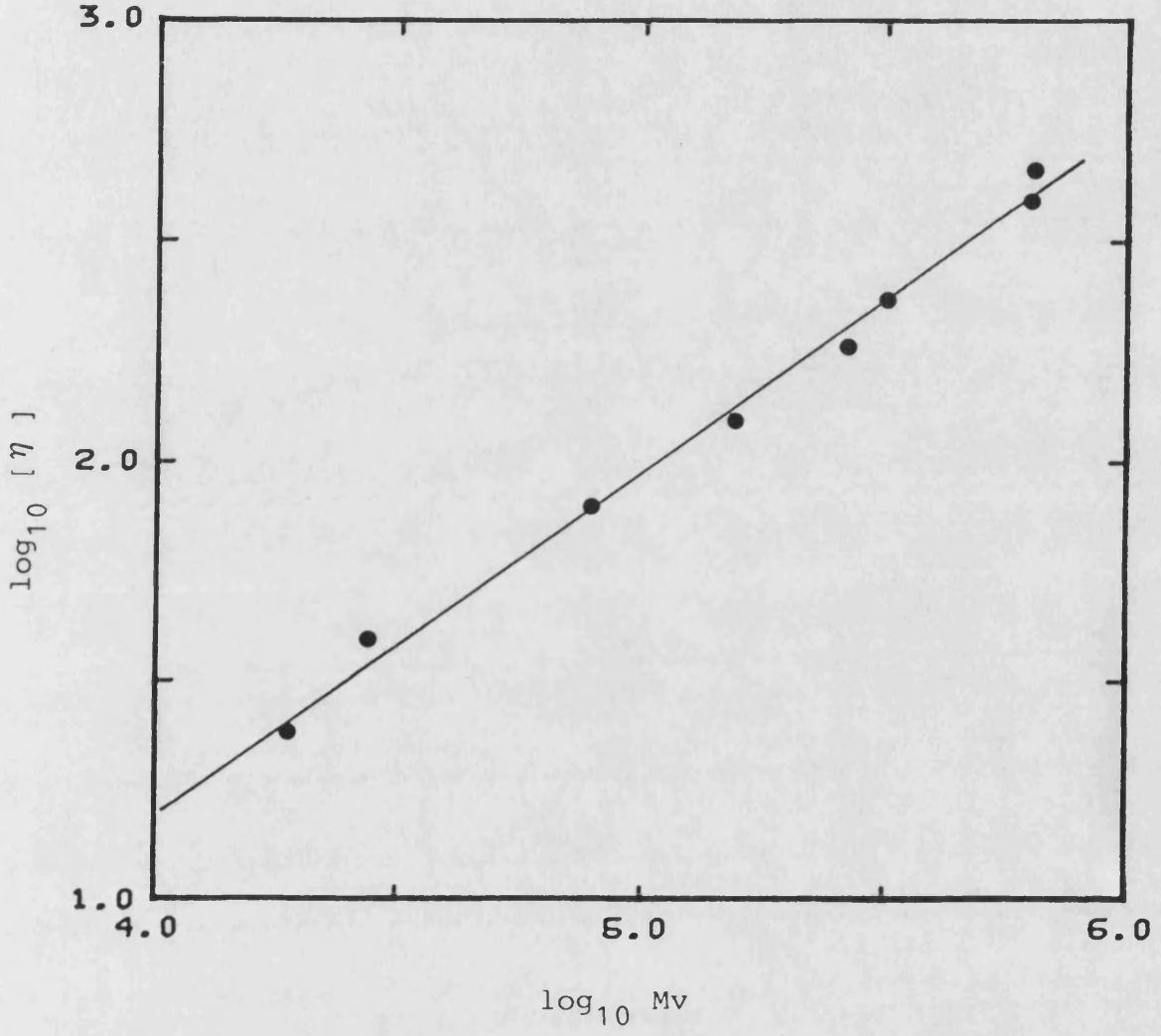

Figure 4.9:- Mark - Houwink plot of PHB after second iteration

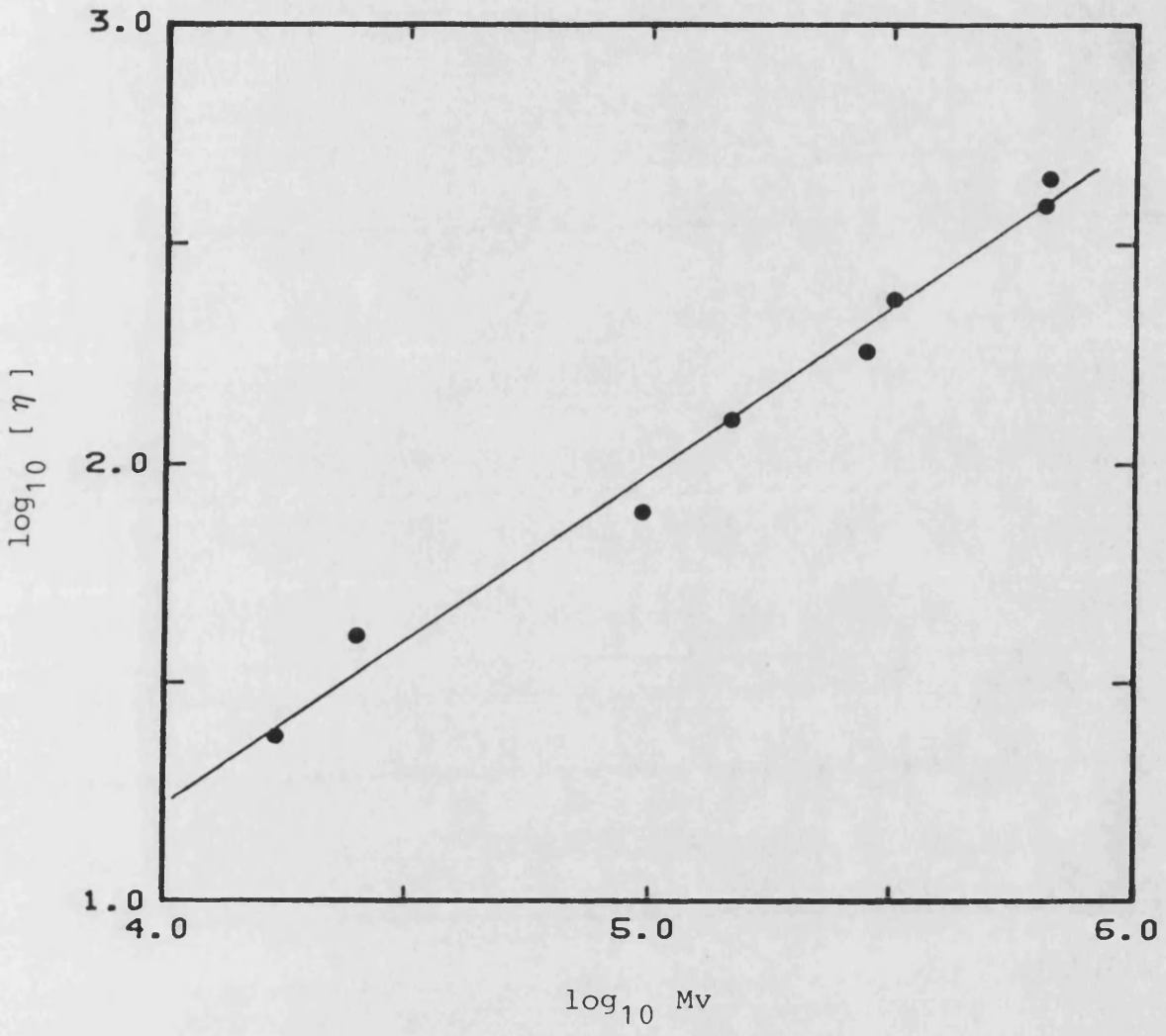

Figure 4.10:- Mark - Houwink plot of PHB after third iteration

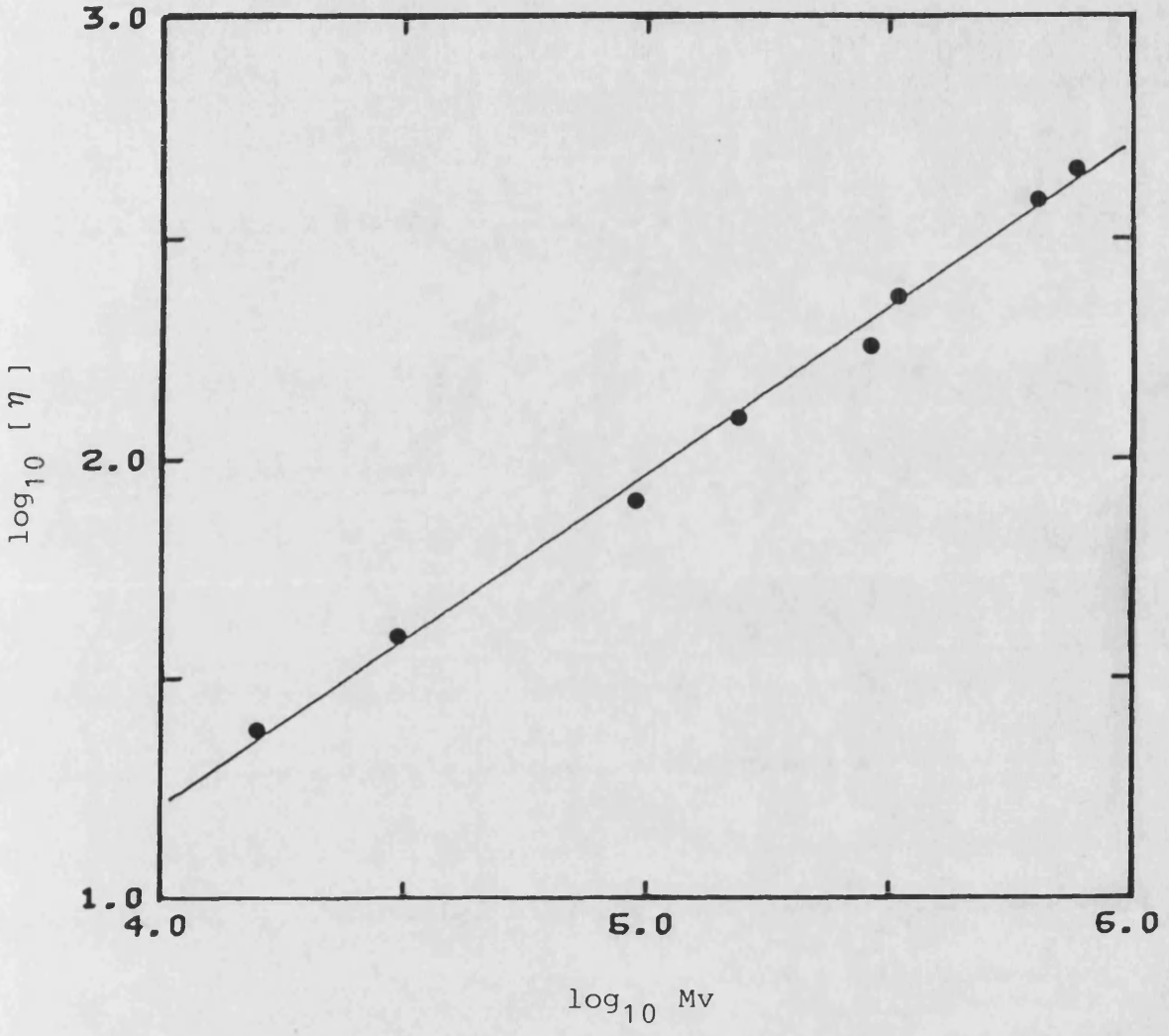

Figure 4.11:- Mark - Houwink plot of PHB after fourth iteration

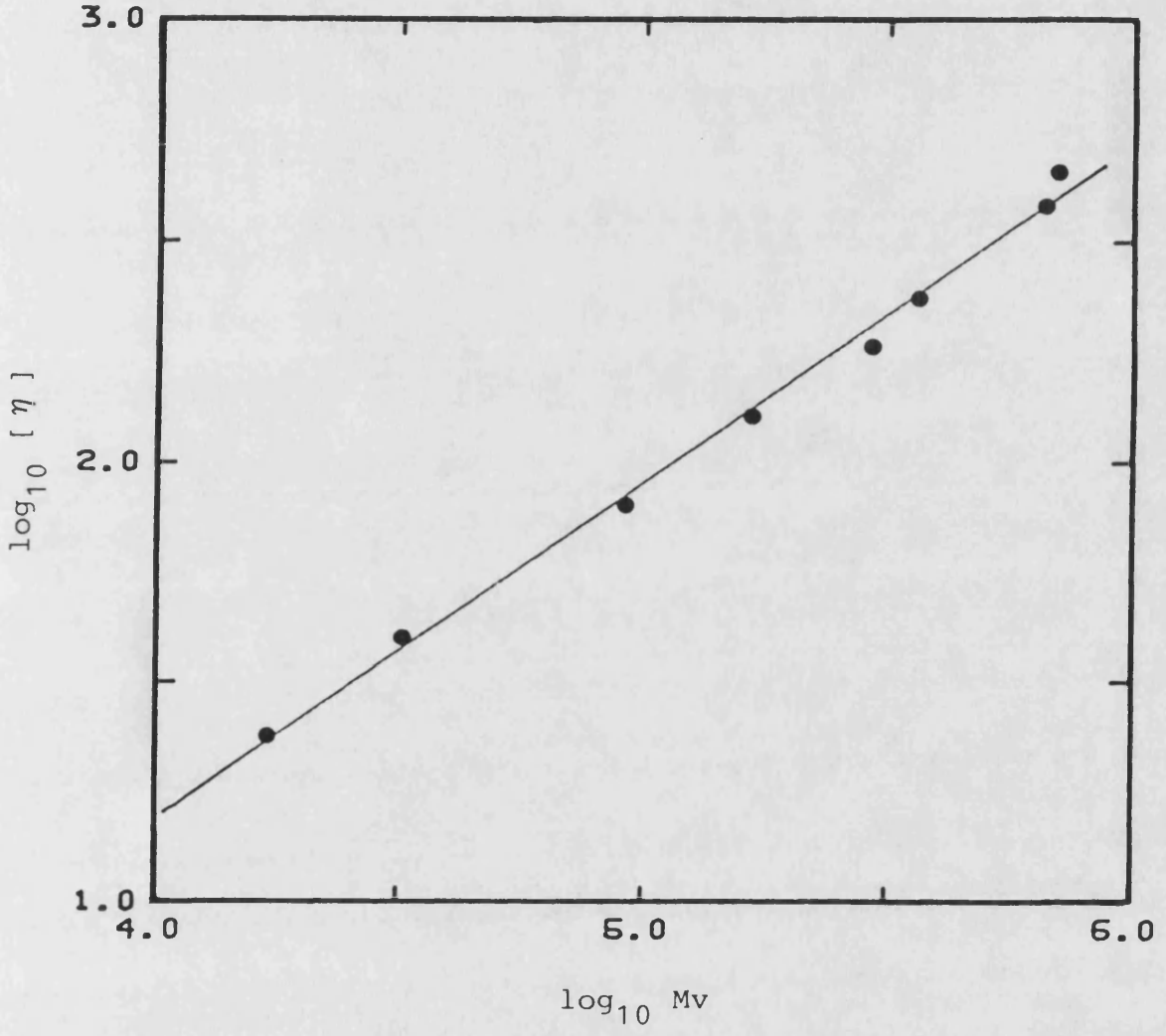

Figure 4.12:- Mark - Houwink plot of PHB after fifth iteration

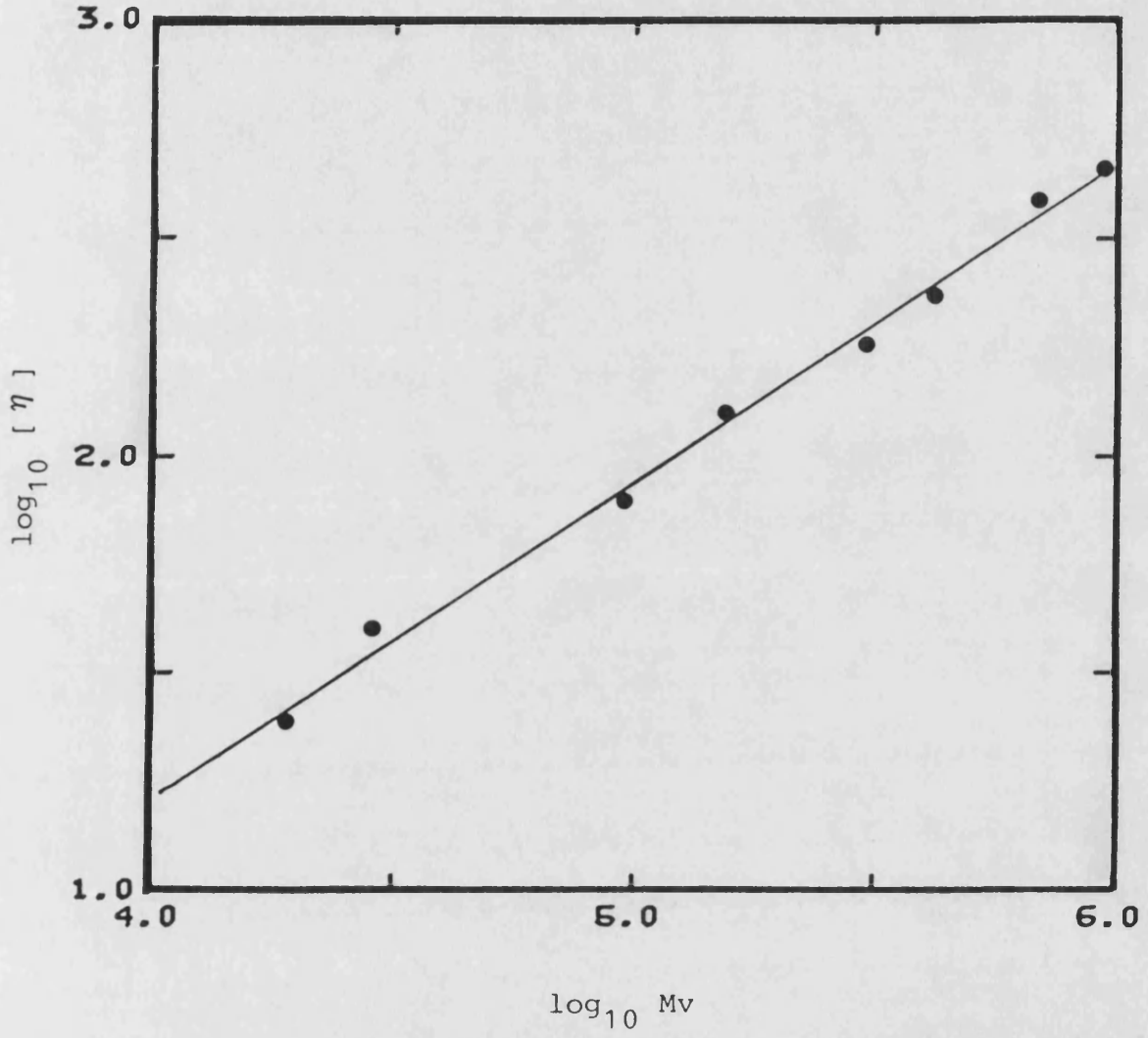

Figure 4.13:- Mark - Houwink plot of PHB after sixth iteration

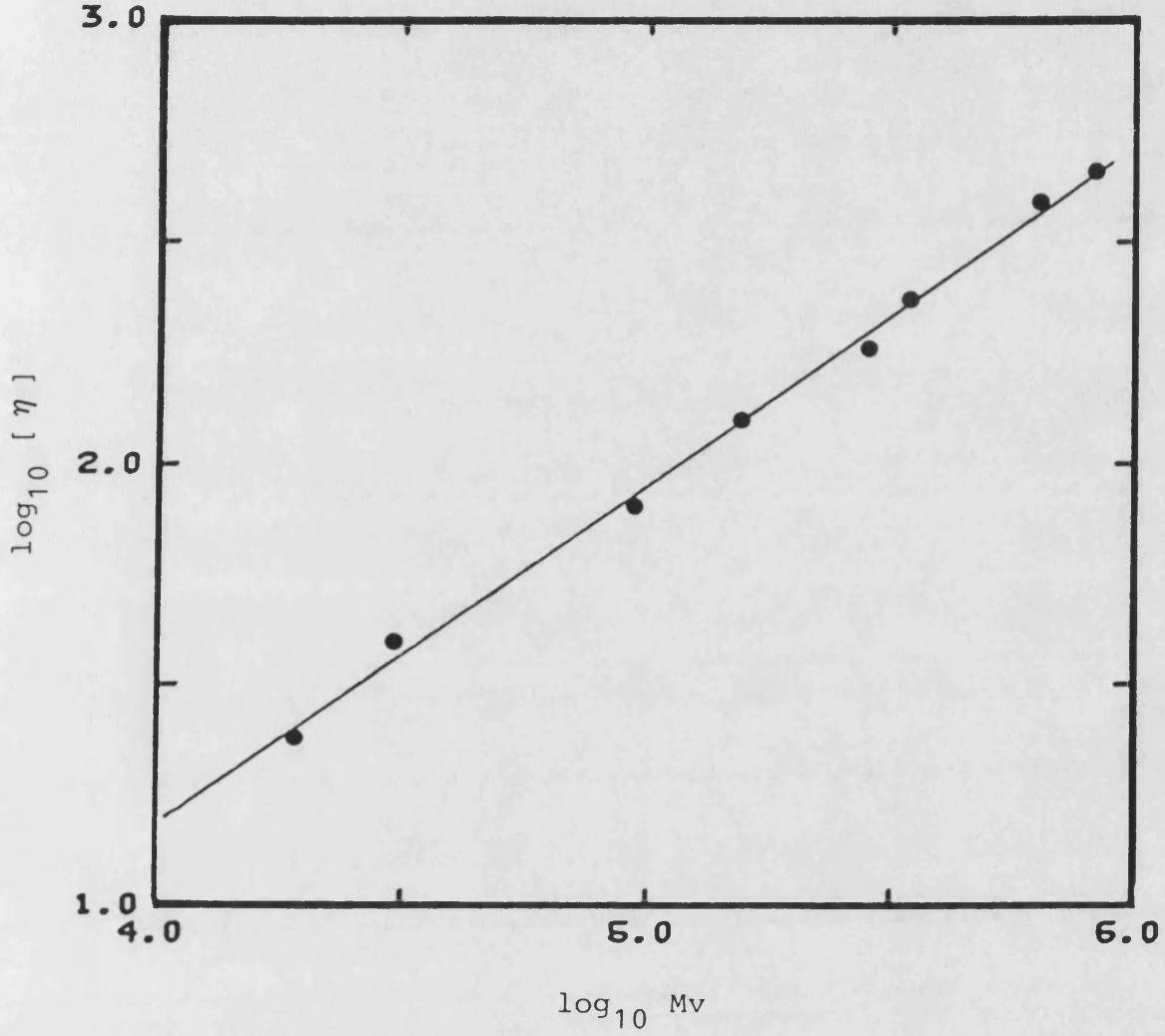

Figure 4.14:- Mark - Houwink plot of PHB after seventh iteration

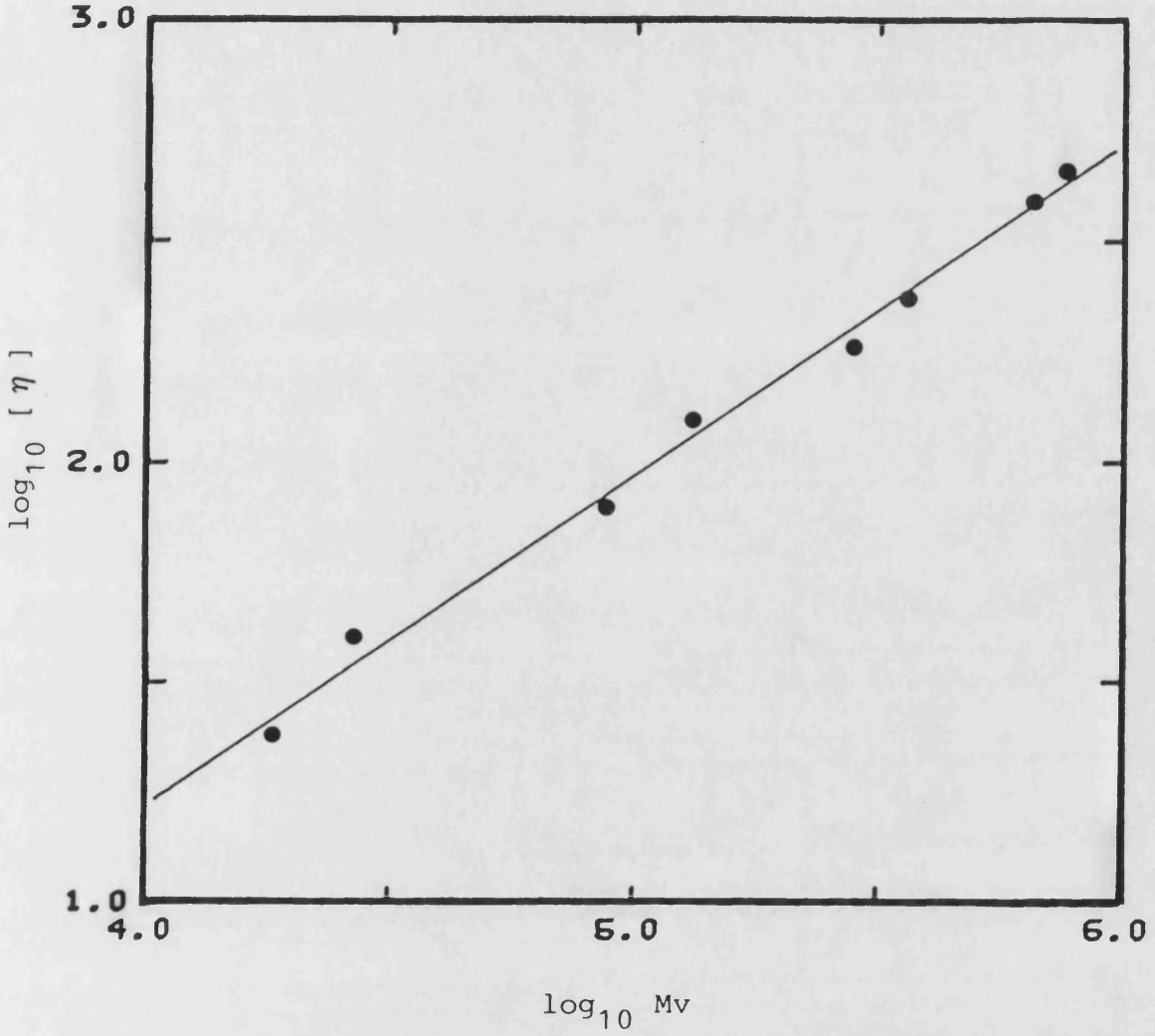

Figure 4.15:- Mark - Houwink plot of PHB after eight iteration

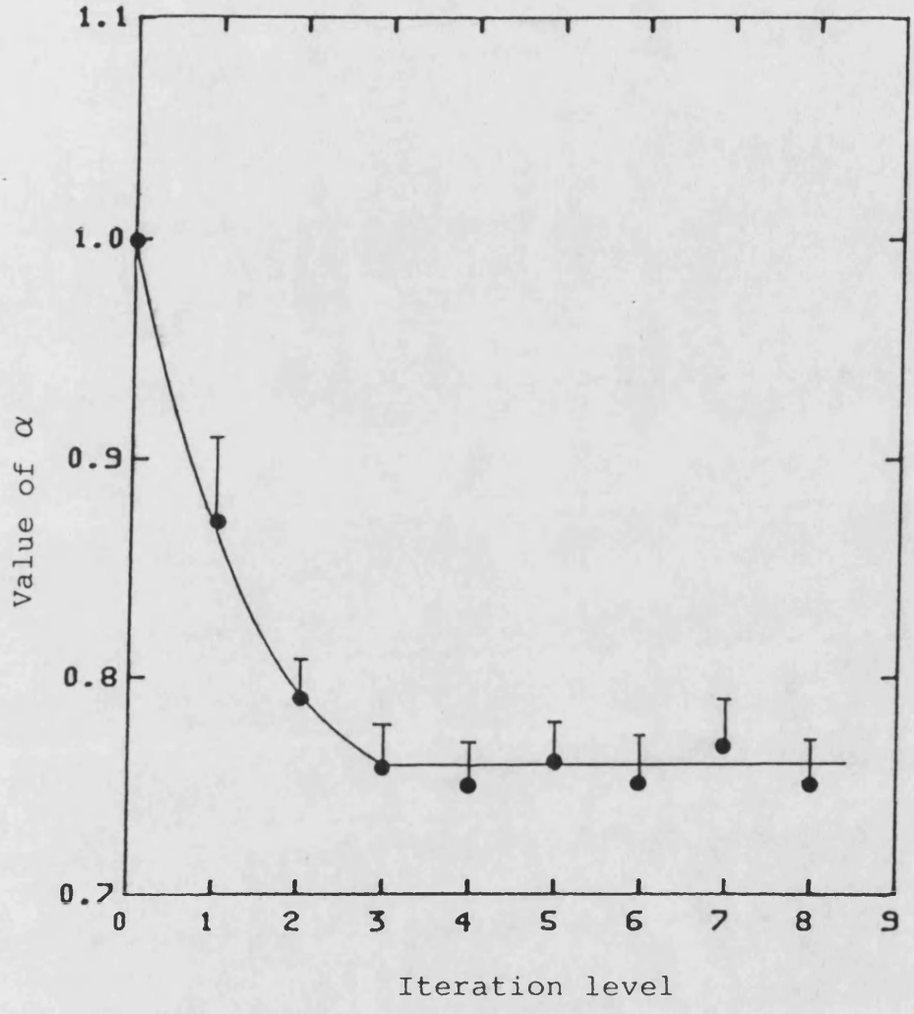

Figure 4.16:- The variation of α after each iteration

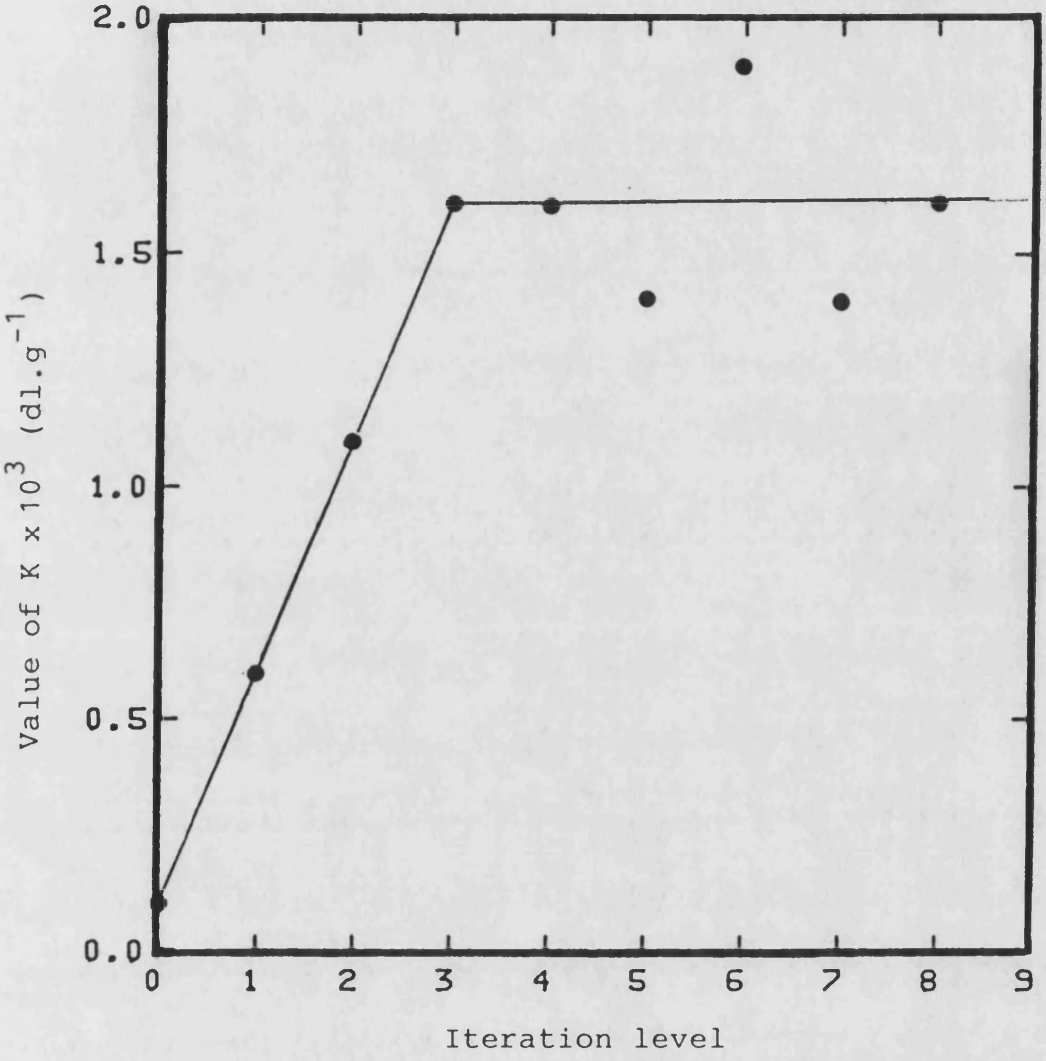

Figure 4.17:- The variation of K after each iteration

Table 4.10 : Mark-Houwink constants of poly(β-hydroxybutyrate) in chloroform.

K ($\frac{ml}{mg}$)	α	Temperature (°C)	References
1.6×10^{-2}	0.76	25	Present work
7.7×10^{-3}	0.82	30	Marchessault *et al.* (1970)
1.2×10^{-2}	0.78	30	Akita *et al.* (1976)

studies suggest that PHB exists in a random coil configuration in chloroform at ambient temperatures although Marchessault *et al.* (1970) have concluded from optical rotation studies that PHB exists as a rigid helix in chloroform.

The iteration procedure described above proved to be a rapid method for determination of Mark-Houwink constants from polydisperse samples of a polymer. The SEC assay was reliable and stable over a period fo three years. However the molecular weight determination was not as precise as that reported by Van Dijk *et al.* (1983). The latter authors used three SEC columns in series. It is likely that the precision of the assay reported here would have been improved by the use of a larger volume of gel but this was a financial constraint on the study. In practical terms,the SEC method described here was useful for routine determination of molecular weight distribution and results could be obtained with as little as 10-20mg polymer.

PARTIII

DEGRADATION AND RELEASE STUDIES FROM PHB AND P(HB/HV) COPOLYMERS

Chapter 5

BIODEGRADABLE POLYMER AND DRUG DELIVERY

5.1 Introduction.

Degradable or erodable polymers in this study are defined as materials that undergo a degradation process in a biological environment and are converted to products that can be readily eliminated from the body. If such polymers are used in implants the degradation products must be small enough to be excreted by the kidney. However, if the polymers are used topically on body sites such as the eye or the uterus, then high molecular weight water-soluble degradation products are acceptable.

Biodegradable polymeric drug delivery systems can be divided into 2 groups (Heller, 1986):

- Monolithic devices in which the therapeutic agent is physically dispersed or dissolved in a polymeric matrix.
- Devices in which the therapeutic agent is covalently bound to the polymer backbone such that the therapeutic agent is released by hydrolysis or enzyme-catalysis.

In an ideal situation, a biodegradable drug delivery device would release therapeutic agent at a constant or controlled rate over a predetermined time by degradation of the polymer backbone into non-toxic, biocompatible subunits which would subsequently be metabolized or eliminated from the body. The advantage of biodegradable polymeric delivery systems, over non biodegradable polymeric delivery systems is that surgical removal of an implanted device, after depletion of the therapeutic agent, is not required.

However, care needs to be exercised when formulating drugs in biodegradable implants, particularly in matrix-type formulations. In some cases, rapid scission of the polymer backbone or crosslinks can compromise the integrity of the device resulting in rapid release of substantial doses of the drug (Jeong and Kim, 1986).

Within the second group of devices in which the therapeutic agent is covalently bound to the polymer, are a specialised group of water-soluble systems which have the potential to both prolong release and to target the drug. Various authors have reported studies of such soluble macromolecular systems (Kopecek, 1984; Feijen *et al*, 1980; Marriott and Pouton, 1986).

The present study is concerned with the aforementioned monolithic delivery systems. The purpose of this chapter is to present a review of previous work in this field. Most of the polymers used in monolithic systems have been aliphatic polyesters with considerable emphasis on poly(lactate), poly(glycolate) and their copolymers. The use of the latter polymers is reviewed in detail since they are closely related to PHB and its copolymers with HV; the materials used in the experimental work reported in this thesis. The special properties of PHB are reviewed in detail in section 5.5.

5.2 Monolithic systems.

The release of the therapeutic agent from a monolithic degradable drug delivery system may be influenced by the mechanism and rate of degradation of the polymeric carrier. The majority of reports relating to drug delivery systems have been concerned with degradation by hydrolysis. Heller (1984) has classified two extreme types of hydrolysis that a polymer can undergo :- bulk hydrolysis and surface hydrolysis.

In bulk hydrolysis, chain cleavage takes place throughout the bulk of the material while in surface hydrolysis the reaction is confined to the outer surface of the solid device.

Monolithic devices which undergo a bulk erosion process may exhibit complex drug release kinetics because these are determined by drug diffusion phenomena and polymer hydrolysis. In general, the initial kinetics of release are comparable with those resulting from diffusion from non-erodable monolithic devices; release rate is often proportional to the square root of time as described by the Higuchi's equation (Higuchi, 1961). However, as the bulk hydrolysis proceeds, the permeability of the polymer increases and thus the rate of diffusion of the drug increases (Heller, 1986; Hadgraft and Guy, 1987).

The kinetics of drug release from monolithic devices which undergo a surface hydrolysis are more predictable. Release by diffusion would be expected with additional release caused by erosion of the polymer. If release by diffusion is slow, such that release by erosion is dominant, then such devices should be capable of providing zero-order drug release as long as the surface area of the device remains constant. In practice the rate of drug release will decrease with decrease of the total surface area of the device, which will be a consequence of the erosion process. In principle, by controlling the geometry of the device one could determine its lifetime, for instance, for a laminate the lifetime of the device would be directly proportional to its thickness.

5.3 Poly(glycolate), poly(lactate) and poly(glycolate-co-lactate).

Poly(lactate)(PLA), poly(glycolate) (PGA) and their copolymers have been used by many researchers for the purpose of investigating

Figure 5.1 :- Chemical structure of related polyesters.

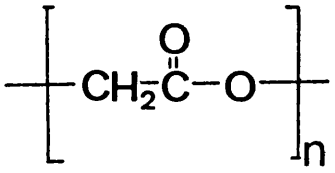

poly (glycolate)

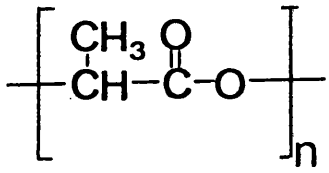

poly (lactate)

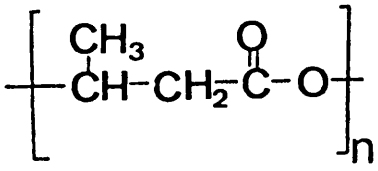

poly (β- hydroxybutyrate)

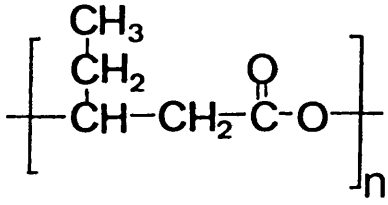

poly (β - hydroxyvalerate)

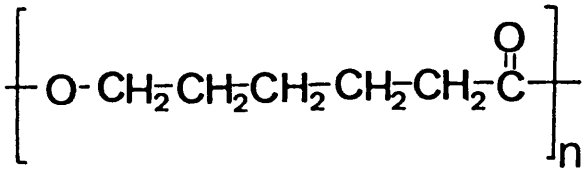

poly (ϵ - caprolactone)

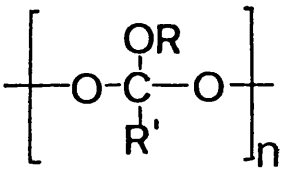

poly (orthoesters)

monolithic biodegradable drug carriers. They belong to a group of related aliphatic polyesters. The structures of these polymers together with other members of the group are shown in figure 5.1.

PLA, PGA and the P(GA/LA) copolymers have been woven for use as surgical sutures which are biodegradable, biocompatible and have mechanical strength greater than catgut. (Frazza and Schmitt, 1971; Gilding and Reed, 1981). PGA sutures are marketed under the tradename of Dexon® and P(GA/LA) sutures are marketed as Vicryl®. As a result of the proven biocompatibility of PGA, PLA and P(GA/LA) copolymer sutures, extensive studies have been reported on the suitability of these polymers for controlled release of drugs. PGA and PLA are produced synthetically by ring-opening polymerisation of the appropriate cyclic diester to produce high molecular weight polymers (Gilding and Reed, 1979).

5.3.1 Physicochemical properties.

The chemical structure of lactic acid (LA) includes a chiral centre, thus, PLA can be prepared in the l(+), d(-) and racemic dl forms. P-l-LA is relatively crystalline (degree of crystallinity about 37%) with a melting point of around 180°C and a glass transition temperature (Tg) at 50-60°C. P-dl-LA is totally amorphous and also has a Tg at about 50-60°C (Gilding and Reed, 1979).

Biodegradation of all polyesters is facilitated by the hydrolysis of the ester bond to yield an alcohol and a carboxylic acid. The example of this reaction is shown opposite.

PGA is the most hydrophilic of this group of polyesters. It has a melting point of 220-230°C and Tg of about 36°C (Bandrup and Immergut, 1975). The degree of crystallinity of Dexon® sutures has

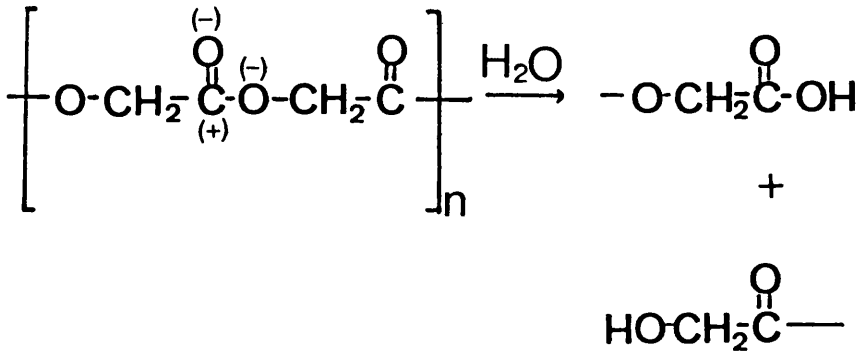

Reaction 1 : Degradation of poly(glycolate) in aqueous solution to yield an acid and an alcohol.

been quoted as 46 - 62% (Gilding and Reed, 1979). The effect of copolymerisation of GA and l-LA has a marked effect on degree of crystallinity as shown in figure 5.2. All copolymer compositions containing between 25 and 67% GA are amorphous. Crystallinity and hydrophobicity in turn effect the absorption of water by these copolymers and influence their rates and mechanisms of degradation.

PGA and P-l-LA homopolymers have been described as hydrophilic and hydrophobic crystalline matrices respectively; PLA being more hydrophobic than PGA due to the presence of the pendant methyl group. Gilding and Reed (1981) have examined the effect of the hydrophilicity/hydrophobicity of P(GA/LA) copolymers by measuring the equilibrium water uptake of immersed polymer films. These authors found that equilibrium water levels were low for the hydrophobic, crystalline P-l-LA and copolymers with low GA content. Equilibrium water absorption increased rapidly to 20-30% w/w for amorphous copolymers, as hydrophilicity (the content of GA) was increased. However, above 70 mole % GA, water uptake decreased as the degree of crystallinity increased. Copolymers containing 70 mole % GA absorbed the highest quantity of water. Such polymers have a high rate of degradation and may degrade by mechanisms involving scission of the polymer backbone within the bulk sample.

Cohn *et al.* (1987) reported that the molecular weight of PGA and PLA homopolymers can influence their degrees of crystallinity. They observed that samples of PGA and PLA of low molecular weight (Mn = 1000) had degrees of crystallinity of 9% and 12.2 % respectively. The degree of crystallinity increased to maximum values of 52% and 37% for PGA (Mn > 20000) and PLA (Mn = 28000) respectively. The authors explained that high molecular weight polymers have fewer

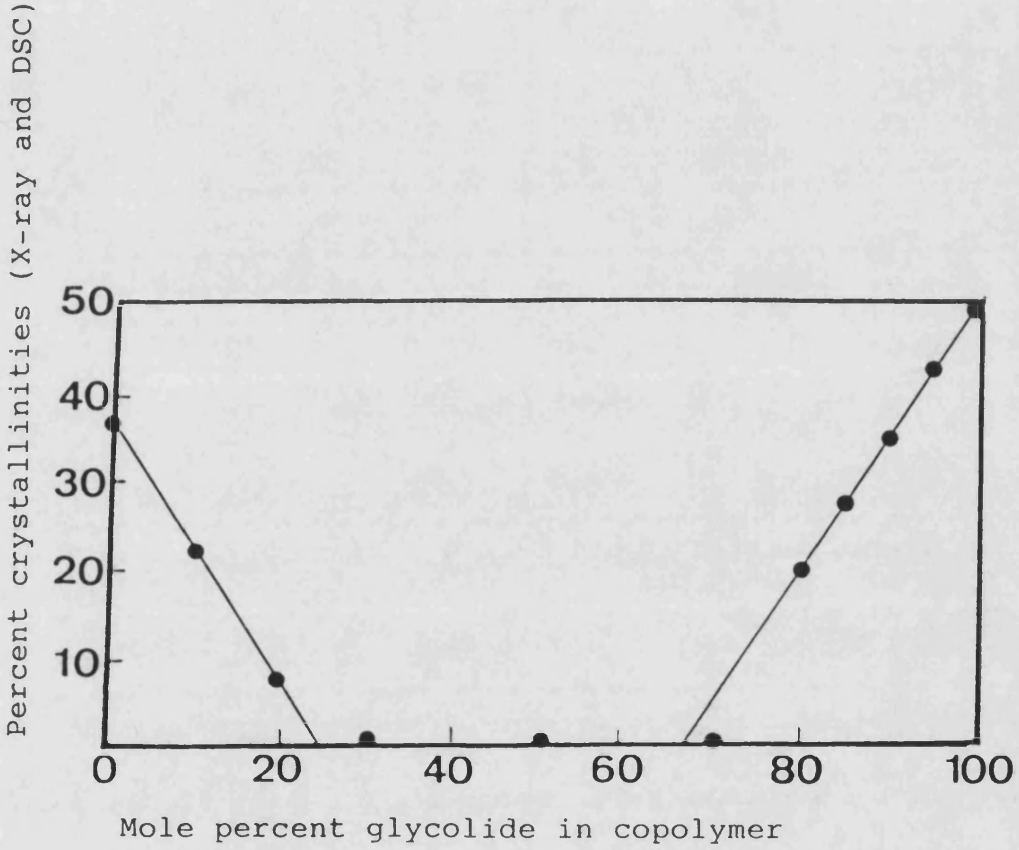

Figure 5.2 :- Percent crystallinities for PGA/PLA copolymers as a function of composition (determined by X-ray and DSC measurement). (Reproduced from Reed and Gilding, 1981).

chain ends which allows crystallisation to proceed without interference from the hydrophilic chain ends which will be present in larger quantities in low molecular weight polymers.

5.3.2 Degradation of PGA, PLA and P(GA/LA) copolymers *in vitro* and *in vivo.*

5.3.2.1. Introduction

The degradation of polyesters has been studied *in vivo* and *in vitro.* It is important to study degradation *in vivo* to determine the effect of enzymatic processes on the rate of degradation, although most polymers are expected to degrade primarily by non-enzymatic processes. Mechanisms of degradation are likely to influence the mechanisms of release of drugs; therefore a considerable number of *in vitro* studies have been reported.

In section 5.2, two distinct mechanisms of degradation of biodegradable polymers were discussed; bulk hydrolysis and surface hydrolysis. Bulk hydrolysis refers to the breaking of backbones of polymer chains resulting in shorter chains. Thus bulk hydrolysis is characterised by changes in the molecular weight of the original polymer sample. In contrast, surface hydrolysis results in the successive erosion of monomers from the exposed end of polymer chains at the polymer surface and thus does not usually lead to changes in the molecular weight of the bulk polymer sample. Differentiation of these two processes is important. Determination of weight loss of polymer is not sufficient and should be accompanied by analysis of the molecular weight distribution during degradation.

5.3.2.2 Degradation of PGA, PLA and P(GA/LA) copolymers *in vitro*.

In vitro studies of Dexon® sutures at pH 7 and 37°C showed that PGA degrades by bulk hydrolysis (Gilding and Reed, 1981). These authors used SEC to measure the changes in the molecular weight of PGA during degradation and also measured the changes in weight by a gravimetric method. The molecular weight distribution of Dexon® changed after 1 week but there was no significant mass loss until the fifth week; a clear indication of bulk hydrolysis.

Chu and Louie (1985) studied the degradation of Dexon® sutures *in vitro* by monitoring the changes in the tensile strength, the pH, the degree of crystallinity and the mass of glycolic acid release from the sutures. The result of their work is shown in Figure 5.3. There appear to be two stages of degradation for Dexon® sutures. These authors have used the microfibrillar model for fibre structure to explain the two stage degradation. This model, shown in Figure 5.4, was proposed by Peterlin in 1972.

The basic element of a fibre is said to be a microfibril which contains crystalline and amorphous regions arranged in parallel to the long axis of the fibre. The crystalline regions are highly packed and composed of chain sequences in ordered conformation. The amorphous regions comprise chain folds, chain ends and tie chain segments which are denoted by A and B in Figure 5.4. The tie chain segments are thought to hold different crystalline regions together. The tie chain segments transmit strain throughout the crystalline zones when a fibre is under stress. Based on this concept, Chu and Louie (1985) have proposed that when PGA fibre is placed in an aqueous solution the degradation proceeds by two stages, first within the amorphous regions and secondly within

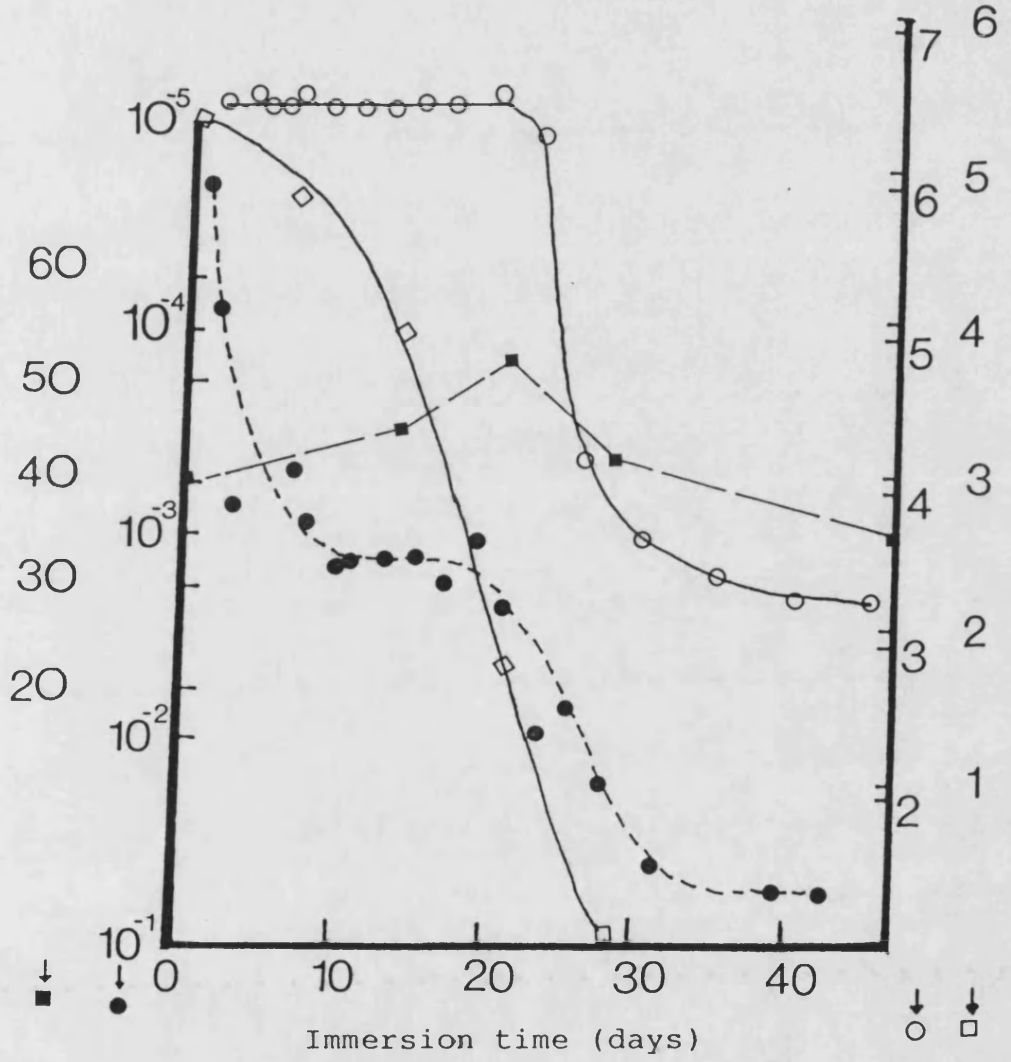

Figure 5.3 :- Interrelationship among glycolic acid concentration (●), tensile strength (□), level of crystallinity (■), and pH level of the medium (O), and their changes as a function of time.
(Reproduced from Chu, 1981).

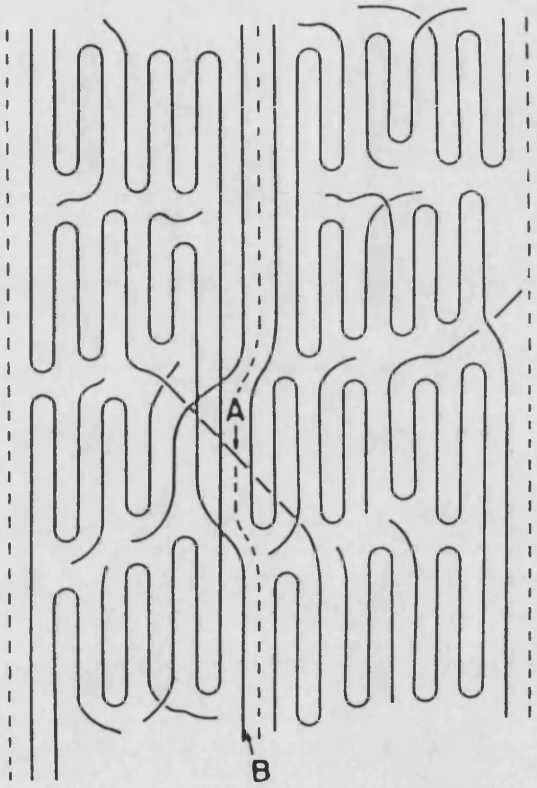

Figure 5.4 :- Schematic drawing of microfibrillar structure of fibres (A) Interfibrillar (B) Intrafibrillar tie molecules (Reproduced from Chu, 1981)

the crystalline regions. Thus, crystallinity increases by reduction in the mass of amorphous polymer and possibly because the remaining undegraded chain segments in the amorphous regions become more mobile, allowing them to reorganize from a disordered to an ordered state.

Tensile strength decreases rapidly perhaps because the tie chain segments in the amorphous regions are degraded first. Chu (1985) has speculated that the drastic change in pH during the second stage, the crystalline hydrolysis, may be due to either of two effects:

> i.the crystalline regions contain more glycolic per unit volume than amorphous regions and hence more glycolic acid is released per unit mass during the second stage of hydrolysis.
>
> ii.destruction of the tie-chain segments in the first stage frees the crystalline blocks, which were previously linked together by tie-chain segments, from restricted motion. As a result the crystals in the microfibrils become less densely and orderly packed, which makes them more susceptible to degradation.

Chu (1981) also found that the pH of solution has an effect on the degradation of Dexon® sutures *in vitro*. He observed that the degradation rate in unbuffered physiological saline (pH = 5.0) was less than that in phosphate buffered physiological saline (pH = 7.4). The proposed reason for the latter observation was that in the unbuffered system the acidic degradation products remained and accumulated. The hydrolysis process was retarded, by the lack of hydroxyl ions, which often catalyse ester hydrolysis, thereby decreasing the rate of degradation.

Initial studies by Gilding and Reed (1981) on the degradation of films of P(50%GA/50%LA) copolymer indicated that it was a suitable

matrix for formulation of drugs. The molecular weight of this copolymer decreased as did its mass under the influence of a water content of about 25% w/w. These features, they claimed, were suitable for the sustained release of hydrophobic drugs. Gilding and Reed (1981) also studied degradation of P-l-LA films and found that, despite the higher crystallinity and low water uptake, degradation still occured by backbone cleavage.

5.3.2.3 Degradation of PLA and P(GA/LA) copolymers *in vivo*.

Miller *et al.* (1977) have reported differences in the rate of degradation of P-l-LA and copolymers of l-LA and GA. Weight loss of ^{14}C and tritium - labelled homopolymer and copolymer pellets was studied after implantation in rats. The results are shown in Figure 5.5 where the degradation half-lives of the samples are plotted against copolymer composition.

The rate of degradation was closely related to the results of the crystallinity study reported by Gilding and Reed (1981) suggesting that the crystallinity of the copolymer is a major determinant of the rate of degradation *in vivo*. For the relatively crystalline homopolymers, the hydrophobicity/hydrophilicity of the polymer appears to determine the rate of the degradation. The more hydrophobic PLA degrades at a slower rate than PGA.

Schindler *et al.* (1977) have studied the *in vivo* degradation of P-l-LA using various initial molecular weights (initial viscosities = 0.47, 1.15, 2.24 and 3.23 dl/g). Polymer films (2 x 1 cm, 100 μm thick) were implanted subcutaneously in rabbits and changes in the molecular weight and the mass remaining were determined during degradation. These authors reported two stages of degradation. The first stage

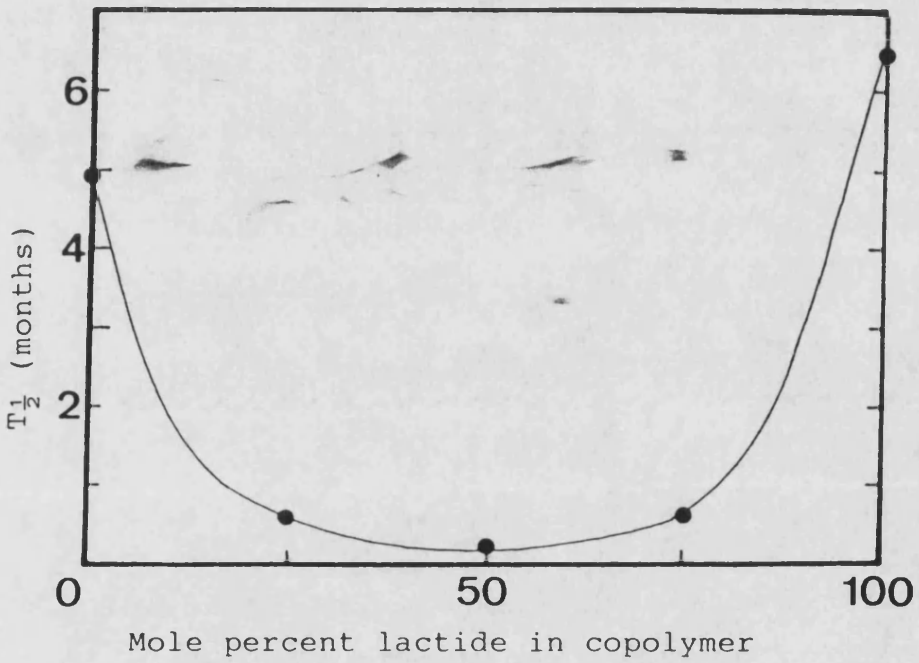

Figure 5.5 :- Half-life (in months) of various ratios of PLA and PGA as copolymers implanted in rat tissue. (Reproduced from Miller et al., 1977)

involved backbone cleavage with no significant weight loss until a critical molecular weight (Mn= 15,000) was reached. The second stage involved a marked weight loss together with an accelerated decrease of molecular weight. The rate of degradation for polymer of different molecular weights was found to be similar (initial viscosities:- 0.47, 1.15, 2.24 and 3.23 dl/g). Chawla and Chang (1985) have also studied the *in vivo* degradation of P-l-LA. These authors used films (1 cm x 1 cm) and monitored mass loss following degradation of four different samples of P-l-LA (M_w = 0.9, 2.0, 2.7, 2.9×10^6) after implantation in rats. The highest molecular weight was reported to have the lowest rate of degradation *in vivo.* Thus, there is some confusion in the literature as to the effects of molecular weight on rate of degradation.

Visscher *et al.* (1985) have studied the *in vivo* degradation of P(50%dl-LA/50%GA) formulated as microspheres. These authors observed the reaction of tissues into which microspheres were implanted and also morphological changes in the microspheres as they degraded. Microscopic studies indicated that the 'microcapsules' became slightly more porous after 4 days of implantation. When they were examined after 49 days of implantation there was a considerable change in the appearance of the internal matrix which was no longer simply porous but was showing signs of extensive erosion. Microcapsule could not be found after 63 days,suggesting that they had been completely absorbed within this time. The tissues showed only minimal response to the presence of these microcapsules with no sign of inflammation.

5.3.3 Release of drugs from P(GA/LA) copolymers

5.3.3.1 Introduction

A variety of P(GA/LA) copolymer systems have been developed for the long term maintenance of therapeutic drug levels. Systems have

been devised for the delivery of a range of chemical classes of drug to achieve delivery periods that vary from days to years. The motivation for formulation in P(GA/LA) copolymer systems has usually been in the improvement of patient compliance. For example, systems for antimalarial drugs, fertily control agents and narcotic antagonists have been studied.

However, a recent review by Wise *et al.* (1987) has highlighted two particular areas where the potential of biodegradable polymers can be exploited. One area is the delivery of biological mediators which would usually be peptides and proteins. Biodegradable polymers may be capable of protecting such labile macromolecules as well as facilitating controlled release. One commercial product which was developed with this approach in mind is Zoladex® which is manufactured by ICI plc (UK) (Hutchinson and Furr, 1985).

Wise *et al.* (1987) considered that a second important area for exploitation was the pulsed release of drugs from biodegradable polymers. Pulse-release could be useful development in controlled release of antigens for immunization. This suggestion relates to previous studies on the release of a steroid from P(LA/GA) copolymer. In the latter study, a biphasic dual pulsed release of d-norgestrel was reported (Figure 5.6). This was in fact a disadvantage in the delivery of d-norgestrel but could be used to advantage for delivery of antigens. Wise *et al.* (1987) consider that research should be directed to engineering release of antigen/vaccine as two distinct, controlled *bursts*. An initial burst of antigen release over a period of several days will be required to induce the primary immune response. After a period of weeks, the system will then be required to release a second antigen pulse. This use of biodegradable polymers is not yet well developed. Literature

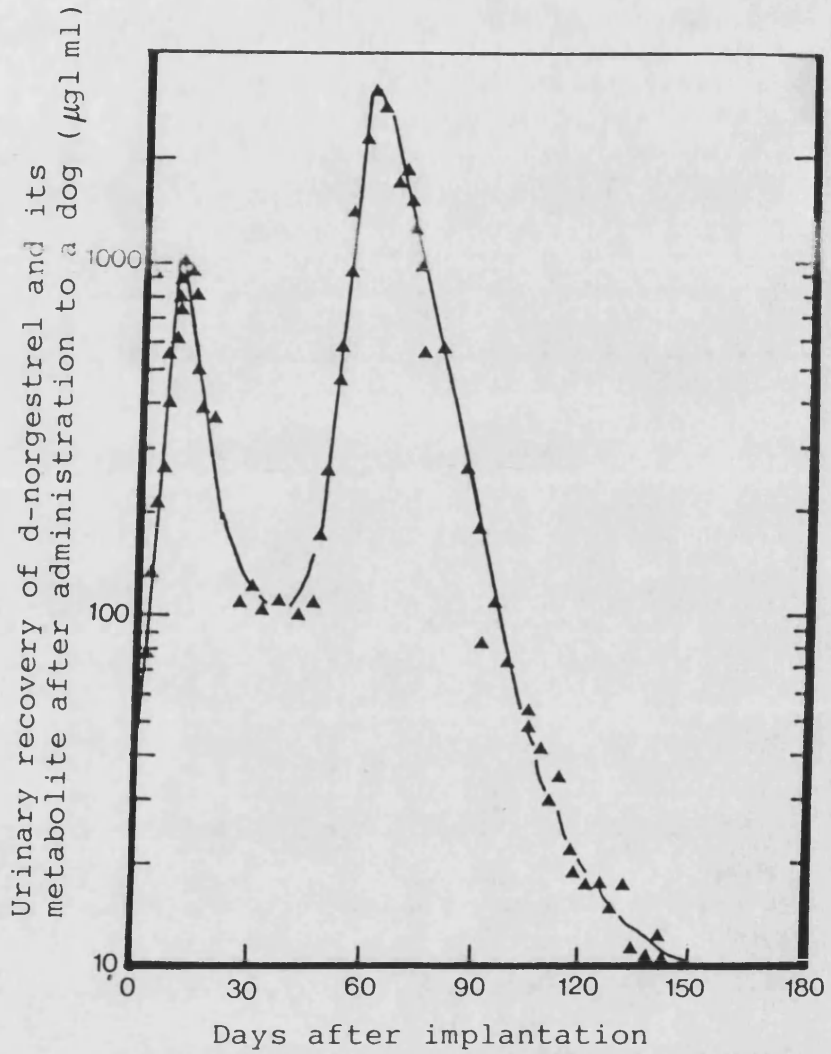

Figure 5.6 :- Biphasic-pulsed release of d-norgestrel from P(LA/GA) copolymer (90% dl-lactate/ 10% glycolate).
(Reproduced from Wise et al., 1987)

reports of release of drugs from biodegradable polymers are reviewed below.

5.3.3.2 Factors affecting release of low molecular weight drugs.

Since P(GA/LA) copolymers undergo bulk hydrolysis, it is important to determine the degradation on the kinetics of drug release. When little or no polymer hydrolysis has occured, drug release is expected to be controlled by diffusion in the same way as would occur in a non-degradable system. However, as the extent of bulk hydrolysis becomes significant, diffusional release rate can accelerate. Heller (1985) presumed that the increase in rate of release was due to an increase in the permeability of polymer arising from increases in chain mobility caused by hydrolytic chain scission.

The effect of copolymer composition on the release of a hormonal steroid, levonorgestrel, was studied by Sharon *et al.* (1984). The release of the steroid was directly related to the susceptibility of each polymer to degradation. Copolymers and homopolymers of l-LA, dl-LA were used. The rank order of polymers with increasing rate of biodegradation was P(75% l-LA/25%GA), P(90%dl-LA/10%GA), P(100%dl-LA), P(50%dl-LA/50%l-LA) and P(100%l-LA). Two polymers, P(100%dl-LA) and P(50%dl-LA/50%l-LA), were selected for further release studies of the steroid since they appeared to have potential for development of a delivery system with a lifetime of 6 months to 1 year.

Wise *et al.* (1978) reported that the molecular weight of P(50%l-LA/50%dl-LA) had an effect on the rate of release of sulphadiazine from spherical beads. The rate of drug release decreased with increase in the molecular weight of the polymer. Below a molecular weight of 150,000, there was no further increase in the release rate. In

another study, Gresser *et al.* (1984) found that by lowering the polydispersity of P(75%l-LA/25%GA) (Mw = 56000) from 2.0 to 1.4, it was possible to produce a system which exhibited a reduced initial rate of release of estradiol with a longer period of constant release. Clearly, the polymer molecular weight distribution is an important determinant of release characteristic although there are few reports in the literature of such studies.

The release rate of a specific drug from a P(GA/LA) matrix can be adjusted by manipulation of the concentration of drug in the drug-polymer mixture. The duration of release is also affected by loading of drug but can also be manipulated by modifying the geometry and size of the device. Generally, the higher the loading of a drug in the matrix, the faster will be the release rate (Suzuki and Price, 1985). The lifetimes of P(GA/LA) systems were also found to be dependent on the aqueous solubility of the drug (Gresser and Sanderson, 1984).

5.3.3.3 Release of peptides from P(GA/LA) copolymers.

Generally, high molecular weight pharmaceuticals, such as polypeptides cannot be administered by the oral route. They are degraded and deactivated by proteolytic enzymes in the gastro-intestinal tract and therefore are usually administered parenterally. Since such drugs often have very short half lives, frequent injections are required to produce an effective therapy.

For polypeptides and hormones, where the pharmacological use of the agent require sustained release, the most appropriate dosage form is one capable of releasing drug continously at a controlled rate over a period of weeks or even months. Examples of such peptides are the highly potent, synthetic analogues of lutenizing hormone releasing

hormone. The controlled release of such peptides from P(dl-LA/GA) systems have been studied extensively (Sanders *et al.* 1986; Hutchinson and Furr, 1987). The uses of such analogues of luteinizing hormone releasing hormone are for reversible chemical castration and suppression of hormone dependent disease states such as prostatic cancer and endometriosis.

Sanders *et al.* (1984) have prepared microspheres by a phase separation method. The peptide, in aqueous solution, was mixed with a solution of p(50%dL-LA/50%GA) in dichloromethane. A non-solvent was then added to precipitate the polymer around the aqueous droplets. The release of the peptide from these microspheres was found to be triphasic(see Figure 5.7) . The primary release phase involved diffusion of drug from the surface of the microsphere (ie the drug which was not trapped within the matrix). During, the second phase of release the rate of release was too low to be therapeutically effective although the polymer molecular weight decreased during this period. Further degradation and dissolution of low molecular weight fragments combined with erosion within the bulk, the polymer then initiated the tertiary release phase of the peptide.

Polypeptides have high molecular weights and are water soluble. Therefore their release from polyesters by partition dependent diffusion through the polymer is likely to be extremely slow. Thus, the degradation of the polymer is a crucial factor in determining the release of the high molecular weight polypeptide from the dosage form.

Hutchinson and Furr (1987) have reported the degradation of P(50%dl-LA/50%GA) in the absence of drug in McIlvanes buffer, pH 7.4 at 37°C. This is shown in figure 5.8. The polymer degraded by bulk hydrolysis resulting in the formation of lower molecular weight

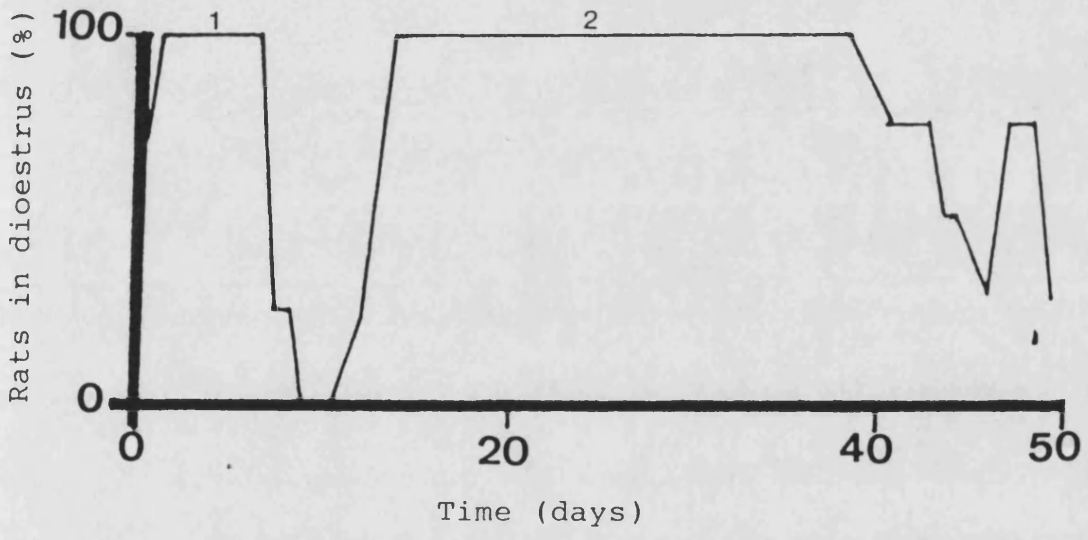

Figure 5.7 :- The effect of subdermal depots containing 300 g of Zoladex^{R} in high molecular weight PGA/PLA copolymer administered to regularly cycling adult female rats. The two release phases are (1) initial release due to leaching from the surface; (2) degradation-induce phase (Reproduced from Hutchinson and Furr, 1985)

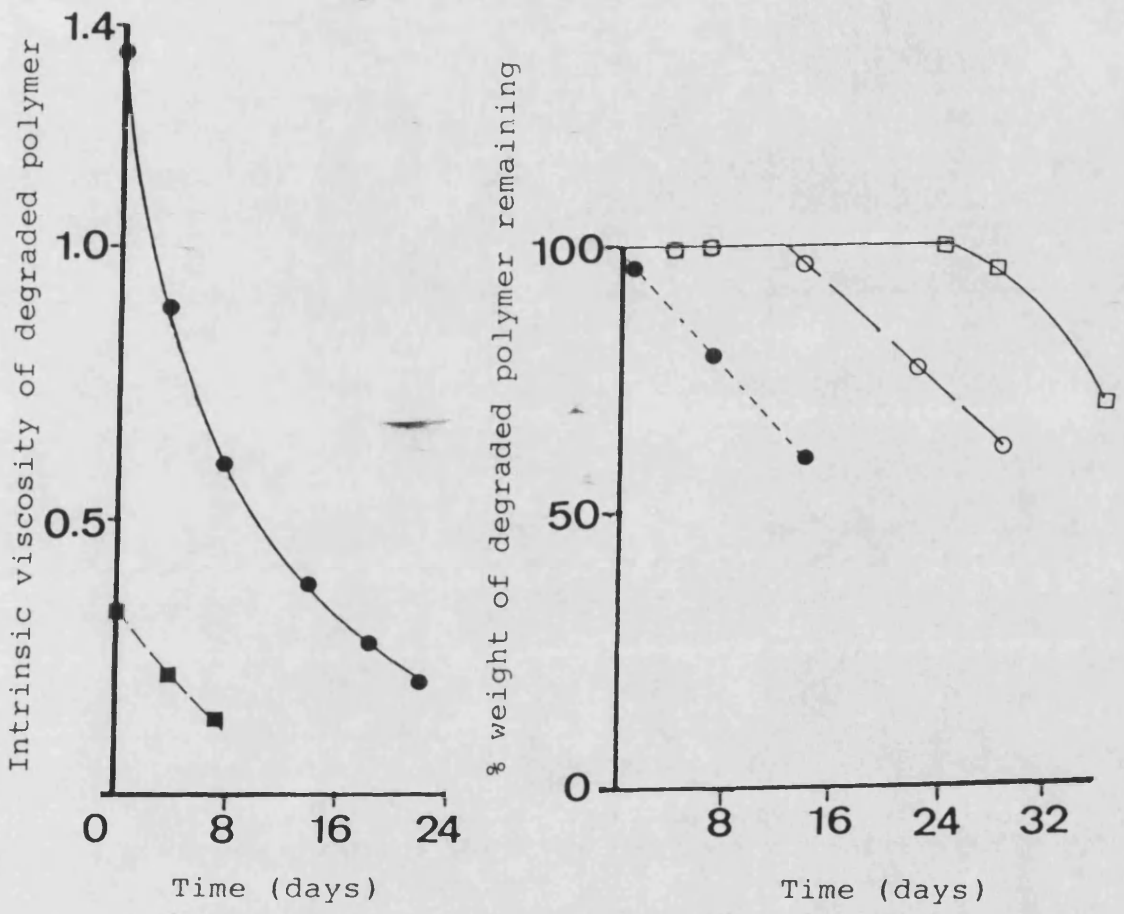

Figure 5.8 (a) and (b):- In vitro degradation of 50/50 molar poly [(±) - lactide - co-glycolide] at 37°C in buffer at pH 7·4. High molecular weight polymers as measured by viscosity (a) and yet retain their water insolubility (b) only after extended time of degradation does any weight loss occur. (Reproduced from Hutchinson and Furr, 1987).

polymers demonstrated by a decrease in intrinsic viscosity. As the molecular weight of the degrading polymer decreased,it became increasingly hydrophilic and exhibited enhanced water uptake, whilst retaining its water insolubility. After an extended period of degradation, the molecular weight decreased to a level at which there was significant water solubility. At this point, the polymer began to erode homogenously allowing the peptide and also polymer degradation products to diffuse away from the loosening polymer matrix. This latter process corresponded to the third phase of peptide release which occurred largely by diffusion through aqueous pores. This triphasic release of water-soluble macromolecules is typical of P(GA/LA) systems although the general profile can be modified by formulation.

Matrices can be formulated to give biphasic release avoiding the slow secondary phase release (Hutchinson and Furr, 1985). This can be achieved by using a low molecular weight polymer and a higher loading of drug; although the rate of release is increased and the duration of release is shortened. Sanders *et al.* (1986) have studied the release of an LHRH analogue from various P(dl-LA/GA) melt-extrusion systems using polymers with equal molecular weights. The copolymer compositions (dl-LA/GA) were 100:0, 95:5, 90:10, 85:15 and 80:20. Increase in the content of dl-LA produced a more hydrophobic system which resulted in the decrease of the duration of the subeffective secondary phase and an increase of the duration of the tertiary release phase.

Further studies examined the effect of molecular weight of P(d-LA) on the release of peptide. Use of a high molecular weight polymer ($[\eta]$ = 1.02 dl/g) resulted in extension of the secondary phase whereas an implant prepared using a low molecular weight polymer ($[\eta]$ = 0.36

dl/g) exhibited no secondary phase of release. In addition, use of a low molecular weight polymer caused overlap of the primary and tertiary phases resulting in continuous release of the peptide for more than 8 months. Another disadvantage of using high molecular weight polymer was that elevated temperatures and extended extrusion times were required for manufacture of the implant which resulted in thermal degradation of the peptide.

Redding *et al.* (1984) compared the effectiveness of administering LHRH analogue as microspherical polymeric implants with the conventional twice daily subcutaneous injection. A pharmacological assay, prostate cancer in rats, was used to compare the two therapies. These authors found that a greater decrease in tumour weight was achieved using the polymeric implant. Since prostate tumours are often heterogeneous consisting of both hormone dependent and hormone independent cells, combination therapy using the implant and mitoxantrone dihydrochloride therapy was studied and proved to be effective against prostatic cancer (Schally *et al.*, 1986).

5.4 Other related biodegradable polymers.

5.4.1 Poly (ϵ-caprolactone)

Poly(ϵ-caprolactone) is likely to have different properties to PGA since it will exist in a rubbery state at body temperature whereas both PLA and PGA are glassy. The glass transition temperature of poly(ϵ-caprolactone) is very low (-60 to -70°C).

Pitt and Gu (1987) studied the degradation of poly(ϵ-caprolactone) films *in vitro*. The polymer underwent 2 stages of degradation. The first stage involved random chain scission involving hydrolytic cleavage of ester group resulting in decrease of the

molecular weight of the original polymer. The formation of carboxylic acid end groups catalysed further chain scission. These authors were also able to show that if the carboxylic acid ends were capped with ethanol, the subsequent rate of degradation was decreased.

The second stage of degradation involved significant loss of weight which was due to the diffusion of dissolved oligomeric fractions away from the bulk polymer. As the polymer degraded, the degree of crystallinity increased from 45% to 90% indicating preferential attack of the amorphous phase.

5.4.2 Poly (orthoesters).

Although polymers based on lactic and glycolic acid have the important advantage of degrading to the natural metabolites of lactic and glycolic acid, they are not ideal materials for controlled drug release. To produce delivery systems having more desirable release kinetics, an erosion mechanism based on surface hydrolysis is significantly more desirable and it is for this reason that poly(orthoesters) have been studied.They have been prepared synthetically by the Alza Corporation (USA) and are marketed under the tradename Alzamer®.

Poly(orthoesters) can be designed to contain pH-sensitive linkages which are relatively stable in basic envrionments but will hydrolyse at progressively increasing rates as the external pH is lowered. (Heller and Himmelstein, 1985). Excipients can be incorporated into poly(orthoester) systems such that the pH in the surface layers of the device are lower relative to the interior of the device. In this way, it is possible to ensure that hydrolysis proceeds at a significant rate only in the surface layers (Heller *et al.*, 1983).

Two different classes of excipients have been used; acidic excipients, which were intended to accelerate the rate of hydrolysis, and basic excipients, which were intended to stabilize the interior of the matrix. Sodium carbonate has been used as a basic excipient in a study of the release of a contraceptive steroid, norethindrone, from poly(orthoester) systems. Release was not in fact mediated by surface erosion of the polymer but rather by the formation of a swollen hydrophilic layer at the surface of the polymer allowing release of the drug by diffusion from the swollen layer. Na_2CO_3, in this case, functioned as an osmotic agent and causing uptake of water into the matrix.

Based on the results obtained using Na_2CO_3, the use of an insoluble acid anhydride was studied. The acid anhydride was intended to act as a catalyst since, in the presence of water, it would hydrolyse to form a diacid which would then catalyse the erosion of the matrix. Pthalic anhydride was used in this way by Sparer *et al.* (1984). These authors were able to show that the release of a model compound, methylene blue, correlated with the surface erosion of the polymer matrix.

The lifetimes of devices using acid anhydrides as excipients could be varied within a range of hours to about one month. However a device with a lifetime of more than one month has been achieved by Heller *et al.* (1985). This involved the use of a basic excipient, magnesium hydroxide, which had sufficiently low solubility to avoid substantial uptake of water. Heller and Himmelstein (1985) have pointed out that no adverse tissue reaction have been observed during *in vivo* release experiments but genuine toxicological studies have not been performed.

5.5 Poly (d-β-hydroxybutyrate), (PHB)

5.5.1 Biosynthesis of PHB and P(HB/HV) copolymers

PHB is an optically active aliphatic polyester consisting of d-β-hydroxybutyric acid as repeating units. It is usually obtained by bacterial biosynthesis and thus has an advantage over synthetic polymers in that there are no residual catalysts or monomers in the bulk polymer. Providing that solvent-based extraction is carried out carefully, a pure product can be obtained.

PHB can be found in many bacteria. Its function is to act as an energy reservoir, rather like glycogen or fat reservoirs in animals (Dawes and Ribbons, 1964; Dawes and Senior, 1973). PHB accumulates as small spherical granules, 0.1 - 0.7 nm in diameter and, under appropriate condition, PHB can account up to 75% w/w of the dry weight of a bacterial culture (Senior, 1984). The synthesis of PHB in bacteria has been discussed by Dawes and Senior (1973) and in simple terms, PHB is produced in response to an imbalance of growth brought about by nutrient limitation.

Imperial Chemical Industries (ICI) UK have patented a fermentation method for the mass production of PHB. This fermentation process involves continuous growth of *Alcaligenes sp.* under nitrogen limitation condition. The species of *Alcaligenes* used are *faecalis*, *ruhlandi*, *latus*, *aquamarinus* and *eutrophus* (ATCC No. 8750, 15749, 29712, 14440 and 17699 respectively). These organisms, of which *eutrophus* is preferred, accumulate PHB during the growth phase while undergoing aerobic fermentation using a variety of substrates that supply hydrogen and carbon dioxide. Mutant strains of *A. eutrophus* are able to utilise glucose which is the preferred raw substrate in terms of cost. The application of PHB as a biodegradable

commodity thermoplastic currently is limited by its cost which prevents it competing with cheap polymers (polyethylene, propylene, etc.). However the cost of the polymer for specialized applications, such as pharmaceutical formulations, is not likely to be prohibitive.

On a smaller scale production, Doi *et al.* (1986) have described the biosynthesis of PHB and P(HB/HV) copolymers by culturing *Alcaligenes eutrophus* H16 in a nitrogen-free mineral medium containing organic acids as carbon sources. PHB was synthesized in the presence of sodium acetate where as P(HB/HV) copolymers were prepared in a medium containing a mixture of sodium acetate and sodium methylacetate. Higher contents of β-hydroxyvalerate can be prepared by culturing the strain in a medium containing only sodium methylacetate.

5.5.2 Physicochemical properties.

The crystal structure of solid PHB has been examined by Cornibert and Marchessault (1972) and also by Yokouchi *et al.* (1973). These studies suggested that the conformation of crystalline PHB molecules was a 2_1 helix. Marchessault *et al.* (1970), in another study reported that the helical structure of PHB was retained in chloroform, trifluoroethanol and ethylenedichloride but the conformation of PHB in dichloroacetic acid was found a random coil. These conclusions were based on viscosity and optical rotary dispersion (ORD) experiments where PHB in solution underwent a sharp change (similar to helix coil transitions of polypeptides) when the binary solvent composition (dichloroacetic acid : ethylene dichloride) was varied at a fixed temperature. However, their viscosity experiments indicated that the exponent α in the Mark Houwink equation for PHB in chloroform was

more representative of a random coil configuration.

Akita *et al.* (1976) reported evidence to support the hypothesis that PHB is a random coil in both chloroform and trifluoroethanol. These authors used samples of PHB with narrow polydispersities in contrast to the samples used by Marchessault *et al.* whose samples had Mw/Mn =6. Akita *et al.* (1976) used viscometric and light scattering techniques to demonstrate that PHB exists as a random coil in both solvents.

Recently, Doi *et al.* (1986) studied the conformation of PHB in chloroform using ^{13}C-nuclear magnetic resonance spectroscopy. Their results suggested that the PHB molecule was not rigid but rather flexible in chloroform supporting the random coil hypothesis.

Lundgren *et al.* (1965) characterized PHB extracted from different bacteria by X-ray diffraction. Samples of PHB extracted from various bacteria had similar X-ray diffraction spectra. The only difference between samples were in intrinsic viscosity (i.e. molecular weight) due to the difference in the polymerisation of PHB in various bacteria.

The chemical synthesis of P-dl-HB has been described by Agostini *et al.* (1971). This study suggested that the degree of crystallinty of P-dl-HB was similar to that of P-d-HB. This property is in marked contrast to the properties of P-l-LA and P-dl-LA where the former is 37% crystalline but the latter is totally amorphous.

The glass transition temperature of PHB was found to be in the range -4 to 1°C. This value was obtained from molten PHB using the dilatometric method (Barham *et al.*, 1984). The crystallinity of PHB lies in the range 60-90% as determined by density measurements, with a heat of fusion for 86% crystalline PHB of 146 J/g (Barham *et al.*, 1984).

Marchessault *et al.* (1981) found that PHB molecules in the weight range 1K-8K had similar heats of fusion. The values obtained by Marchessault *et al.* (1981) were in good agreement with those obtained by Barham *et al.* (1984). This indicates that low molecular weight polymers have the same equilibrium crystallinity as high molecular weight polymers.

The degree of crystallinity of PHB can be reduced by incorporating d-β-hydroxyvalerate (HV) into the PHB chain (Holmes, 1985). Mitomo *et al.* (1986) determined the degrees of crystallinity of a series of copolymers. When the HV content was increased from 0% to 30 mole %, the crystallinity apparently decreased from 75% to 39% for solution grown crystals. However Bloembergen *et al.* (1986) reported that for solution precipitated and aged P(HB/HV) samples, the degree of crystallinity was independent of HV content, but the rate of crystallization of the samples was dependent upon and retarded by increasing HV content. It is possible that the measurements reported by Mitomo *et al.* (1986) were made before equilibrium crystallinity had been achieved. Further work is required to establish the crystalline nature of P(HB/HV) copolymers.

Bluhm *et al.* (1986) studied the effect of copolymer composition on the melting temperature using HV contents from 0% to 47 mole %. The melting point decreased to a minimum at 30 mole % HV and then increased. To explain this phenomena, these authors introduced the concept of isodimorphism which explained their results in terms of two crystalline phases within the bulk polymer. At high HV contents, the bulk sample apparently included an HV dependent crystalline phase which raised the onset of melting.

Copolymerization of HB and HV leads to changes in the mechanical properties of PHB films. Akhtar *et al.* (1987) reported the mechanical properties of copolymer films containing 0%, 6.6%, 12.6% and 20% HV, determined using a static tensile test. Increase in HV content resulted in tougher, less brittle and more pliable materials. Mechanical properties were not affected by molecular weight above Mw = 200,000 although films cast from solution were fragile if the molecular weight was much below Mw = 200000

5.5.3 Random degradation of PHB

An ability to control the molecular weight of PHB by degradation in non-aqueous solution has been an integral part of the present study. It is of interest to consider whether or not this degradation occurs by random chain scission. (Majid *et al.*, 1987). The kinetics of random chain scission have been derived by Jellinek (1978). The theory is based on the rupture of main chain links according to the laws of probability. Jellinek (1978) derived equations which described the random degradation, mathematically, using the following assumptions.

- the polymer sample was actually monodisperse (i.e. it consisted of linear chains of one length only)
- the rate of scission of chain links was directly proportional to the number of chain links present at any time t of the scission process. The main chain links were of equal strength and were equally likely to break under the scission process.

The degree of degradation, α , which represents the probability of breaking one link in the original chain at time t is given by

$$\alpha = \frac{\bar{s}}{DP_o - 1} \quad \ldots\ldots (5.1)$$

where $\bar{s}$ is the average number of main chain links which have been

broken in one original chain at time t.

DP_o is the original chain length of the monodisperse polymer sample. i.e. the degree of polymerisation of the polymer. If DP_o is large, equation 5.1 reduces to

$$\alpha = \frac{\bar{s}}{DP_o} \quad \ldots\ldots \quad (5.2)$$

Thus the rate of breaking main chain links, n, in a closed system at time t is given by

$$\frac{-dn}{dt} = kn \quad \ldots\ldots \quad (5.3)$$

The number of links, n_o, present in the system at time t = 0 is related to n at any stage of the scission process as follows:

$$n = n_o - \alpha n_o$$
$$= n_o (1 - \alpha) \quad \ldots\ldots \quad (5.4)$$

Inserting equation 5.4 into 5.3, we then have

$$\frac{-d\, n_o(1 - \alpha)}{dt} = k\, n_o(1 - \alpha) \quad \ldots\ldots \quad (5.5)$$

Integrating the above equation (5.5) gives:-

$$-\ln(1 - \alpha) = k\, t \quad \ldots\ldots \quad (5.6)$$

for small values of α , equation 5.6 then becomes

$$\alpha = k\, t \quad \ldots\ldots \quad (5.7)$$

or by inserting equation 5.2 to replace α in equation 5.7

$$\bar{s} = DP_o\, k\, t \quad \ldots\ldots \quad (5.8)$$

Since number-average molecular weight is likely to be obtained experimentally, equation 5.9 is used:-

$$n_{DP_o}(DP_o-1) = n_o \quad \ldots\ldots \quad (5.9)$$

where n_{DP_o} is the number of chain of original chain length DP_o. When s links, the average for each original chain, have been scissioned, one has for time t

$$n_o = n + n_{DP_o}\bar{s} \quad \ldots\ldots \quad (5.10)$$

or

$$\bar{s} = \frac{n_o-n}{n_{DP_o}}$$

Thus the number average chain length at any time t of the scission process is given by

$$\frac{DP_{n,t}}{DP_o} = \frac{1}{\bar{s}+1} = \frac{n_{DP_o}}{n_o-n+n_{DP_o}} \quad \ldots\ldots \quad (5.11)$$

Hence

$$\frac{d}{dt}\left(\frac{n_{DP_o}DP_o}{DP_{n,t}}-n_o-n_{DP_o}\right) = k\left(n_o+n_{DP_o}-\frac{n_{DP_o}DP_o}{DP_{n,t}}\right) \quad \ldots\ldots \quad (5.12)$$

or,

$$-\frac{d(DP_{n,t})}{dt} = k(DP_{n,t}^2-DP_{n,t}) \quad \ldots\ldots \quad (5.13)$$

Integrating equation 5.13 gives,

$$-\ln\left(1-\frac{1}{DP_{n,t}}\right) = kt-\ln\left(1-\frac{1}{DP_o}\right) \quad \ldots\ldots \quad (5.14)$$

Equation 5.14 reduces for large values of $DP_{n,t}$ and DP. (i.e small α) to

$$\alpha = \frac{1}{DP_{n,t}}-\frac{1}{DP_o} = kt \quad \ldots\ldots \quad (5.15)$$

This is a useful form of the theory. From equation 5.15, it can be seen that a plot of $\frac{1}{DP_{n,t}}-\frac{1}{DP_o}$ gives a straight line with a gradient equal to

the rate constant, k, whenever random chain scission occurs.

5.5.3 Aqueous degradation of PHB and P(HB/HV) copolymers.

Recently, Miller and Williams (1987) have studied the hydrolytic degradation of PHB monofilaments in terms of changes in their mechanical properties with time. These authors concluded that there was little degradation of PHB microfilaments both *in vivo* and *in vitro*. Two P(HB/HV) copolymers (containing 8 and 17 mole % HV) were subjected to accelerated tests *in vitro*. These were stored at higher temperature (60°C and 70°C) at pH 7.4. HV content apparently retarded the rate of high temperature hydrolysis.

In the same study, PHB monofilaments were subjected to various intensities of γ-irradiation after which the degradation experiments were repeated, again by observing changes in the mechanical properties of the monofilaments. A minimum intensity of γ-irradiation that could initiate the degradation process was found (10 MRad). 20MRad caused total loss of integrity of the monofilament as a suture material even before exposure to water.

Miller and Williams (1987) found that γ-irradiation has the ability to reduce the molecular weight of the bulk polymer which subsequently increases its susceptibility to degradation. However, the molecular weight changes were not determined. These authors also reported that there was a difference in the rate of *in vitro* and *in vivo* degradation following γ-irradiation. *In vivo* degradation was more rapid. They attributed this difference to the involvement of enzymes in the degradation process *in vivo*. It should be noted that no attempt was made to study weight loss or change in molecular weight in the above study. All conclusions were based on measurements of mechanical

strength. These measurements were variable and the thickness of the microfilaments was not reported in detail.

Holland *et al.* (1987) have shown that one possible reason for the relative stability of the drawn PHB monofilaments reported by the previous authors may have been a high degree of crystallinity. This is a typical consequence of the extrusion process used to produce monofilamental fibers. The latter authors studied the *in vitro* degradation of different morphological forms of PHB including solvent cast films, melt-pressed discs, injection moulded samples and compressed tablets. These different forms were subjected to aqueous buffer solutions at pH 2.3, 7.4 and 10.6 at 37°C and at 70°C. Degradation was examined by determining the loss in weight as a function of time. The various forms of PHB had different resistances to hydrolytic attack, the compressed tablet being the least resistant. Resistance of PHB complied with the following rank order: compressed tablets < solvent cast films < melt-pressed discs < injection moulded pieces. These differences correlated with the difference in degrees of crystallinity as measured using a differential scanning calorimeter. High degree of crystallinity was associated with high resistance to hydrolytic attack. These authors also reported that the rate of degradation increased with increase in pH suggesting that the degradation mechanism was base-catalysed as would be expected for an ester hydrolysis. The degradation rate was also increased by raising the incubation temperature to 70°C.

Holland *et al.* (1987) have also studied the effect of molecular weight and copolymer composition on the hydrolysis of solvent cast films. Two molecular weights (36K and 300K) of copolymer containing 20 mole % HV were subjected to hydrolytic degradation. The high molecular weight

polymer degraded more slowly although no explanation for this finding was discussed.

Two high molecular weight copolymers (12 mole % and 20 mole %, Mw = 350K and 300K respectively) showed different degradation rates; the 20 mole% HV polymer degraded more rapidly. This may have been due to a difference in the crystallinity of the copolymers. The 20 mole % HV polymer, whilst being more hydrophobic, was less crystalline which may have promote degradation.

5.5.5 Drug release from PHB and P(HB/HV) copolymers.

Korsatko *et al.* (1983a, 1983b) have prepared PHB matrix tablets as sustained release formulations by compressing homogenous mixtues of PHB and 7- hydroxyethyltheophyline (HET); a model hydrophilic drug. The tablets were 2.0mm in thickness and 6.0 mm in diameter. A variety of drug loading were studied between 5% and 80% w/w. The molecular weight of PHB used was 260,000. *In vitro* release studies were performed in non-sterile 0.9% NaCl at 37°C. When drug loadings were below 30%w/w, the release of drug took place over periods of up to 50 days whereas with drug loadings of 60 - 80% w/w the release was completed within 24 hours. Release of drug occured initially from the surface and then proceeded by diffusion through the aqueous pores formed by water penetration of the matrix of the tablet. The degradation of PHB had no significant effect on the release of HET *in vitro.*

A comparison of *in vitro* and *in vivo* release rates from tablets containing 10% HET indicate that the *in vivo* release rate was slower than that measured *in vitro.* These authors postulated that a lower supply of aqueous fluid around the implanted tablets *in vivo* could have caused the reduced release rate However, the possibility of the release rate being increased *in vitro* due to microbial degradation of PHB cannot

be ruled out. Experience at Bath has indicated that non-sterile distilled water unless absolutely fresh can be contaminated with microorganisms which are capable of rapid degradation of PHB. This could have explained the higher release of HET *in vitro*.

Bissery *et al.* (1984) have prepared PHB microspheres containing an anticancer drug, lomustine [1-(2 chloro-ethyl)-3-cyclohexyl-nitrosourea (CCNU)]. A solvent evaporation method was used which involved dissolving the drug and PHB in chloroform and then emulsifying this solution in an aqueous solution of polyvinyl alcohol. The emulsion was then stirred into a solution of methylcellulose and mixed until the chloroform had completely evaporated. Microspheres (1-13μm) were obtained by filtration. Microscopic examination revealed that each sample of PHB microspheres was composed of a mixture of individual particles and assorted aggregates. Thus, the particles were not entirely spherical.

In vitro and *in vivo* release of CCNU was studied. In this buffer, pH 7.2 at 37°C, more than 90% of the loaded drug (7.4% w/w) was released in 10 hours. Comparison of this release rate with that from P-dl-LA microspheres containing CCNU, prepared by the same method, showed that the P-dl-LA microspheres had a longer sustaining effect (60% of the loaded CCNU being released in 90 hours). The authors were not able to explain these effects. Their *in vivo* studies involved monitoring the distribution of ^{14}C-labelled PHB microspheres (1-12μm) following an intravenous injection into mice. Thus these authors had a targetting application in mind rather than conventional implantation. One and seven days after injection, most of the radioactivity was found in the lungs, liver and spleen. Presumably, the

larger particles were trapped in lung capillaries and the smaller particles taken up by the reticuloendothelial system. The anticancer activity of CCNU-loaded microspheres was assessed in mice bearing AKR leukemia. Intravenous injection of PHB microspheres containing the anticancer drug had little effect on increasing the life span of the animals.

Juni *et al.* (1986) have prepared PHB microspheres containing an anthracycline anticancer drug, aclarubicine hydrochloride, by a similar solvent evaporation process. These authors dissolved the required drug, an additive and PHB in methylene chloride. The solution was then dispersed in 1% gelatin solution dissolved in 0.1M phosphate buffer, and then stirred to evaporate off the methylene chloride. The diameter of microspheres obtained in this case were considerably larger; in the range 50-400μm. *In vitro* release studies from microsphere containing 13% aclarubicine hydrochloride (170μm in mean diameter) showed that only 10% of the drug was released in 5 days in an isotonic sodium chloride solution at 37°C. The release rate was enhanced by the inclusion of fatty acids in the microspheres. Accelerated release of the drug was apparent when the number of carbon atoms in the fatty acid chain was greater than 12; the longer the carbon chain, the faster the release rate. The release of the drug could be enhanced further by using an ester of a fatty acid as the adjuvant.

Brophy and Deasy (1986) have prepared PHB microspheres containing sulphamethizole by another solvent evaporation process. The amount of drug incorporated into the matrix was higher than the solubility of the drug in the PHB matrix such that the drug existed as a dispersion in the matrix. Their *in vitro* studies showed that release rate was influenced by the particle size of the dispersed drug. Fine

particles led to more rapid release.

Brophy and Deasy (1986) also showed, in agreement with the general properties of matrix systems, that an increase in drug content caused an increase in the fraction of drug released per unit time. In common with other systems, an initial rapid release was caused by diffusion of drug from the surface of the microparticles. Coating the particles with PLA reduced the burst effect observed from non-coated particles.

Brophy and Deasy (1986) also studied the release of sulphamethizole from P(HB/HV) copolymers containing 17% and 30 mole% HV. Higher HV content resulted in slower release of the drug. The authors explained that copolymerization may have resulted in better alignment and deposition of the drug in the matrix, thereby reducing its diffusivity. Release of the drug was essentially due to the diffusion processes and was independent of polymer degradation.

Gould *et al.* (1987) studied the effect of molecular weight of model hydrophilic drugs, fluorescein labelled dextrans, from direct compressed tablets of P(HB/HV) copolymers. Two copolymers were used containing 12 and 20 mole % HV with molecular weights quoted as 350,000 and 300,000 respectively. The *in vitro* release of the dextrans was dependent on the copolymer composition and also on the molecular weights of the dextrans. The authors found that increasing the HV content from 12 to 20 mole % resulted in lower release rates of the drugs. This was thought to be due to the high compressibility of the 20 mole % copolymer although the molecular weights of the two polymers were also different. Increase of the molecular weight of the dextrans from 4000 to 40,000 resulted in an increase in the release rate from both copolymers. Gould *et al.* (1987) proposed that the release of dextran was controlled by the

porosity of the matrix and the rate of the fluid influx into the matrix. Fluid influx was induced artificially by incorporating either lactose or microcrystalline cellulose into the matrix. Release rate was increased by both adjuvants. Lactose had a greater effect than microcrystalline cellulose. This was explained by the formation of a porous network by lactose rather than the microporous (wicking) network formed in the presence of microcrystalline cellulose.

The nature of the polymer-drug matrices described above were varied. Clearly the manner in which the drug is mixed with the polymer, the effects of its polarity and crystallinity are important determinants for the rates and mechanisms of release. These factors require further study to aid in the design of drug delivery systems.

5.5.6 *In vivo* degradation and biocompatibility of PHB.

Korsatko *et al.* (1984) studied the biocompatibility of compressed PHB tablets implanted in mice. The dimensions of the PHB tablets were 2.0 mm in thickness and 6.0 mm in diameter with a mean weight of 60.0mg. There was a fairly constant degradation rate throughout a 20 week period. The rate constant for degradation was reported to be 2.21 x 10^{-1}mg/week. These authors assumed that enzymatic processes had contributed to degradation of the polymer resulting in monomeric β-hydroxybutyric acid. Histological examinations showed that there was an acute inflammation at the site of implantation followed by continuous mild inflammation throughout the 20 weeks period. The inflammatory response was considered to be an important influence on the degradation rate of PHB in that it would have provided a source of enzymes from cells of the immune system. Korsatko *et al.* (1984) also used a tissue culture technique using mice fibroblasts to determine the effect of PHB on

the cellular growth rate and their metabolic function. These experiments indicated no significant differences in cellular growth and metabolism between the control and PHB exposed cultures.

Juni and Nakano (1987a) have also reported biocompatibility studies using PHB microspheres (diameter = 100μm) implanted into the thigh muscles of rats. The inflammatory reaction was described as mild and was restricted to the implant site. Four weeks after implantation, the microspheres were encapsulated by connective tissues.

Kennedy *et al.* (1987) used microspheres of 40 μm in diameter prepared by spray-drying for biocompatibility studies. Microspheres were implanted into the thigh muscles of rats and the tissue and serum levels of acid and alkaline phosphatase were used as a monitor of inflammation and as an indicator of biocompatibility. There were transient increases of both enzyme levels in the tissue surrounding the injection site although there were no differences between test and control injections. The mild acute responses were either due to the vehicle (1% methylcellulose in phosphate buffered saline, pH7.4) or to the trauma caused by the injection itself.

Generally, PHB appears to be acceptable for implantation but there is confusion in the literature regarding the mechanisms and extent of degradation *in vivo*. A recent report of subcutaneous implantation of sutures has suggested that little or no degradation occurred after six months (Miller and Williams, 1987).

Chapter 6

DEGRADATION AND RELEASE STUDIES FROM PHB AND P(HB/HV) COPOLYMERS : MATERIALS , EQUIPMENT AND METHODS

6.1 MATERIALS

6.1.1 Chloroform.

Chloroform for the formation of PHB films and P(HB/HV) copolymer films was obtained by distilling standard laboratory reagent grade chloroform obtained from Fisons (UK). Chloroform for SEC was high performance liquid chromatography (HPLC) grade obtained from Fisons (UK). Deuterated chloroform, $CDCl_3$ was used to dissolve PHB homopolymer and P(HB/HV) copolymer samples for NMR studies. This solvent was obtained from Aldrich (UK).

6.1.2 PHB homopolymer and P(HB/HV) copolymers.

PHB and P(HB/HV) copolymers were obtained from Marlborough Biopolymers (UK). The following batches were used:

- i. High molecular weight PHB (high purity grade). Batch number Bx IC 83/2 . The viscosity-average molecular weight of this batch as determined by SEC was 720K
- ii. High molecular weight PHB (technical grade). Batch number Bx GV 9(EE). The viscosity-average molecular weight was 765K
- iii. P(HB/HV) copolymer, purchased as 6.6 mole % HV. Batch number Bx PV 7(EE). The equivalent viscosity-average molecular weight as compared to PHB was 465K

- iv. P(HB/HV) copolymer, purchased as 12.6 mole% HV. Batch number Bx PV 12(EE). The equivalent viscosity-average molecular weight as compared to PHB was 1050K
- v. P(HB/HV) copolymer, purchased as 20 mole% HV. Batch number P/V/I . The equivalent viscosity-average molecular weight as compared to PHB was 1480K

The hydroxyvalerate contents of each copolymer were determined by proton NMR (see section 6.3.9). The contents determined in this study, expressed as mole %, were as follows: (iii) 6.5% (iv) 12.3% (v) 19.2%.

6.1.3 Other materials

Methanol (analytical grade) was obtained from Fisons (UK). p-Toluene sulphonic acid (pTSA) (standard laboratory reagent) was used as obtained from Fisons (UK).

The salts for the preparation of buffer solutions, their respective grades and their sources were shown in Table 6.1.

Ethyl acetate for gas chromatography was high performance liquid chromatography grade obtained from Fisons (UK).

Tetrahydrofuran for size exclusion chromatography was high performance liquid chromatography grade obtained from Aldrich (UK).

n-Propionic acid for gas chromatography was standard laboratory reagent grade obtained from BDH (UK).

Water was freshly distilled from an all glass apparatus.

Poly(ethylene glycol) standards for calibration of size exclusion columns were obtained from Polymer Laboratories (UK). These standards were characterized by the manufacturer as having narrow polydispersity (Mw/Mn) indices. ($Mw/Mn < 1.1$)

Table 6.1: Salts for the preparation of various buffer solutions.

Buffer salts	Reagent grade	Source
Sodium carbonate anhydrous	Standard laboratory reagent	BDH (UK)
Sodium hydrogen carbonate	Standard laboratory reagent	BDH (UK)
Citric acid monohydrous	Analytical reagent	Fisons (UK)
Trisodium citrate dihydrous	Laboratory reagent	BDH (UK)
Disodium hydrogen orthophosphate anhydrous	Analytical reagent	Fisons(UK)
Potassium dihydrogen orthophosphate anhydrous	Analytical reagent	Fisons (UK)
Sodium chloride	Analytical reagent	Fisons (UK)
Sodium hydroxide	Analytical reagent	Fisons (UK)
Potassium chloride	Analytical reagent	Fisons (UK)

Methyl red which was used as a model compound for release studies from polymer films was obtained from BDH (UK).

Poly (l-lactate) (weight average molecular weight quoted as 300,000) was obtained from Polyscience Ltd (UK).

Poly (lactate-co-glycolate) (9:1 mole ratio) was obtained as a gift from Cyanamid of Great Britain (UK).

6.2 Equipments

6.2.1 Size exclusion chromatography.

Molecular weight distributions of PHB were determined using the equipment described in Chapter Four. Molecular weight distributions of copolymers were estimated as PHB equivalents by using the same techniques.

Size exclusion chromatography was also used for determination of low molecular weight degradation products of PHB. In this case, the column used was Micropak TSK 1000H obtained from Varian Associates Inc (USA). The column dimensions were 3/8" OD, 7.5 mm ID, length 30 cm. This column packing material was spherical, cross-linked styrene/divinylbenzene copolymer particles, 8-10 μm in diameter with a pore size of 40A.

6.2.2 Gas liquid chromatography.

A Perkin Elmer model F33 gas liquid chromatograph was used. The column packing for analysis of degradation products of PHB was 10% Carbowax 20M on Chromosorb W HP (mesh 100/120). This packing material was obtained from Phase Separation (UK).

6.2.3 Nuclear Magnetic Resonance Spectroscopy.

^{1}H-NMR spectra were recorded on a JEOL GX270MHz Fourier Transform (FT) nuclear magnetic resonance spectrometer.

6.2.4 Differential Scanning Calorimetry.

A Du Pont model 910 Differential Scanning Calorimeter was used in association with a Du Pont model 9900 Thermal Analyser.

6.2.5 Weighing balance.

A Mettler model AE163 digital balance enabled weighing to a precision of ± 0.01 mg. This was used to determine the dry weight of PHB and P(HB/HV) copolymer films during degradation experiments.

6.2.6 Infrared and UV spectrophotometry.

For infrared studies, a Perkin Elmer model 782 infrared spectrophotometer was used. Measurements of visible and UV absorption were undertaken using a Perkin Elmer model 550S Ultraviolet/Visible spectrophotometer.

6.3 Methods

6.3.1 Catalytic degradation of PHB in non-aqueous solution.

1 g of high molecular weight PHB (Batch number : Bx IC 83/2) was refluxed in 85 ml chloroform for 15 minutes. The dissolved polymer solution was then cooled to room temperature. The required mass of p-toluenesulphonic acid (pTSA) was added in 15 ml methanol. The chloroform/methanol solution was refluxed at 60°C during the course of a degradation experiment. The start of the experiment was taken to be when the solution started to boil.

Samples were withdrawn for immediate analysis of molecular weight distribution using SEC. Two concentrations of pTSA were investigated i.e. 0.2% w/v and 0.02% w/v. A control experiment was performed using the same procedure in the absence of pTSA. The effect of methanol concentration on the rate of degradation was studied by varying the amount of methanol from 15% v/v to 30% v/v in the absence of pTSA.

For determination of molecular weight distribution, 1ml of the refluxing solution was removed from the reaction vessel. This was diluted to 10ml with chloroform and assayed using SEC.

6.3.2 Preparation of polymer films.

PHB and P(HB/HV) copolymers, received from the manufacturer, were purified prior to film casting. 2% w/v of the required polymer was refluxed in redistilled chloroform until it had dissolved (usually less than 15 minutes). The polymer was then precipitated in the presence of excess methanol. The precipitated polymer was collected using Whatman No. 52 filter paper placed in a Buchner funnel. It was then washed with excess methanol and distilled water and dried in an oven at 40°C before use.

For the casting of PHB films, a 2% w/v polymer solution was prepared. The solution was then concentrated to a final concentration of 5% w/v PHB using a Rotary evaporator (Buchii Rotavapor model R110). For the preparation of the P(HB/HV) copolymer films, a 5% w/v solution was prepared. This solution was then concentrated by rotary evaporation to give a final concentration of 10% w/v. Polymer solutions were cast onto clean, dry glass plates using a thin layer chromatography (TLC) applicator.

The clearance setting of the TLC applicator was chosen to produce dry films of thickness 80-90 μm. The resultant cast films were dried slowly in draught-free conditions for 2 hours and then overnight in a vaccuum oven at 40°C. Films were stored at room temperature for one week prior to use.

6.3.3 Preparation of pH buffer solutions.

Buffer solutions were prepared at constant ionic strength (I = 0.153M). Ionic strength was calculated according the Equation 6.1

$$I = \frac{1}{2} \sum i^2 C \quad \ldots\ldots \quad (6.1)$$

where

i is the charge of each of the ionic species

C is the concentration of each of the ionic species in mole/dm^3

Buffer solutions for the degradation experiments were sterilized, using a bench top autoclave, at 121°C for 30 minutes prior to the degradation experiment. The following formulae were used as shown in Table 6.2

6.3.4 Degradation of polymer films in the presence of aqueous solutions.

Cast films were cut into pieces measuring approximately 2 cm by 1 cm. Each piece was weighed individually and stored. Samples used for the degradation experiments were within 0.3mg of the mean weight.

Degradation experiments were conducted as follows. 15 pieces of the cut films were divided into 3 groups, each group containing 5 pieces. The total weight of each group of five was monitored during the degradation experiment. The mean weight loss was taken as the mean of the three groups.

Table 6.2 : Formulae for preparation of buffer solutions.

pH	Types of salt used	Quantity used
5.0	Trisodium citrate dihydrous	5.71 gm
	Citric acid monohydrous	0.92 gm
	Sodium chloride	2.38 gm
	Distilled water to	1000 ml
7.4	Disodium hydrogen orthophosphate anhydrous	6.28 gm
	Potassium dihydrogen orthophosphate anhydrous	1.36 gm
	Sodium chloride	0.67 gm
	Distilled water to	1000ml
10.0	Sodium carbonate anhydrous	1.59 gm
	Sodium hydrogen carbonate	0.84 gm
	Sodium chloride	5.76 gm
	Distilled water to	1000ml
10.5	Sodium carbonate anhydrous	1.84 gm
	Sodium hydrogen carbonate	0.17 gm
	Sodium chloride	5.96 gm
	Distilled water to	1000 ml
11.0	Disodium hydrogen orthophosphate anhydrous	3.55 gm
	Sodium hydroxide	0.32 gm
	Sodium chloride	4.15 gm
	Distilled water to	1000ml

Each piece of film was identified and placed in a 30 ml screw-capped specimen tube in the presence of 20 ml of the required buffer solution. As well as the aforementioned 15 pieces, another set of 10 pieces were treated in the same manner for each degradation experiment. These ten pieces were used to study changes in molecular weight and crystallinity during the degradation process. Samples removed for crystallinity studies were stored at -80°C until DSC was performed. Buffer solutions were replaced at least once weekly and after every weight determination.

Degradation experiments were performed at 37°C, to simulate physiological temperature, and at higher temperatures to enable study of degradation at an accelerated rate. Samples were stored at physiological temperature, 37± 1°C, in a thermostatted room.

High temperature experiments were carried out in ovens (usually Gallenkamp vacuum ovens) set at the appropriate temperature. The temperature of these ovens was always within 1.0°C of the stated temperature.

6.3.5 Determination of weight loss

Samples were removed from the buffer solutions at regular intervals and were dried in a vacuum dessicator over phosphorus pentoxide for twelve hours. After drying, samples were weighed to determine the cumulative weight loss. After weighing, the individual film samples were returned to storage with fresh buffer solution.

6.3.6 Gas liquid chromatography of degradation products

1 gm of PHB was boiled with 50ml 0.1M sodium hydroxide for 24 hours to obtain alkali-soluble degradation products. The solution was filtered and the filtrate acidified to pH 1.0 (using 1M hydrochloric acid

solution) to ensure that carboxylic acid derivatives were unionized.The solution was extracted twice with 50ml ethyl acetate. The ethyl acetate portions were pooled and concentrated to about 5 ml using a rotary evaporator. The concentrated product was then injected onto the gas liquid chromatograph operating under the following conditions:

injection volume:- 2 μl

oven temperature:- 100°C

injector and detector temperature:- 150°C

column:- 10% carbowax 20M on chromosorb W HP (mesh 100/120)

length : 1 metre

internal diameter : 1.75 mm.

carrier gas :- nitrogen

pressure of nitrogen used :- 15lb/in2

flow rate of nitrogen:- 15ml/min

detector :- flame ionization detector

operating condition of detector: hydrogen : 17 lb/in2

air : 25 lb/in2

A similar extraction and assay process was carried out after boiling 1g PHB in 50ml phosphate buffer (pH 7.4) for 48 hours.

The GLC column for this experiment was chosen on the basis of its reported ability to separate carboxylic acids. The resolution of the GLC method was investigated using two aliphatic carboxylic acids, (n-propionic acid and n-butyric acid) and two hydroxy acids (lactic acid and β-hydroxybutyric acid). The ethyl acetate extraction process was tested by extracting the above acids from HCl solutions using the

standard extraction procedure.

6.3.7 Size exclusion chromatography of low molecular weight degradation products.

6.3.7.1 Calibration of column.

Polyethylene glycol molecular weight standards were used to calibrate a Micropak TSK 1000H column. This column is designed to separate molecules which are soluble in tetrahydrofuran and have relative molecular masses below 1000. An infrared spectrophotometer was used as a flow-through detector as described in section 3.2.

The infrared spectrum for poly(ethylene glycol) was obtained by placing a liquid oligomer between sodium chloride cells. The strong peak at 2930 cm^{-1} which corresponded to the C-H stretching band, was used to detect the elution of poly(ethylene glycol).

Standards were dissolved in tetrahydrofuran (0.5% w/v) and 20 μl of each solution was injected onto the column to obtain a calibration plot.

6.3.7.2 SEC of non-aqueous degradation products.

5 gm of low molecular weight PHB (approximately 20K) was refluxed in 90ml chloroform. 2 gm p-toluene sulphonic acid (pTSA) was added in 100ml methanol. The mixed solution was refluxed for 3 days. During this period, samples were taken for analysis of molecular weight distribution. The chloroform and methanol were removed from these samples by rotary evaporation until a viscous liquid was obtained. 0.1ml of the viscous liquid was dissolved in 10ml tetrahydrofuran (THF). This solution was diluted 1 in 10 in THF before injection onto the SEC column.

The aqueous solubility of the non-aqueous degradation products of

PHB was examined as follows. 3 ml of the viscous liquid referred to above was mixed with 100ml distilled water. The mixture was shaken for 5 minutes and filtered through a Whatman membrane filter type WCN (pore size = 0.45 μm). The water was removed from the filtrate using a rotary evaporator. The remaining liquid was collected and about 0.1 ml was dissolved in THF, diluted 1 in 10 as before and injected onto the SEC column.

6.3.7.3 SEC of aqueous degradation products

1 g PHB was boiled with 50ml of 0.1M sodium hydroxide for 3 days. The solution was filtered through Whatman No. 1 filter paper to remove the suspended polymer. The filtrate obtained was acidified to pH 1.0 using 1M hydrochloric acid. The acidified solution was then evaporated to dryness using a rotary evaporator. 10ml of tetrahydrofuran was added to the dried products and the solution was injected onto the SEC column.

6.3.8 Differential scanning calorimetry

6.3.8.1 Introduction.

Differential scanning calorimetry (DSC) was used to study the melting behaviour of PHB homopolymer and PHB/PHV copolymers. In addition DSC was used to provide estimates of polymer crystallinity.

In the event of a thermal transition occuring within the sample pan, the DSC is required to supply different quantities of heat to the sample and reference pans to maintain isothermal condition between the two pans. This thermal change is equivalent to the energy absorbed or evolved and is represented by the peak area of a DSC thermogram.

The peak areas for any transition can be quantified provided the instrument has been calibrated with a reference material of known heat of fusion.

The degree of crystallinity of a polymer can be estimated using equation 6.2, provided that the heat of melting for a 100% crystalline polymer is known.

$$\text{percent crystallinity} = \frac{\Delta H_m \text{ of semicrystalline polymer}}{\Delta H_m \text{ of 100\% crystalline polymer}}$$

6.3.8.2 Experimental methods

In this study the differential scanning calorimeter was calibrated with indium. (ΔH_m= 28.47 KJ/kg) . Approximately 3 mg polymer was accurately weighed into aluminium pans using a microbalance and the samples were covered with aluminium lids. Test samples were placed in one DSC cell and an empty aluminium pan was placed in the other cell as the reference. The pans were heated from ambient temperature to 220°C at a heating rate of 10°C/min unless otherwise stated. The values of heat of fusion, onset and peak melting temperatures were obtained using the computerized thermal analyser.

6.3.9 Nuclear Magnetic Resonance spectroscopy.

50mg PHB homopolymer or P(HB/HV) copolymers were dissolved in deuterated chloroform and the spectra of the polymers were determined using ^1H nuclear magnetic resonance. These spectra (Figures 6.2 to 6.5) used to determine the hydroxyvalerate composition of the copolymers supplied by their manufacturer. Figure 6.2 shows the NMR spectrum of the homopolymer, PHB and the assigned chemical shift of various proton groups of PHB. Figures 6.3 to 6.5 represent the NMR spectra of copolymers with increasing hydroxyvalerate (HV) content.

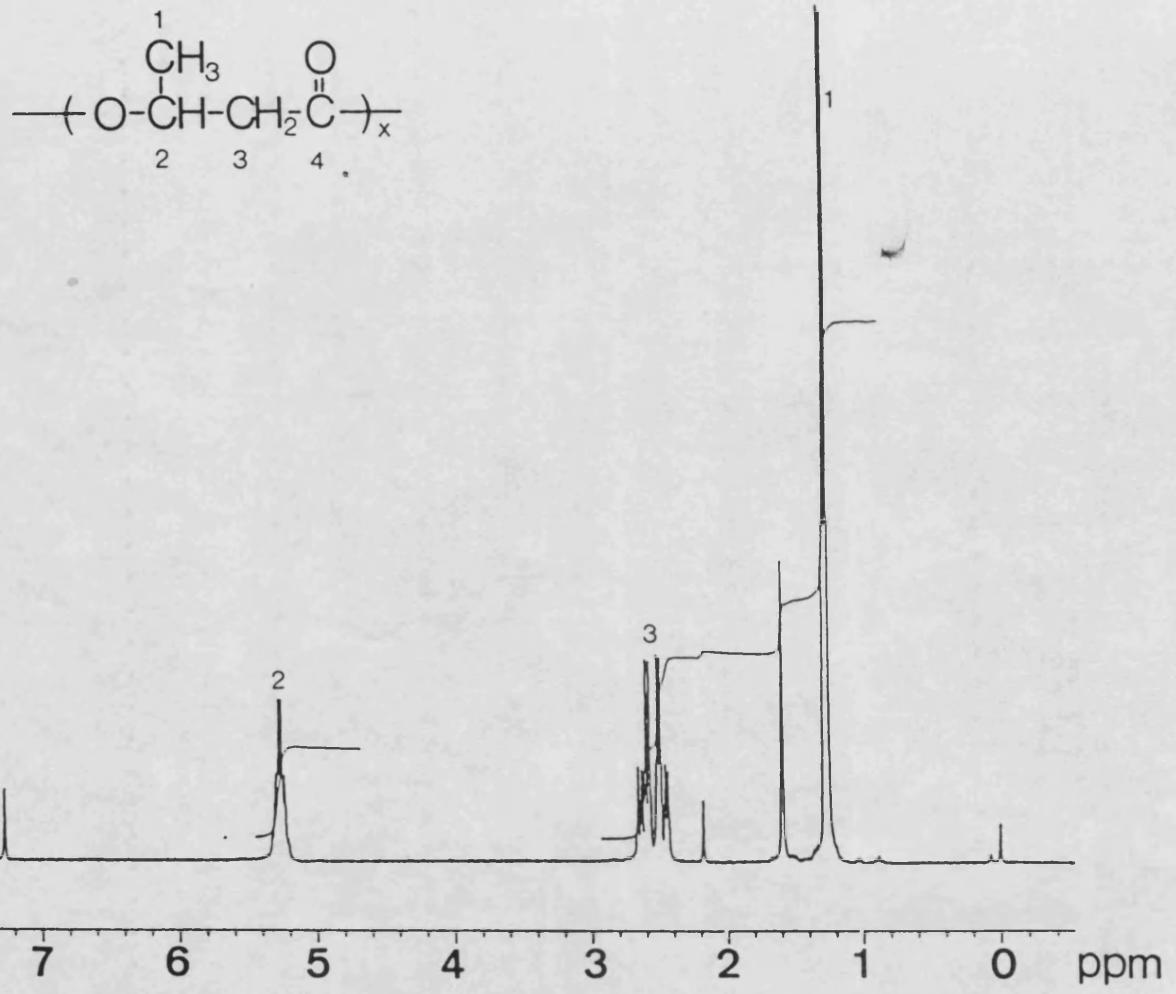

Figure 6.2 :- 270 - MHz ^{1}H NMR spectrum of PHB homopolymer in dueterated chloroform. Chemical shifts are ppm downfield from Me_4Si.

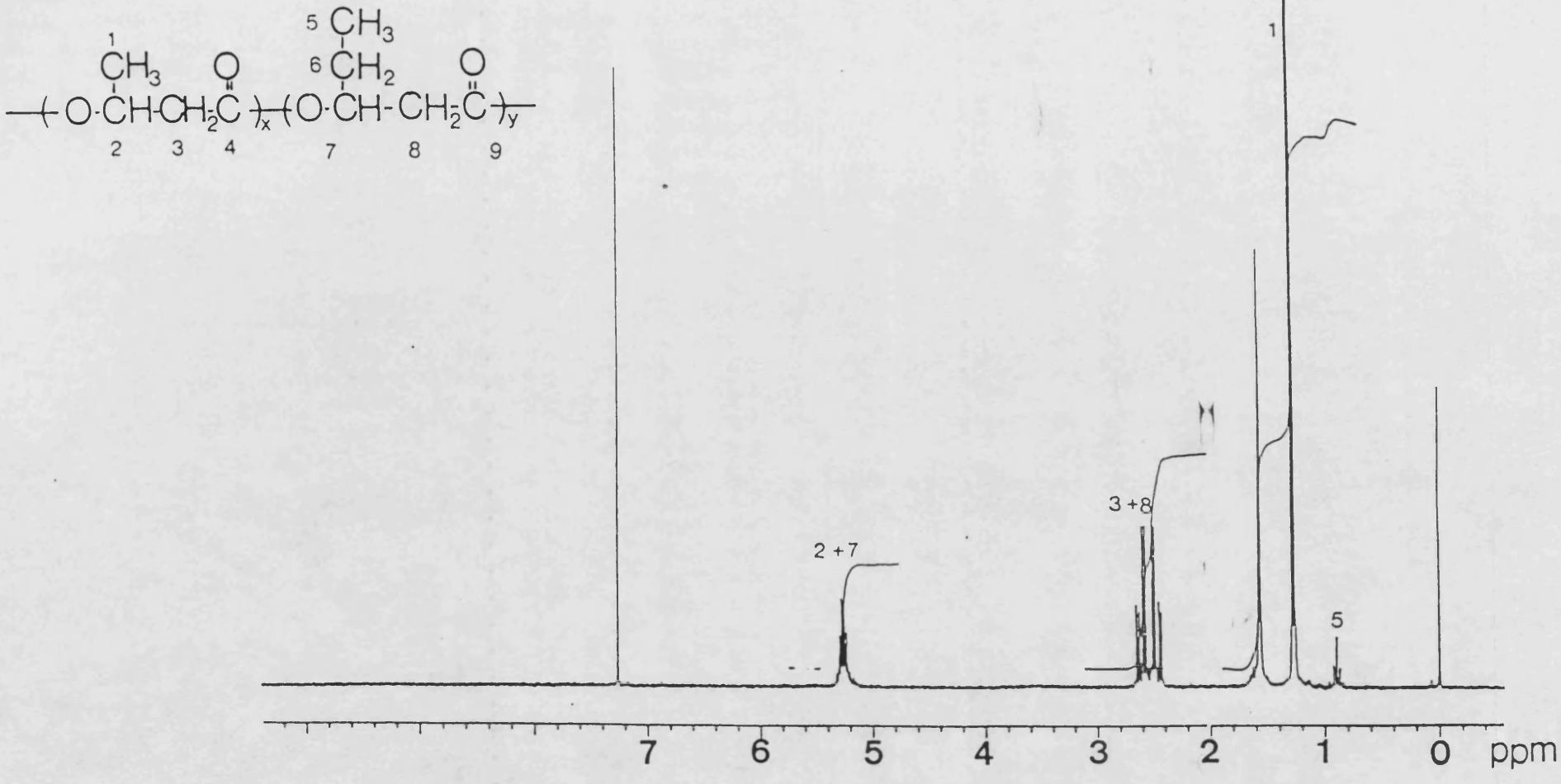

Figure 6.3 :- 270 - MHz ^{1}H NMR spectrum of a copolyester containing β-hydroxybutyrate and β-hydroxyvalerate units in dueterated chloroform. Chemical shifts are ppm downfield from Me_4Si. The amount of HV unit = 6·5 mole %.

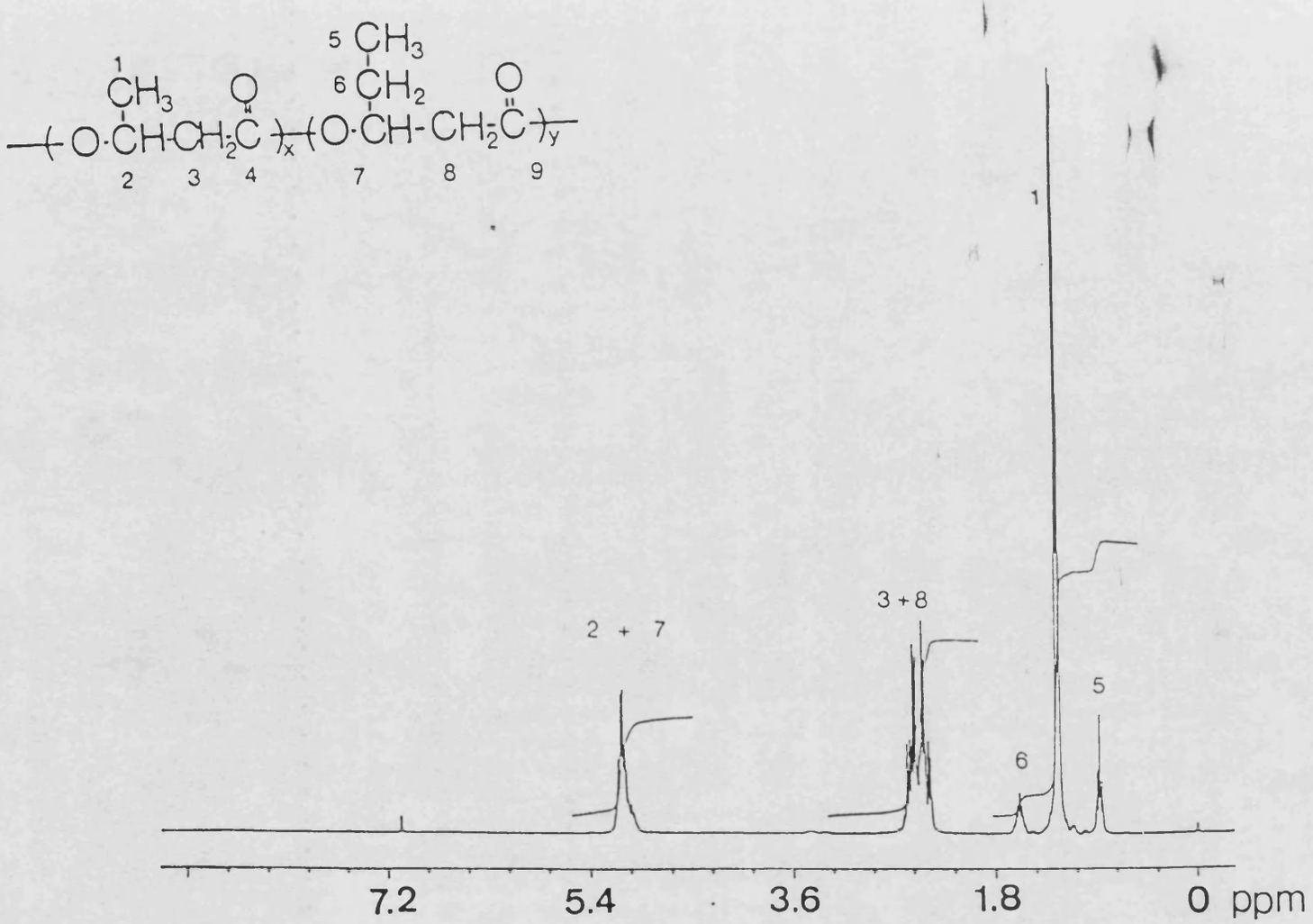

Figure 6.4 :- 270 - MHz ^{1}H NMR spectrum of a copolyester containing β-hydroxybutyrate and β-hydroxyvalerate units in dueterated chloroform. Chemical shifts are ppm downfield from Me_4Si. The amount of HV unit = 12·3 mole %.

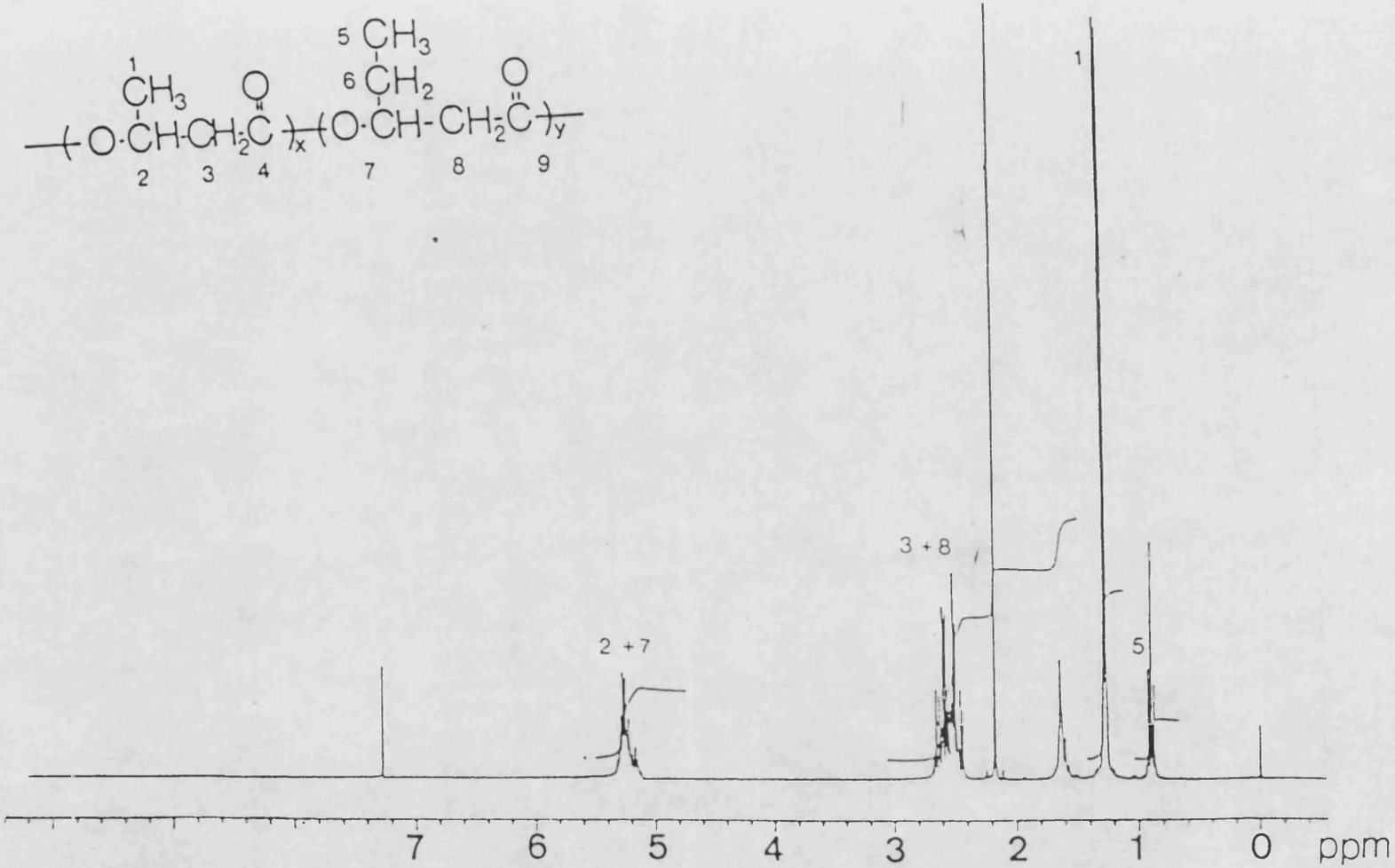

Figure 6.5 :- 270 - MHz ^{1}H NMR spectrum of a copolyester containing β-hydroxybutyrate and β-hydroxyvalerate units in dueterated chloroform. Chemical shifts are ppm downfield from Me_4Si. The amount of HV unit = 19·2 mole %.

The amount of HV was calculated by integrating the areas under the methyl proton peaks for HV and HB. This amount of HV, expressed as mole percent of HV, was obtained by dividing the area of peak which correspond to the methyl proton of HV by the sum of areas which correspond to methyl protons of HV and HB .

6.3.10 Release of Methyl Red from polymer films.

6.3.10.1 Assays of Methyl Red in phosphate butter (pH 7.4), 0.1M sodium hydroxide and chloroform.

Methyl red was assayed by visible light spectrophotometry in both aqueous and organic solvents.

Stock solutions of methyl red in the above solvents were prepared in the range of 5×10^{-5} M . From these stock solutions, samples were taken and diluted to obtain a range of concentrations of methyl red in the appropriate solvent. The absorption spectra of methyl red in each solvent were obtained by scanning the absorption of electromagnetic radiation from 400nm to 600nm. The wavelength corresponding to maximum absorption was noted in each case and Beer-Lambert calibration plots were obtained for each solvent. Absorption coefficients from Beer-Lambert plots were used in the normal manner and the day-to-day performance of the spectrophotometer was monitored using solutions of known concentration.

6.3.10.2 Preparation of films containing methyl red.

Polymer solutions in chloroform were prepared as described in section 6.3.2 . Methyl red was dissolved in the chloroform solutions of polymers to give the desired ratio of drug to polymer. Films were cast and dried in the normal manner (section 6.3.2). The mass of methyl red

in the resultant films was determined by dissolving a known mass of film in a known volume of chloroform and assaying for methyl red using a spectrophotometric technique (section 6.3.10.1).

6.3.10.3 Release experiments.

A rectangular glass template measuring 2 cm by 7 cm was used to cut specimens from polymer films. The release of methyl red was examined using two specimens from each film. The mean cumulative mass of methyl red released from each film was calculated. Two films were prepared to represent each concentration of drug in each polymer although the exact concentratons of methyl red in films could not be replicated precisely. Release experiments were usually performed at 37°C in phosphate buffer (pH 7.4). All experiments were performed in 50ml conical flasks containing 50 ml buffer solution without agitation. The polymer was fully submerged without significant contact with the vessel walls. A separate set of experiments was performed to determine the effect of polymer degradation on the release of methyl red from various polymer films. These experiments were performed at 37°C in 0.1M sodium hydroxide which increased the rate of degradation of the polyesters.

Sink conditions were maintained throughout the release studies by ensuring that the concentration of methyl red in the aqueous phase was always lower than 1% of its solubility. It was assumed that the thermodynamic activity of methyl red in each polymer film was in excess of that in the aqueous phase.

Chapter 7

DEGRADATION AND RELEASE STUDIES FROM PHB AND P(HB/HV) COPOLYMERS : RESULTS AND DISCUSSION

7.1 Degradation of PHB in non-aqueous solution.

Degradation of PHB in non-aqueous solution to obtain a range of molecular weights of PHB was carried out in methanol-chloroform mixtures in the presence of a catalyst, p-toluenesulphonic acid (pTSA). It was of interest to determine the kinetics of degradation under the influence of the catalyst and to determine whether or not the degradation process was random. In addition, the effect of refluxing PHB in the absence of the catalyst was important. Refluxing was necessary to dissolve high molecular weight PHB, thus it was of interest to determine whether or not any changes in molecular weight occurred during 15-30 minutes refluxing in organic solvents. Size exclusion chromatography was used to monitor the degradation process as described in Part I of this thesis.

Figure 7.1.1 shows the variation in the number-average molecular weight of PHB after refluxing in methanol-chloroform mixtures in the absence of pTSA. The concentration of PHB was 1%w/v in all cases. The methanol was used as a cosolvent to allow dissolution of both PHB and pTSA. Concentrations of 15% and 30% v/v methanol were studied. Higher contents of methanol were not used as these caused precipitation of PHB as a gel. Each point on Figure 7.1.1 represents the mean Mn from two separate experiments. Standard deviations shown for the data obtained in chloroform were representation of the other data. Replicate experiments in each solvent were conducted with polymer sampled from

the same batch. The large values of standard deviation were a reflection of the polydispersity of the samples or the precision of the assay at high molecular weights. The difference between the mean values obtained in chloroform and the other solvents were a result of the use of different batches of polymer. Figure 7.1.1 indicates that there was no measurable change in Mn in any of the non-aqueous solvents after refluxing for three hours in the absence of pTSA.

Figure 7.1.2 and Figure 7.1.3 show the changes in the weight-average molecular weight and the polydispersity index, Mw/Mn, respectively during the same experiments. The variability in Mw was less than the variability in Mn. There were no significant differences in Mn or polydispersity index throughout the refluxing process. These results indicated that refluxing could be used as a means of dissolving polymer for film casting without fear of causing degradation.

Degradation of PHB in the presence of catalyst was carried out at two different concentrations of pTSA; 0.02% w/v and 0.2% w/v. The solvent used was methanol-chloroform in the ratio 15:85 (volume ratio). Tables 7.1.1, 7.1.2 and 7.1.3 show the number-average, weight-average molecular weights and degrees of polydispersity, Mn, Mw and Mw/Mn respectively, as a function of time during the degradation of PHB in the presence of 0.02% pTSA. Each sample was examined twice by SEC and the experiments were replicated to determine the sources of error.

Tables 7.1.4, 7.1.5. and 7.1.6. list the equivalent data obtained at the higher concentration, 0.2% w/v pTSA. There were no significant differences between replicate degradation experiments. The standard deviation of the assay, on replicate injection was usually within ± 5% of the mean although as one would expect the precision of the assay was a

Table 7.1.1 : Changes in the number-average molecular weight (M_n) with time for non-aqueous degradation of PHB in the presence of 0.02% w/v pTSA

Time (minutes)	Number-average molecular weight (M_n)	
	1st experiment	2nd experiment
0	182000 ± 6000	177000 ± 700
15	171000 ± 9000	176000 ± 4000
30	145000 ± 3000	149000 ± 7000
45	129000 ± 9000	138000 ± 2000
60	122000 ± 0	126000 ± 700
90	107000 ± 1000	108000 ± 700
120	97000 ± 700	102000 ± 4000
150	91000 ± 5000	88000 ± 700
180	83000 ± 0	85000 ± 0

Table 7.1.2 : Changes in the weight-average molecular weight (M_w) with time for non-aqueous degradation of PHB in the presence of 0.02% w/v pTSA

Time (minutes)	Weight-average molecular weight (M_w)	
	1st experiment	2nd-experiment
0	844000 ± 45000	761000 ± 18000
15	723000 ± 30000	692000 ± 18000
30	624000 ± 28000	604000 ± 49000
45	530000 ± 18000	532000 ± 34000
60	471000 ± 13000	465000 ± 4000
90	384000 ± 3000	398000 ± 9000
120	323000 ± 3000	339000 ± 6000
150	282000 ± 2000	286000 ± 8000
180	248000 ± 1000	254000 ± 5000

Table 7.1.3 : Changes in the degree of polydispersity (M_w/M_n) with time for non-aqueous degradation of PHB in the presence of 0.02% w/v pTSA

Time (minutes)	Degree of polydispersity ($\frac{M_w}{M_n}$)	
	1st experiment	2nd experiment
0	4.64 ± 0.09	4.31 ± 0.08
15	4.25 ± 0.06	3.95 ± 0.04
30	4.31 ± 0.11	4.05 ± 0.14
45	4.12 ± 0.16	4.01 ± 0.03
60	3.85 ± 0.11	3.71 ± 0
90	3.59 ± 0.01	3.68 ± 0.04
120	3.36 ± 0.01	3.34 ± 0.07
150	3.12 ± 0.18	3.28 ± 0.05
180	2.98 ± 0.03	2.99 ± 0.08

Table 7.1.4 : Changes in the number-average molecular weight (M_n) with time for non-aqueous degradation of PHB in the presence of 0.2% w/v pTSA

Time (minutes)	Number-average molecular weight (M_n)	
	1st experiment	2nd experiment
0	192000 ± 6000	187000 ± 16000
15	110000 ± 6000	107000 ± 0
30	49000 ± 2000	65000 ± 3000
45	39000 ± 2000	51000 ± 0
60	33000 ± 700	42000 ± 700
90	25000 ± 0	29000 ± 0
120	20000 ± 700	25000 ± 0
150	17000 ± 0	20000 ± 0
180	15000 ± 0	17000 ± 0

Table 7.1.5 : Changes in the weight-average molecular weight (M_w) with time for non-aqueous degradation of PHB in the presence of 0.2 % w/v pTSA

Time (minutes)	Weight-average molecular weight (M_w)	
	1st experiment	2nd experiment
0	836000 ± 37000	821000 ± 37000
15	418000 ± 24000	414000 ± 4000
30	154000 ± 0	214000 ± 6000
45	118000 ± 4000	151000 ± 1000
60	94000 ± 1000	118000 ± 3000
90	70000 ± 1000	82000 ± 1000
120	52000 ± 1000	64000 ± 1000
150	43000 ± 0	52000 ± 1000
180	37000 ± 1000	43000 ± 0

Table 7.1.6 : Changes in the degree of polydispersity ($\frac{M_w}{M_n}$) with time for non-aqueous degradation of PHB in the presence of 0.2 % w/v pTSA

Time (minutes)	Degree of polydispersity ($\frac{M_w}{M_n}$)	
	1st experiment	2nd experiment
0	4.36 ± 0.04	4.41 ± 0.18
15	3.81 ± 0.01	3.87 ± 0.03
30	3.18 ± 0.13	3.28 ± 0.04
45	3.06 ± 0.04	2.94 ± 0.01
60	2.89 ± 0.02	2.82 ± 0.11
90	2.73 ± 0.06	2.84 ± 0.04
120	2.64 ± 0.04	2.59 ± 0.01
150	2.56 ± 0.02	2.55 ± 0.08
180	2.40 ± 0	2.53 ± 0.07

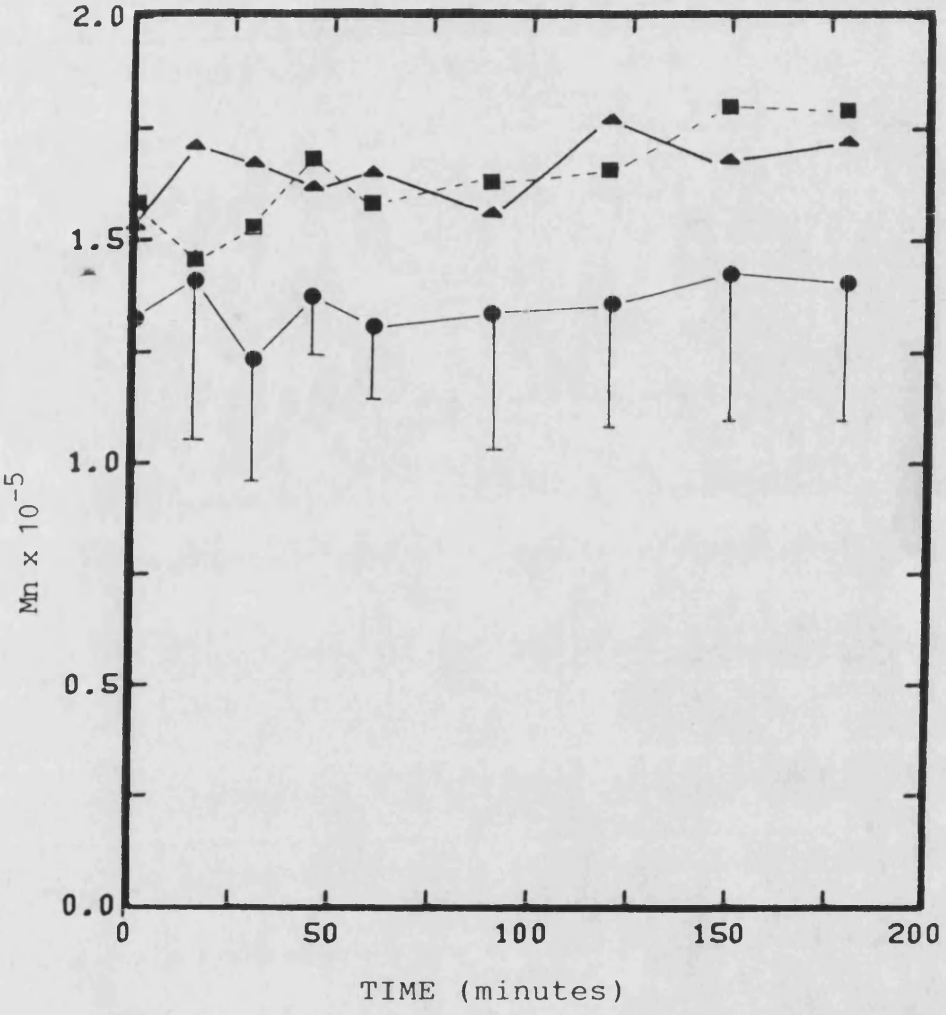

Figure 7.1.1:- The variation of the number-average molecular weight (Mn) of PHB with time during reflux in various non-aqueous solutions. (●), 1% $w/_v$ polymer in chloroform; (■), 1% $w/_v$ polymer in 85:15 chloroform:methanol (volume ratio); (▲), 1% $w/_v$ polymer in 70:30 chloroform; methanol (volume ratio)

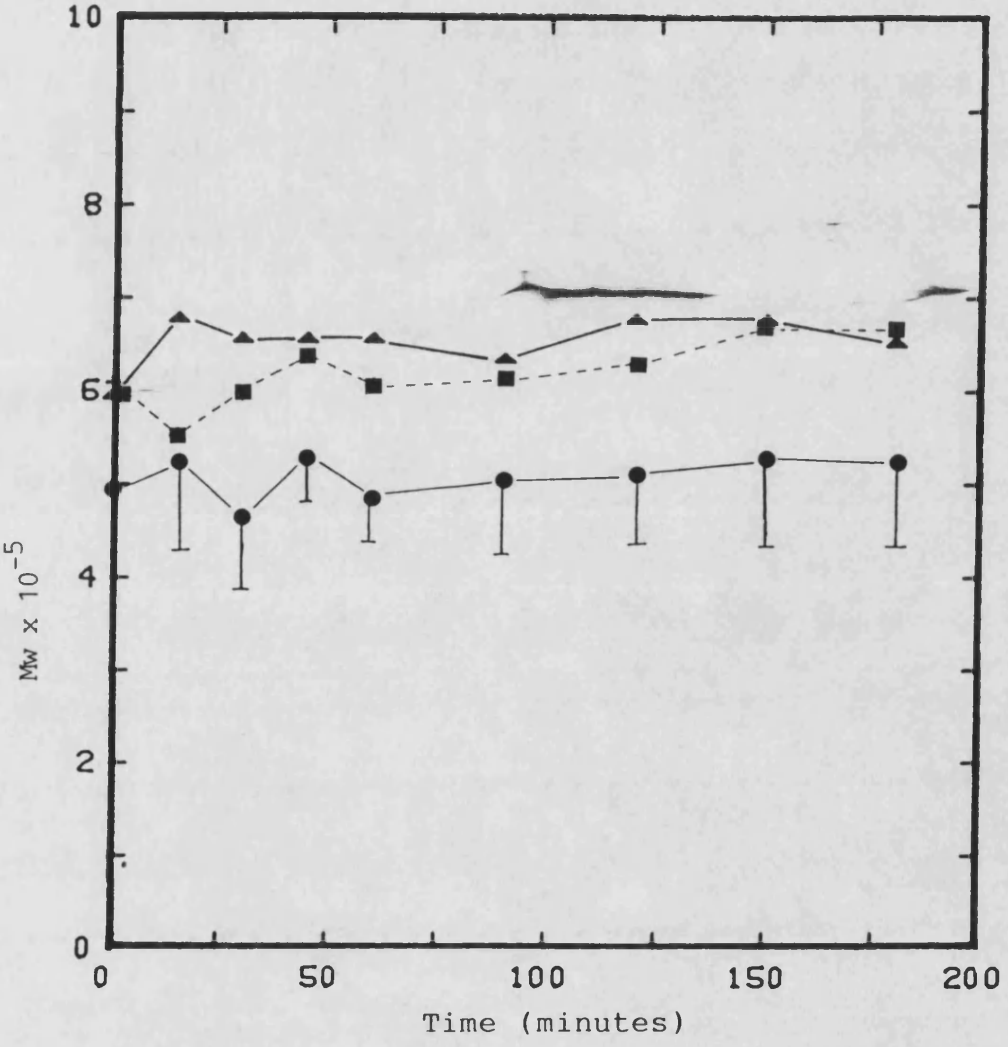

Figure 7.1.2:- The variation of the weight-average molecular weight (Mw) of PHB with time during reflux in various non-aqueous solutions. (●), 1% w/v polymer in chloroform; (■), 1% $w/_v$ polymer in 85:15 chloroform: methanol (volume ratio); (▲), 1% $w/_v$ polymer in 70:30 chloroform: methanol (volume ratio)

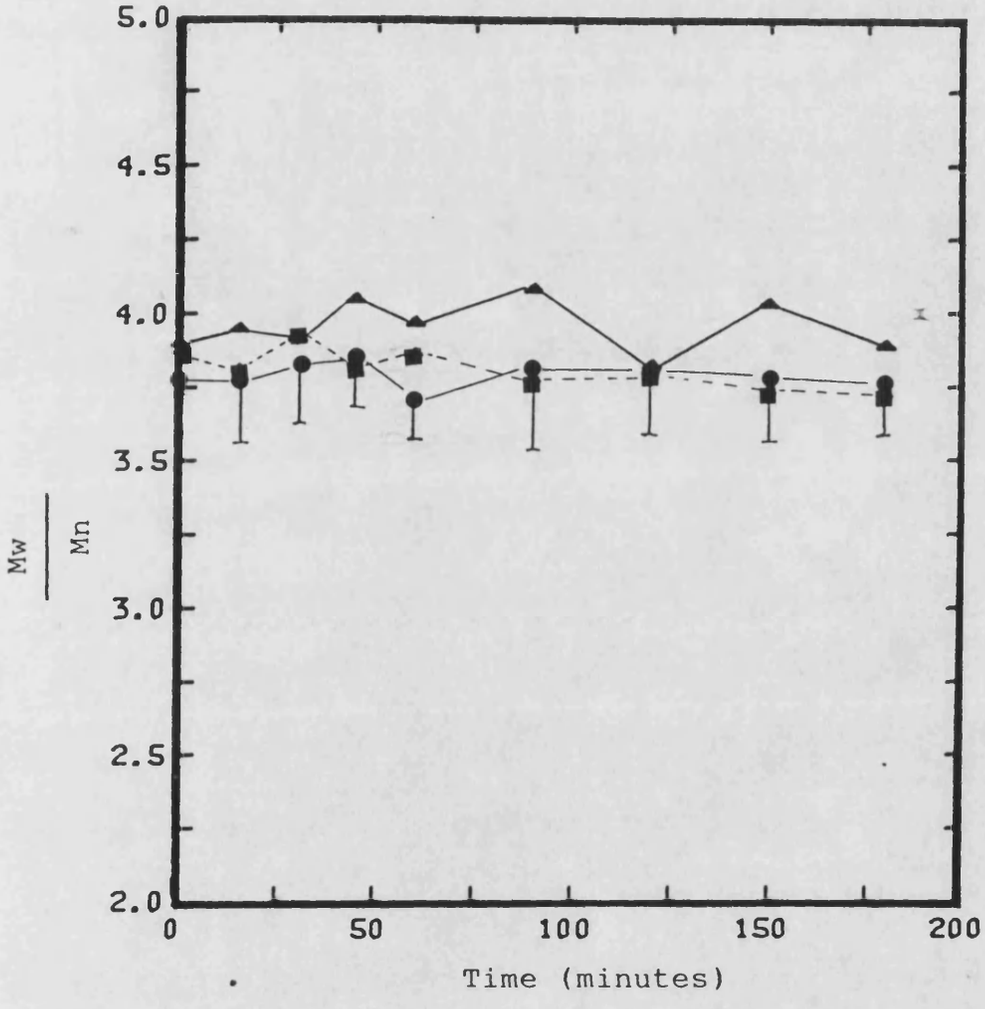

Figure 7.1.3:- The variation of the degree of polydispersity (Mw/Mn) of PHB with time during reflux in various non-aqueous solutions. (●), 1% $w/_v$ polymer in chloroform; (■), 1% $w/_v$ polymer in 85:15 chloroform: methanol (volume ratio); (▲) 1% $w/_v$ polymer in 70:30 chloroform: methanol (volume ratio)

function of retention time; longer retention was associated with greater precision.

Figures 7.1.4, 7.1.5 and 7.1.6 are plots of mean Mn, Mw and Mw/Mn respectively against time, pooling all the data for each concentration of pTSA. From these three figures, it can be seen that Mn, Mw and Mw/Mn decreased progressively with time. Closer inspection of Figure 7.1.6 suggests that the polydispersity index, Mw/Mn, was approaching a minimum value of 2 which represents the most probable molecular weight distribution (MWD). Theoretically, the most probable MWD of 2 is achieved when random chain scission is operative. Random chain scission implied that each polymeric repeat unit has the same probability of undergoing scission. If non-random chain scission was operative, the MWD would be narrower than that obtained by random chain scission usually leading to a polydispersity index is in the range of 1-2 (Scott, 1974). Figure 7.1.6. is not sufficient to show which of these processes is operative for the pTSA degradation. However a more detailed criteria can be used to establish the occurrence of random main chain scission. The theory is based on equations developed by Scott (1974). Linear polymers undergoing random main chain scission possess a Schulz-Zimm molecular weight distribution (MWD). The use of this analysis is discussed below.

Tables 7.1.7. and 7.1.8 show the relative changes in molecular weights for each degradation in the presence of 0.02% w/v and 0.2% w/v pTSA respectively. The results from each experiment were calculated separately since the initial average molecular weights differed slightly.

Figure 7.1.7. shows a plot of $\frac{u'_2}{u_2}$ against $\frac{u'_1}{u_1}$ in comparison with the theoretical Schulz-Zimm plot which should be obtained during random chain scission of a linear polymer (see

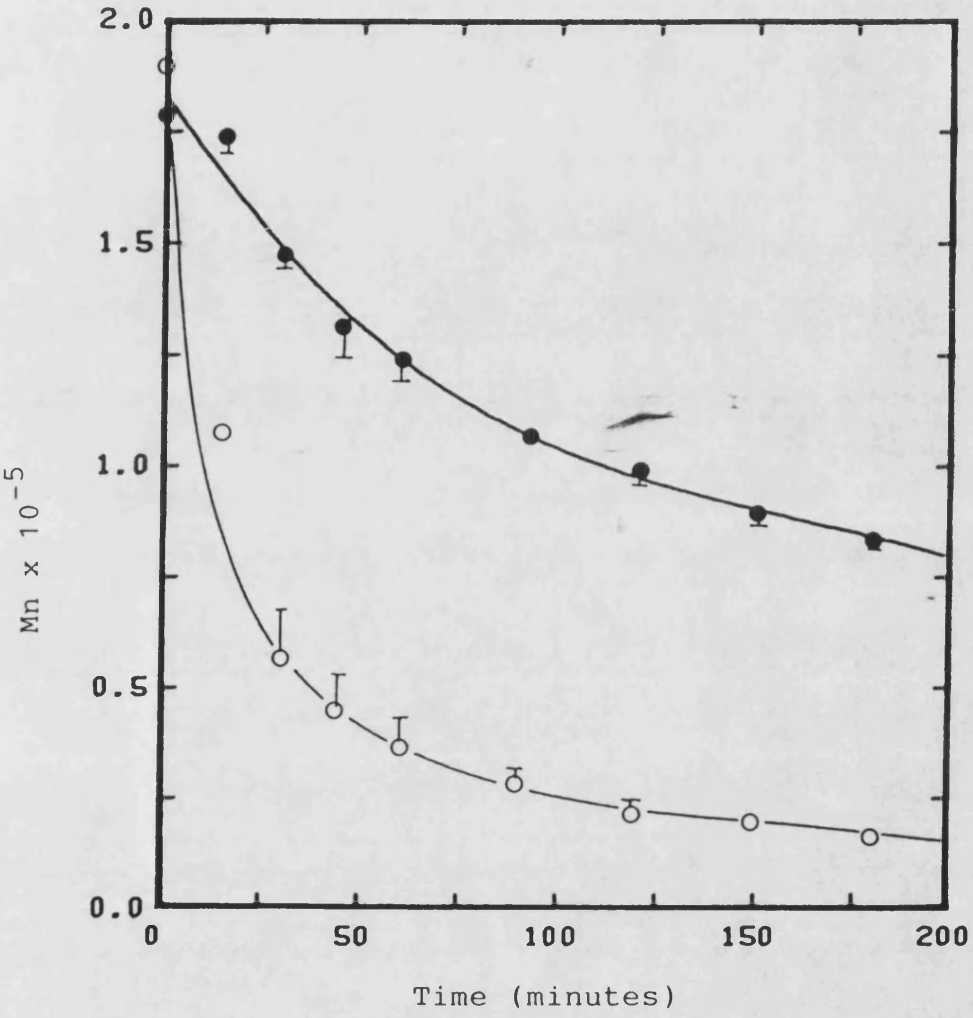

Figure 7.1.4:- Decrease in the number-average molecular weight (Mn) of PHB with time during reflux in the presence of pTSA. (○), 0·2% $w/_v$ pTSA; (●), 0·02% $w/_v$ pTSA.

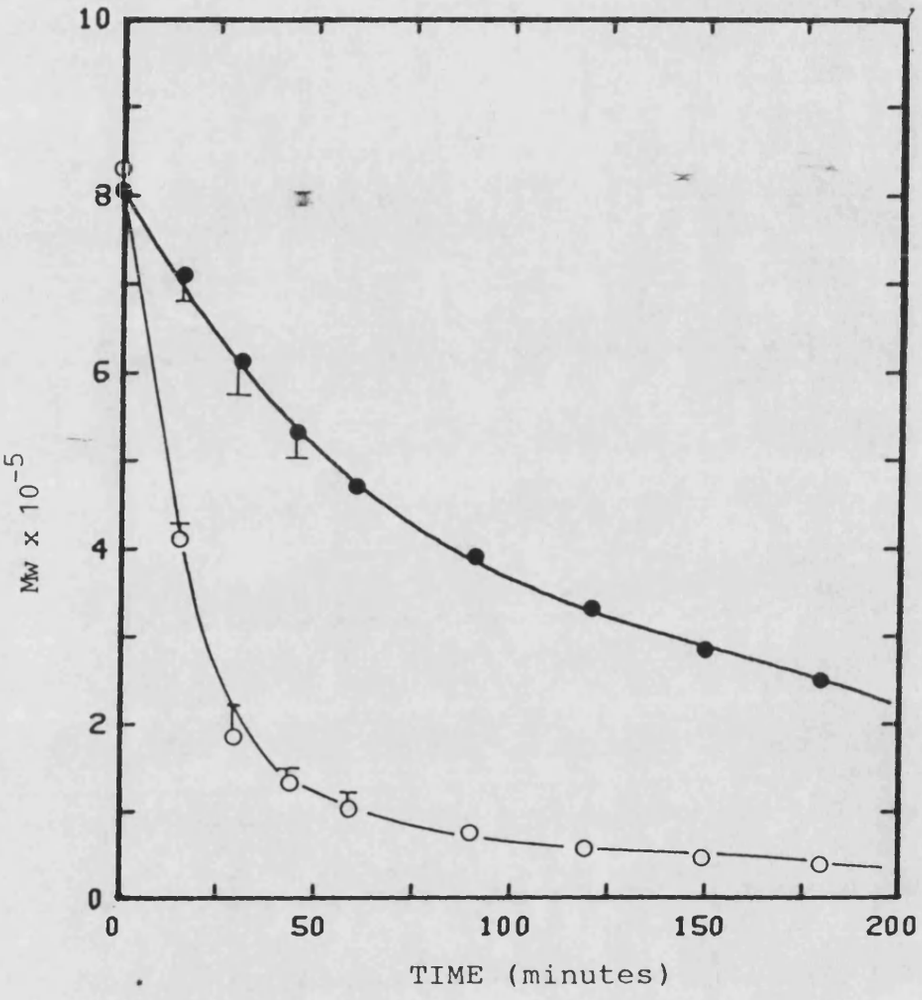

Figure 7.1.5:- Decrease in the weight-average molecular weight (Mw) of PHB with time during reflux in the presence of pTSA. (●), 0·02% $w/_v$ pTSA (O), 0·2% $w/_v$ pTSA.

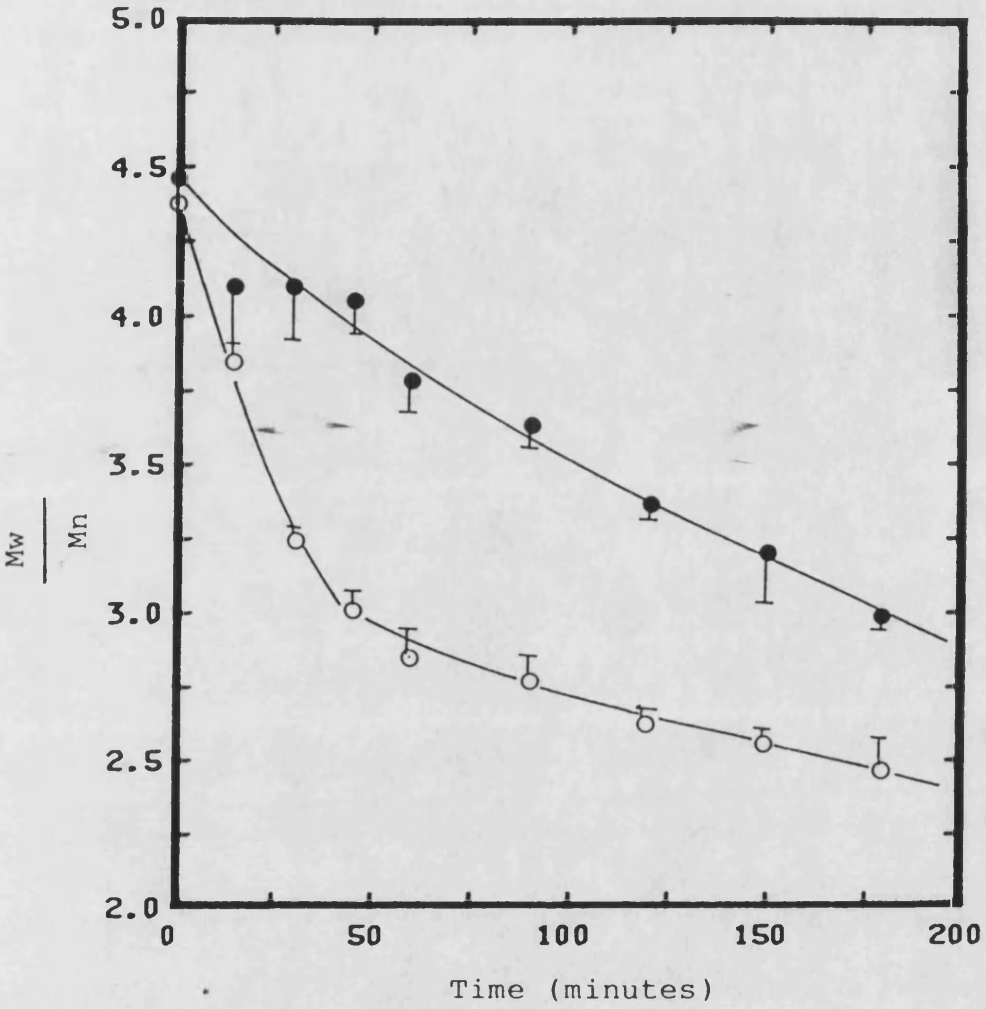

Figure 7.1.6:- Decrease in the degree of polydispersity (Mw/Mn) of PHB with time during reflux in the presence of pTSA. (●), 0·02% w/v pTSA; (○), 0·2% w/v pTSA.

Table 7.1.7 : Relative change in number-average molecular weight , u_1'/u_1 , and weight-average molecular weight , u_2'/u_2, against time (see text) for degradation of PHB in the presence of 0.02% pTSA

Time (minutes)	First experiment		Second experiment	
	$\frac{u_1'}{u_1}$	$\frac{u_2'}{u_2}$	$\frac{u_1'}{u_1}$	$\frac{u_2'}{u_2}$
0	1.000	1.000	1.000	1.000
15	0.940	0.857	0.994	0.909
30	0.797	0.739	0.841	0.794
45	0.709	0.628	0.780	0.699
60	0.670	0.558	0.712	0.611
90	0.588	0.455	0.610	0.523
120	0.500	0.334	0.497	0.376
150	0.500	0.334	0.497	0.376
180	0.456	0.294	0.480	0.334

Table 7.1.8 : Relative change in number-average molecular weight, u_1'/u_1 , and weight-average molecular weight, u_2'/u_2 , against time (see text) for degradation of PHB in the presence of 0.2% w/v pTSA

Time (minutes)	First experiment		Second experiment	
	$\frac{u_1'}{u_1}$	$\frac{u_2'}{u_2}$	$\frac{u_1'}{u_1}$	$\frac{u_2'}{u_2}$
0	1.000	1.000	1.000	1.000
15	0.573	0.500	0.572	0.504
30	0.255	0.184	0.348	0.260
45	0.203	0.141	0.273	0.184
60	0.172	0.112	0.225	0.144
90	0.130	0.084	0.155	0.100
120	0.104	0.062	0.134	0.078
150	0.089	0.051	0.107	0.063
180	0.078	0.044	0.091	0.052

below). The linear polymer was assumed to have a Schulz Zimm MWD with a polydispersity index (Mw/Mn) of 4.40 at zero time. This value was taken to represent the average value of the polydispersity indices of PHB samples measured by SEC (see Table 7.1.6). The theoretical plot was obtained using Equations 7.1 and 7.2 as shown below:-

$$\frac{u'_1}{u_1} = \frac{1}{1+x} \quad \ldots\ldots (7.1)$$

$$\frac{u'_2}{u_2} = \frac{2}{xH}\left\{1+\frac{1}{x}[(1+\frac{x}{b})^{-b}-1]\right\} \quad \ldots\ldots (7.2)$$

where

u'_1 and u'_2 are, respectively,the number and weight-average degrees of polymerization after scission

u_1 and u_2 are the corresponding values before scission.

x is the number of scission per initial number-average molecular weight molecules.

H is the degree of polydispersity (or Mw/Mn).

b is equal to the inverse of (H-1)

As can be seen from figure 7.1.7, there is a close similarity between the degradation of PHB in the presence of pTSA and the theoretical Schulz-Zimm plot for a random chain scission. Hence it can be assumed that in the presence of pTSA, PHB degrades by a process modelled by random chain scission and that the molecular weight distribution of PHB will tend towards that represented by the Schulz-Zimm distribution, [(Mn + Mz)/Mw = 2 and $1<Mz/Mw<2$].

Figure 7.1.7:- The relative change in weight average molecular weight, u_2'/u_2, versus the relative change in number average molecular weight, u_1'/u_1, during reflux of PHB in the presence of pTSA.

○ and ▲ experimental data obtained using 0·02%w/v pTSA

□ and ■ experimental data obtained using 0·2% w/v pTSA

——— theoretical Schulz-Zimm plot for random scission

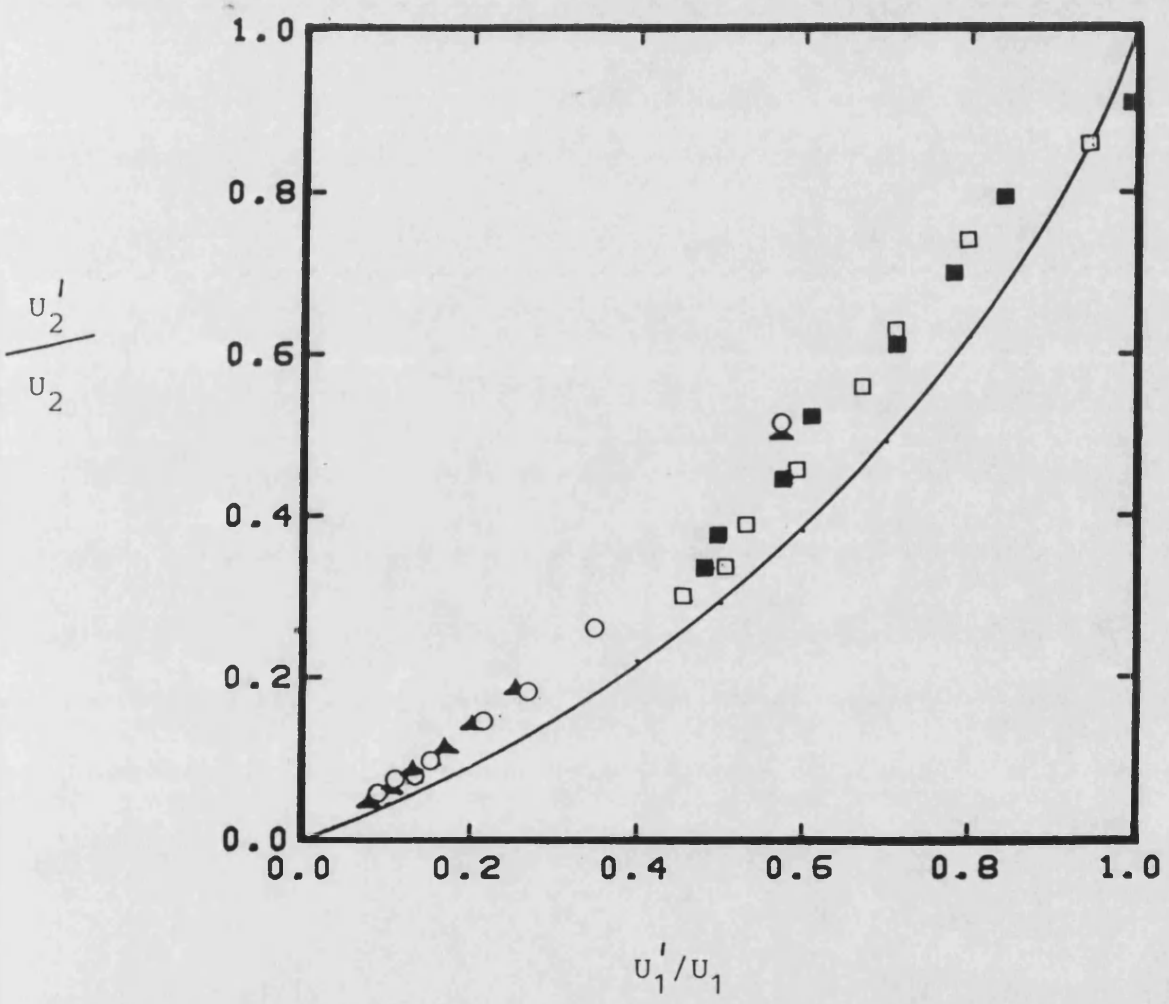

In order to determine the rate of bond cleavage, Jellinek (1978) stated that for random chain scission in solution, the following relationship should hold (see section 5.5.3);

$$\left| \frac{1}{DP} - \frac{1}{DP_o} \right| = k\,t \quad \ldots\ldots \quad (7.3)$$

where

DP is the degree of polymerization at time t

DP_o is the initial degree of polymerization.

Tables 7.1.9 and 7.1.10 show the function $\frac{1}{DP} - \frac{1}{DP_o}$ with respect to time for each experiment in the presence of 0.02% w/v and 0.2% w/w pTSA respectively. The differences between the values obtained for the two experiments again reflect the polydisperse nature of the high molecular weight PHB being used and also the limited precision of the SEC column. The assay used during this study could be improved by the use of several PL gel columns linked in series although this would result in the practical disadvantage associated with long retention times.

Values of $\frac{1}{DP} - \frac{1}{DP_o}$ are plotted according to Jellinek's equation in Figure 7.1.8. The plots were linear for both concentrations of pTSA and the rate constant for each concentration was calculated from the slope of the curve. The rate constants were $(2.68 \pm 0.09) \times 10^{-5}$ min^{-1} and $(0.31 \pm 0.01) \times 10^{-5}$ min^{-1} for degradation in the presence of 0.2% w/v and 0.02% w/v pTSA, respectively . pTSA proved to be a useful catalyst for controlled degradation of PHB in this non-aqueous system. Since the purification of PHB from fermentation mixtures involves precipitation from chloroform into excess methanol followed by filtration, it would be easy to include a pTSA degradation step to obtain lower molecular weights as required.

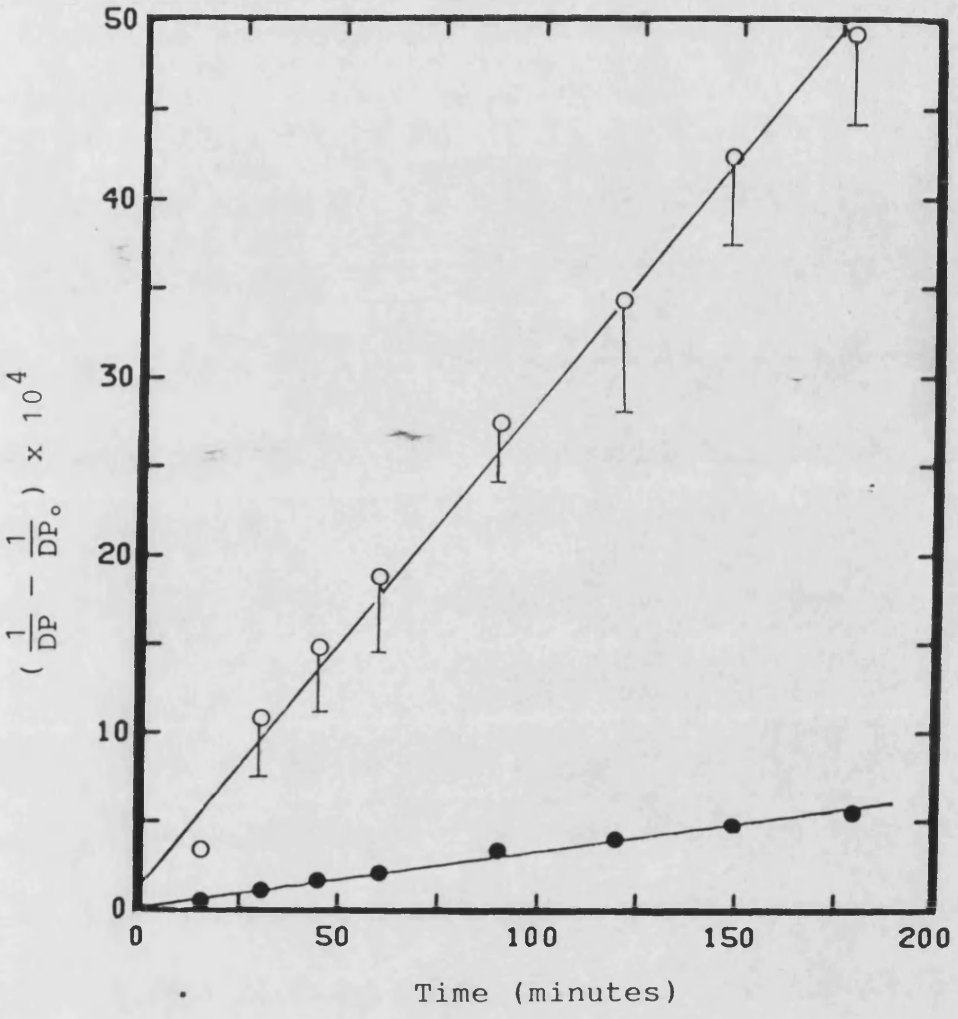

Figure 7.1.8:- The relationship between the function $(\frac{1}{DP} - \frac{1}{DP_o})$ with time for degradation of PHB in the presence of pTSA. (●), 0·02% $w/_v$ pTSA (O), 0·2% $w/_v$ pTSA.

Table 7.1.9 : Changes in the function of ($1/DP - 1/DP_0$) with time in the presence of 0.02% w/v pTSA

Time (minutes)	($1/DP - 1/DP_0$) ($\times 10^4$)	
	1st experiment	2nd experiment
15	0.3	0.03
30	1.2	0.9
45	1.9	1.4
60	2.3	2.0
90	3.3	3.1
120	4.1	3.6
150	4.7	4.9
180	5.6	5.3

Table 7.1.10 : Changes in the function of ($1/DP - 1/DP_0$) with time in the presence of 0.2% w/v pTSA.

Time (minutes)	($1/DP - 1/DP_0$) ($\times 10^4$)	
	1st experiment	2nd experiment
15	3.3	3.5
30	13.1	8.6
45	17.6	12.3
60	21.6	15.9
90	29.9	25.1
120	38.5	29.8
150	45.5	38.4
180	52.8	46.0

7.2 Degradation of PHB and P(HB/HV) copolymers in aqueous solution.

Hydrolysis studies of PHB were carried out using solvent-cast films at different values of pH at 37°C. Figure 7.2.1 shows the weight loss of these films as a function of storage time. The weight loss from polymer films followed a zero-order pattern. This could be explained by surface erosion if degradation took place through a constant surface area such that the degradation from the sides of the film were not significant compared to degradation from the planar surface.

However, this conclusion was drawn with caution, since the zero-order fit was not always significantly better than a first -order fit, as can be seen in Figure 7.2.2, which expresses the degradation of films at pH 7.4 and 37°C plotted on a logarithm scale against time. Such uncertainty is not surprising since the degradation of PHB probably results in the formation of pores which change the effective surface area throughout the degradation process. This phenomenon was observed by Holland *et al.* (1987) who studied the degradation of PHB discs. These authors studied the morphology of PHB discs using scanning electron microscopy and found that the surface of the discs became more porous as a result of degradation. Generally, the data obtained during the present study was best modelled using a zero-order plot. Therefore subsequent data is plotted as cumulative weight loss against time.

Each point on Figure 7.2.1 represents the mean of three experiments. The standard deviations obtained at each time were within 2% of the mean values. The linear rate constants for the degradation of PHB films in various pH buffers were obtained from the gradient of the appropriate curves. Rate constants are shown in Table 7.2.1.

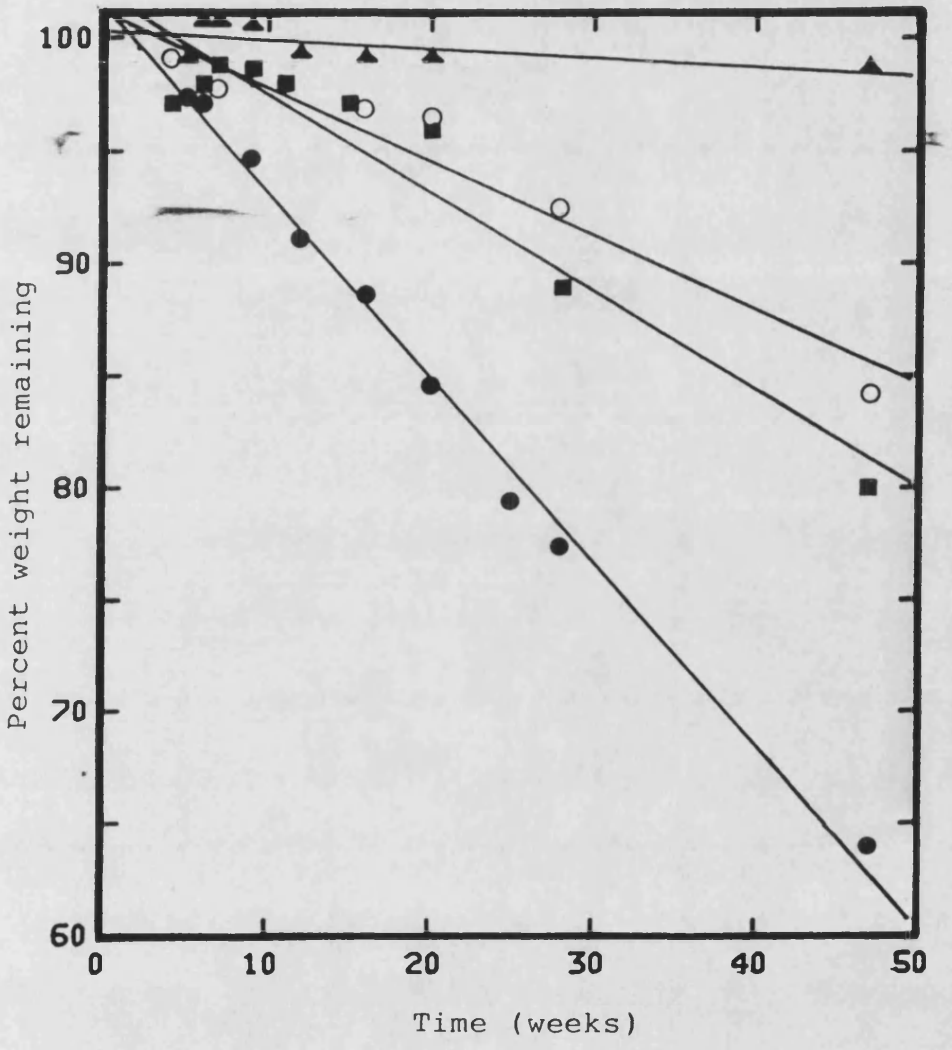

Figure 7.2.1:- Progressive weight loss of PHB film in buffer solutions at 37°C; (▲), pH 1·0; (○), pH 7·4; (■), pH 10·0; (●), pH 13·0.

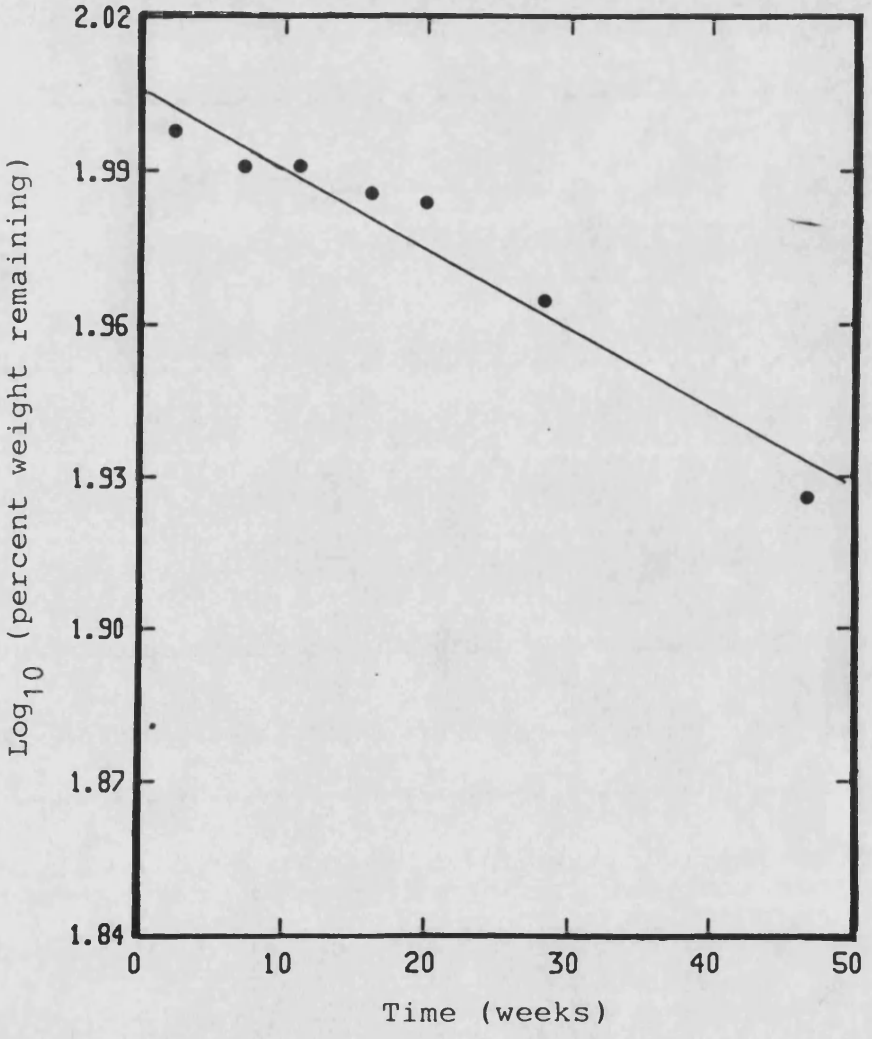

Figure 7.2.2:- First - order plot of weight loss of PHB film in phosphate buffer (pH 7·4) at 37°C.

Table 7.2.1 : Rate constants for degradation of PHB in different pH at 37°C

pH	Rate constant(k) (% $weeks^{-1}$ $\times 10^2$)
1.0	4.0 ± 1.9
7.4	32.9 ± 2.8
10.0	43.7 ± 4.9
13.0	81.9 ± 2.5

Figure 7.2.3 shows the rate constants for the degradation of PHB films at 37°C plotted against pH. This figure shows that there was minimal degradation at pH 1 and a progressive increase in degradation as the pH was increased. The degradation appeared to be base-catalysed but not acid-catalysed.

The mechanism of ester hydrolysis can be explained by the hypothesis put forward by Schnabel (1981) according to which two types of bond cleavage can occur depending on the pH of the solution. In acidic conditions, hydrolysis is initiated by a protonation process which is followed by the addition of water and the cleavage of the ester linkage as shown on the opposite pages. In the case of PHB, presumably, this mechanism is slow.

In contrast in alkaline media, hydroxyl ions attack the carbonyl carbons resulting in rapid hydrolysis of ester linkages as illustrated on the same page as above. Thus the degradation of PHB appears to be similar to copolymers of polyethylene oxide/polyethylene terepthalate (PEO/PET)' which are known to be pH-sensitive (Reed and Gilding, 1981).

Figure 7.2.1 shows that the maximum weight loss determined during degradation experiments at 37°C over a 50 week period was about 36%. This partial degradation study cannot truly represent the whole degradation process. Hence, accelerated testing was carried out to obtain information on the course of the degradation process as it proceeded until most of the film had degraded. It was also hoped that an extrapolation procedure could be used to model the degradation process which would take place in the physiological environment at pH 7.4 and 37°C.

Figure 7.2.4 shows the degradation of PHB films in 0.1M sodium hydroxide as a function of temperature. Degradation rate increased with

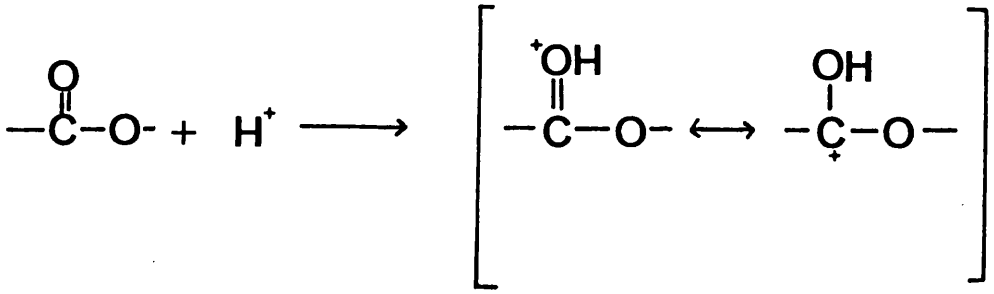

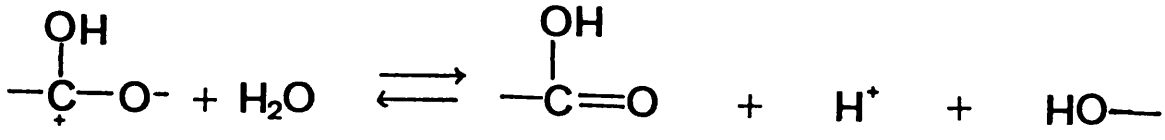

Reaction 2 : Degradation of polyesters in acidic solutions.

(from Schnabel , 1981)

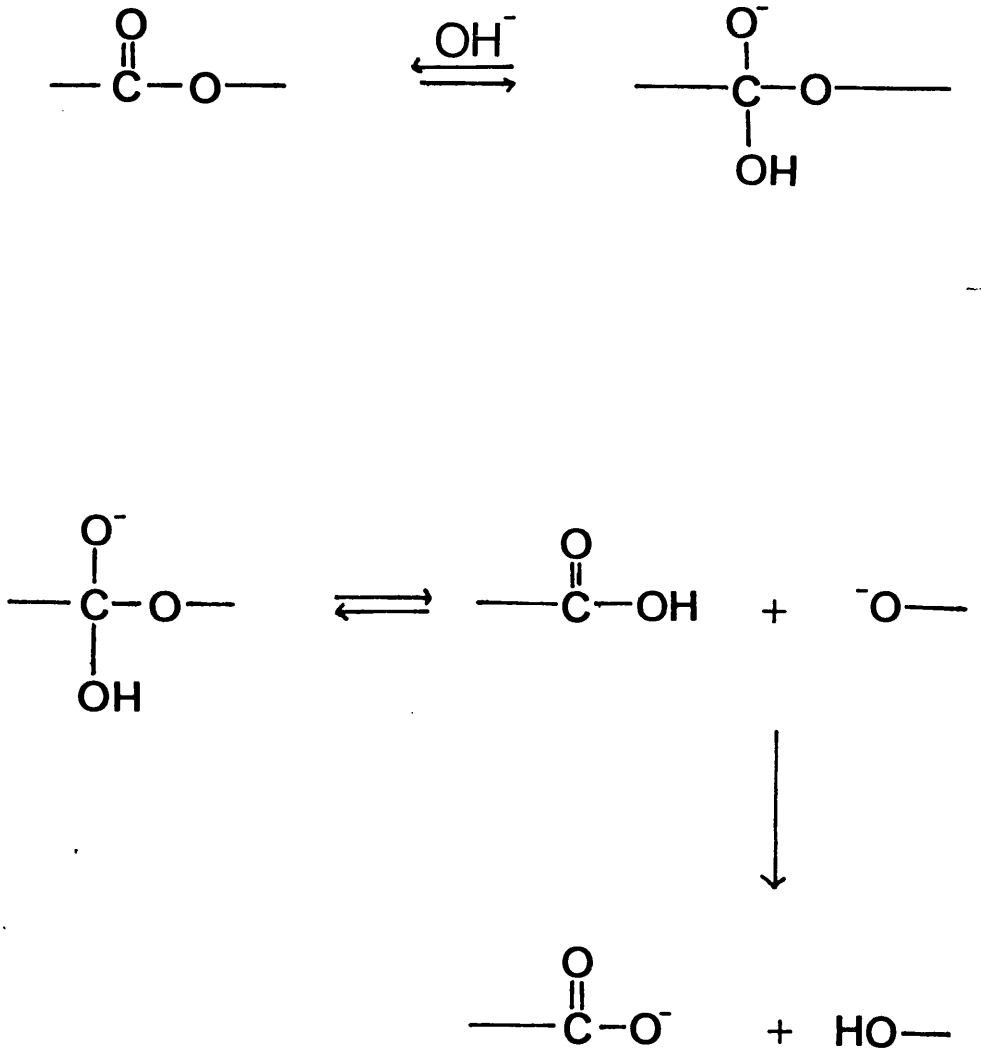

Reaction 3 : Degradation of polyesters in basic solutions.
(from Schnabel, 1981)

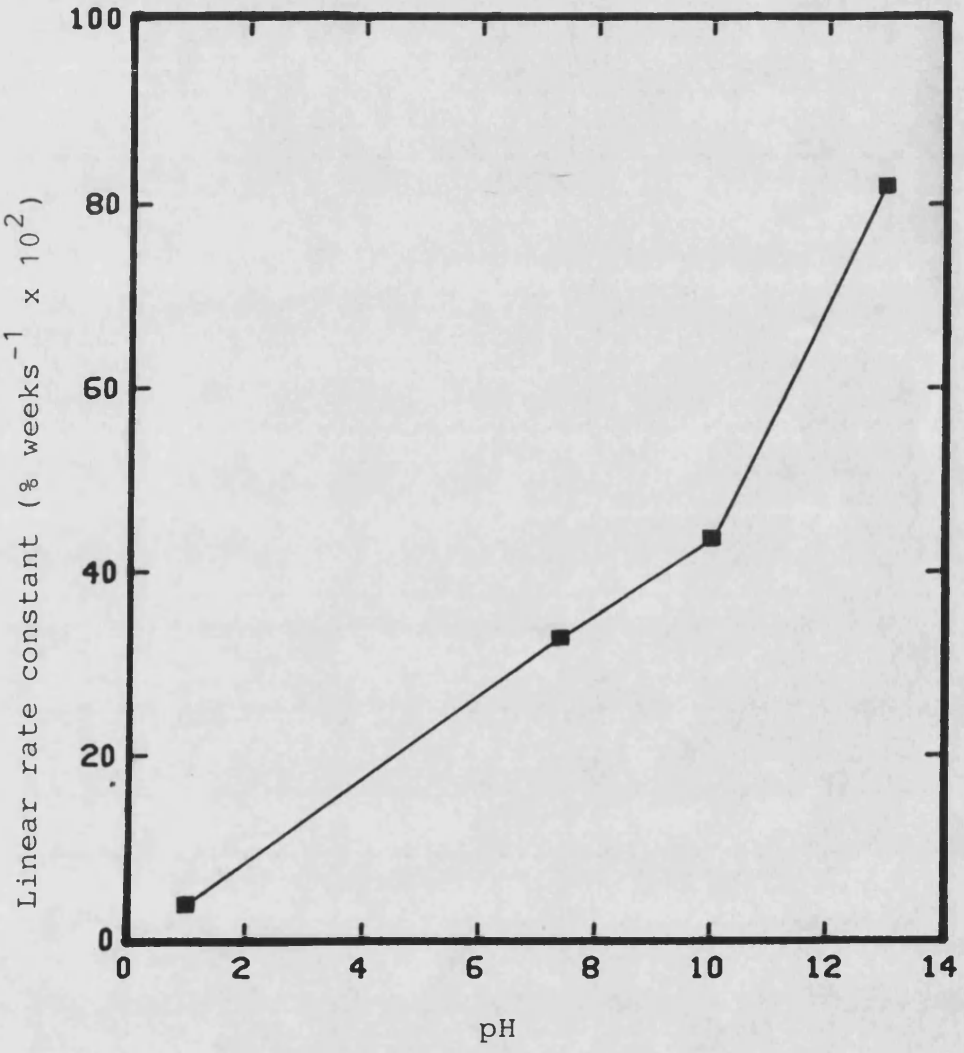

Figure 7.2.3:- Variation of linear degradation rate constant for PHB films as a function of pH stored in buffer solutions at 37°C.

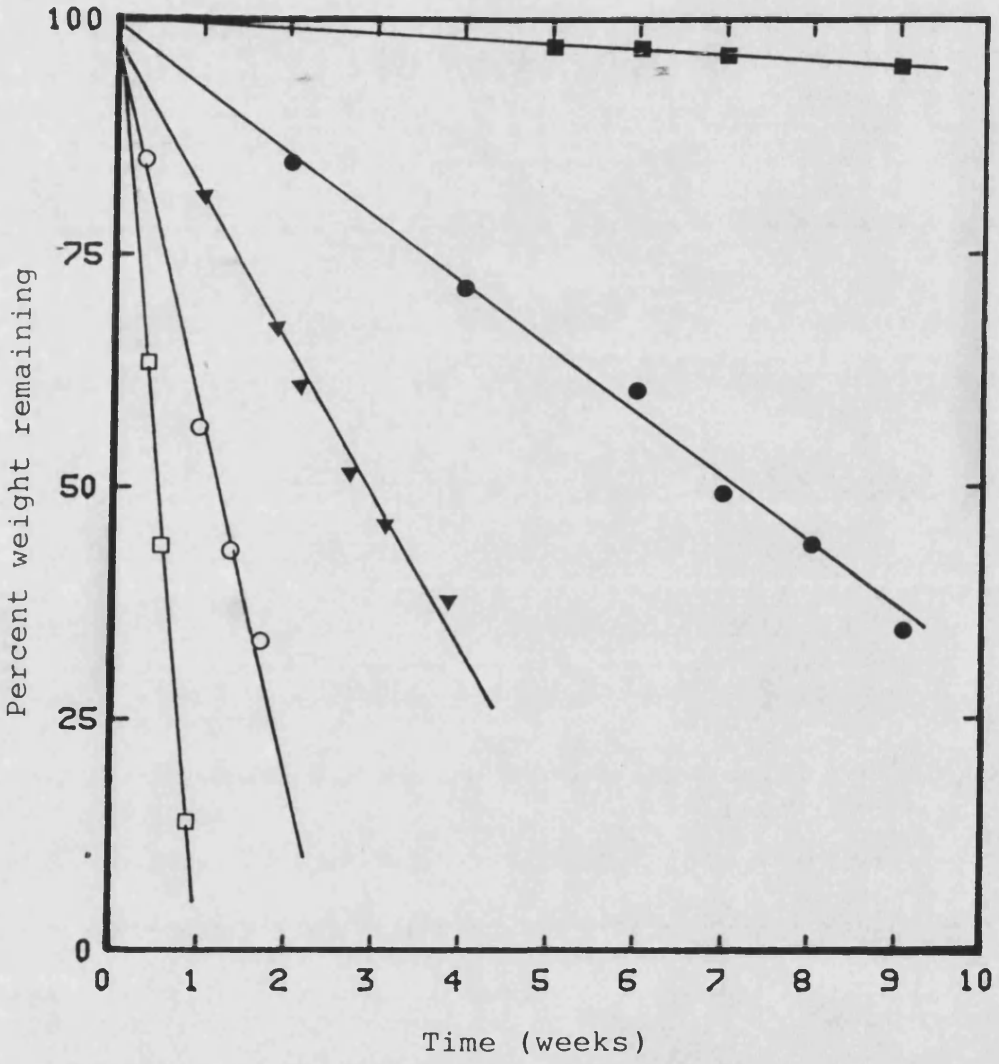

Figure 7.2.4:- Progressive weight loss of PHB film in 0·1M NaOH as a function of temperature. (■), at 37°C; (●), at 65°C; (▲), at 75°C; (○), at 85°C; (□), at 95°C.

temperature as expected. Table 7.2.2 shows the linear degradation rate constants (k) obtained at each temperature (T) from the slope of the graphs. The values of $\frac{1}{T}$ (K^{-1}) and log k are also tabulated. These values were used to plot log k against $\frac{1}{T}$ (Figure 7.2.5) according to the Arrhenius' equation as shown below:-

$$\ln k = \ln A - \frac{E}{R T} \quad \ldots\ldots \quad (7.4)$$

where

E is the activation energy

R is the gas constant

k is the rate constant

T is the absolute temperature in K

A is the pre-exponential factor.

The slope of the straight line gives the value of the activation energy calculated as 16.6 ± 0.6 kcal/mole. This value is lower than that obtained for the hydrolytic degradation of poly(esterurethanes) (PUR) by Cohen and Van Aartsen (1973). These authors determined that the activation energy for the hydrolysis of PUR which occured through backbone cleavage was 23.8 ± 0.9 kcal/mole.

The effect of pH on the hydrolysis of PHB films at high temperature was studied as a comparison with the results obtained at 37°C. Figure 7.2.6. shows weight loss as a function of time at 75°C. Linear degradation rate constants for each pH are shown in Table 7.2.3. The change from physiological temperature (Table 7.2.1) to 75°C (Table 7.2.3) caused an increase in degradation rate throughout the pH range studied. The increase in the degradation rate in 0.1M sodium hydroxide

Table 7.2.2 : Arrhenius' plot for the effect of temperature on the degradation of PHB in 0.1M sodium hydroxide.

Temperature(T) (°C)	1/T ($K^{-1} \times 10^3$)	Rate constant(k) (% $days^{-1} \times 10$	ln k
37	3.2	1.2	-2.12
65	3.0	10.2	0.02
75	2.9	22.0	0.79
85	2.8	52.8	1.66
95	2.7	163.8	2.80

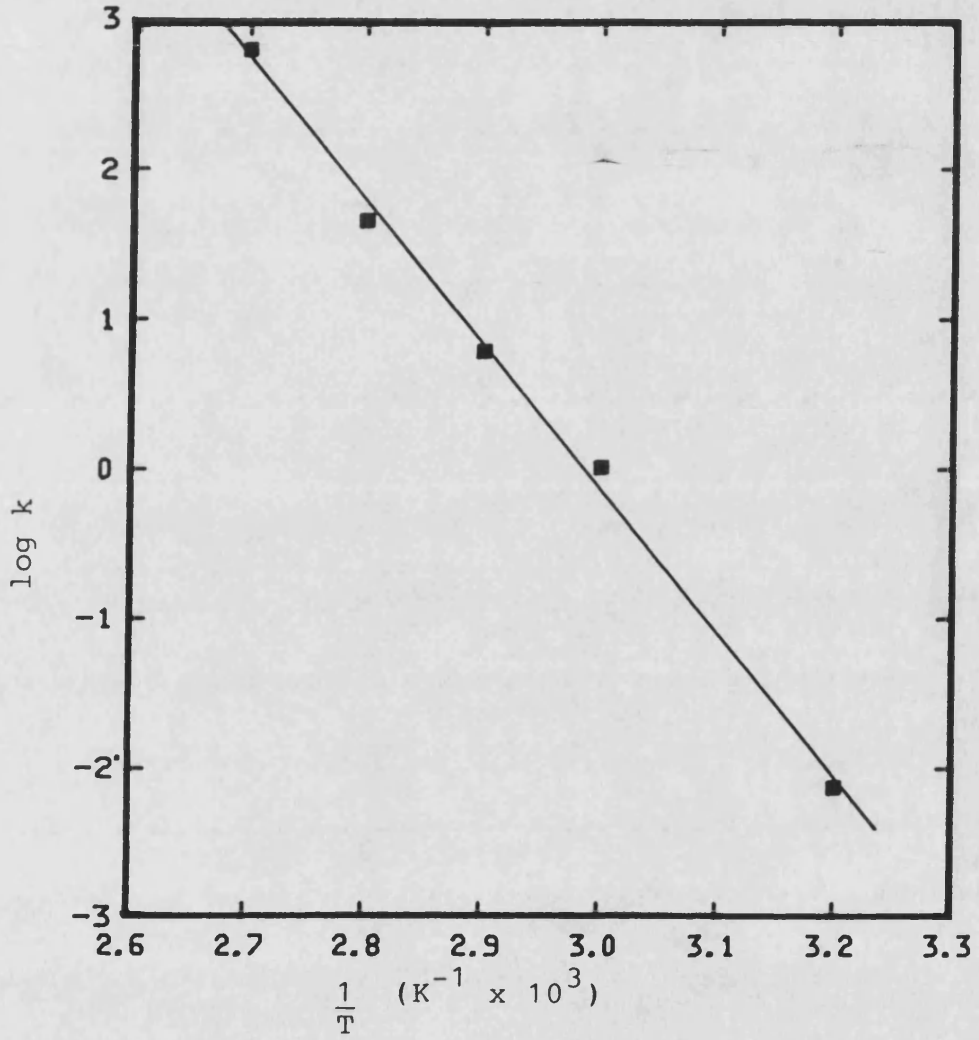

Figure 7.2.5:- Arrhenius' plot for the hydrolytic degradation of PHB films in 0·1M NaOH.

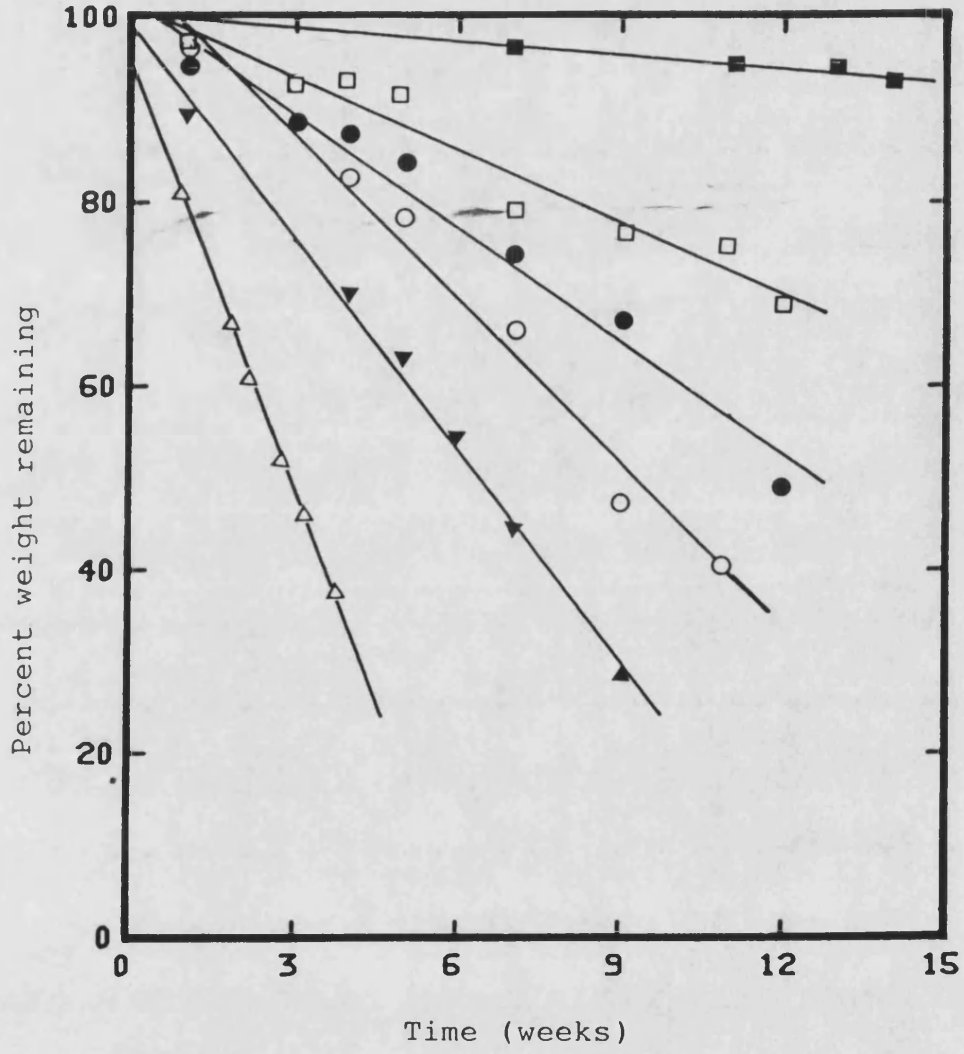

Figure 7.2.6:- Progressive weight loss of PHB films in buffer solutions at 75°C; (■), pH 7·4; (□), pH 10; (●), pH 10·5; (○), pH 11·0; (▲), pH 11·5; (△), pH 13·0.

Table 7.2.3 : Rate constant for degradation of PHB in different pH at 75°C

pH	Rate constant(k) (% $weeks^{-1}$ $\times 10^{1}$)
7.4	4.9 ± 0.7
10.0	26.1 ± 2.6
10.5	41.0 ± 2.5
11.0	59.2 ± 4.0
11.5	76.6 ± 2.9
13.0	154.0 ± 2.3

was about twenty fold when the temperature was increased from 37°C to 75°C.

Figure 7.2.7 shows the relationship between linear degradation rate constant and pH at 75°C. The general shape of the curve is the same as that obtained at 37°C (Figure 7.2.3). These results suggest that degradation at 75°C proceeded by the same mechanisms as degradation at 37°C and that accelerated tests could be used to extrapolate the kinetics of degradation to lower temperatures. The advantage of the high temperature study was that the complete profile of PHB degradation was obtained within a short duration.

The degradation of PHB was compared with that of P(HB/HV) copolymers to determine the effect of HV content on degradation. The mole fractions of hydroxyvalerate in the copolymers used, measured by proton NMR spectroscopy, were 0.065, 0.123 and 0.193.

Figures 7.2.8 to 7.2.10 show weight loss at pH 7.4 and 37°C from PHB and copolymer films as a function of HV content. Linear degradation rate constants from these experiments are shown in Table 7.2.4, although it should be noted that the data obtained for two of the copolymers (Figures 7.2.8 and 7.2.9) did not fit a zero-order model convincingly.

Table 7.2.4 shows that all of the copolymers degraded more rapidly than PHB but the maximum degradation rate occured at 12.3 mole % PHV. The copolymer containing 19.3 mole % HV degraded at a slightly higher rate than PHB (Figure 7.2.11). These differences in degradation rate could be explained in terms of the crystalline natures and polarities of the copolymers. The crystallinity of PHB is decreased by the introduction of HV. This decrease in crystallinity is indicated in Table 7.2.5. where the heat of fusion, ΔH_f, for each

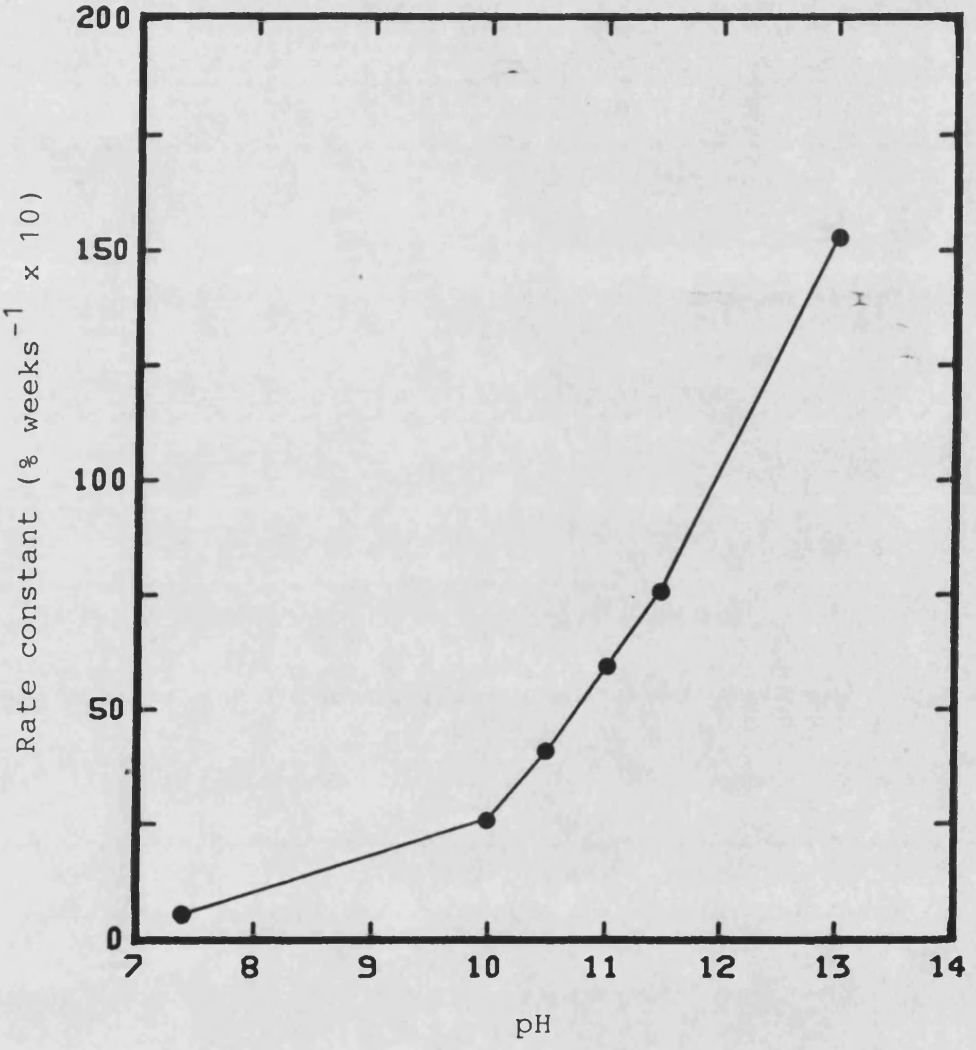

Figure 7.2.7:- Variation of linear degradation rate constant as a function of pH for PHB films stored in buffer solutions at 75°C.

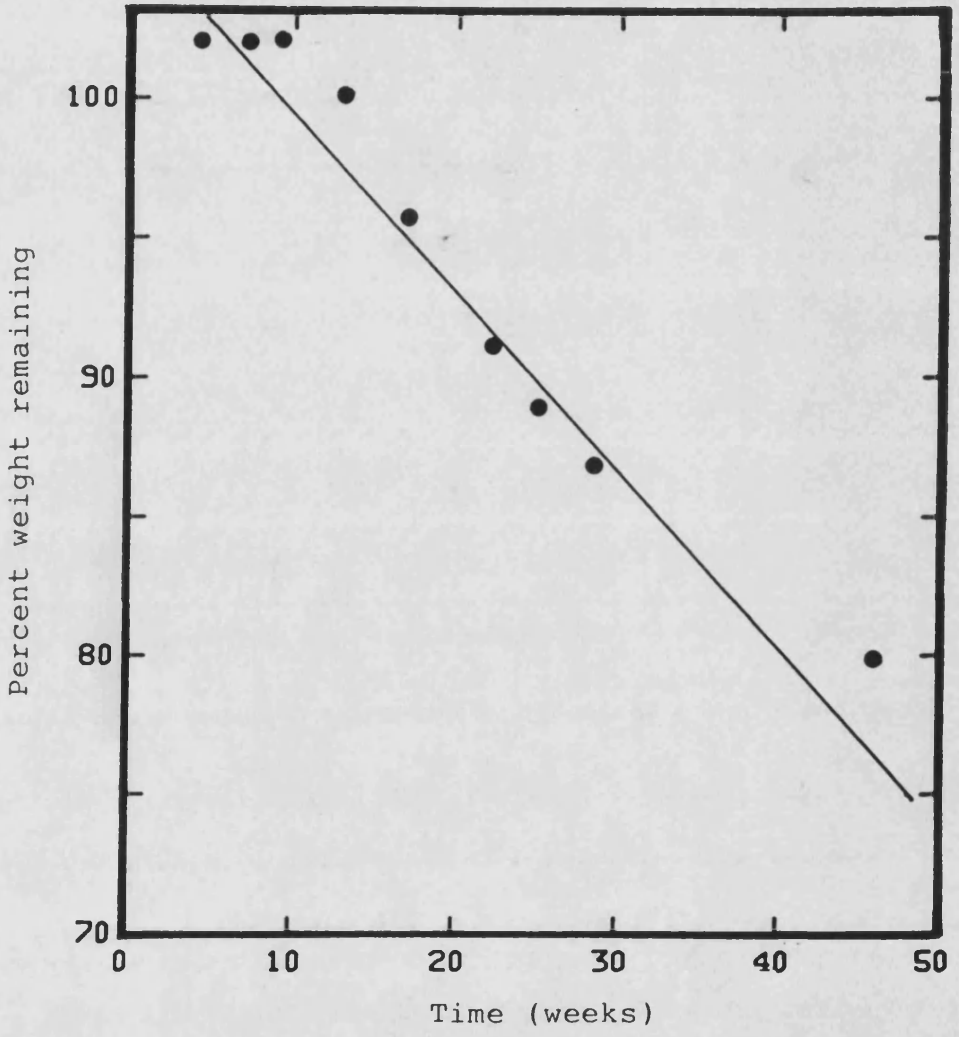

Figure 7.2.8:- Progressive weight loss of PHB/PHV copolymer (6·5 mole % HV) film stored in phosphate buffer (pH 7·4) at 37°C.

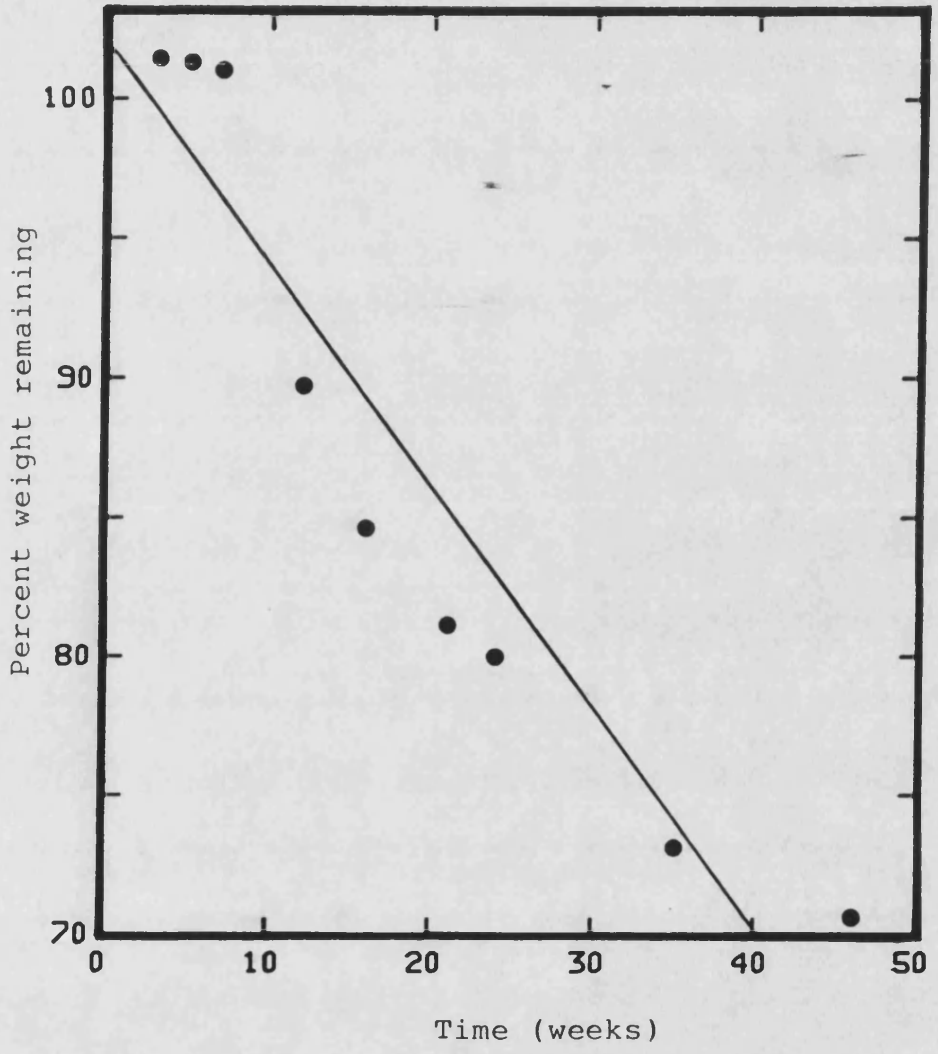

Figure 7.2.9:- Progressive weight loss of(12·3 mole % HV) PHB/PHV copolymer films in pH 7·4 at 37°C.

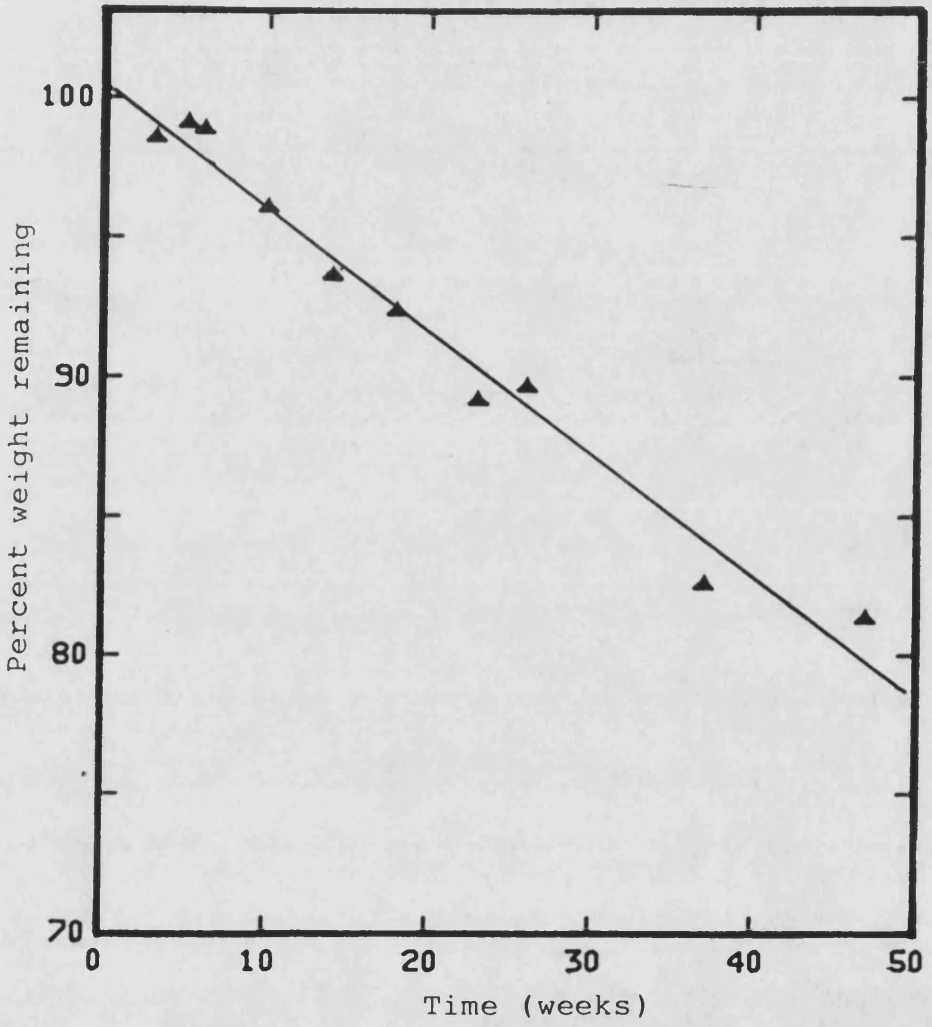

Figure 7.2.10:- Progressive weight loss of (19·3 mole %) PHB/PHV copolymer films in pH 7·4 at 37°C.

Table 7.2.4 : Rate constant for degradation of PHB and its copolymers in pH 7.4 (I = 0.153M) at 37°C

Polymer composition (mole % HV)	Rate constant (k) (% $weeks^{-1}$ ×10)
0	3.3 ± 0.3
6.5	6.4 ± 0.9
12.3	7.9 ± 1.0
19.2	4.4 ± 0.2

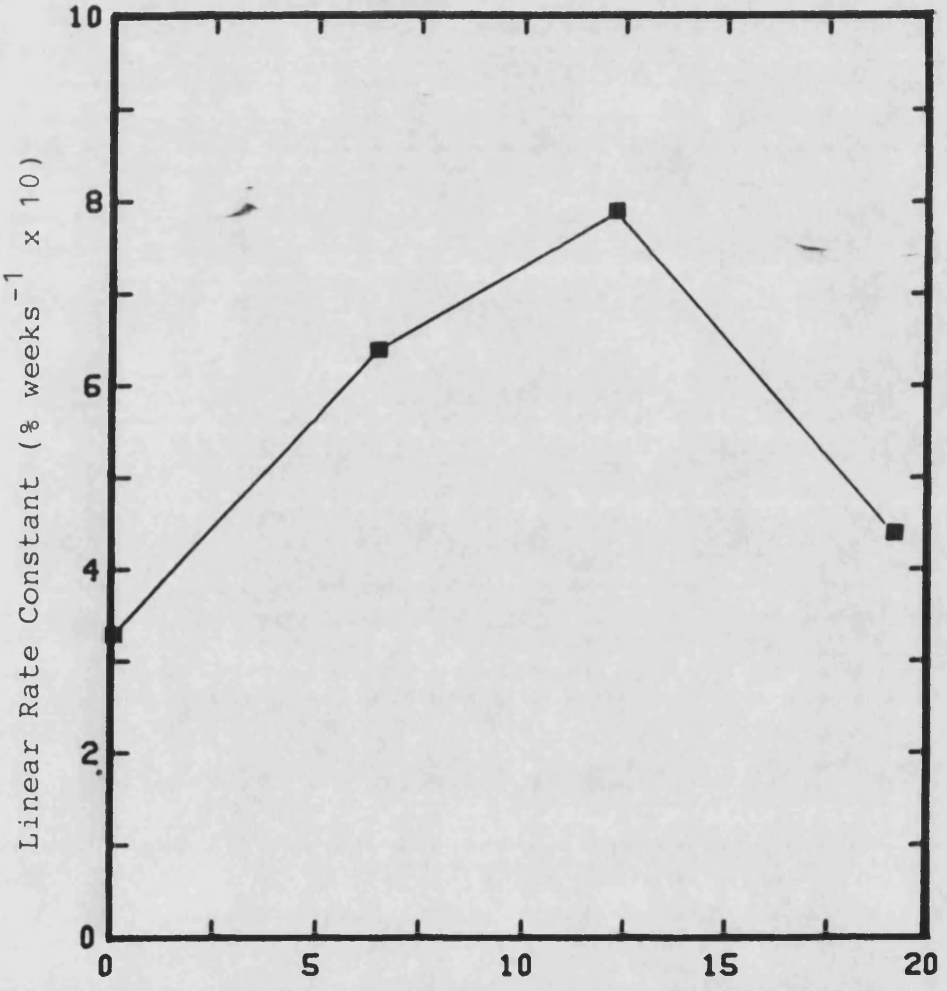

Figure 7.2.11:- Variation of linear degradation rate constants as a function of PHB/PHV copolymer composition for films stored in phosphate buffer (pH 7·4) at 37°C.

Table 7.2.5 : Heats of fusion, ΔH_f , for PHB and P(HB/HV) copolymer films

Polymer composition (mole % HV)	Heat of fusion ΔH_f ($\frac{J}{g}$)
0	86.0 ± 7.7
6.5	64.4 ± 0.6
12.3	44.5 ± 3.7
19.2	35.3 ± 2.5

for each copolymer is tabulated. ΔH_f was obtained using differential scanning calorimetry. The degree of crystallinity would not in this case be proportional to the value of ΔH_f, since the values of ΔH_f would be different for mixed crystals of HV and HB. However the steep fall in overall ΔH_f - is indicative of a substantial change in crystallinity which decreases steadily with increase in HV content.

Keller (1957, 1962) introduced the concept of chain folding to explain crystallinity in polymers. According to Keller, polymer crystals arise from the lamellar folding of polymer chains in such a way that the thickness of a crystal is determined by the fold length of the polymer chain. Following the introduction of this concept, Mandelkern (1975) represented the morphology of a semicrystalline polymer as shown in Figure 7.2.12. When the amorphous content is increased, as in this study by the intoduction of HV units, more polymer chain-ends are exposed to the degradative process. Hence, when the degree of crystallinity decreases, the degradation rate increases. This effect of the degree of crystallinity on polymer degradation has been demonstrated *in vivo* (Miller *et al*, 1977) for P(LA/GA) systems.

Despite the decrease in degree of crystallinity, which continued for the P(HB/HV) copolymers as HV content increased, there was a change in behaviour as the HV content increased from 12.3 to 19.3 mole %. The degradation rate was slower for the polymer containing 19.3 mole% HV. This may have been due to an increase in hydrophobicity which may have reduced wetting or penetration of water at the polymer/solution interface.

The precise crystalline nature of P(HB/HV) copolymers is yet to be determined and there is some confusion in the literature. Certainly the copolymers are not amorphous in the manner of P(LA/GA) copolymers.

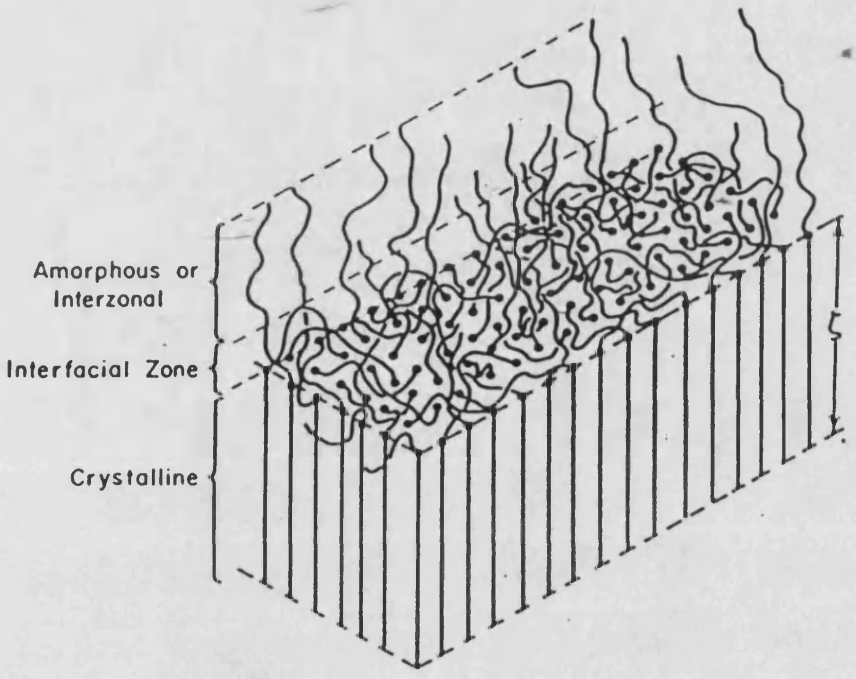

Figure 7.2.12:- Schematic representation of crystalline and associated non crystalline regions in polymers (from Mandelkern, 1970).

It was reported by Bluhm *et al.* (1986) that over the range of copolymers containing between 0 and 47 mole % HV, there exists an unexpected minimum in the heat of fusion (ΔH_f) at approximately 30 mole % of HV. They attributed this phenomenon to the isodimorphism of these copolymers such that two crystalline phases due to β-hydroxybutyric acid (HB and HV units exist on either side of this minimum value heat of fusion). It is possible that as HV contents increase towards 30 mole %, the regions of HV content are associated in the amorphous regions causing increased hydrophobicity. At higher HV contents, the major crystalline areas would be based on the unit cell for HV. More work on the crystalline nature of copolymers is required so that the nature of polymer-drug mixtures can be understood. At present the degree of randomness in the copolymer chain is not known. At present it can be assumed that the degradation of P(HB/HV) copolymers containing between zero and 30 mole % HV depends on the balance between the crystallinity and the hydrophobicity of the polymer. Such a balance has been shown to control the degradation of P(LA/GA) copolymers over a wide range of composition. (Gilding and Reed, 1981).

Figure 7.2.13 shows the accelerated degradation study of P(HB/HV) copolymer in 0.1M sodium hydroxide at 75°C. These weight loss profiles show that the rank order of degradaton rates is in agreement with that obtained under physiological conditions (at 37°C and pH 7.4).

Table 7.2.6. and Figure 7.2.14 show the linear degradation rate constants obtained from the slopes of Figure 7.2.13. There was no significant difference between the linear rate constants for the 6.5 mole % HV and 19.2 mole % HV copolymers. The 12.3 mole % HV copolymer had the highest degradation rate constant and the general shape of the curve was similar to that obtained under physiological conditions. The

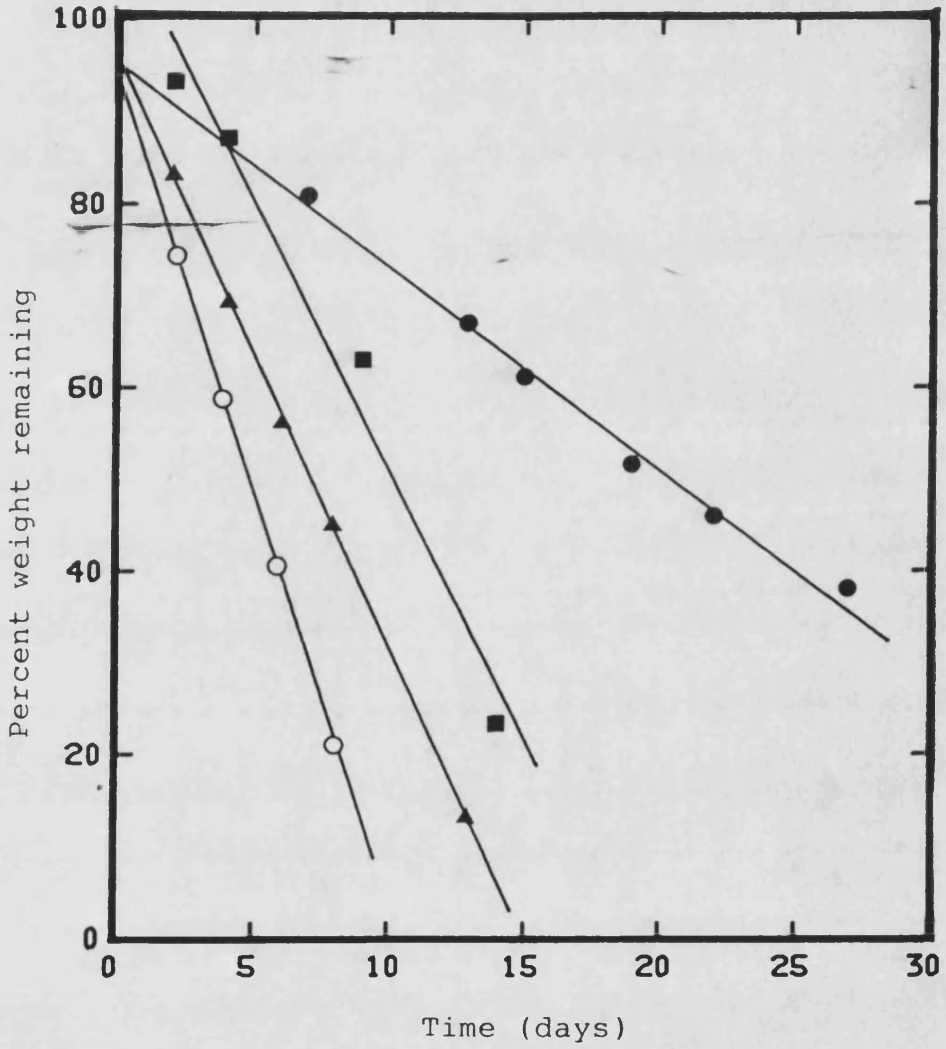

Figure 7.2.13:- Progressive weight loss of PHB/PHV copolymer films stored in 0·1M sodium hydroxide at 75°C; (●), PHB; (▲), 6·5 mole % HV; (○), 12·3 mole % HV; (■), 19·2 mole % HV.

Table 7.2.6 : Linear rate constant for degradation of PHB and P(HB/HV) copolymers in 0.1M sodium hydroxide at 75°C

Polymer composition (mole % HV)	Rate constant (k) (% $days^{-1}$)
0	2.2 ± 0.1
6.5	6.4 ± 0.1
12.3	8.9 ± 0.4
19.2	5.8 ± 0.7

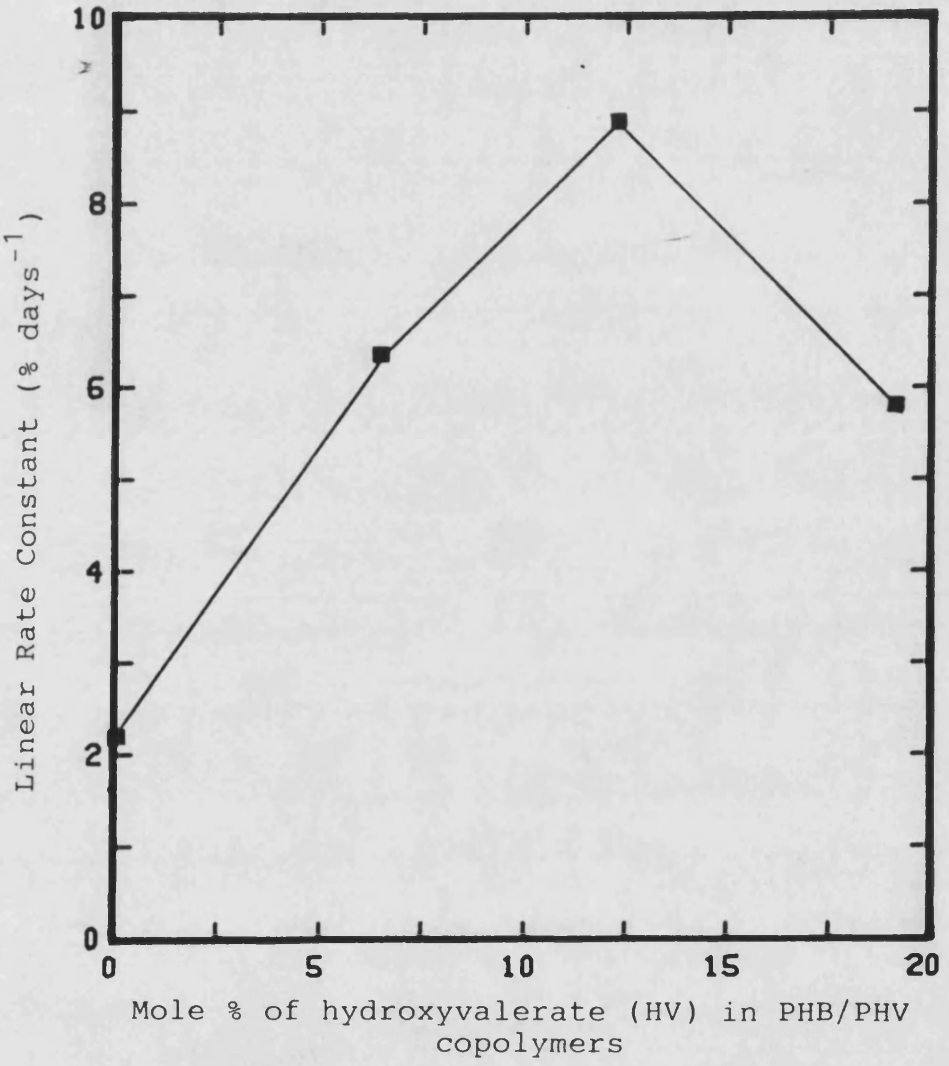

Figure 7.2.14:- Variation of linear degradation rate constants as a function of PHB/PHV copolymer composition for films stored in 0·1M sodium hydroxide at 75°C.

main difference between the data obtained under physiological conditions and those obtained under accelerated conditions was that, in the latter case, PHB homopolymer degraded much more slowly than all copolymers. However it would appear that the accelerated tests could be used as an indicator of changes in degradation rate.

Figure 7.2.15 shows the weight loss profile for P-l-LA and P(LA/GA) containing 10 mole % glycolate. The degradation rate for P-l-LA was slower than that for P(LA/GA). This was expected due to the nature of P-l-LA which is relatively hydrophobic and more crystalline than the P(LA/GA) copolymer. A comparison of these results with those obtained using PHB under the same conditions shows that the relative order of increasing resistance of hydrolysis was P(GA/LA) < PLA << PHB.

Previous studies of P(LA/GA) systems have shown that these polymers degrade by bulk hydrolysis followed by extensive mass loss (Reed and Gilding, 1981). It was of interest to compare the mechanisms of degradation of P(LA/GA) systems with PHB. SEC studies were carried out to observe changes in the molecular weight of the polymer during degradation. Such data are shown in Table 7.2.7. These were determined during the degradation of PHB in 0.1M sodium hydroxide at 85°C. The molecular weight of the bulk polymer remained constant as the film progressively lost weight. Ths implies that the mass loss occured through surface hydrolysis while the bulk matrix of PHB remained unchanged. The same study was also carried out on P-l-LA using an assay of PHB molecular weight-equivalent. The weight-average molecular weight (Mw), decreased from 258K to 15K within one day of degradation. The remaining weight of PLA after this degradation was 22%. Thus PLA degraded by both hydrolysis of the surface and bulk polymer chains. Hydrolysis of the chains within the bulk was

Table 7.2.7 : Weight loss and changes in molecular weight during degradation of PHB films in 0.1M sodium hydroxide at 85°C

Duration of degradation (days)	Mass loss (%)	Molecular weight changes (M_w)
0	0	609000 ± 85000
2	14.9 ± 1.5	607000 ± 54000
7	43.3 ± 1.9	629000 ± 37000
9	56.7 ± 1.8	607000 ± 54000
12	66.3 ± 1.6	598000 ± 66000

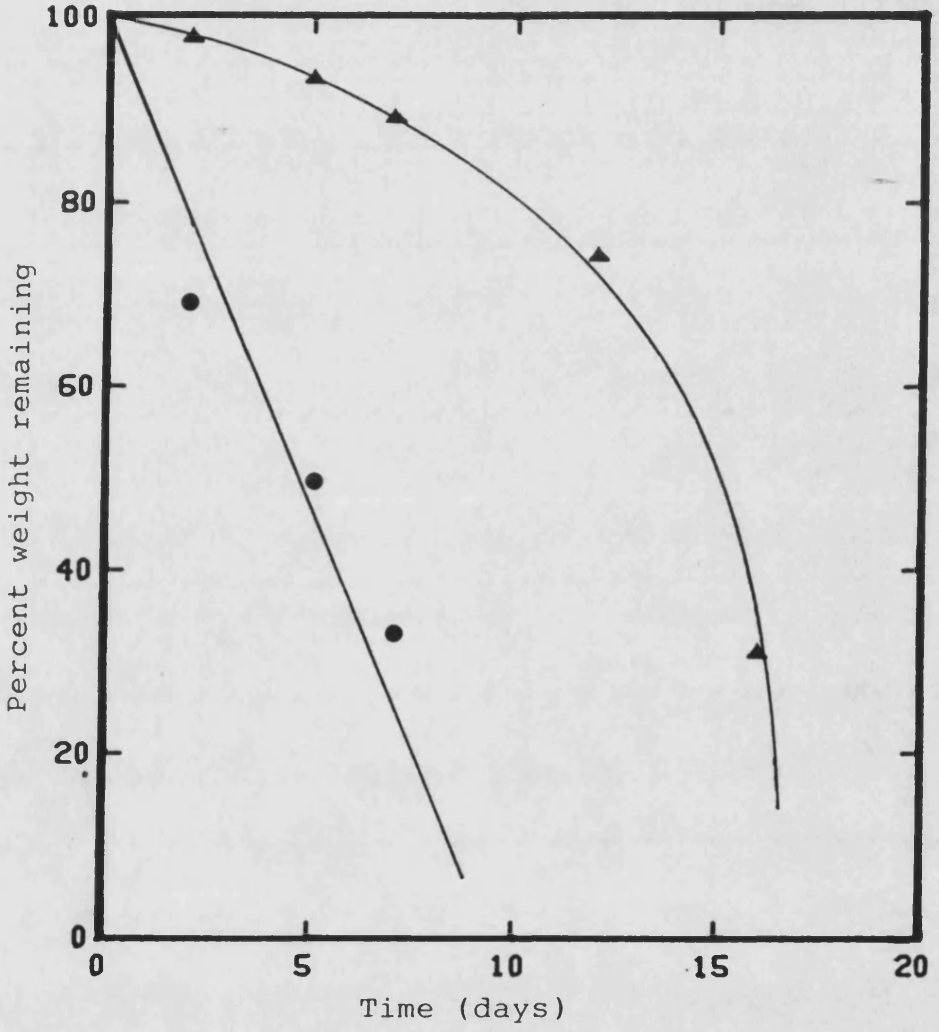

Figure 7.2.15:- Progressive weight loss of PGA/PLA copolymer (10 mole % glycolate) (●) and PLA homopolymer (▲) films stored in phosphate buffer (pH 7·4) at 75°C.

responsible for the decrease in bulk molecular weight. Table 7.2.8 shows changes in the molecular weights and masses of various polymer films during degradation under various conditions. The degradative conditions to which these polymers were exposed are stated in the table (Table 7.2.8). P(HB/HV) copolymers degraded in the same manner as PHB homopolymer, that is, by surface hydrolysis without any change in the molecular weight of the bulk copolymer films. This studied showed clearly that the degradation of P(LA/GA) copolymer occurred by hydrolysis of the surface and polymeric chains.

Differential scanning calorimetric (DSC) studies of the degraded films were also undertaken. Films removed after degradation were stored at -80°C until the DSC studies were carried out to avoid any equilibration of degree of crystallinity. The heats of fusion, ΔH_f , obtained before and after degradaton are shown in Table 7.2.8. There were no changes in ΔH_f for PHB or P(HB/HV) copolymers after degradation indicating no changes in the bulk properties of the polymers. This is a conformation that degradaton proceeded by surface erosion. Thermograms for the P-l-LA and P(LA/GA) films were different before and after degradation. The melting endotherm peaks were broader after degradation indicating bulk changes in these two polymers but the values of ΔH_f were lower after degradation. These values of ΔH_f indicate lower degrees of crystallinity after degradation; an unexpected result, although there was some doubt associated with these values due to difficulties in establishing the baselines of the thermograms after degradation.

7.3 Analysis of water-soluble degradation products

Although weight loss and molecular weight determinations provide information relating to the mechanisms of polymer degradation, they do not establish the degradation products which are released into

Table 7.2.8 : Changes in the weight,weight-average molecular weight and heats of fusion for various polyesters

Identity of polymer and degradative condition	Final mass loss (%)	Molecular weight loss (M_w)		Heat of fusion ΔH_f (J/g)	
		Initial	Final	Initial	Final
PGA/PLA(1:9) in pH 7.4 at 75°C	76.6	94K	12K	25.0	17.6
PLA in pH 7.4 at 75°C	69.5	258K	113K	40.2	28.6
PHB in pH 7.4 at 37°C	15.6	868K	868K	86.0	86.3
6.5 mole % PHB/PHV in 0.1M NaOH at 75°C	78.9	430K	430K	64.4	64.0
12.3 mole % PHB/PHV in 0.1M NaOH at 75°C	87.2	1050K	1050K	44.5	44.2
19.2 mole % PHB/PHV in 0.1M NaOH at 75°C	76.6	1480K	1480K	35.3	35.6

aqueous solution. These degradation products may provide further information on the mechanisms of degradation and are of interest from a toxicological viewpoint. Studies on the presence of water-soluble degradation products focused on whether the monomer or oligomers were released from polymer films as a result of surface hydrolysis.

Since the monomer released from PHB would be d-β-hydroxybutyric acid, initial studies on water-soluble degradation products were aimed at detection of β-hydroxybutyric acid. Two simple methods that have been used to quantify β-hydroxybutyric acid; the spectrophotometric method used by Slepecky and Law (1960) and the gas liquid chromatography used by Cosmi *et al.* (1983). β-hydroxybutyric acid is freely available as its sodium salt but dimers, trimers and higher oligomers are not available from chemical suppliers. A fractionation method for oligomers having degrees of polymerization ranging from 10 to 20 has been developed by Coulombe *et al.* (1978) and methods for synthesis of dimers and trimers have been reported. A method allowing detection of the monomer and low molecular weight oligomers simultaneously would be preferable and hence efforts were directed towards this aim.

One series of experiments used gas liquid chromatography(GLC) on a column capable of resolving carboxylic acids, such as n-butyric acid and propionic acid (see Chapter 6). Figure 7.3.1a shows the separation of n-butyric acid and propionic acid using this column. Butyric acid was retained longer due to its hydrophobicity and lower molecular weight. When dl-lactic acid and β-hydroxybutryric acid were injected into this column, no separation between these two compounds was observed, as shown in Figure 7.3.1b. This indicated that the column was not capable of resolving low molecular weight hydroxy acids presumably due to their higher polarity. Hydroxy acids are notoriously difficult to separate using

Operating temperature

Oven: 100°C
Detector: 150°C

(a) Attenuation:- 100 x 512
Retention time for
i n-propionic acid = 2.8 min
ii butyric acid = 5.6 min

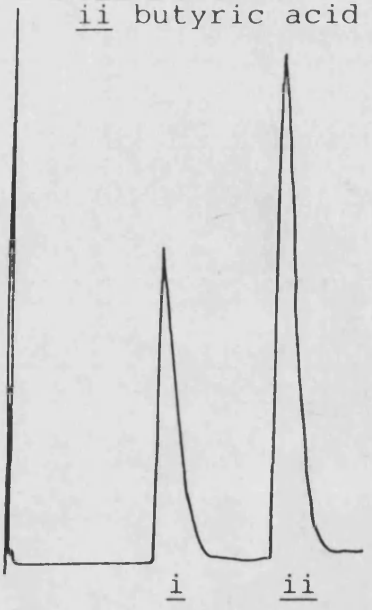

(b) Attenuation:- 100 x 8
Retention time = 2.8 min

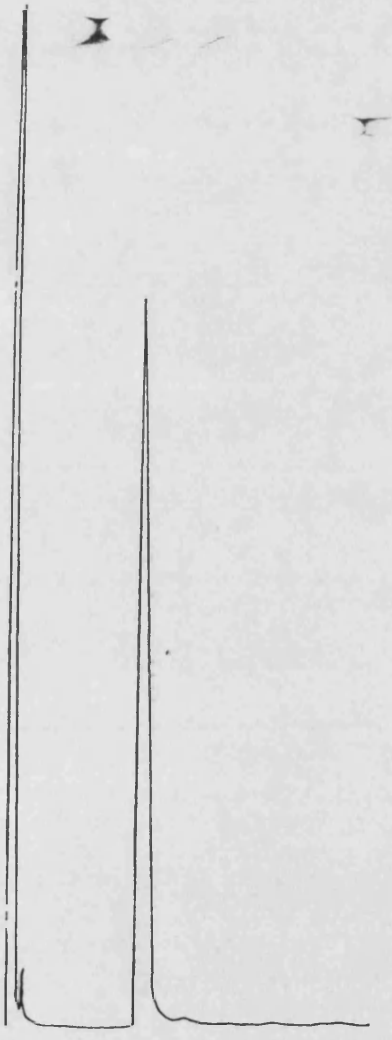

(c) Attenuation:- 100 x 80
Retention time = 2.8 min

Figure 7.3.1:- Gas liquid chromatograms (GLC) of (a) n-butyric acid and propionic acid. (b) dl-lactic acid and β-hydroxybutyric acid (c). Aqueous soluble product(s) from degradation of PHB in 0·1M NaOH.

GLC. When the water-soluble degradation products were injected into the column, only one peak was observed with a retention time corresponding to that of β-hydroxybutyric acid. No higher molecular weight peaks were detected suggesting that dimers and trimers of β-hydroxybutyric acid were not present in aqueous solution. Unfortunately this could not be established because no standards were available to test for chromatographic retention. Synthesis of dimer and trimer was beyond the scope of this study. Olsen *et al.* (1965) has shown that the chemical synthesis of the dimeric ester of β-hydroxybutyric acid involves a sequence of several reactions and higher oligomers are difficult to purify.

A second chromatographic method was examined; namely, low molecular weight size exclusion chromatography (SEC). A column was available which separated molecules below a threshold of about 1000 daltons. This column was calibrated with poly(ethylene glycol) (PEG) standards. Direct calibration of this column with PHB standards was not possible due to lack of pure oligomers as mentioned above.

Figure 7.3.2 shows the infrared spectrum of polyethylene glycol. Calibration of the SEC column was facilitated by detection of PEG at 2930 cm^{-1} which corresponded to the C-H stretching region. Degradation products of PHB were detected by infrared absorption in the C=0 stretching region as in previous experiments.

Table 7.3.1 shows the molecular weights of PEG fractions ($Mw/Mn<1.1$) used for the calibration curve and their corresponding retention times. The calibration curve obtained is shown in Fiugre 7.3.3. The column was expected to resolve oligomers of PHB from the monomer to the hexamer.

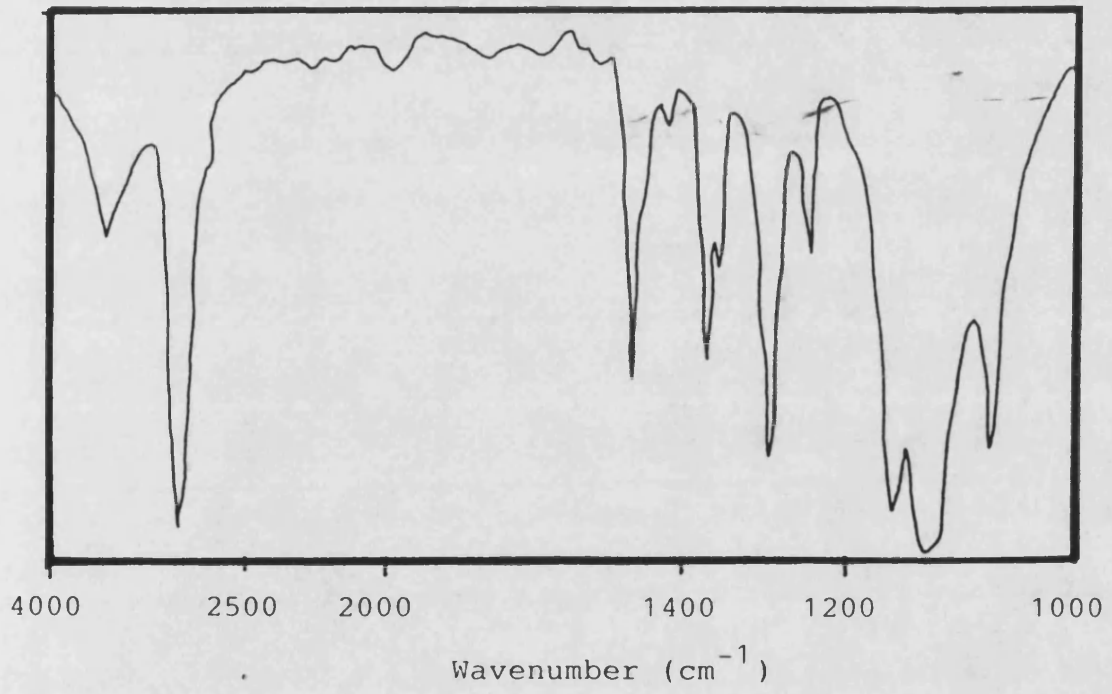

Figure 7.3.2:- Infrared spectrum of polyethylene glycol

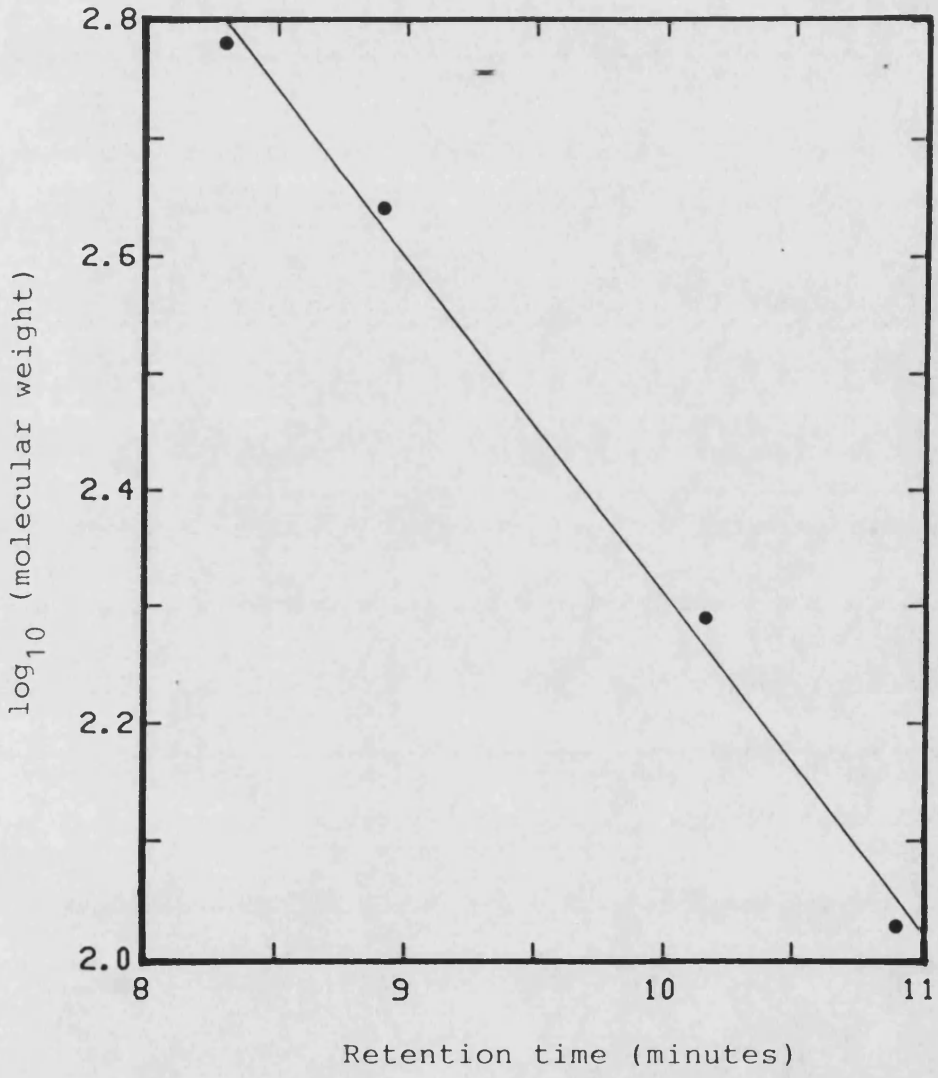

Figure 7.3.3:- SEC Calibration curve of polyethylene glycol

Table 7.3.1 : SEC calibration curve of poly(ethylene glycol)

Peak molecular weight	Retention times (minutes)
106	10.90
194	10.15
440	8.90
660	8.30

Figure 7.3.4a shows the chromatographic retention of the monomer, β-hydroxybutyric acid. Based on the calibration curve of poly(ethylene glycol), this retention time corresponded to a molecular weight slightly lower than the exact molecular weight of β-hydroxybutyric acid. (True MW = 104). A small unidentified peak at higher molecular weight was evident in the reagent supplied.

Figure 7.3.4.b shows the chromatogram for water-soluble degradation products obtained from PHB film. Only one peak was evident with a retention time corresponding to that of the monomer. This data suggests that the degradation of PHB films occurs through surface hydrolysis such that the monomer breaks off from the chain end. Alternatively, if dimers or higher oligomers are released into the aqueous phase, they are rapidly degraded to the monomer.

Figure 7.3.4c shows the chromatogram of degradation products obtained from P(HB/HV) copolymer film containing 12.3 mole % HV. The main peak eluted with a retention time corresponding to that of β-hydroxybutyric acid. The overlapping higher molecular weight peak was presumably due to β-hydroxyvaleric acid, indicating that copolymers degrade by the same process as PHB.

In summary, both the SEC and GLC studies indicate that aqueous, surface hydrolysis of PHB and P(HB/HV) copolymers is achieved by cleavage of monomers from the exposed chain ends.

When random chain scission of polymers occurs in non-aqueous solution, a whole range of oligomers are produced, as has been demonstrated in Part I of this study. It was of interest to test the resolution of the SEC method for oligomers of PHB obtained by pTSA catalysed degradation. In addition an attempt was made to determine aqueous solubility of oligomers.

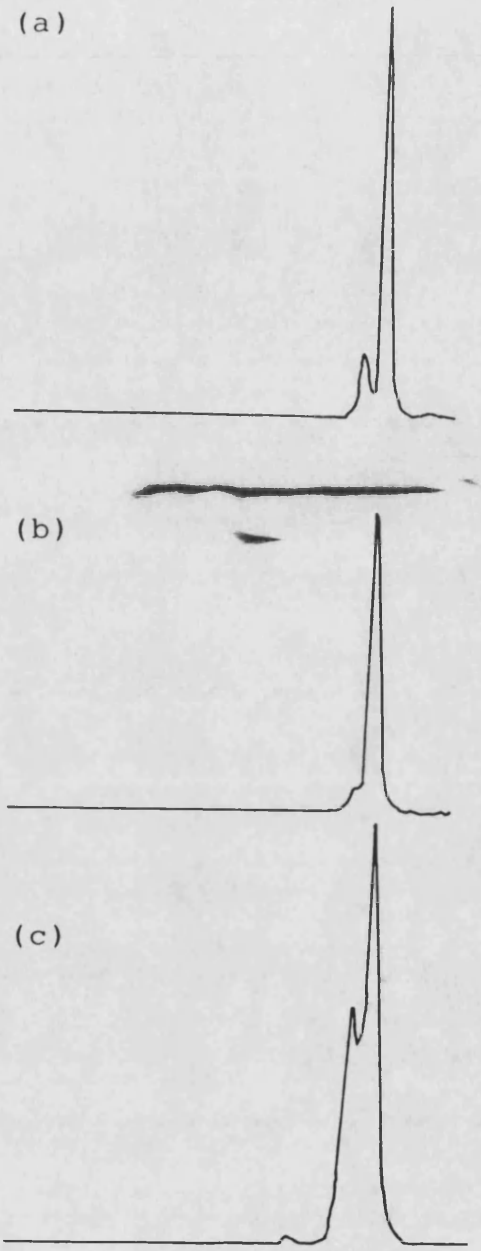

Figure 7.3.4:- Size exclusion chromatograms of (a) β-hydroxybutyric acid (b). Degraded product obtained from degradation of PHB film in 0·1M NaoH (c). Degraded products from 12·3 mole % PHB/PHV copolymer film in 0·1M NaOH.

Figures 7.3.5a and 7.3.5b show the SEC chromatograms of products from degradation of PHB in chloroform in the presence of pTSA and those products which appeared to dissolve in water.

Figure 7.3.5a shows that three peaks were obtained after extensive degradation of this sample and their retention times are shown in Table 7.3.2. Based on the calibration curve of poly(ethylene glycol) the molecular weights for these peaks corresponded roughly to those of the monomer, dimer, and trimer respectively. The value of the molecular weight for the third peak was higher than that of trimer although one would not expect SEC to perform ideally at low molecular weights when solute geometry is highly dependent on molecular weight.

Figure 7.3.5b indicates that the monomer, dimer and trimer appeared to be soluble in water. This was in agreement with Dawes and Ribbons (1964) who showed that dimer and trimer exist as part of the metabolic pathway in microorganisms. It appeared that dimer and trimer are capable of dissolving in water. This re-emphasised the finding that erosion of films occurred primarily by cleavage of monomer from the surface.

However, further studies of this type have shed doubt on this evidence. Figures 7.3.6a and 7.3.6b show equivalent experiments performed after a partial degradation in the presence of pTSA. The length of degradation was reduced to 19 hours. The chromatogram for pTSA degradation, shown in Figure 7.3.6a, indicates the presence of monomer, dimer , trimer, tetramer and other oligomers which appeared in the void volume of the column. Figure 7.3.6b shows that chromatogram of degradation products which were apparently soluble in water. It is unlikely that these high molecular weight oligomers were genuinely soluble in water but may have been suspended as a colloidal

Table 7.3.2 : Retention times and PEG-equivalent molecular weights for degraded products from pTSA degradation

Peak number	Retention times (minutes)	Molecular weight based PEG calibration curve
1	11.15	92
2	10.00	204
3	9.35	321

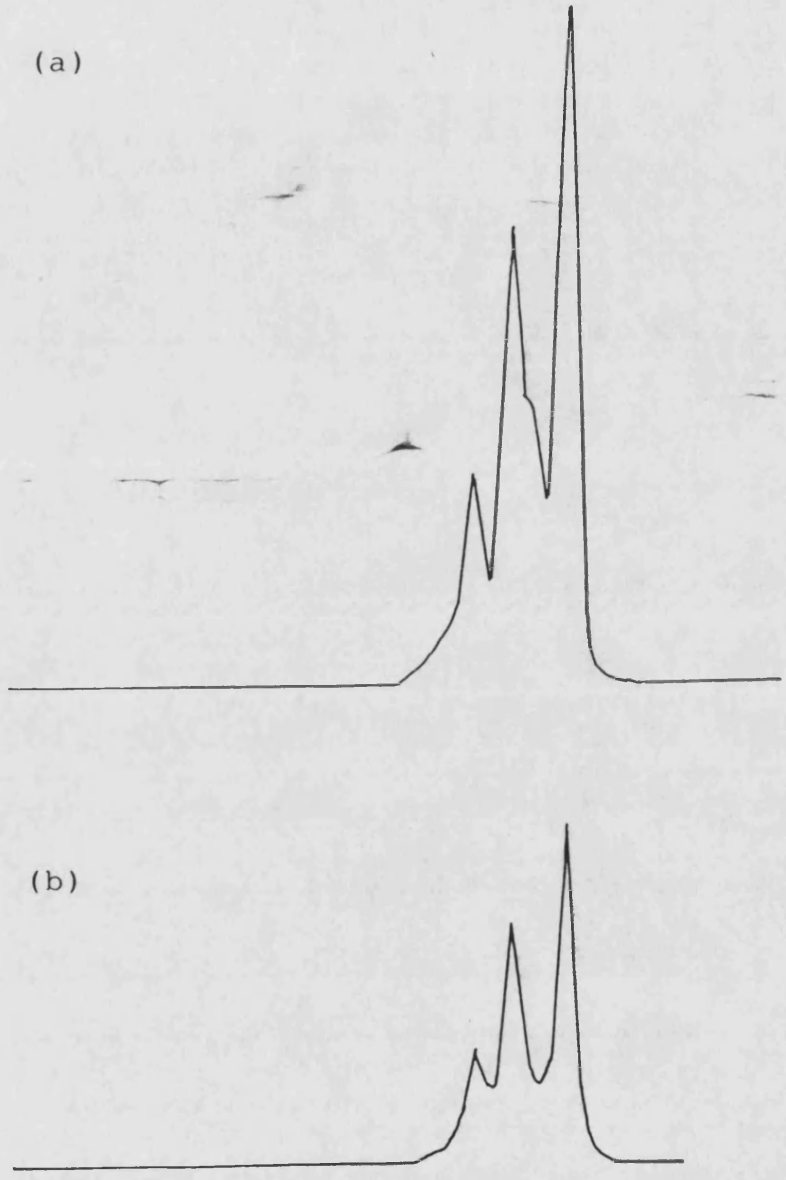

Figure 7.3.5:- Size exclusion chromatograms of (a) degraded products from pTSA degradation (3 days refluxing with 2 % $^{w}/_{v}$ pTSA)

(b) water-soluble fractions recovered from the above product after extraction as detailed in text.

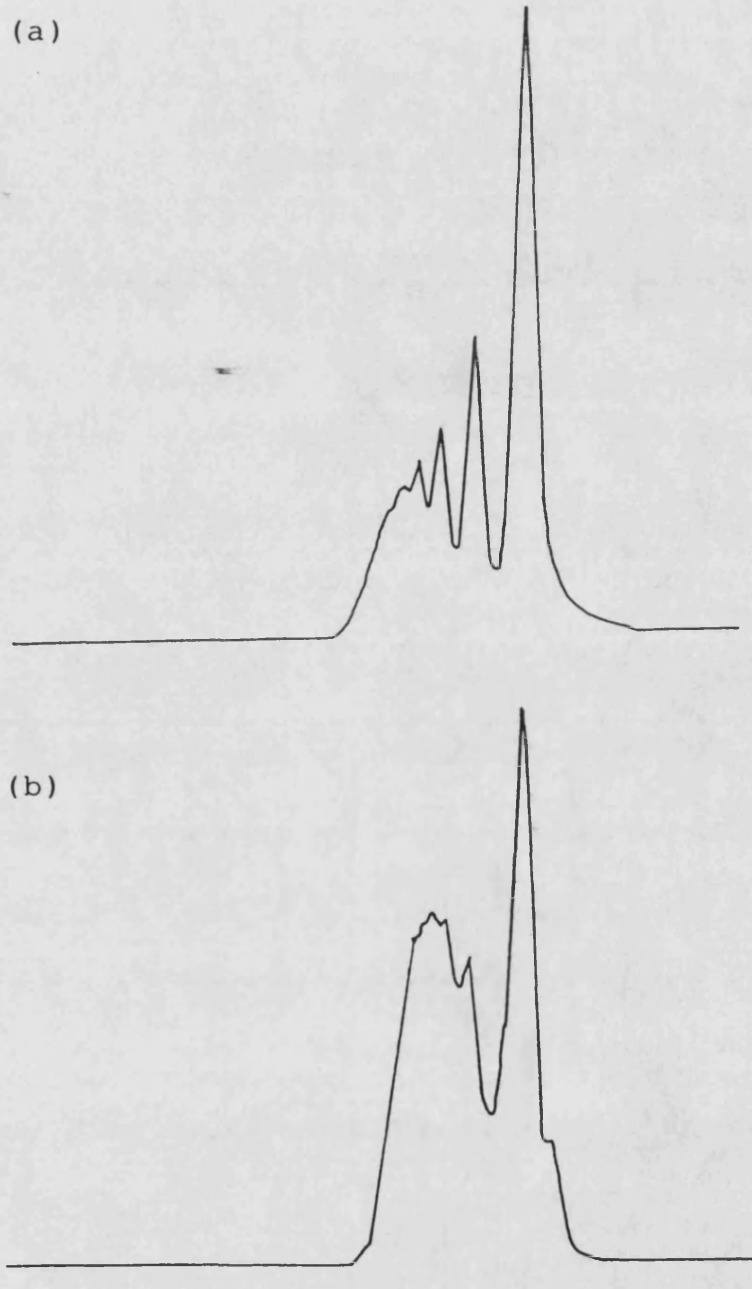

Figure 7.3.6:- Size exclusion chromatogram of (a) degraded products from pTSA degradation (19 hours refluxing with 2% $^{w}/_{v}$ pTSA) (b) 'water-soluble' fraction recovered from the above product after extraction as detailed in text.

microemulsion which resisted filtration. Thus higher molecular weight fragments of PHB were transfered onto the column artificially (see section 6.3.7.3).

Further work is required to establish the degradation products of PHB and PHV. The synthesis of dimers and trimers for validation of chromatrographic methods is necessary.

7.4. Release of methyl red from polymer films.

Several workers (Korsatko *et al.* 1983, Brophy and Deasy, 1986 and Gould *et al.*, 1987) have investigated the effect of formulation on the release of drugs from PHB and P(HB/HV) matrices. The aim of the present study has been to examine the factors which affect release of chloroform-soluble compounds from PHB and copolymers films. Chloroform is a good solvent for the polymers. Thus films could be cast from solutions containing drug and polymer. Methyl red was chosen as a model compound because it is readily soluble in water and chloroform and was easily assayed by ultraviolet spectrophotometry.

Figure 7.4.1 shows the ultraviolet spectra of methyl red in different pH buffers and chloroform. It can be seen that there was no change in the absorption maximum above pH 7.4 due to the similarities in the fraction of dye ionised at pH 7.4, 10.0 and 13.0. The pKa of methyl red is 5.1 (Martin *et al.*, 1969) and hence the degree of ionisation at pH 7.4 and above would be almost 100 % . This indicates the suitability of methyl red as a model compound for the release studies under physiological conditions (pH 7.4 at 37°C) and also under extreme conditions of degradation (0.1M sodium hydroxide).

The loading of methyl red in cast PHB and copolymer films was determined using a spectrophotometric assay of methyl red in chloroform.

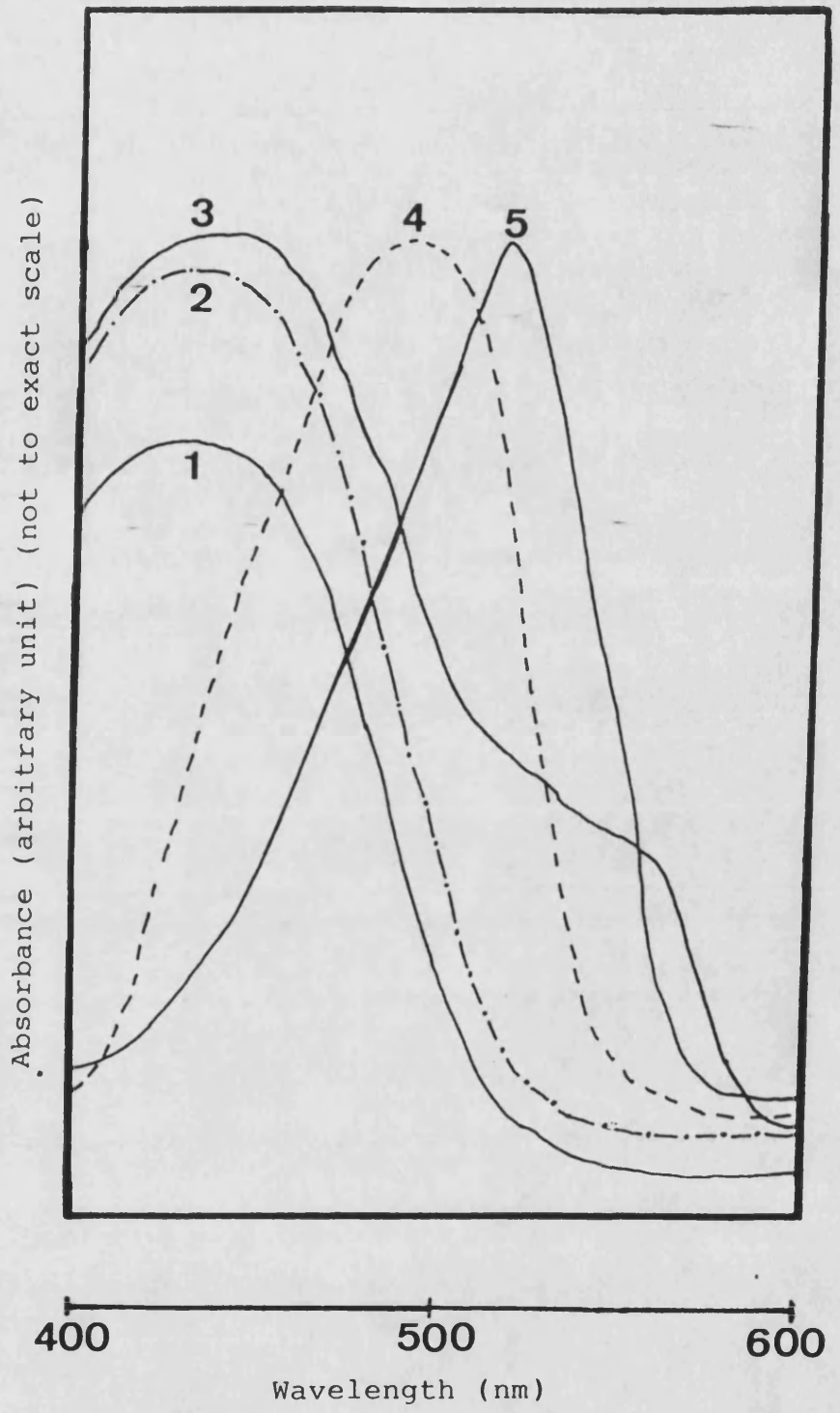

Figure 7.4.1:- Ultraviolet spectra of methyl red in chloroform and aqueous pH buffer solutions; (1) 0·1M sodium hydroxide; (2) pH 10 bicarbonate buffer; (3) pH 7·4 phosphate buffer; (4) chloroform; (5) 0·1M hydrochloric acid.

Figure 7.4.2 and Table 7.4.1 show the calibration curve obtained and the reproducibility of the assay.

The release of methyl red from polymer films was studied at pH 7.4 and in 0.1M sodium hydroxide. Figure 7.4.3 and Table 7.4.2 show the calibration curves and their reproducibility at pH 7.4. Figure 7.4.4 and Table 7.4.3, show the analogous assay of methyl red in 0.1M sodium hydroxide.

7.4.1 Effect of methyl red loading on its release.

The cumulative release of methyl red under static conditions was plotted against time for different loadings of methyl red in PHB films and this is shown in Figure 7.4.5 for films containing 0.71% w/w, 2.78% w/w, 5.21% w/w and 7.36% w/w methyl red. Data plotted is the mean of three replicate release studies from each film. The highest standard deviation for the data was less than 2% of the mean. The higher the initial loading the faster was the release rate. The release of methyl red from films containing more than 10% w/w methyl red was completed within six hours. In these cases the release mechanism was thought to be through pores and channels.

High loading probably resulted in crystals of methyl red within the film which were in close contact. Dissolution of methyl red at the surface would have allowed further penetration of water gradually forming a series of interconnecting pores throughout the matrix. The lower loadings of methyl red would have led to fewer points of contact between crystallites of methyl red. Thus pore formation would have been more tortuous leading to a slower rate of release.

The role of diffusion through the polymer itself was thought to be minimal at high drug loadings although it may have played a part at

Table 7.4.1 : Calibration curves of methyl red in chloroform at 490 nm

Calibration code	Absorption coefficient E^{1M} for 1cm cell ± standard deviation	Correlation coefficient
1	47000 ± 450	0.9980
2	45000 ± 200	0.9990
3	40000 ± 900	0.9993
4	43000 ± 900	0.9993
AVERAGE=	43750 ± 3000	

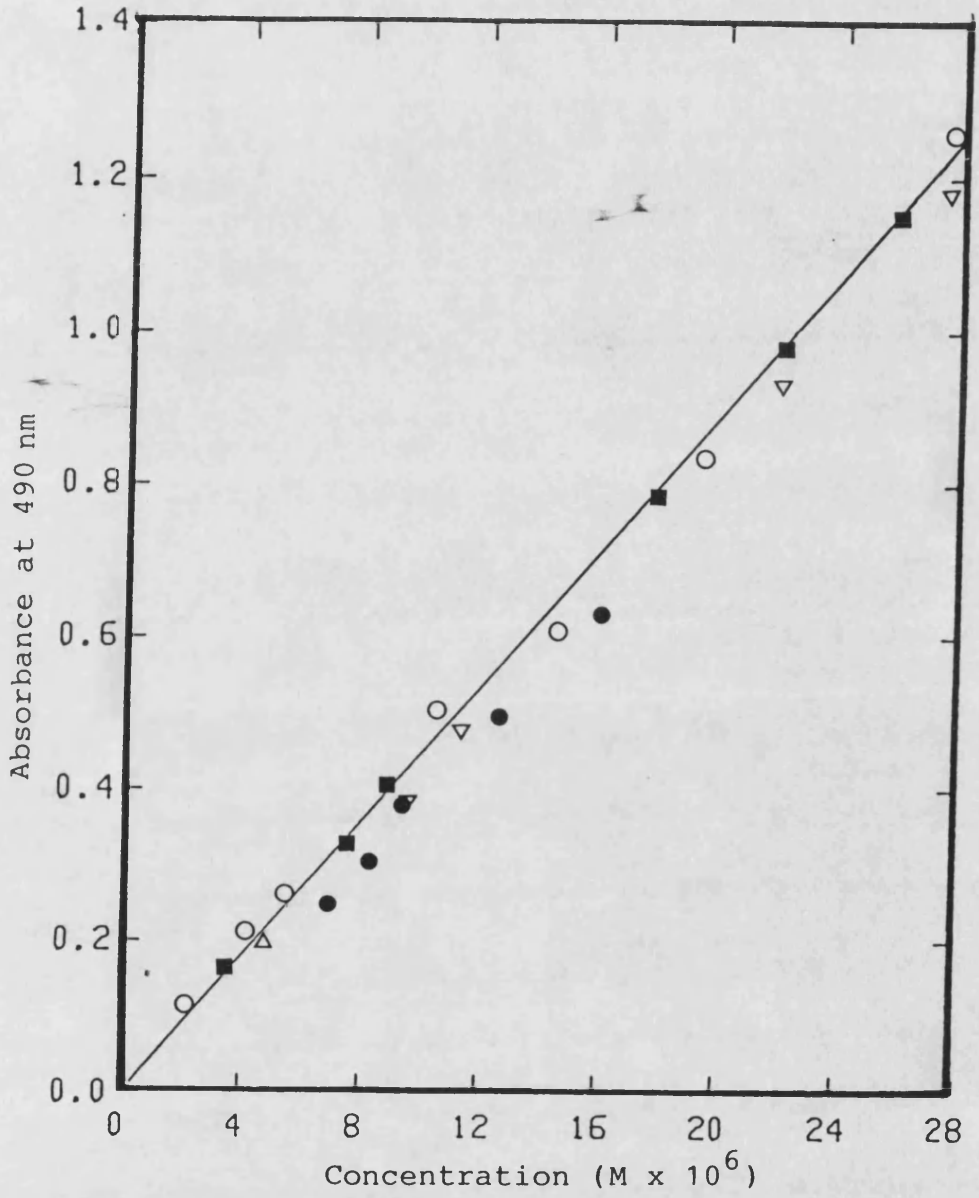

Figure 7.4.2:- Beer Lambert plot of methyl red in chloroform.

Table 7.4.2 : Calibration curves of methyl red in pH 7.4 (I = 0.153 M) at 435 nm

Calibration code	Absorption coefficient E^{1M} for 1cm cell ± standard deviation	Correlation coefficient
1	16200 ± 200	0.9994
2	15700 ± 40	0.9999
3	16300 ± 200	0.9994
AVERAGE=	16100 ± 320	

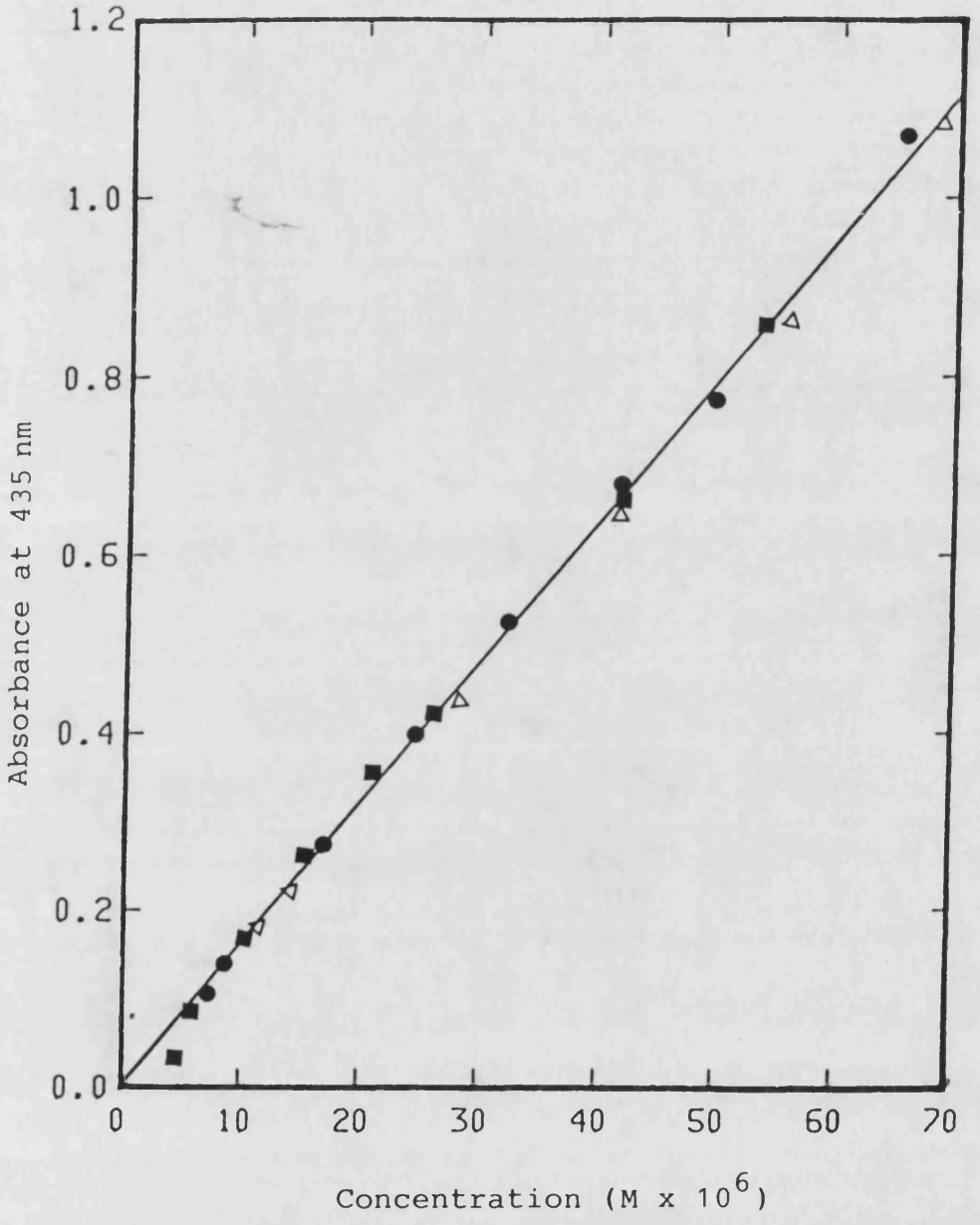

Figure 7.4.3:- Beer Lambert plot of methyl red in phosphate buffer (pH 7·4, I = 0·153M).

Table 7.4.3 : Calibration curves of methyl red in 0.1M sodium hydroxide at 430 nm

Calibration code	Absorption coefficient E^{1M} for 1cm cell ± standard deviation	Correlation coefficient
1	19000 ± 92	0.9999
2	19000 ± 81	0.9999
3	18000 ± 230	0.9996
4	22000 ± 220	0.9997
AVERAGE=	19500 ± 1700	

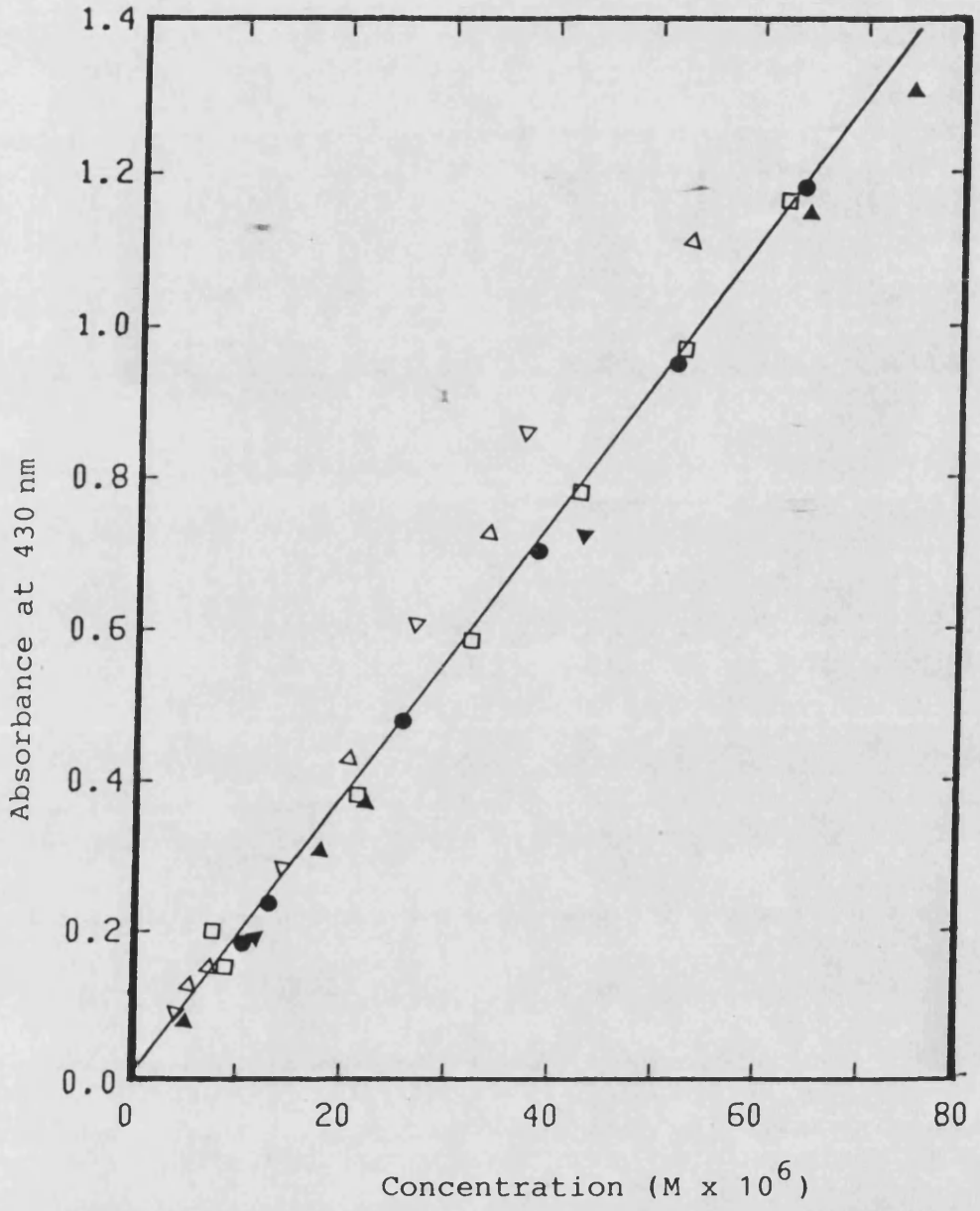

Figure 7.4.4:- Beer Lambert plot of methyl red in 0·1M sodium hydroxide.

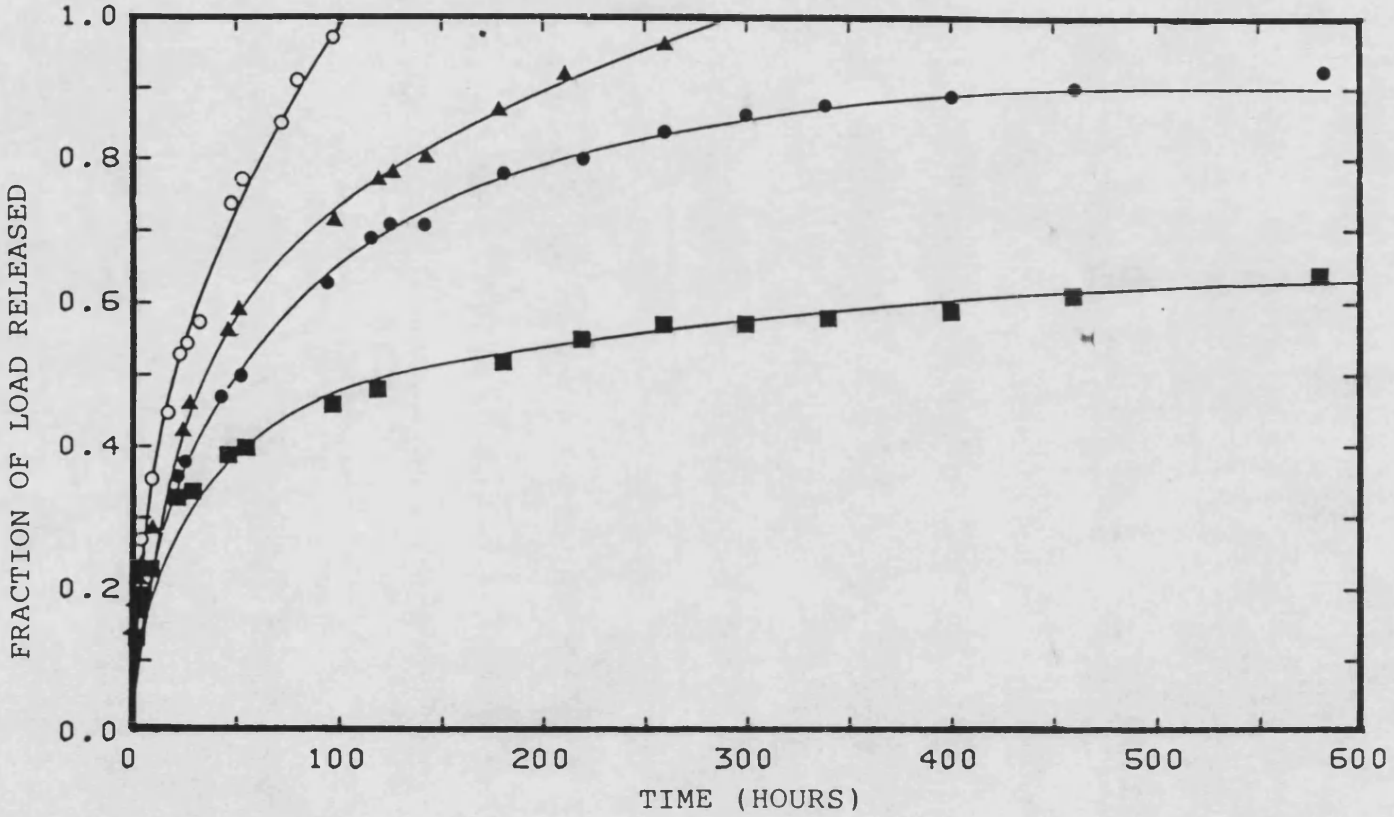

Figure 7.4.5:- Release of methyl red from PHB films, as a function of methyl red content in film, after storage in phosphate buffer (pH 7·4) at 37°C; Loading of methyl red: (■), 0·71% $w/_w$; (●), 2·78% $w/_w$; (▲), 5·21% $w/_w$; (O), 7·36% $w/_w$.

low drug loadings. The involvement of diffusion through the polymer would have been a function of the morphology of the mixtures. For films containing low loading an attempt was made to determine the morphology of methyl red in the films using DSC. It was of interest to determine whether methyl red existed as a suspension of crystallines or whether the methyl red was dispersed at a molecular level in PHB films. Unfortunately the results of this study were inconclusive since the melting point of methyl red was too close to that of PHB and could not be separated from the large polymer melting endotherm. Visual and microscopic inspection of the films showed that despite the high solubility of methyl red in chloroform, most of the drug existed as a suspension in PHB matrix. Presumably, the highly crystalline nature of PHB was not disrupted by the presence of methyl red.

Brophy and Deasy (1987) have used the following equation to describe the *in vitro* release of sulphamethizole from PHB microparticles.

$$f(t)=B_1\, t^{1/2}-B_2\, t \quad \ldots\ldots \quad (7.3)$$

where f(t) is the fraction of drug released at time t.

Equation 7.3 can be derived by extending the theory used by Higuchi (1962). A complete derivation is shown in Appendix 3. This theory has been used in the present study to model release of methyl red from polymer films. Equation 7.3 was a good model for the experimental release of methyl red from PHB and P(HB/HV) films. An example is shown in Figure 7.4.6 which represents the release of methyl red from P(HB/HV) film containing 6.5 mole % HV in pH 7.4 and 37°C. The values of B_1 and B_2 were used to characterise the release of methyl red from PHB and copolymer films throughout our study. These values were obtained by transforming Equation 7.3 into a straight line

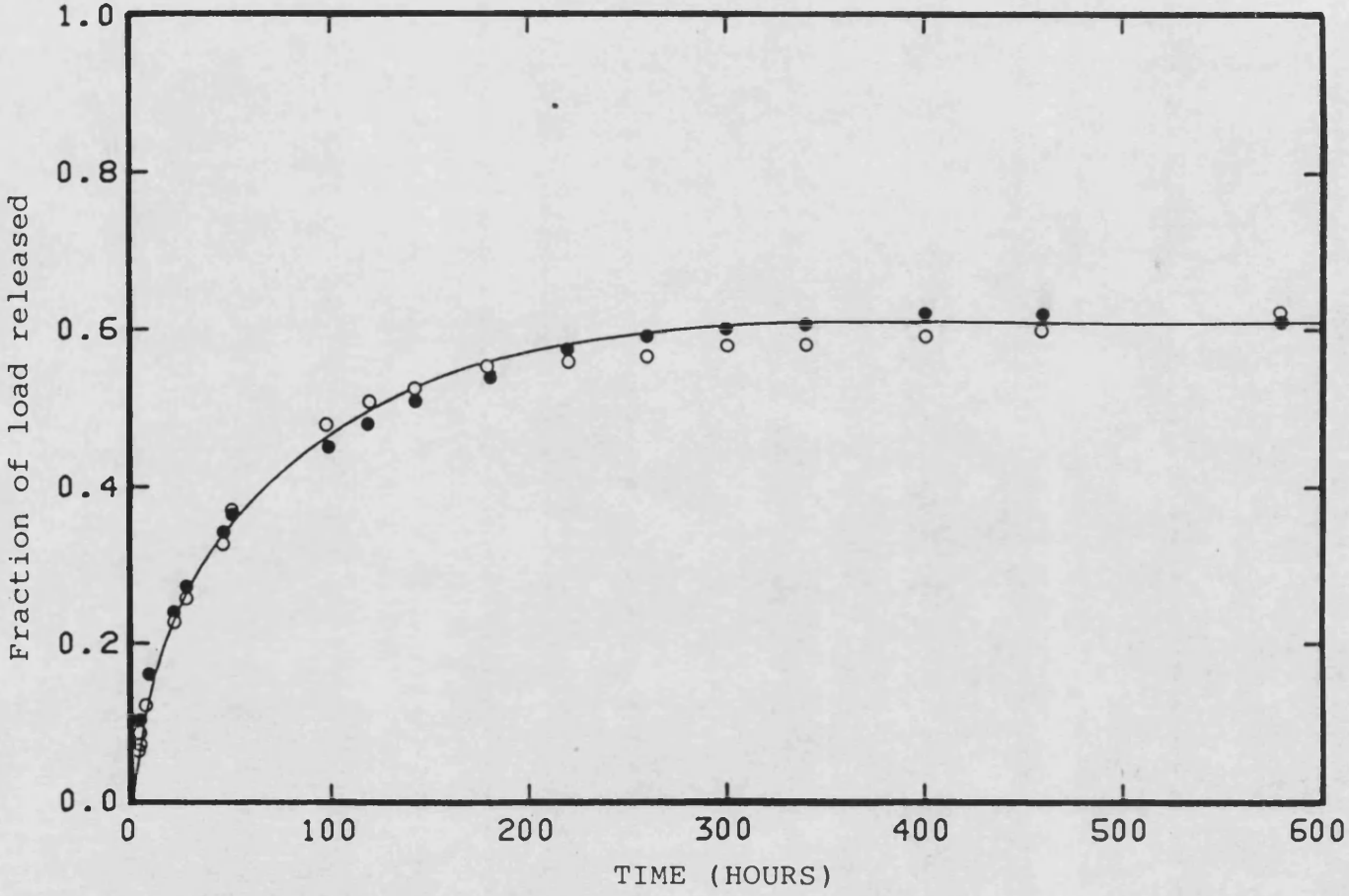

Figure 7.4.6:- Release of methyl red from PHB/PHV copolymer film (6·5 mole% HV) after storage in phosphate buffer (pH 7·4) at 37°C (o) experimental data (●) release predicted by fitting data to modified equation.

curve such that the intercept and the slope giving the values of B_1 and B_2 respectively (see Appendix 3).

Figure 7.4.7, 7.4.8 and 7.4.9 show the relationship of the function $([\frac{f(t)^2}{t}]^{1/2})$ against the square root of time, ($t^{1/2}$) for PHB films containing 0.71% w/w, 0.89% w/w and 0.82% w/w methyl red. The objective of this study was to determine the variation between replicate batches of film. It was not possible to replicate the drug loading precisely in this study but these three films had similar loadings. The data obtained from the 0.71% loading (Fig. 7.4.7) was not as good a fit to the model as these obtained for other films. There was no obvious explanation for this concept that the 0.71% loading was the lowest used and the data may have indicated a change in the mechanism of release at very low loadings. Values of B_1 and B_2 obtained from these three films are shown in Table 7.4.4. Statistical t-test analysis of the values of B_1 and B_2 showed that there were no significant differences between these values at 95% level of confidence for the 0.82% and 0.89% films. Thus the release of drug from similar batches of film was reproducible.

Figures 7.4.10 to 7.4.12 show the function $([\frac{f(t)^2}{t}]^{1/2})$ plotted against the square root of time, ($t^{1/2}$), for PHB films containing 2.78%, 5.21% w/w and 7.36% w/w methyl red. The values of B_1 and B_2 obtained are shown in Table 7.4.5. The values of B_1 and B_2 obtained from methyl red loading of 2.78% w/w were not significantly different to those obtained for the 0.89% w/w film (Table 7.4.4). However, comparison between data obtained at loadings of 2.48% w/w and 5.21% w/w and 7.36% w/w were clearly different.

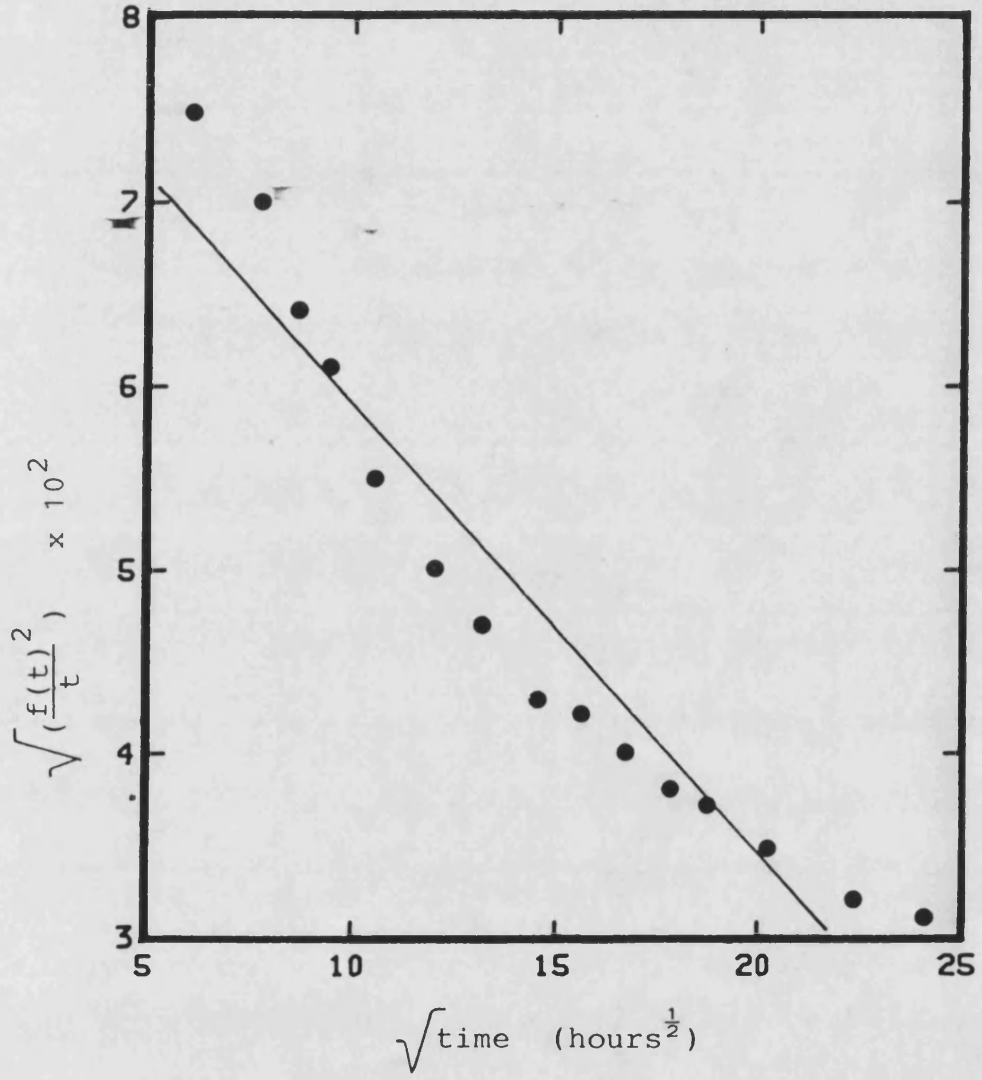

Figure 7.4.7:- The function $\sqrt{(\frac{f(t)}{t})^2}$ against $\sqrt{t}$ for release of methyl red from PHB film containing 0·71% $w/_w$ methyl red (in pH 7·4 at 37°C).

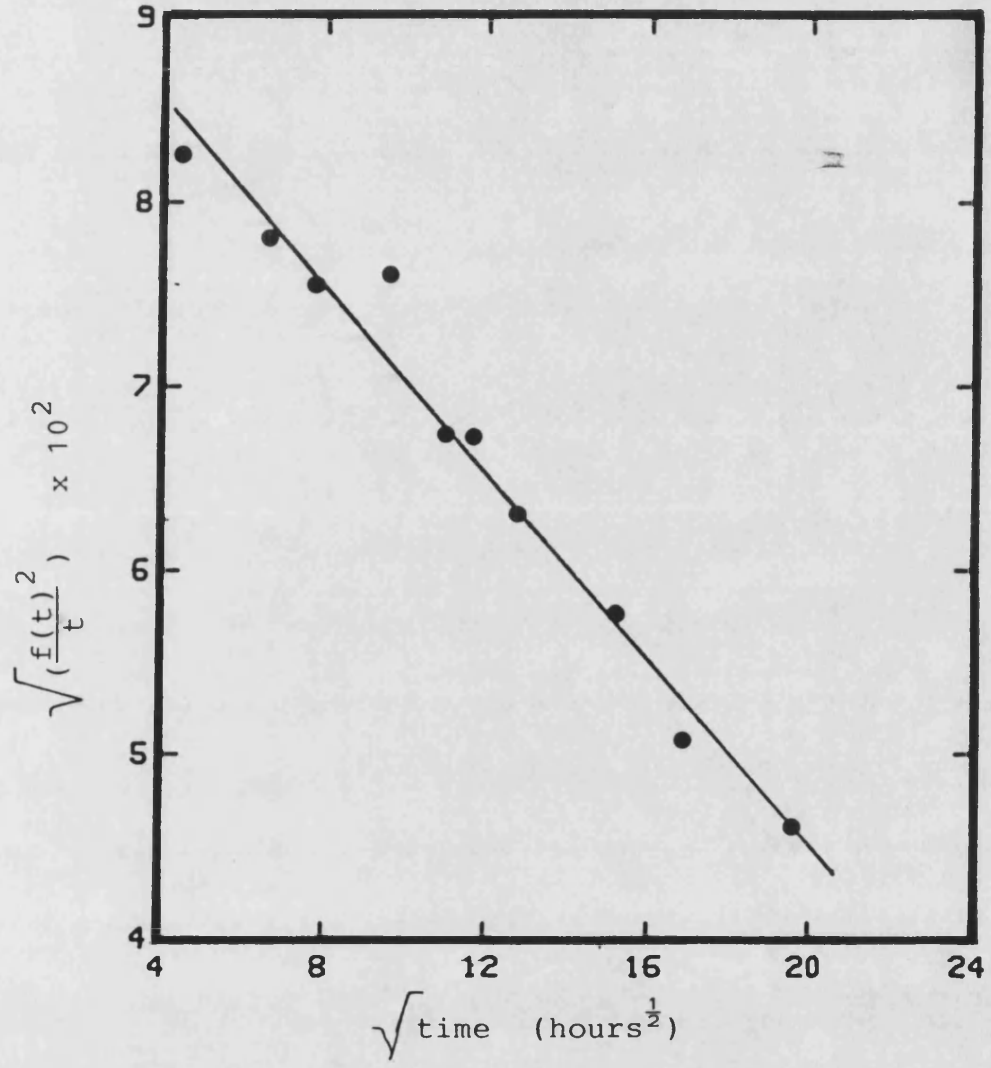

Figure 7.4.8:- The function $\sqrt{(\frac{f(t)}{t})^2}$ against $\sqrt{t}$ for release of methyl red from PHB film containing 0·89% $w/_w$ methyl red (in pH 7·4 at 37°C).

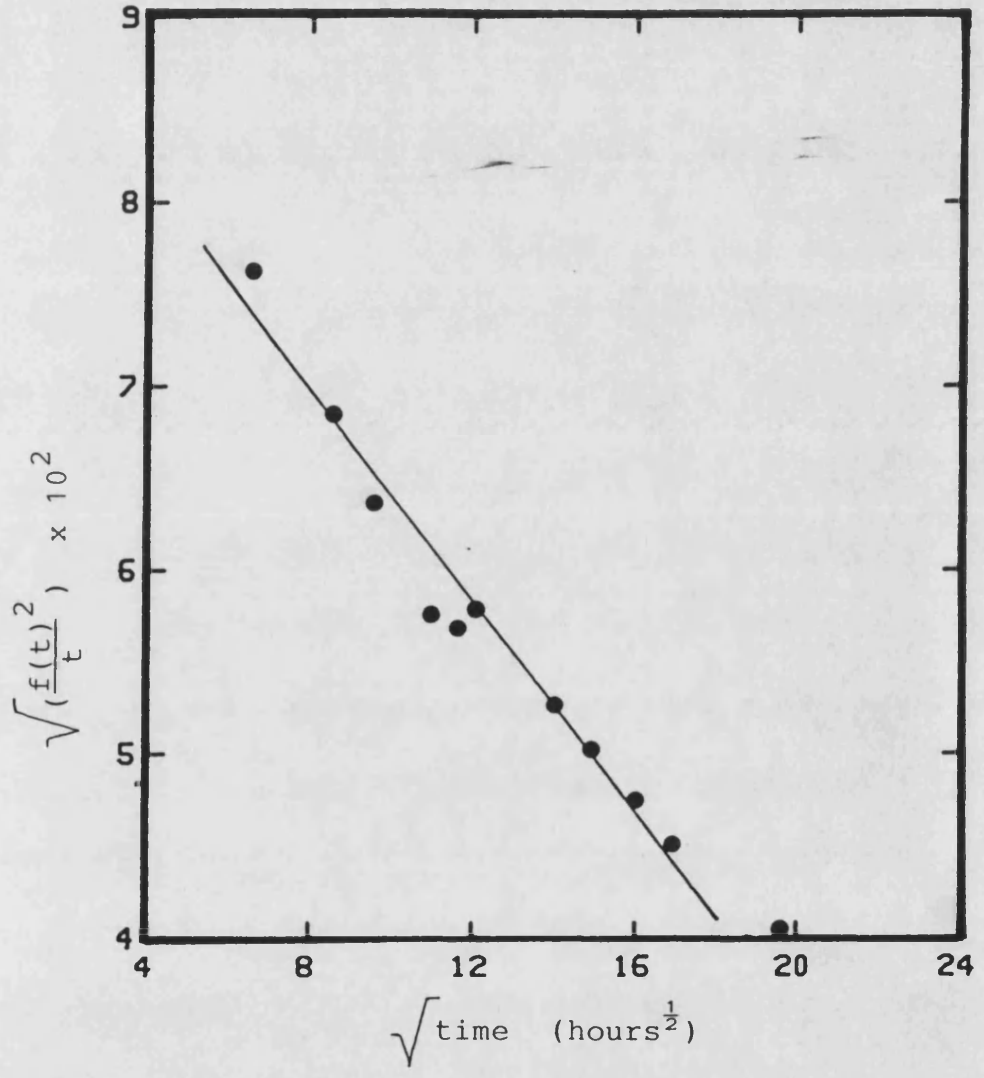

Figure 7.4.9:- The function $\sqrt{(\frac{f(t)}{t})^2}$ against $\sqrt{t}$ for release of methyl red from PHB film containing 0·82% w/w methyl red (in pH 7·4 at 37°C).

Table 7.4.4 : Kinetic parameters for release of methyl red from PHB films stored in phosphate buffer (pH 7.4, I = 0.153 M) at 37°C

Percent w/w methyl red in PHB film	Rate constant ($hours^{-1} \times 10^3$)	
	B_1	B_2
0.71	76.2 ± 3.2	2.40 ± 0.22
0.82	89.4 ± 3.7	2.62 ± 0.30
0.89	95.7 ± 2.4	2.53 ± 0.19

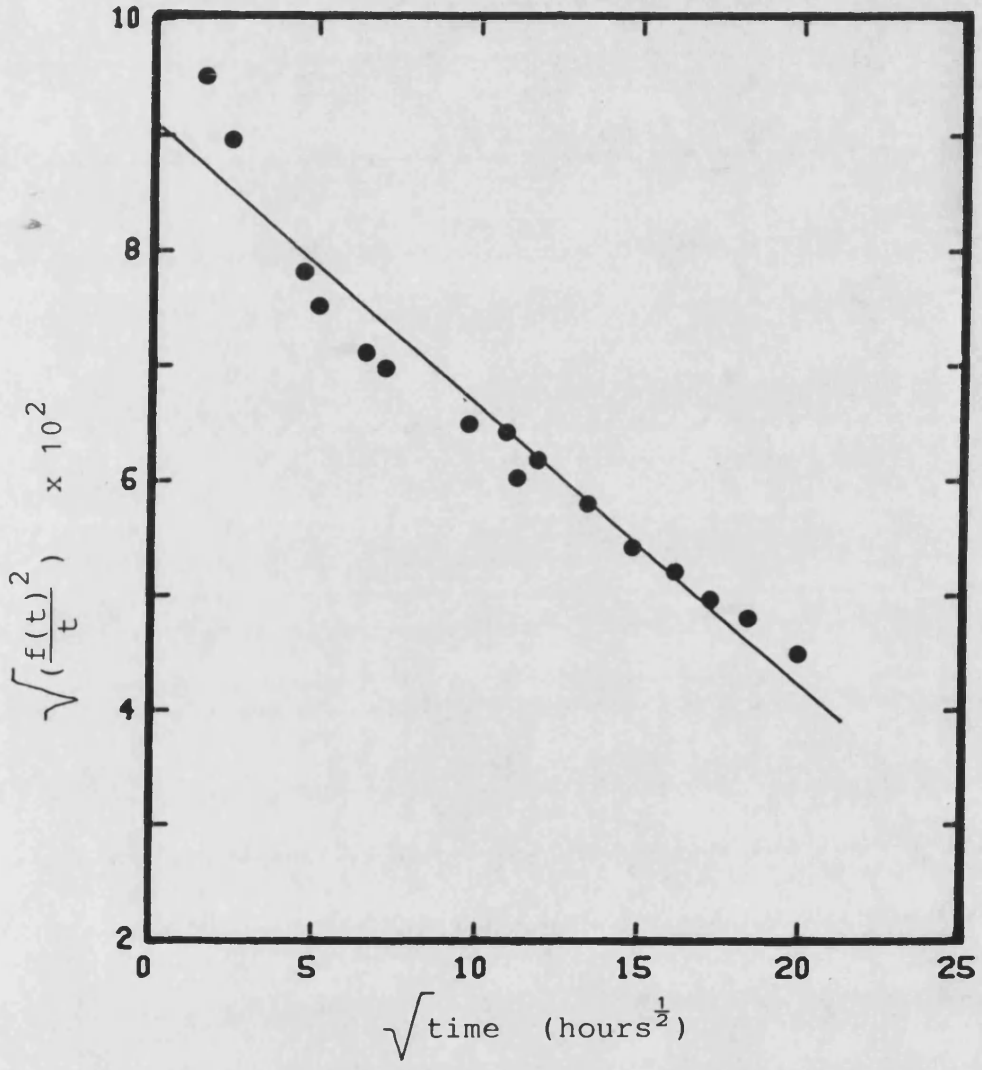

Figure 7.4.10:- The function $\sqrt{(\frac{f(t)}{t})^2}$ against $\sqrt{t}$ for release of methyl red from PHB film containing 2·78% $w/_w$ methyl red (in pH 7·4 at 37°C).

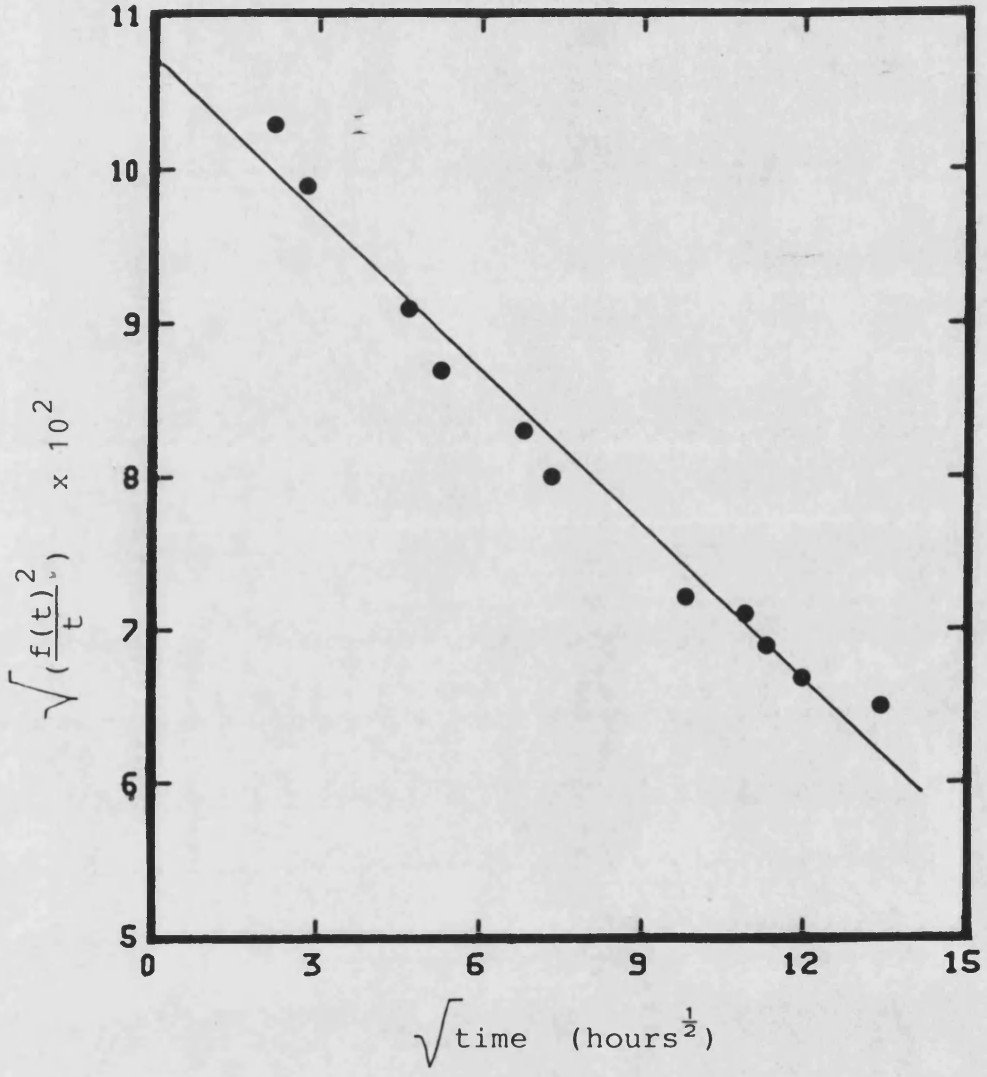

Figure 7.4.11:- The function $\sqrt{(\frac{f(t)}{t})^2}$ against $\sqrt{t}$ for release of methyl red from PHB film containing 5·21% $w/_w$ methyl red (in pH 7·4 at 37°C).

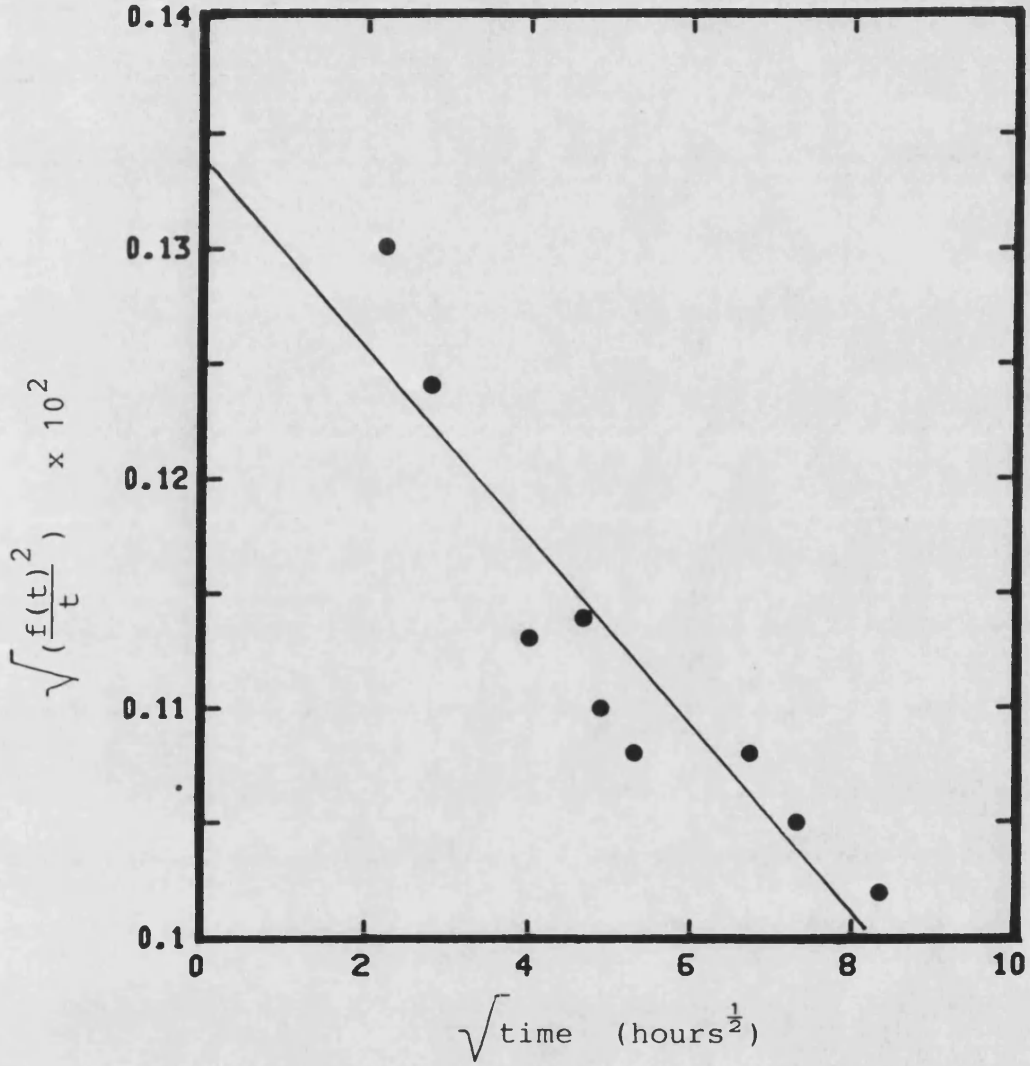

Figure 7.4.12:- The function $\sqrt{(\frac{f(t)}{t})^2}$ against $\sqrt{t}$ for release of methyl red from PHB film containing 7·36% w/w methyl red (in pH 7·4 at 37°C).

Table 7.4.5 : Kinetic parameters for release of methyl red from PHB films in phosphate buffer (pH 7.4 , I= 0.153M) at 37°C

Percent w/w methyl red in PHB film	Rate constants ($hours^{-1} \times 10^3$)	
	B_1	B_2
2.78	90.9 ± 1.8	2.44 ± 0.20
5.21	107.0 ± 1.5	3.37 ± 0.20
7.36	123.1 ± 2.5	2.46 ± 0.40

7.4.2 Effect of copolymer composition on the release of methyl red.

Figure 7.4.13 shows the cumulative release of methyl red from P(HB/HV) copolymer films containing approximately 1% w/w methyl red at pH 7.4 and 37°C. The precise loadings of methyl red in copolymers containing 6.5 mole % HV, 12.3 mole w/w HV and 19.2 mole % HV were 1.03 %w/w, 0.86 %w/w and 0.78 % w/w respectively. The relationships between the function $([\frac{f(t)^2}{t}]^{1/2})$ and $(t^{1/2})$ for various copolymer films are shown in Figures 7.4.14 to 7.4.17 and the functions B_1 and B_2 are summarised in Table 7.4.6.

The two loading studied using 6.5 mole% HV copolymer films (1.03% and 0.86% w/w methyl red) had very different values of B_1 and B_2 . Both released drug at a slower rate than similar PHB films. There were large differences in rates of release from the other copolymer films (Table 7.4.6). At 12.3 and 19.2 mole % HV , the rate of release was rapid. The most likely reason for this rapid release lies in the more amorphous nature of P(HB/HV) copolymers. Penetration of water and movement of drug away from the polymer was probably slower for polymers having a higher degree of crystallinity (Gordon,1963).

However the molecular weights of the polymers were somewhat different and the morphology of polymer drug matrices was not examined in this study. A more comprehensive study of the factors affecting the release from copolymers is required. This study has indicated that release can be controlled by selection of the polymer as well as the loading of the drug. Polymers of equal molecular weight should be used and a knowledge of the effect of polymer crystallinity on the morphology of the drug would be required to intepret the results of

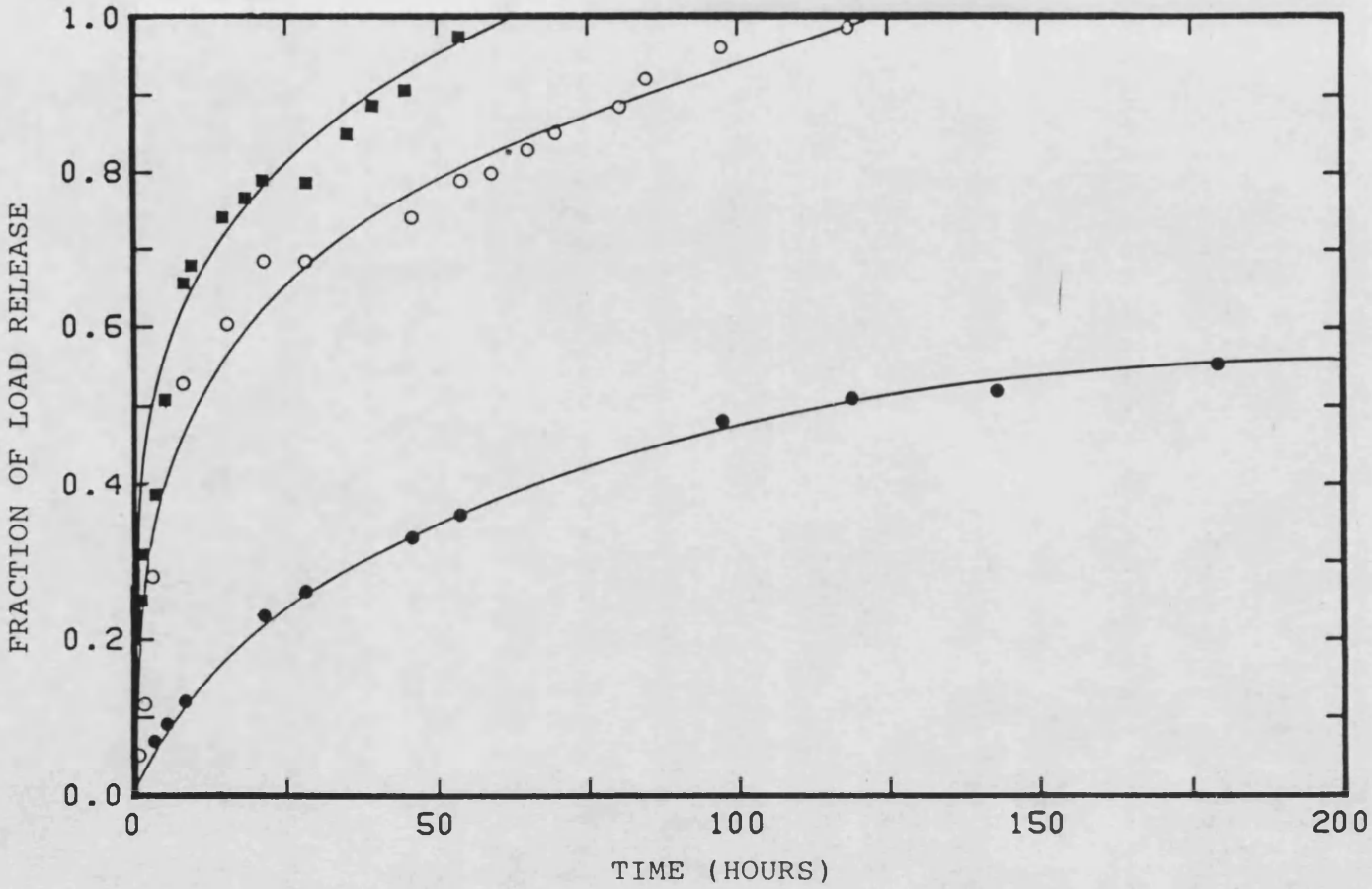

Figure 7.4.13:- Release of methyl red from PHB/PHV copolymer films stored in phosphate buffer (pH 7·4) at 37°C. (●), 6·5 mole % HV (1·03% w/w methyl red loading); (○), 12·3 mole % HV (0.86 % w/w methyl red loading); (■), 19·2 mole % HV (0.78 % w/w methyl red loading).

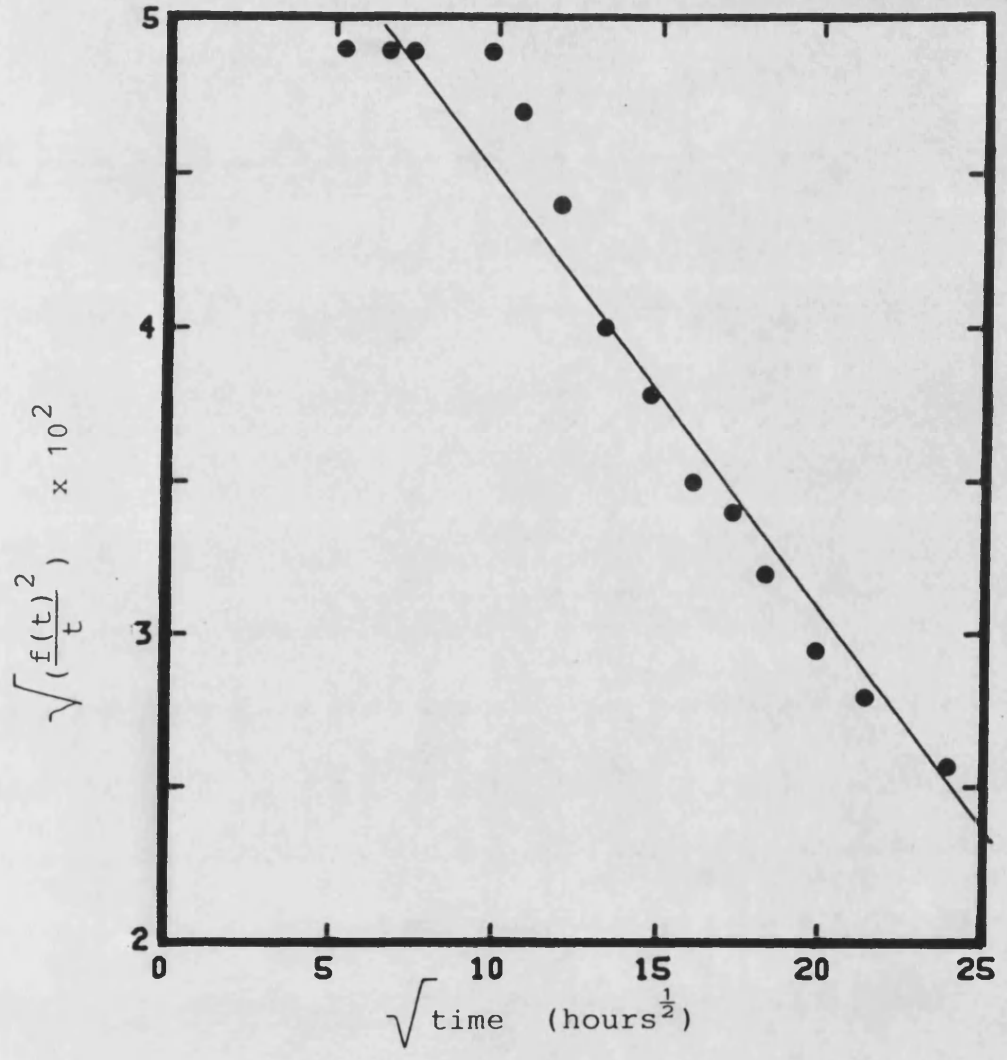

Figure 7.4.14:- The function $\sqrt{(\frac{f(t)}{t})^2}$ against $\sqrt{t}$ for release of methyl red from PHB/PHV copolymer film (6·5 mole % HV) containing 1·03% w/w methyl red (in pH 7·4 at 37°C).

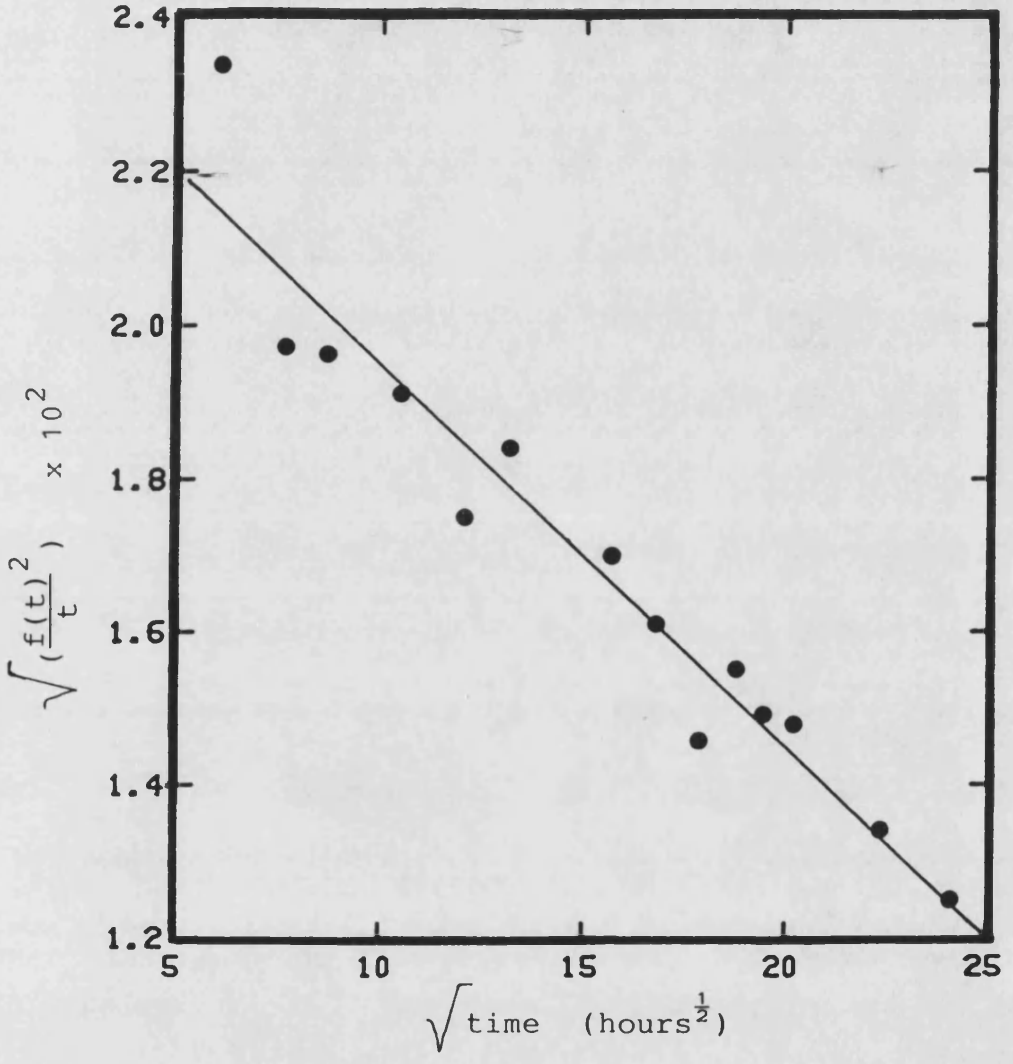

Figure 7.4.15:- The function $\sqrt{(\frac{f(t)}{t})^2}$ against $\sqrt{t}$ for release of methyl red from PHB/PHV copolymer film (6·5 mole % HV) containing 0·86% w/w methyl red (in pH 7·4 at 37°C).

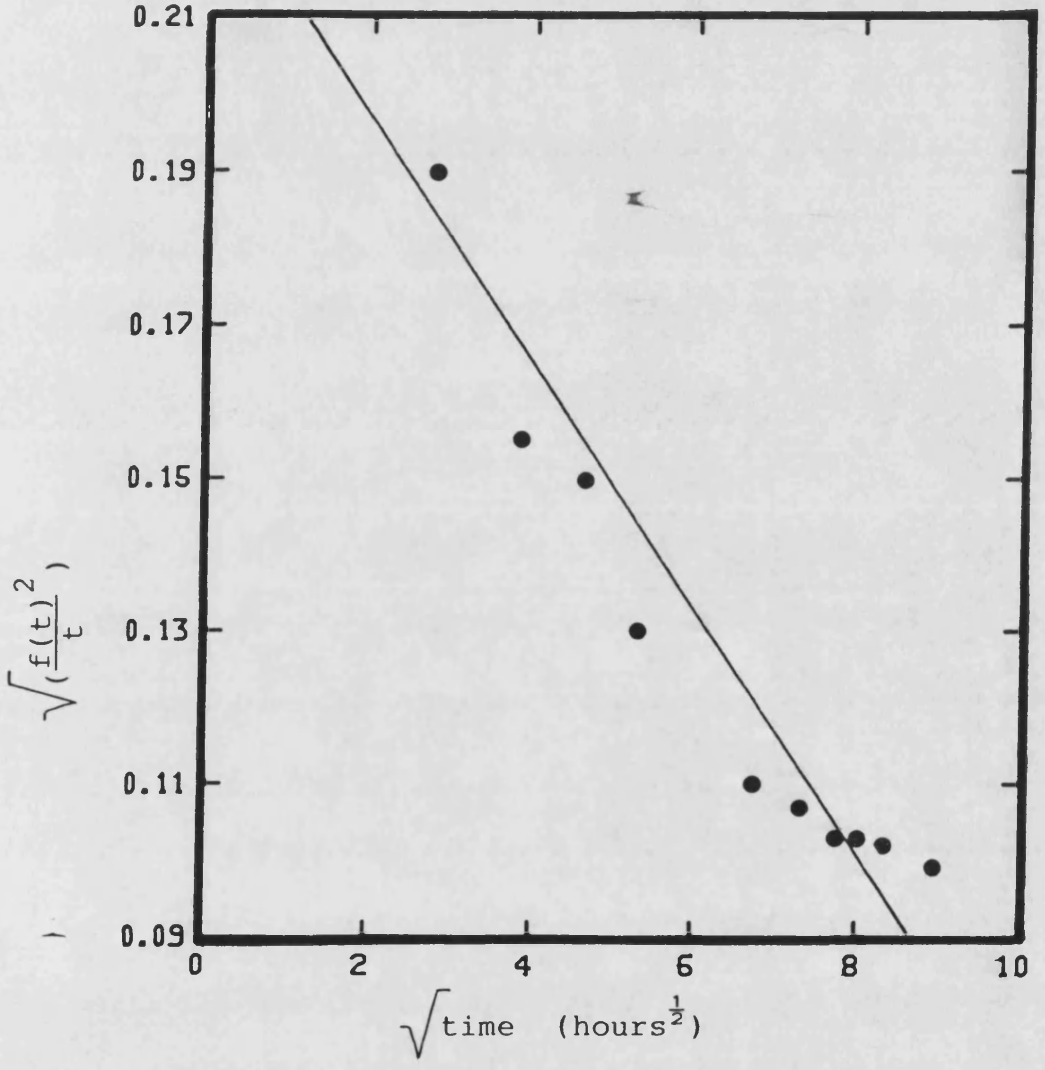

Figure 7.4.16:- The function $\sqrt{(\frac{f(t)}{t})^2}$ against $\sqrt{t}$ for release of methyl red from PHB/PHV copolymer film (12·3 mole % HV) containing 0·74% w/w methyl red (in pH 7·4 at 37°C).

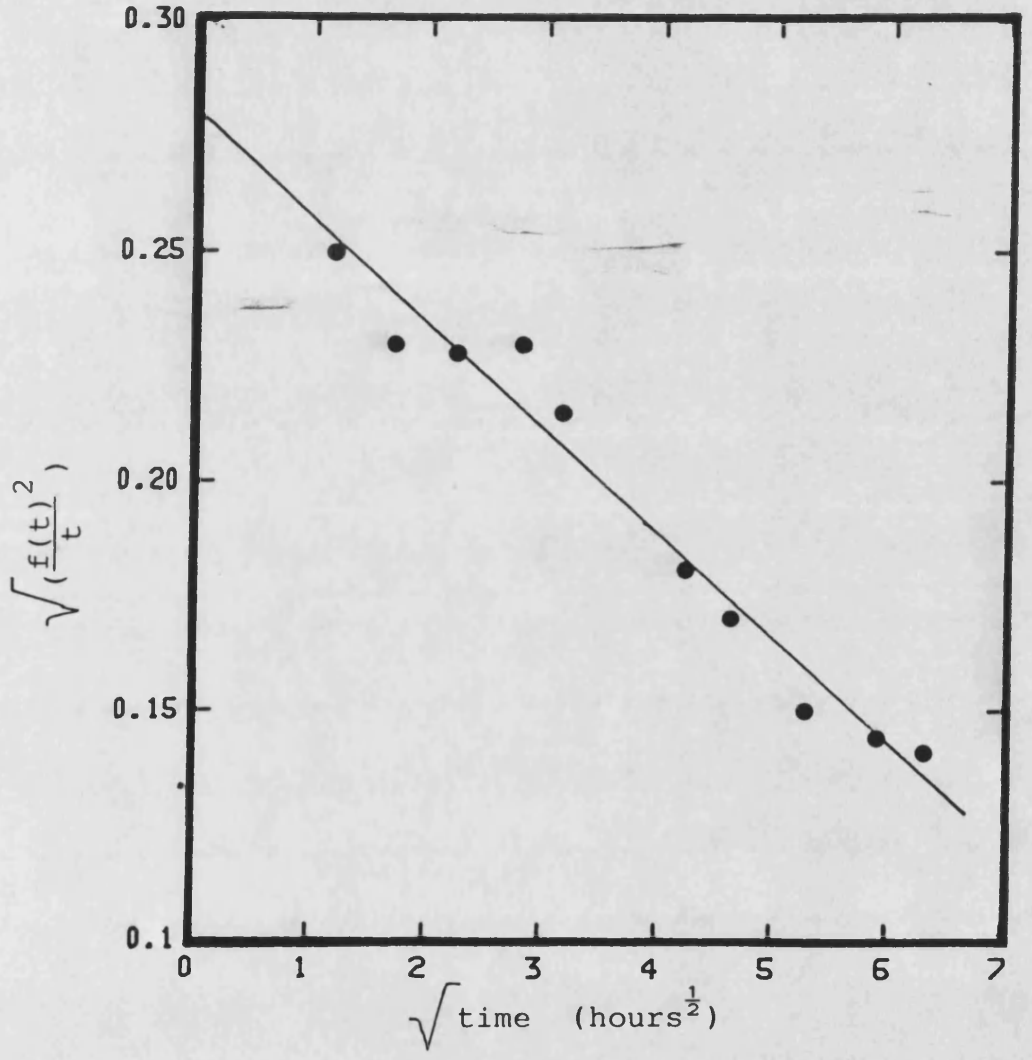

Figure 7.4.17:- The function $\sqrt{(\frac{f(t)}{t})^2}$ against $\sqrt{t}$ for release of methyl red from PHB/PHV copolymer film (19·2 mole % HV) containing 0·78% w/w methyl red (in pH 7·4 at 37°C).

Table 7.4.6 : Kinetic parameters for release of methyl red from copolymer in phosphate buffer (pH 7.4 , I = 0.152M) at 37°C

Polymer composition (mole % HV)	Methyl red loading (% w/w)	Rate constants (hours^{-1} $\times 10^3$)	
		B_1	B_2
6.5	1.03	59.0 ± 1.2	1.41 ± 0.08
6.5	0.86	24.5 ± 1.1	0.58 ± 0.08
12.3	0.74	233.3 ± 10.9	16.58 ± 1.70
19.3	0.78	279.0 ± 5.8	22.70 ± 1.41

release studies. Brophy and Deasy (1986) observed that the *in vitro* release of sulphamethizole from PHB microparticles was dependant on polymer molecular weight. As the polymer molecular weight decreased, the release rate also decreased. This could explain the slow release rate from the 6.5 mole % HV films used in this study, which were lower in molecular weight than other films used.

However there is no obvious explanation for the effect of molecular weight on drug release since the crystallinity of the polymers used in this study was not dependant on molecular weight. In addition the work of Akhtar *et al.* (1987) showed that there were no changes in the mechanical propeties of polymer films over the molecular weight range used in the release studies reported here. Thus differences between release rates from the copolymers were probably a genuine function of morphology of the matrices rather than their molecular weights but a conclusion cannot be drawn from the available data.

7.4.3 Effect of degradation on the release of methyl red.

The release studies reported here took place over a timespan which appeared to be too short to be influenced by degradation of the polymers. This hypothesis was tested by comparing release rates at 37°C in 0.1M sodium hydroxide with those obtained previously at pH 7.4.

Figures 7.4.18 to 7.4.21 show the function of $([\frac{f(t)^2}{t}]^{1/2})$ plotted against $(t^{1/2})$ for a representative series of four films, one for each polymer studied. The values of B_1 and B_2 obtained from these relationships are shown in Table 7.4.7. Data for release from these films at pH 7.4 is shown in tables 7.4.5 and 7.4.6. Using a student t-test, it was found that the values of B_1 and B_2 obtained in 0.1M sodium hydroxide were significantly higher than the values obtained at pH

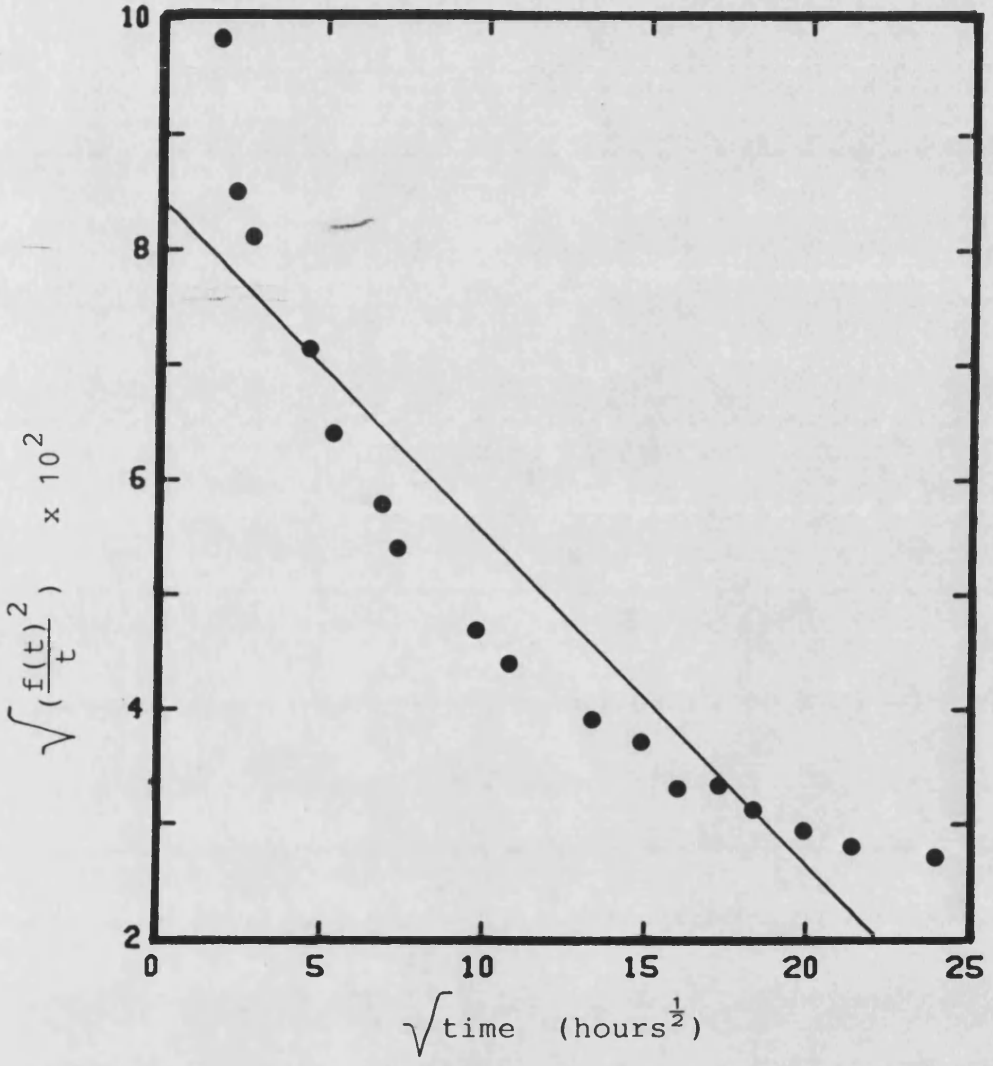

Figure 7.4.18:- The function $\sqrt{(\frac{f(t)}{t})^2}$ against $\sqrt{t}$ for release of methyl red from PHB film containing 0·71% w/w methyl red (in 0·1M sodium hydroxide at 37°C).

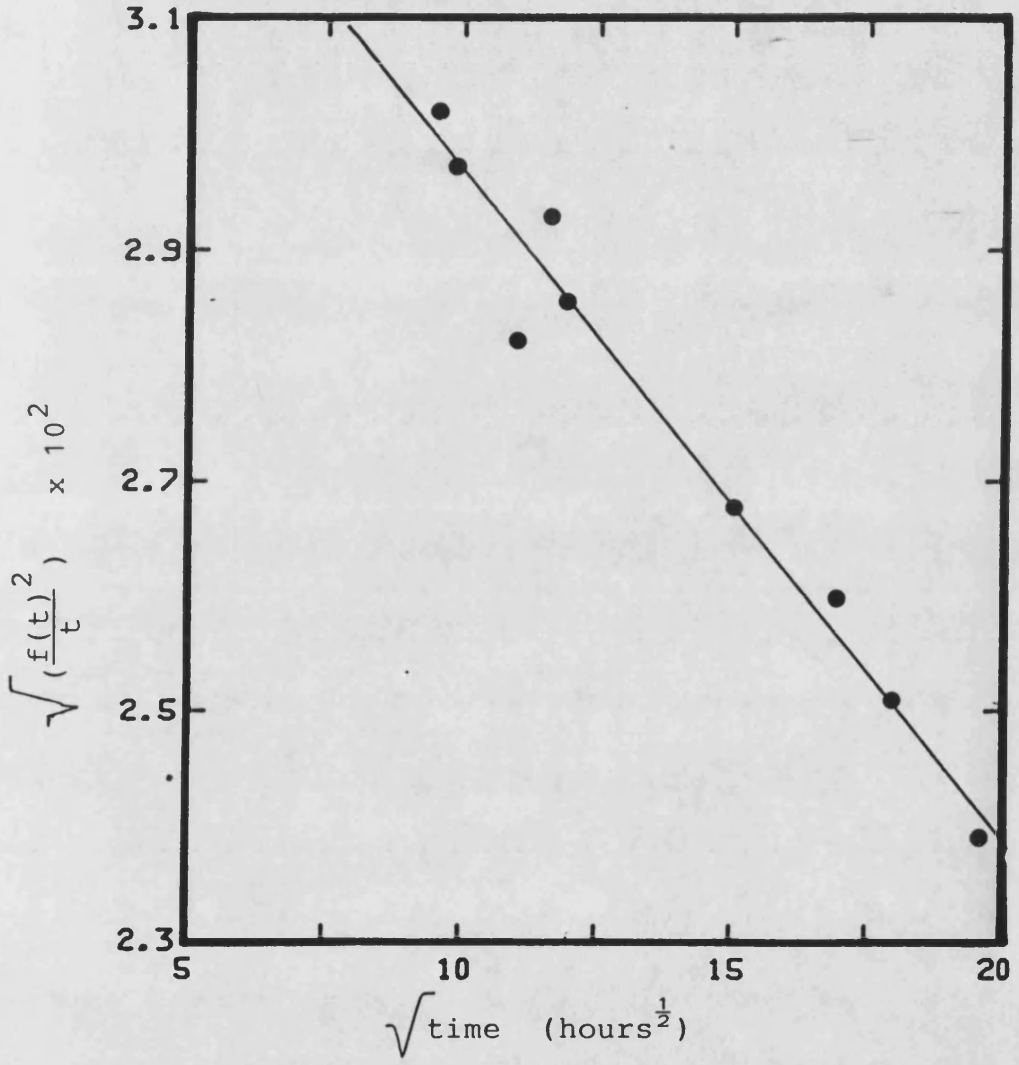

Figure 7.4.19:- The function $\sqrt{(\frac{f(t)}{t})^2}$ against $\sqrt{t}$ for release of methyl red from PHB/PHV copolymer film (6·5 mole % HV) containing 0·86% methyl red (in 0·1M sodium hydroxide at 37°C).

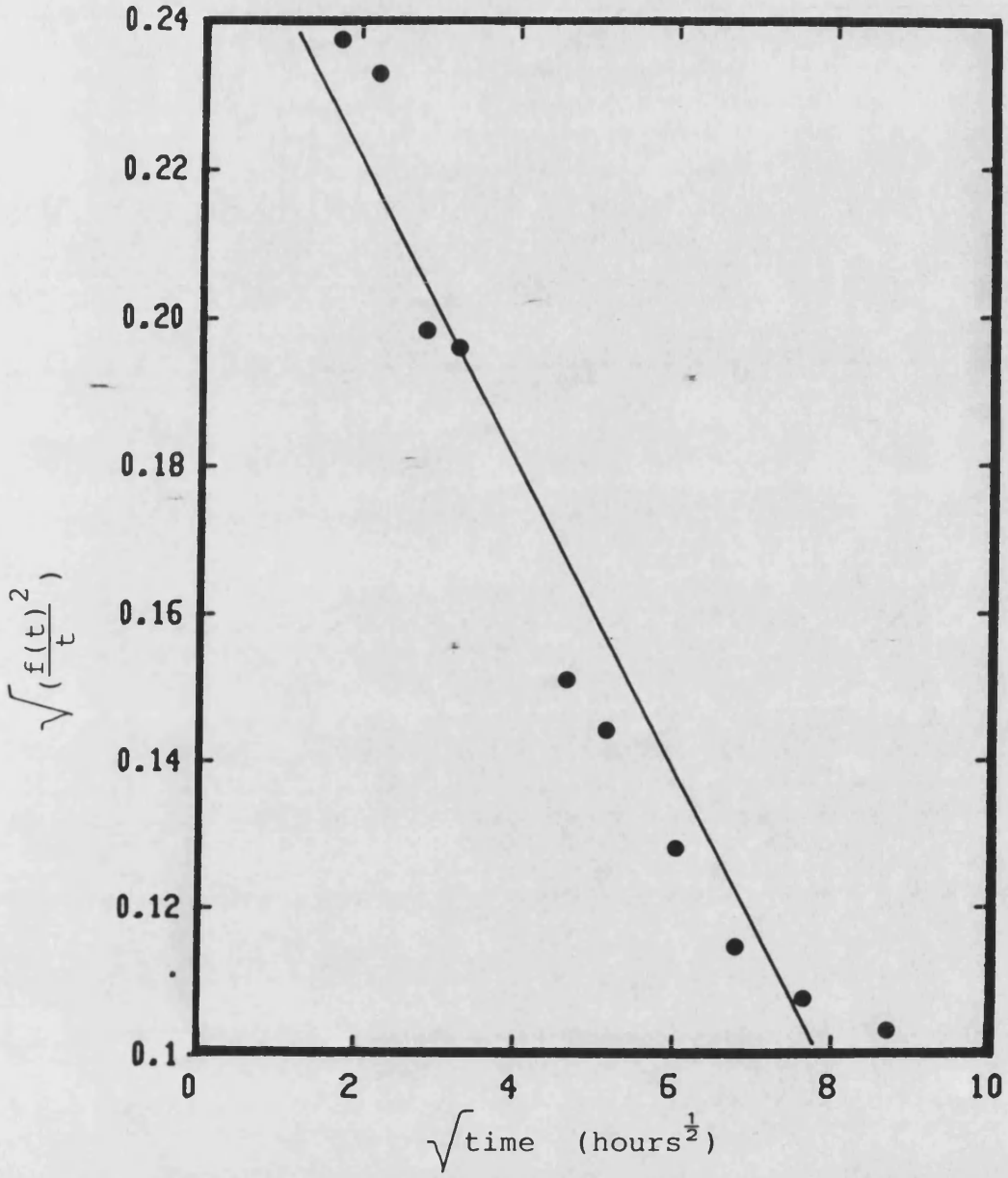

Figure 7.4.20:- The function $\sqrt{(\frac{f(t)}{t})^2}$ against $\sqrt{t}$ for release of methyl red from PHB/PHV copolymer film (12·3 mole % HV) containing 0·74% $w/_w$ methyl red in (0·1M sodium hydroxide at 37°C).

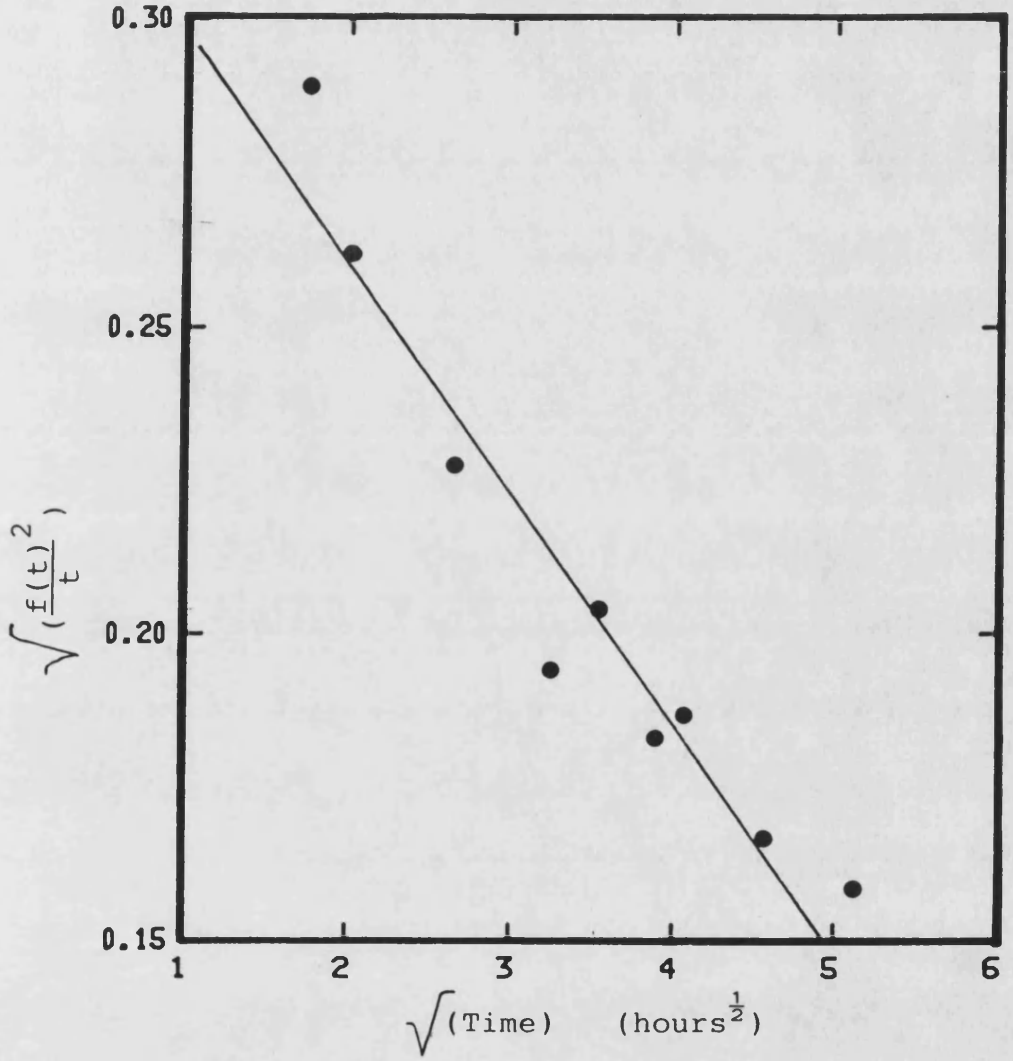

Figure 7.4.21:- The function $\sqrt{(\frac{f(t)}{t})^2}$ against $\sqrt{t}$ for release of methyl red from PHB/PHV copolymer film (19·2 mole % HV) containing 0·78% $w/_w$ methyl red (in 0·1M sodium hydroxide at 37°C).

Table 7.4.7 : Kinetic parameters for release of methyl red from copolymer films in 0.1M sodium hydroxide at 37°C

Polymer composition (mole % HV)	Methyl red loading (% w/w)	Rate constants (hours^{-1} $\times 10^3$)	
		B_1	B_2
0	0.71	83.5 ± 3.0	2.45 ± 0.20
6.5	0.86	35.7 ± 1.2	0.78 ± 0.08
12.3	0.74	263.1 ± 15.3	20.83 ± 5.25
19.3	0.78	335.0 ± 26.1	37.40 ± 7.44

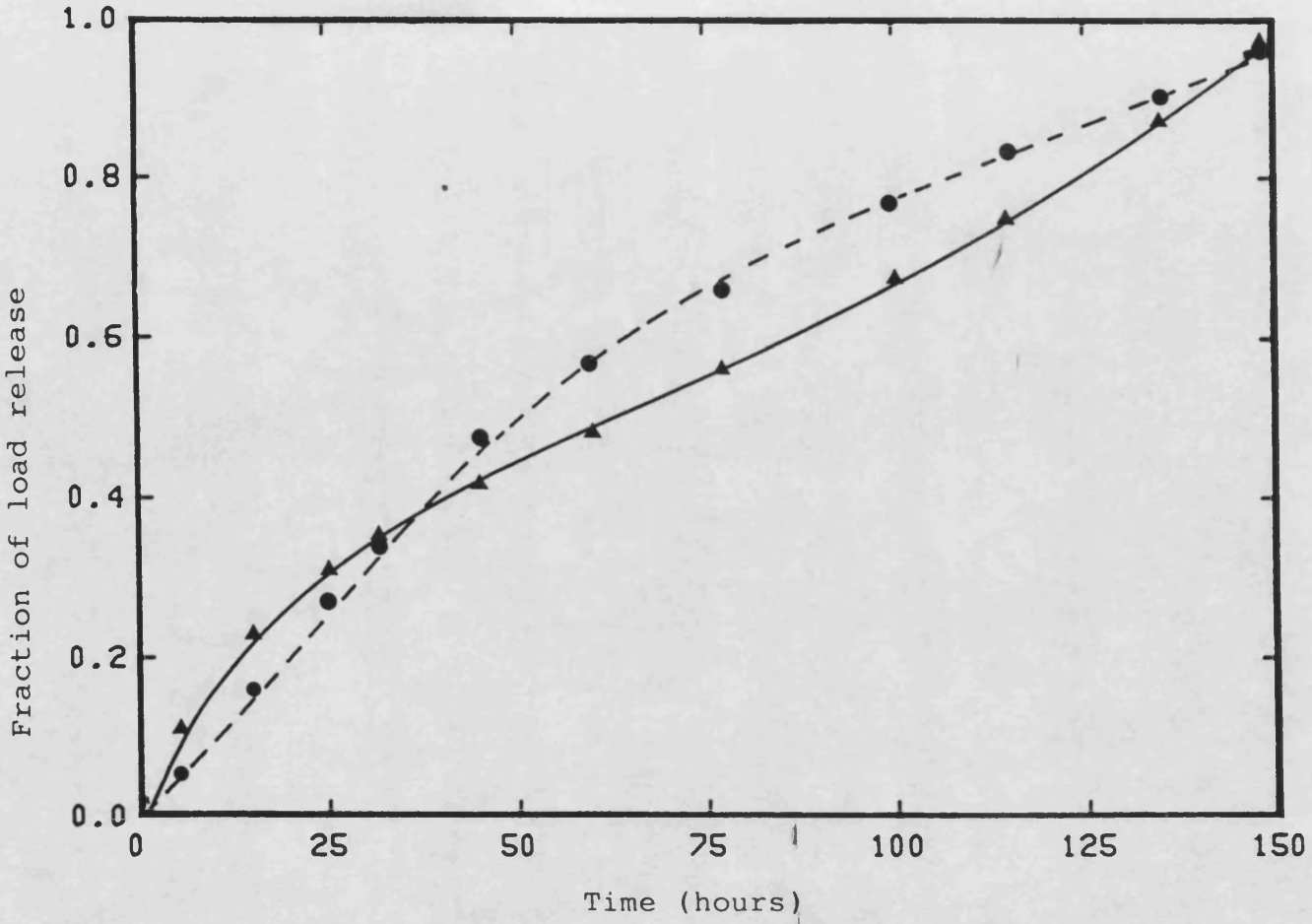

Figure 7.4.22:- The effect of degradation on the release of methyl red from P(GA/LA) copolymer and PLA films after storage in 0·1M NaOH at 37°C.
(▲), 10 mole % glycolic acid (1·03% $w/_w$ methyl red loading); (●), PLA homopolymer (0·99% $w/_w$ methyl red loading).

7.4. These data indicate that release of methyl red frm the films was influenced by an increased rate of surface erosion of the polymer. However the proportional increase in release was generally 10-20% whereas the increase in degradation rate was approximately threefold (Figure 7.2.3). Thus, for PHB and its copolymer films the release of methyl red at pH 7.4 occured by diffusional processes with a minor contribution from polymer erosion. This was in contrast with release of methyl red from P-l-LA and P(LA/GA) films which was significantly affected by erosion and was drastically different in 0.1M NaOH. The release profiles for these two films are shown in Figure 7.4.22 showing that drug from these films occured by a mixture of matrix diffusion and erosion. Consequently, the modified matrix release equation (Equation 7.3) was inappropriate for these systems.

Chapter 8

GENERAL CONCLUSIONS AND SCOPE FOR FUTURE WORK.

8.1 General conclusions.

Viscosity measurements of dilute solutions of molecular weight fractions of PHB in chloroform at 25°C allowed calculation of the intrinsic viscosities. From the Huggins' plots of each fraction, the value of Huggins' constant, k', was found to be in the range between 0.3 to 0.4. This indicated that the molecular conformation of PHB in chloroform was essentially a random coil and that chloroform was a good solvent for PHB.

Size exclusion chromatography was employed to obtain the molecular weight distribution of PHB. The quantitative evaluation of chromatographic data involved a universal calibration of the column using polystyrene standards and an iterative process leading to the establishment of Mark-Houwink constants for PHB. SEC proved to be a powerful, rapid method for determination of Mark-Houwink constants and, once the calibration had been performed, proved to be a rapid method for determintion of molecular weights distributions for PHB. Only 10-20mg polymer was required for assay. However, the precision of the assay using one mixed gel column was not high enough to determine small changes in molecular weight. Several columns in series could be used to increase precision. Low molecular weight samples of PHB could be obtained from initially high molecular weight PHB using p-toluenesulphonic acid (pTSA) to catalyse degradation in chloroform-methanolic mixtures. Degradation of PHB under these conditions occured by random chain scission. During this non-aqueous degradation,

the polydispersity of PHB samples was determined, in terms of the molecular weight averages, and the ratios obtained indicated that the molecular weight distribution approached the Schulz-Zimm distribution.

The use of SEC and weight loss experiments during aqueous degradation of PHB and its copolymer films indicated that the degradation occurred by surface hydrolysis. However, the rate of surface hydrolysis was very slow and could be enhanced by making the hydrolytic medium more alkaline. Altering the P(HB/HV) copolymer composition changed polymer resistance to surface hydrolysis. DSC studies indicated that increase in the valerate content caused a decrease in crystallinity, hence exposing more chain ends to degradation. However,there is some doubt as to the crystallinity of the P(HB/HV) copolymers at present.

Degradation products were isolated and characterized from *in vitro* experiments. Chromatographic studies indicated that surface hydrolysis of PHB and P(HB/HV) copolymer films occurred through the scission of monomers from chain ends resulting in release of monomers.

In vitro studies of release of methyl red from polymer films have shown that the release form PHB and P(HB/HV) copolymers was dependent on the loading and the crystallinity of these polymers. Increasing the loading of methyl red produce an increase in the release rate. Comparative release studies on different copolymer compositions with similar loading of methyl red have indicated that films containing 10-20 mole % HV cause more rapid release for low molecular compounds compared to the homopolymer. The *in vitro* release profiles can be modelled by a modified Higuchi's equation which takes into consideration the release over longer times. This equation adequately described the *in vitro* release of methyl red at loadings

between 1% and 10% w/w. Release of methyl red from PHB and P(HB/HV) polymers at pH 7.4 was controlled by diffusional processes in contrast to release from PLA or P(LA/GA) systems where the polymer degradation process was important.

8.2 Future work.

Investigation of the *in vitro* degradation of PHB and P(HB/HV) copolymer films has shown that degradation occurs only by surface hydrolysis. Thus if drugs could be trapped within the polymer matrix, their release could be controlled by the area of polymer surface exposed to the aqueous environment. This may be of particular value in delivery of macromolecules such as peptides. Thus, there is great scope for formulation in PHB or P(HB/HV) polymers and entrapment of drug need to be studied in detail.

However, before such biomedical applications can be contemplated experiments must be carried out to determine the degradation process which occurs *in vivo* and also the blood and tissue compatibility of these polymers. *In vivo* degradation studies should be aimed at providing information regarding the contribution of enzyme-catalysed degradation to the mechanism and the rate of degradation of these polymers. Experience with other polymers indicates the need for such studies. For example, poly(ϵ-caprolactone) was found to degrade *in vitro* by non-enzymatic random hydrolytic cleavage of ester linkages (Schindler *et al.*, 1977). In contrast to the above mechanism, Woodward *et al.* (1985) found that the *in vivo* degradation of low molecular weight poly (ϵ-caprolactone) powders in rats occurred mainly through enzymatic degradation. Tissue compatibility should be studied to determine the toxicology and mutagenicity of

PHB and the copolymers. Blood compatibility testing may also be useful in view of possible uses of PHB for targetting of drugs to macrophages and the use of PHB in surgery.

Release studies with the model compound, methyl red, showed that erosion played a minor part in the release of the marker. In a practical sense, this is not desirable since the degradation of these polymers was slow, thus the absorption of the depleted device would be slow in comparison to its useful life as a delivery system. PLA or P(LA/GA) systems would be a more appropriate choice for delivery of low molecular systems. A more desirable approach would be to utilize the surface hydrolysis as a rate limiting step for the release of higher molecular weight drugs; utilizing the special surface erosion properties of PHB.

However, the possibility of accelerating degradation could be investigated for low molecular weight compounds through the incorporation of basic agents, such as amines, in the polymer matrix. An example of such a process occuring was shown by Maulding *et al.* (1986) where the hydrolysis of PLA microspheres was increased by incorporating thioridazine, which is a tertiary amino compound, into the matrix. An analogous approach has been studied extensively with poly (ortho-esters), although these compounds showed the reverse sensitivity to degradation. The control of drug release from these polymers was achieved by incorporating acid anhydrides into the polymer matrix (Shih *et al.*, 1984; Nguyen *et al.*, 1984). The incorporation of higher molecular weight compounds has been reported by Sandow and Siedel (1986) and Koenig *et al.* (1985). In both examples, a polypeptide, buserelin acetate, was incorporated into PHB microspheres.

Apart from the suggestions being discussed previously, a full characterisation of the release experiments presented in the thesis would be useful. In this thesis, the effect of the environmental diffusion layer (or hydrodynamic layer) on the rate of release has been totally neglected. A more rational evaluation of drug relase would incorporate studies of the intrinsic release profile of methyl red from polymer films. From the literature, the method that can be adopted for the intrinsic release has been described by Collett *et al.* (1972) and this has been applied to matrix-type drug delivery systems using the Higuchi's model (Tojo,1985). An update version with using the modified Higuchi's equation may be useful to evaluate the experimental release data from this study. Further studies on release of low molecular weight compounds should include morphological studies which were not possible by DSC for methyl red.

REFERENCES

Ackers, G.K., (1964). Molecular exclusion and restricted diffusion processes in molecular sieve chromatography. *Biochemistry* , **3** , 723-730.

Agostini, D.E., Lando, J.B. and Reid, J.S., (1971). Synthesis and characterization of PHB. I. Synthesis of crystalline DL-PHB from DL -Butyrolactone. *Journal of Polymer Science, Part A1* , 2775-2787

Akhtar, S., Pouton, C.W., Notarianni, L.J. and Gould, P.L., (1987). Mechanical properties of Biopol polyester films and the effect of inclusion of solid crystalline drug. *Journal of Pharmacy and Pharmacology* , **39** :43P

Akita, S., Einaga, Y., Miyaki, Y. and Fujita, H., (1976). Solution properties of PHB . 1. Biosynthesis and characterization . *Macromolecules* , **9(5)** , 774-780

Artursson, P., (1987). The fate of microparticulate drug carrier after intravenous administration. In : Polymers in controlled drug delivery (L. Illum and S.S. Davis eds.) Bristol : Wright

Bandrup, J. and Immergut, E.H., (1975). Polymer Handbook, 2nd. edition. New York : Wiley Interscience.

Barham , P.J., Keller, A., Otun, E.L. and Holmes, P.A., (1984). Crystallization and morphology of a bacterial thermoplastic: PHB. *Journal of Material Science* , **19** , 2781-2794

Bawn, C.E.H., Freeman, R.F.J. and Kamaliddin, A.R., (1962) . High polymer solutions. 3. The relation between intrinsic viscosity and

molecular weight for polystyrene fractions in benzene, toluene, chloroform, ethyl benzene and methyl ethyl ketone. *Transaction of Faraday Society* , 46 , 1107-1112

Billmeyer, F.W., (1962). Textbook of Polymer Science. New York : Interscience Publisher.

Bissery, M.C., Valeriote, F. and Thies, C., (1984). *In vitro* and *in vivo* evaluation of CCNU-loaded microspheres prepared from poly(lactate) and PHB. In: Microspheres and drug therapy: Pharmaceutical , Immunological and Medical Aspects. (S.S. Davis, L.Illum , J.G.Mcvie and E.Tomlinson eds.) New York: Elsevier.

Bloembergen, S., Holden, D.A., Hamer, D.K., Bluhm, T.L. and Marchessault, R.H., (1986).Studies of composition and crystallinity of bacterial PHB/PHV. *Macromolecules* , 19 , 2865-2871

Bluhm, T.L., Hamer.D.K., Marchessault, R.H., Fyfe, C.A. and Veregin, R.P., (1986). Isodimorphism in bacterial PHB/PHV. *Macromolecules* , 19 , 2871-2876

Brenner, P.F., Cooper, D.L. and Mishell, D.R., (1975). Clinical study of a progesterone-releasing intrauterine contraceptive device. *American Journal of Obstetric and Gynaecology* , 121 , 704-706

Brophy, M.R. and Deasy, P.B., (1986). *In vitro* and *in vivo* studies on biodegradable polyester microparticles containing sulphamethizole. *International Journal of Pharmaceutics* , 29 , 223-231

Cantow, M.J.R., Porter, R.S. and Johnson, J.F., (1967). Effect of temperature and polymer type on gel permeation chromatography. *Journal of Polymer Science, A1* , 5 , 987-991

Carmichael, J.B., (1968). Stochastic model for gel permeation separation of polymers. *Journal of Polymer Science, A2* , **6** , 517-527

Casassa, E.F., (1971). Theoretical models for peak migration in GPC. *Journal of Physical Chemistry* , **75(26)** , 3929-3938

Chawla, A.S. and Chang, T.M.S., (1985). *In vivo* degradation of PLA of different molecular weights. *Biomaterial Medical and Artificial Organs* , **13(3-4)** , 153-162

Chien, Y.W., (1980). Controlled drug release from polymeric delivery systems:biomedical applications and physicochemical principles. In: Drug delivery systems: Characteristic and biomedical applications. (R.L. Juliano ed.) New York: Oxford University Press

Chu, C.C., (1981). An *in vitro* study of the effect in the degradation of PGA suture. *Journal of Biomedical Materials Research* , **15** , 19-27

Chu, C.C. and Louie, M., (1985). A chemical means to study the *in vitro* hydrolytic degradation of PGA. *Journal of Applied Polymer Science* , **30** , 3133-3141

Cohen, J.L. and Van Aartsen, J.J., (1973). The hydrolytic degradation of polyurethanes. *Journal of Polymer Science: Polymer Symposium* , **42** , 1325-1338

Cohn, D., Younes, H. and Marom.G., (1987). Amorphous and crystalline morphologies in glycolic acid and lactic acid polymers. *Polymer* , **28** , 2018-2022

Coll, H. and Gilding, D.K., (1970). Universal calibration in GPC: A study of polystyrene, poly- α -methylstyrene and polypropylene.

Journal of Polymer Science: A2 , 8 , 89-103

Collett, J.H., Rees, J.A. and Dickinson, N.A., (1972). Some parameter describing the dissolution of salicylic acid at controlled pH. *Journal of Pharmacy and Pharmacology* , 24 , 724-728

Cooper, A.R., (1982). Analysis of polymer systems by gel permeation chromatography . In: Analysis of polymer systems (L.S. Bark and N.S. Allen eds.) London: Applied Science

Cornibert, J. and Marchessault, R.H., (1972). Physical properties of PHB: 4. Conformational analysis and crystalline structure. *Journal of Molecular Biology* , 71 , 735-756

Cosmi, G., Di Gorcia, A., Samperi, R. and Vinci, G., (1983). Gas chromatograhic measurement of 3-hydroxybutyrate and lactate in plasma and 3-hydroxybutyrate in whole blood. *Clinical Chemistry* , 29(2) , 319- 321

Coulombe, S., Schauwecker, P., Marchessault, R.H. and Hauttecoeur, B., (1978). High pressure liquid chromatography for fractionating oligomers from degraded PHB. *Macromolecules* , 11(1) , 279-281

Couvreur, P., Grislain, L., Lenaerts, V., Brasseur, F., Guiot, P. and Biernacki, A., (1986). Biodegradable polymeric nanoparticles as drug carrier for antitumour agents. In: Polymeric nanoparticles and microspheres (P. Guiot and P. Couvreur eds.) Boca Raton : CRC Press

Cowie, J.M.G., (1973). Polymers: Chemistry and physics of modern materials. Aylesbury: International Textbook

Crank, J., (1975). The mathematics of diffusion. 2nd. edition.Oxford: Oxford University Press

Dawes, E.A. and Ribbons, D.W., (1964). Some aspects of the endogenous metabolism of bacteria. *Bacteriology Review* , 28(2) , 126-149

Dawes, E.A. and Senior, P.J., (1973). The role and regulation of energy reserve polymers in microorganisms. In: Advances in microbial physiology (A.H. Rose and D.W. Tempest eds.) London : Academic Press

Dawkins, J.V., (1967). Thermodynamic interpretation of polystyrene retention on crosslinked polystyene gel in poor and theta solvents. *Journal of Polymer Science:A2* , 14 , 569-571

Deasy, P.B., (1984). Microencapsulation and related drug processes. New York: Marcel Dekker

De Haan, P. and Lerk, C.F., (1984). Oral controlled release dosage forms. A review. *Pharmaceutisch Weekblad* , 6(2) , 57-67

Di Marzio, E.A. and Guttman, L.M., (1969). Separation by flow. *Journal of Polymer Science:B* , 7 , 267-272

Doi, Y., Kuniska, Y., Nakamura, Y. and Soga, K., (1986). NMR studies on PHB and a copolyesters of PHB/PHV isolated from Alcaligenes eutrophus H 16. *Macromolecules* , 19 , 2860-2864

Douglas, S.J., Davis, S.S. and Illum, L., (1987). Poly(alkyl 2-cyanoacrylate)(PAC) microspheres as drug carrier systems. In: Polymers in controlled drug delivery (L. Illum and S.S. Davis eds) Bristol:Wright

Eckenhoff, B. and Yum, S.I., (1981). The osmotic pump novel research tool for optimizing drug regimens. *Biomaterials* , 2 , 89-97

Endo, R., and Takeda, M., (1962). Note on the relationship between the intrinsic viscosity and the molecular weight of crystalline and amorphous polystyrene. *Journal of Polymer Science* , **56** , S28

Fara, J.W., (1985). Osmotic delivery systems for research . *Methods in Enzymology* , **112(35)** , 471-484

Feijen, F., Gregonis, D., Anderson, C., Petersen, R.V. and Anderson, J., (1980). Coupling of steroid hormones to biodegradable poly(α -amino acids) 1. Norehindrone coupled to poly-N -(3-hydroxypropyl)-L-glutamine. *Journal of Pharmaceutical Sciences* , **69(7)** , 871-872

Florence, A.T. and Attwood, D., (1981). Physicochemical principles of pharmacy . London: Macmilan Press

Flory, P.J., (1953). Principles of polymer chemistry. Ithaca: Cornell University Press

Frazza, E.F. and Schmitt, E.E., (1971). A new absorbable suture. *Journal Of Biomedical Material Research Symposium* , **1** , 43-58

Gander, B., Gurny, R. and Doelker, E., (1987). Crosslinked poloxamers as a versatile monolithic drug delivery system. In: Pharmaceutical Technology: Controlled drug release Volume 1 (M.H. Rubinstein, ed.) Chicester:Ellis Horwood

Giddings, J.C., Kucera, E., Russel, C.P. and Myers, M.N., (1968). Statistical theory for the equilibrium distribution of rigid molecules in porous networks exclusion chromatography. *Journal of Physical Chemistry* , **72(13)** , 4397-4408

Gilding, D.K., (1980). Biodegradable polymer. In: Biocompatibility of clinical implant materials (D.F. Williams ed) Boca Raton: CRC Press

Gilding, D.K. and Reed , A.M., (1979). Biodegradable polymers for use in surgery. PGA/PLA homo- and copolymers:1 . *Polymer* , 20 , 1459-1464

Gilding, D.K., Reed, A.M. and Askill, I.N., (1981). Calibration in gel permeation chromatography: Primary, universal and empirical methods. *Polymer* , 22 , 505-512

Gordon, M., (1963). High polymers. Structures and physical properties. London: The Plastics Institute

Gould, P.L., Holland, S.J. and Tighe, B.J.(1987). Polymers for biodegradable medical devices: 4 . PHB/PHV copolymers as non disintegrating matrices for controlled release oral dosage forms. *International Journal of Pharmaceutics* , 38 , 231-237

Gresser, J.D., Howes, J.F., Worth, D.F. and Wise, D.L., (1984). Controlled release drug formulation. In: Biopolymeric controlled release systems (D.L. Wise ed.) Boca Raton: CRC Press

Gresser, J.D. and Sanderson, J.E., (1984). Basis for design of biodegradable polymers for sustained release of biologically active agents.In: Biopolymeric controlled release systems(D.L. Wise, ed.) Boca Raton: CRC Press

Grinshpun, V., O'Driscoll, K.F. and Rudin, A., (1984). On the accuracy of SEC .Analysis of molecular weight distributions of polyethylenes. *Journal of Applied Polymer Science* , 29 , 1071-1077

Grubisic , Z., Rempp , P. and Benoit , A.,(1967). A universal calibration for gel permeation chromatography. *Journal of Polymer Science:B* , 5 , 753-759

Hadgraft, J. and Guy, R.H., (1987). Release and diffusion of drugs from polymers. In: Polymers in controlled drug delivery .(L. Illum and S.S. Davis eds.) Bristol: Wright

Hadgraft, J., (1985). Skin absorption:past, present and future. *Journal of Pharmacy and Phamacology* , **37** :Supplement

Hawkins, D.B. and Thompson, H.O., (1953). The *in vivo* evaluation of conspergent on selected enteric coating. *Journal American Pharmaceutical Association [Science]* , **42** , 424-430

Heilmann, K.(1984). Therapeutic systems:Rate controlled drug delivery:Concept and development. Stuggart:Georg Thieme Verlag

Heller, J. (1984). Biodegradable polymers in controlled drug delivery . *CRC Critical Reviews in Therapeutic Drug Carrier Systems* , **1(1)** , 39-90

Heller, J. (1986). Controlled drug release from monolithic bioerodible polymer devices. *Pharmacy International* , **7(12)** , 316-318

Heller, J. and Himmelstein, K.J. (1985). Poly(ortho esters) biodegradable polymer systems. *Method in Enzymology* , **112** , 422-436

Heller, J., Penhale, D.W.H., Fritzinger, B.K., Rose, J.E. and Helwing, R.F.(1983). Controlled release of contraceptive steroids from biodegradble poly(otho esters). *Contraceptive Delivery Systems* , **4(1)** , 43-53

Higuchi, T., (1961). Rate of release of medicaments from ointment bases containing drugs in dispersion. *Journal of Pharmaceutical Science* , **50** , 874-875

Higuchi, T., (1963). Mechanism of sustained action medication. Theoretical analysis of rate of release of solid drugs dispersed in solid matrices. *Journal of Pharmaceutical Sciences* , 52(12) , 1145-1149

Holland, S.J., Jolly, A.M., Yasin, M. and Tighe, B.J., (1987). Polymers for bioderadable medical devices. 2. PHB/PHV copolymers: hydrolytic degradation studies. *Biomaterials* , 8 , 289-295

Holmes, P.A., (1985). Application of PHB: A micrbially produced biodegradable thermoplastic. *Physical Technology* , 16 , 32-36

Hsu, T.T.P. and Langer, R., (1985). Polymers for the controlled release of macromolecules: Effect of molecular weight of ethylene-vinyl acetate copolymer. *Journal of Biomedical Materials Research* , 19 , 445-460

Huggins, M.L., (1942). The viscosity of dilute solution of long chain molecules . 4. Dependence on concentration. *Journal of American Chemical Society* , 64 , 2716-2718

Hutchinson, F.G. and Furr, B.J.A., (1985). Biodegradable polymers for the sustained release of peptides. *Biochemical Society Transactions* , 13 , 520-523

Hutchinson, F.G. and Furr, B.J.A., (1987). Biodegradable carriers for the sustained release of polypeptides. *Trends Biotechnology* , 5 , 102-106

Jeong, S.Y. and Kim, S.W., (1986). Biodegradable polymeric drug delivery system. *Archives of Pharmaceutical Research* , 9(2) , 63-73

Juni, K. and Nakano, M., (1987a). Poly(hydroxy acids) in drug delivey. *CRC Critical Review in Therapeutic Carrier Systems* , 3(3) , 209-232

Juni, K. and Nakano, M., (1987b). PLA microspheres as drug carrier systems. In: Polymers in controlled drug delivery. (L. Illum and S.S. Davis eds) Bristol: Wright

Juni, K., Nakano, M. and Kubota, M., (1986). Controlled release of aclarubicin, an antitumour antibiotic from PHB mirospheres. *Journal of Controlled Release* , **4** , 25-32

Keller, A., (1957). A note on single crystals in polymers: Evidence for a folded chain configuration . *Philosophical Magazine* , **2** , 1171-1175

Keller, A., (1962). Polymer single crystals. *Polymer* , **3** , 393-421

Kennedy, J.E., Notarianni, L.J. and Pouton, C.W., (1987). Biocompatibility of a biodegradable polyesters in rats. *Journal of Pharmacy and Pharmacology* , **39** :58P

Knox, J.H. and Scott, H.P., (1984). Theoretical models for SEC and calculation of pore size distribution from SEC data. *Journal of Chromatography* , **316** , 311-332

Koenig, W., Siedel, H.R. and Sandow, J.K., (1985). Hoechst A.-G. Sustained release of peptide hormone pharmaceuticals. *European Patent Application EP 133, 988* ;through *Chemical Abstract (1985)* , **102** 226045e

Kopecek, J., (1984). Controlled biodegradability of polymers- a key to drug delivery systems . *Biomaterials* , **5** , 19-25

Kopecek, J. and Duncan, R., (1987). Poly HPMA macromolecules as drug carrier systems. In: Polymers in controlled drug delivery. (L. Illum and S.S. Davis eds) Bristol: Wright

Korsatko, W., Wabnegg, W., Braunegg, G. and Lafferty , R.M., (1983a). PHB - A biodegradable carrier for long term medication. *Pharmazetische Industrie* , 45(2) , 525-527

Korsatko, W., Wabnegg, W., Tillian, H.M., Braunegg, G. ang Lafferty, R.M., (1983b) PHB - A biologically degradable vehicle to retard release of a drug. *Pharmazeutische Industrie* , 45(10) , 1004-1007

Korsatko, W., Wabnegg, W., Tillian, H.M., Egger, G., Pfragner, R. and Walser, V., (1984). PHB - a biodegradable drug vehicle to slow down release. *Pharmazeutische Industrie* , 46(9) , 952-954

Kulkarni, R.K., Moore, E.G., Hegyli, A.F. and Leonard, F., (1971). Biodegradable poly(lactate) polymers. *Journal of Biomedical Material Research* , 5 , 169-181

Levy, G. and Hollister, L.E., (1965). Dissolution rate limited absorption in man . *Journal of Pharmaceutical Sciences* , 54 , 1121-1125

Majid, M.I.A., Pouton, C.W. and Notarianni, L.J., (1987). Catalytic degradation of PHB in non-aqueous solution. *Journal of Pharmacy and Pharmacology* , 39 : 35P

Marchessault.R.H., Coulombe, S., Morikawa, H., Okamura, K. and Revol, J.F., (1981). Solid state properties of PHB and of its oligomers. *Canadian Journal of Chemistry* , 59 , 38-44

Marchessault, R.H., Okamura, K. and Su, C.J., (1970). Physical properties of PHB. 2. Conformational aspects in solution. *Macromolecules* , 3 , 735-740

Mandelkern, L., (1975). Morphology and properties of semicrystalline polymers. *Journal of Polymer Science:Polymer*

Symposium , 50
, 457-468

Marriot, R.J. and Pouton, C.W., (1986). Hydrolytic degradation of MTX-Albumin conjugates in the presence of trypsin. *Journal of Pharmacy and Pharmacology* , 38 : 62P

Martin, A.N., Swarbrick, J. and Cammarata, A. , (1969). Physical pharmacy: Physical principles in the Pharmaceutical sciences. Philadelphia: Lea and Febiger.

Maulding, H.V., Tice, T.R., Cowsar, D.V., Fong, J.W., Pearson, J.E. and Nazareno, J.P., (1986). Biodegradable microspheres: Acceleration of polymeric excipient hydrolytic rate by incoporation of a basic medicament. *Journal of Controlled Release* , 3 , 103-117

Miller, N.D. and Williams, D.F., (1987). On the biodegradation of PHB homopolymer and PHB/PHV copolymers. *Biomaterials* , 8 , 129-137

Miller, R.A., Brady, T.M. and Cutright, D.E., (1977). Degradation rates of oral resorbable implants (polylactates and polyglycolates): Rate modification with changes in PLA/PGA copolymer ratios. *Journal of Biomedical Material Research* , 11 , 711-719.

Mills, S.N. and Davis, S.S., (1987). Controlled drug delivery. In: Polymers in controlled drug delivery (L. Illum and S.S. Davis eds.) Bristol:Wright

Mitomo, H., Barham, P.J. and Keller, A., (1986). Lamellar thickening behaviour of PHB and its copolymer on annealing. *Sen-I-Gakkaishi* , 42(11) , 45-52

Nguyen, T.H., Shih, C., Himmelstein, K.J. and Higuchi, T., (1984). Hydrolysis of some poly(ortho esters)s in homogenous solution. *Journal of Pharmaceutical Sciences* , **73(11)** , 1563-1568

Olsen, I., Merrick, J.M. and Goldstein, I.J., (1965). Chemical synthesis of theisomeric dimeric ester of hydroxybutyric acid. *Biochemistry* , 4(3) , 453-456

Oth, J. and Desreux, V., (1954). Sur les properietes hydrodynamiques des solutions de grande molecules en chaine. Dimension et. viscosite du polystyrene dans differents solvants. *Bulletin Society of Chemistry Belgium* , **63** , 285-329

Pickett, H.E., Cantow, M.J.R and Johnson, J.F., (1966). Column fractionation of polymers. 7. Computer program for determination of MWD from GPC. *Journal of Applied Polymer Science* , **10** , 917-924

Pitt, C.G., Chasalow, F.I., Hibionada, Y.M., Klimas, D.M. and Schindler, A., (1981) Aliphatic polyesters 1. The degradation of poly(ϵ -caprolactone) *in vivo* *Journal of Applied Polymer Science* , **26** , 3779-3787

Pitt, C.G. and Gu, Z.W., (1987). Modification of the rates of chain cleavage of poly(ϵ -caprolactone) and related polyester in the solid state. *Journal of Controlled Release* , 4 , 283-292.

Pitt, C.G., Jeffcoat, A.R., Zweidinger, R.H. and Schindler, A., (1979). Sustained drug delivery systems. 1. The permeability of poly(ϵ -caprolactone), poly(dl-lactate) and their copolymer. *Journal of Biomedical Materials Research* , **13** , 497-507

Pharmaceutical Journal, (1987). Prescription products. 238(6422), p. 341

Pharmaceutical Journal, (1988). Clinical Pharmacy. 240(6463), p. 20

Pokorny, S., (1984). Precision and accuracy of results . In: Steric exclusion liquid chromatography of polymers (J.Janca , ed). New York:Marcel Dekker

Polymer Laboratories., (1985). Technical information on mixed gel column.

Porath, J., and Flodin, P., (1959). Gel filtration : A method for desalting and group separation. *Nature* , 183 , 1657-1659

Porter, R.S., Cantow, M.J.R., and Johnson, J.F., (1967). Polymer degradation 5: Changes in molecular weight distributions during sonic irradiation of polyisobutylene. *Journal of Applied Polymer Science* , 11 , 335-340

Poznansky, M.J. and Cleland, L.G., (1980). Soluble macromolecules as drug carriers. In: Drug delivery systems: Physicochemical and biomedical application (R.L. Juliano ed) New York: Oxford University Press

Ptitsyn, O.B. and Eizner, Y.E., (1960).[Hydrodynamics of polymer solutions.2. Hydrodynamic properties of macromolecules in active solvents.] *Soviet Physics Journal of Technical Physics* , 4 , 1020-1036 (in Russian)

Ratcliffe, J.H., Hunneyball, I.M., Wilson, C.G., Smith, A. and Davis, S.S., (1984). Microsphere system for intraarticular drug administration. In: Microspheres and drug targetting. Pharmaceutical, Immunological

and medical aspects (S.S. Davis, L.Illum, J.G.Mcvie and E.Tomlinson eds.) Amsterdam: Elsevier.

Ratledge, C., (1986) Lipids. In: Biotechnology Volume 4; Microbial prducts 2 (H. Pape and H.-J. Rehm. eds) Weinheim: VCH

Redding, T.W., Schally, A.V., Tice, T.R., and Meyers, W.F., (1984). Long acting delivery systems for peptides.Inhibition of rat prostate tumours by controlled release of ($D\text{-}^{6}Trip$) luteinizing hormone-releasing hormone from injectable microcapsules. *Proceedings of the National Academy of Science USA* , **81** , 5845-5848.

Reed, A.M. and Gilding, D.K., (1981). Biodegradable polymers for use in surgery: PGA/PLA homo and copolymer;2. *In vitro* degradation. *Polymer* , **22** , 494-499

Rodriguez, F., (1982). Principles of polymer systems. Washington: Hemisphere Publishing

Rubinstein, A. and Robinson, J.R., (1987). Controlled drug delivery. *Progress in Clinical Biochemistry and Medicine* , **4** , 71-107

Sadtler Research Laboratories (1962). Number 26 : Frequently used spectra for the infrared spectroscopist. Philadelphia : Sadtler

Sanders, L.M., Kell, B.A., Mc Rae, G.I., and Whitehead, G.W., (1986). Prolonged controlled release of nafarelin, a LHRH analogue from biodegradable polymer implants: Influence of composition and molecular weight of polymer. *Journal of Pharmaceutical Sciences* , **75(4)** , 356-360

Sanders, L.M., Kent, J.S., Mc Rae, G.I., Vickery, B.H., Tice, T.R., and Lewis, .D.H., (1984). Controlled release of luteinizing hormomne-

releasing hormone analogue from poly(d, l-lactide-co-glycolide) microsphere. *Journal of Pharmaceutical Sciences* , 73(9) , 1294-1297.

Sandow, J. and Siedel, H.R., (1986). Hoechst A.-G. Microcapsules of regulatory peptides with controlled release - manufacture and injection preparation. *German Offenlegungschrift [patent document] DE 3428372* ;through *Chemical Abstract (1986)* , 105 30058d

Schally, A.V., Kook, A.I., Monje, E., Redding, T.W., and Paz-Bouza, J.I., (1986). Combination of a long acting delivery system for luteinizing hormone-releasing hormone agonist with Novantrone chemotheraphy: Increased efficacy in the rat prostate cancer model. *Proceedings of the National Academy of Science* , 83 , 8764-8768

Schindler, A., Jeffcoat, R., Kimmel, G.L., Pitt, C.G., Wall, M.E. and Zweidinger (1977). Biodegradable polymers for sustained drug delivery. In: Contemporary Topics in Polymer Science. Volume 2. (E.M. Pearce and J.R. Schaefgen eds). New York:Plenum Press

Schnabel, W., (1981). Polymer degradation: Principles and practical applications. Munich: Carl Hanser

Scott, K.W., (1974). Criteria for random degradation of linear polymers. *Journal of Polymer Science : Polymer Symposium* , 46 , 321-334

Senior, P.J., (1984).Continous culture 8. Poly (β-hydroxybutyrate), a speciality polymer of microbial origin. In: Biotechnology, Medicine and the Environment (A.C.R. Dean, D.C. Ellwood, C.G.T. Evans, eds) Chicester: Ellis Horwood

Sharon, A.C., Wise, D.L. and Howes, J.F., (1984). Biodegradable cylindrical implants for fertility control. In: Biopolymeric controlled

release systems. (D.L. Wise ed.) Boca Raton: CRC Press

Shaw, J., (1985). Transdermal dosage forms. *Methods in Enzymology* , 112(33) , 448-460

Shih, C., Higuchi, T. and Himmelstein, K.J., (1984). Drug delivery from catalysed erodible polymeric matrices of poly(ortho esters). *Biomaterials* , 5 , 237-240

Shihabeddin, M.H., (1984). Investigation in the use of a biodegradable polymer to microencapsulate and control the release of drugs. Ph.D thesis, University of Connecticut.

Siegel, R.A. and Langer, R., (1984). Controlled release of polypeptides and other macromolecules. *Pharmaceutical Research* , 1 , 2-10

Sjoholm, I. and Edman, P., (1984). The use of biocompatible microparticles as carriers of enzymes and drugs *in vivo* . In: Microspheres and drug therapy : Pharmaceutical, immunological and medical aspects. (S.S. Davis, L.Illum, J.G.Mcvie and E. Tomlinson eds.) Amsterdam:Elsevier

Slepecky, R.A., and Law, J.H. (1960) A rapid spectrophotometric assay of α-unsaturated acids and β-hydroxy acids. *Analytical Chemistry* , 32(12) , 1697-1699

Smith, K.L., (1985). Membrane systems:Practical Applications. *Methods in Enzymology* , 112(38) , 505-520

Smith, K.L. and Lonsdale, H.K., (1985). Membrane systems : Theoretical aspects. *Methods in Enzymology* , 112(38) , 494-504

Sparer, R.V., Shih.C., Ringeisin, C.D., and Himmelstein, K.J., (1984).

Controlled release from erodible poly(ortho ester) drug delivery system. *Journal of Controlled Release* , 1 , 23-32

Suzuki, K. and Price, J.C., (1985). Microencapsulation and dissolution of a nueroleptic in biodegradable polymer, poly(d, l-lactate). *Journal of Pharmacetuical Science* , 74(1) , 21-24

Technical Insights Inc., (1985). Industrial/Speciality chemicals via biological sources/routes. Fort Lee: Technical Insights Inc. Advances in bioprocess technology.

Tojo, K., (1985). Intrinsic release rate from matrix type drug delivery systems. *Journal of Pharmaceutical Sciences* , 74(6) , 685-687

Tomlinson, E., Burger, J.J., Schoonderwoerd, E.M.A. and Mc Vie, J.M.G., (1984). Human serum albumin microspheres for intraarterial drug targetting of cytostatic compounds. In: Microspheres and drug therapy: Pharmaceutical, immunological and medical aspects. (S.S. Davis, L.Illum, J.G. Mc Vie and E. Tomlinson eds) Amsterdam: Elsevier

University of Bath (1982). Basic formulae and statistical tables .

Van Dijk, J.A.P.P., Smit, J.A.M., Kohn, F.E., and Feijen, J., (1983). Characterization of poly(d, l-lactate) by gel permeation chromatography. *Journal of Polymer Science: Polymer Chemistry edition* , 21
, 197-208.

Van Kreveld, M.E. and Van den Hoed, W., (1973). Mechanism of gel permeation chromatography distribution coefficient. *Journal of Chromatography* , 83 , 111-124

Visscher, G.E., Robinson, R.L., Maulding, H.V., Fong, J.W., Pearson, J.E. and Argentierri, G.J., (1985). Biodegradation of and tissue reaction to 50:50 poly(d, l-lactate-co-glycolate) microcapsules. *Journal of Biomedical Material Research* , **19** , 349-365

Wheatley, L.M. and Langer, R., (1987). Particles as a drug delivery systems. *Particulate Science and Technology* , **1** , 53-64

Willmott, N., Kamel, H.M.H., Cummings, J., Stuart, J.F.B. and Florence, A.T., (1984). Adriamycin-loaded albumin microspheres: lung entrapment and fate in rats. In : Microsphere and drug therapy : Pharmaceutical, immunological and medical aspects. (S.S. Davis, L.Illum, J.G. Mc Vie and E. Tomlinson eds.) Amsterdam : Elsevier

Wise, D.L., Mc Cormick, G.J., Willet, G.P., Anderson, L.C. and Howes, J.F., (1978). Sustained release of sulphadiazine. *Journal of Pharmacy and Pharmacology* , **30** , 686-689

Wise, D.L., Benagiano.G., Schmitt, G.E. and Goodman, M., (1979). Sustained release hormonal preparations for the delivery of fertility-regulating agents. *Journal of Polymer Science: Polymer Symposium* , **66**
, 129-148

Wise, D.L., Trantolo, D.J., Marino, R.T. and Kitchell, J.P., (1987). Opportunities and challenges in the design of implantable biodegradable polymeric systems for the delivery of antimicrobial agents and vaccines. *Advanced Drug Delivery Review* , **1** , 19-39

Woodward, S.C., Brewer, P.S., Moatamed, F., Schindler, A. and Pitt, C.G., (1985). The intracellular degradation of poly(ϵ-caprolactone). *Journal of Biomedical Material Research* , **19** , 437-444

Yau, W.W., Grinnard, C.R. and Kirkland, J., (1978). Broad range linear calibration in high performance size exclusion chromatography using column packings with bimodal pores. *Journal of Chromatography* , **149** , 465-487

Yau, W.W., Kirkland, J.J. and Bly, D.D., (1979). Modern size exclusion chromatography. New York: Wiley Interscience

Yokouchi, M., Chatani, Y., Tadokoro, H., Teranishi, K. and Tani, H., (1973). Structural studies of polyesters: 5. Molecular and crystal structures of optically active and racemic poly(β-hydroxybutyrate). *Polymer* , **14** , 267-272

APPENDIX 1: Data for viscosity experiment of PHB fractions.

Table 1 : Flow times of different concentrations of Fraction 1 (Experiment 1)

Concentration % w/v	Flow times (seconds)		
	1	2	3
0	116.12	116.20	116.08
1.001	168.20	168.28	168.34
0.871	160.97	160.94	161.05
0.646	155.45	155.50	155.62
0.556	143.86	143.57	143.69
0.488	140.18	140.06	140.04
0.393	135.13	135.04	135.07

Table 2 : Flow times of different concentrations of Fraction 1 (Experiment 2)

Concentration % w/v	Flow times (seconds)		
	1	2	3
0	116.03	115.99	115.96
0.871	160.67	160.72	160.74
0.770	155.22	155.11	155.11
0.646	148.47	148.37	148.23
0.556	143.63	143.52	143.48
0.488	140.02	139.94	139.93
0.435	137.11	137.20	137.17

Table 3 : Flow times for different concentrations of Fraction 2 (Experiment 1)

Concentration % w/v	Flow times (seconds)		
	1	2	3
0	116.02	116.08	116.08
0.224	186.16	186.12	186.09
0.177	169.85	169.89	169.89
0.158	163.45	163.48	163.47
0.142	158.30	158.23	158.29
0.129	154.41	154.30	154.51

Table 4 : Flow times for different concentrations of Fraction 2 (Experiment 2)

Concentration % w/v	Flow times (seconds)		
	1	2	3
0	116.06	116.07	116.09
0.243	192.13	192.17	192.27
0.192	174.77	174.69	174.64
0.159	163.80	163.65	163.60
0.144	158.80	158.99	158.79
0.132	155.00	154.80	154.90
0.121	151.71	151.66	151.63
0.107	147.31	147.21	147.14
0.096	143.85	143.68	143.70

Table 5 : Flow times for different concentrations of Fraction 3 (Experiment 1)

Concentration % w/v	Flow times (seconds)		
	1	2	3
0	116.08	116.03	116.03
0.353	151.12	151.12	151.07
0.312	146.88	146.82	146.83
0.280	143.48	143.53	143.45
0.239	139.18	139.16	139.14
0.166	131.93	131.79	131.91

Table 6 : Flow times for different concentrations of Fraction 3 (Experiment 2)

Concentration % w/v	Flow times (seconds)		
	1	2	3
0	116.03	116.00	116.01
0.353	150.66	150.62	150.73
0.307	146.05	145.95	145.97
0.272	142.37	142.25	142.26
0.221	137.29	137.24	137.12
0.202	135.30	135.21	135.22
0.157	130.89	130.83	130.81

Table 7 : Flow times for different concentrations of Fraction 4 (Experiment 1)

Concentration % w/v	Flow times (seconds)		
	1	2	3
0	115.98	116.03	115.98
0.288	160.45	160.35	160.37
0.248	154.01	154.03	154.03
0.218	149.19	149.15	149.15
0.171	141.70	141.76	141.72
0.157	139.40	139.44	139.27

Table 8 : Flow times for different concentrations of Fraction 4 (Experiment 2)

Concentration % w/v	Flow times (seconds)		
	1	2	3
0	116.06	116.03	115.95
0.595	220.50	220.30	220.34
0.476	196.95	197.04	196.83
0.410	184.21	184.22	184.41
0.360	175.22	175.34	175.14
0.321	168.03	168.17	168.13
0.283	161.07	161.07	161.13
0.253	155.81	155.79	155.75

Table 9 : Flow times for different concentrations of Fraction 5 (Experiment 1)

Concentration % w/v	Flow times (seconds)		
	1	2	3
0	115.98	116.04	115.97
0.117	174.85	174.82	174.74
0.093	161.80	161.73	161.67
0.084	157.14	156.98	157.04
0.073	151.12	151.00	151.00
0.064	146.59	146.50	146.44

Table 10 : Flow times for different concentrations of Fraction 5 (Experiment 2)

Concentration % w/v	Flow times (seconds)		
	1	2	3
0	116.03	116.04	116.03
0.147	195.42	195.69	195.58
0.130	185.17	185.15	185.07
0.117	177.17	177.25	177.14
0.106	170.84	170.94	170.89
0.081	156.57	156.76	156.47
0.072	151.85	151.76	151.47

Table 11 : Flow times for different concentrations of Fraction 6 (Experiment 1)

Concentration % w/v	Flow times (seconds)		
	1	2	3
0	116.11	116.05	116.02
0.289	187.11	187.23	187.17
0.272	182.60	182.38	182.56
0.250	176.57	176.65	176.57
0.231	171.60	171.63	171.61
0.215	167.30	167.21	167.28
0.201	163.55	163.62	163.60
0.189	160.43	160.33	160.33
0.178	157.59	157.58	157.57

Table 12 : Flow times for different concentrations of Fraction 6 (Experiment 2)

Concentration % w/v	Flow times (seconds)		
	1	2	3
0	116.00	116.05	116.10
0.256	178.22	178.13	178.11
0.223	169.73	169.34	169.39
0.197	162.73	162.70	162.65
0.177	157.49	157.37	157.43
0.151	150.66	150.82	150.78
0.131	145.87	145.86	145.91
0.116	142.37	142.25	142.30

Table 13 : Flow times for different concentrations of Fraction 7 (Experiment 1)

Concentration % w/v	Flow times (seconds)		
	1	2	3
0	116.40	116.17	116.24
0.129	198.73	198.60	198.77
0.112	186.38	186.31	186.48
0.099	177.04	177.14	177.11
0.083	165.97	165.98	165.74
0.072	158.50	158.35	158.40
0.063	152.76	152.83	152.63
0.056	148.67	148.60	148.41

Table 14 : Flow times for different concentrations of fraction 7 (Experiment 2)

Concentration % w/v	Flow times (seconds)		
	1	2	3
0	115.83	115.90	115.91
0.126	197.43	197.48	197.52
0.110	185.46	185.34	185.33
0.097	176.17	176.35	176.30
0.082	165.56	165.39	165.69
0.070	157.90	157.86	157.91
0.062	152.31	152.18	152.14
0.058	149.44	149.74	149.55

Table 15 : Flow times for different concentrations of Fraction 8 (Experiment 1)

Concentration % w/v	Flow times (seconds)		
	1	2	3
0	116.10	116.07	116.04
2.000	179.84	180.00	180.03
1.739	170.75	170.75	170.71
1.539	163.91	163.84	163.82
1.290	155.54	155.42	155.41
1.111	149.46	149.33	149.47
0.976	145.06	145.20	145.32
0.870	141.72	141.60	141.98
0.784	139.08	139.16	139.29

Table 16 : Flow times for different concentrations of Fraction 8 (Experiment 2)

Concentration % w/v	Flow times (seconds)		
	1	2	3
0	116.02	116.05	116.01
2.000	180.42	180.39	180.46
1.600	166.05	166.20	166.12
1.427	160.41	160.28	160.18
1.290	155.45	155.73	155.72
1.111	149.86	149.47	149.56
0.784	139.23	139.04	139.51

Table 17 : Flow times for different concentrations of Fraction 11 (Experiment 1)

Concentration % w/v	Flow times (seconds)		
	1	2	3
0	116.12	116.08	116.07
0.492	174.10	174.13	174.09
0.410	163.51	163.56	163.60
0.352	156.35	156.34	156.44
0.308	150.91	150.97	150.92
0.274	146.80	146.97	146.78
0.246	143.70	143.58	143.55
0.224	140.89	140.98	141.10
0.205	138.85	138.83	138.83

Table 18 : Flow times for different concentrations of Fraction 11 (Experiment 2)

Concentration % w/v	Flow times (seconds)		
	1	2	3
0	115.98	116.01	116.02
0.409	170.55	170.58	170.55
0.356	162.81	162.80	162.88
0.315	157.19	157.46	157.00
0.282	152.47	152.46	152.40
0.256	148.89	148.71	148.76
0.221	143.92	143.98	143.89
0.195	140.47	140.43	140.50
0.174	137.76	137.69	137.66

Table 19 : Flow times for different concentrations of Fraction 12 (Experiment 1)

Concentration % w/v	Flow times (seconds)		
	1	2	3
0	115.97	116.00	116.04
0.311	157.77	157.50	157.56
0.281	153.20	153.13	153.16
0.256	149.78	149.59	149.66
0.235	146.66	146.66	146.51
0.218	144.12	144.03	144.11
0.202	141.94	141.87	141.89
0.189	140.09	140.00	140.03

Table 20 : Flow times for different concentrations of Fraction 12 (Experiment 2)

Concentration % w/v	Flow times (seconds)		
	1	2	3
0	115.99	116.02	115.94
0.373	170.55	170.75	170.71
0.321	162.35	162.33	162.39
0.282	156.22	156.16	156.21
0.245	150.66	150.60	150.57
0.222	147.17	146.97	147.04
0.203	144.38	144.16	144.20
0.186	141.77	141.69	141.73

Table 21 : Flow times for different concentrations of Fraction 13 (Experiment 1)

Concentration % w/v	Flow times (seconds)		
	1	2	3
0	115.92	116.05	115.97
0.290	223.49	223.56	223.53
0.249	205.70	205.69	205.67
0.235	200.18	200.22	200.24
0.218	192.99	193.02	193.05
0.202	187.14	186.97	187.01
0.189	181.62	181.63	181.64
0.178	177.16	177.13	177.09
0.167	173.07	173.00	172.95

Table 22 : Flow times for different concentrations of Fraction 13 (Experiment 2)

Concentration % w/v	Flow times (seconds)		
	1	2	3
0	115.94	115.99	116.03
0.243	209.33	209.33	209.33
0.203	191.57	191.65	191.75
0.168	176.92	176.83	176.91
0.143	167.07	166.95	167.11
0.125	159.78	159.85	159.79
0.113	155.29	155.26	155.38
0.104	151.64	151.63	151.66

Table 23 : Flow times for different concentrations of Fraction 14 (Experiment 1)

Concentration % w/v	Flow times (seconds)		
	1	2	3
0	116.12	116.15	116.10
0.276	208.23	208.14	208.20
0.197	179.03	179.06	179.10
0.178	172.48	172.41	172.23
0.163	167.01	166.99	166.97
0.149	162.61	162.50	162.51
0.138	158.89	158.70	158.77
0.123	153.52	153.57	153.61

Table 24 : Flow times for different concentrations of Fraction 14 (Experiment 2)

Concentration % w/v.	Flow times (seconds)		
	1	2	3
0	115.93	115.91	115.90
0.290	208.54	208.59	208.66
0.241	191.38	191.33	191.34
0.200	176.80	176.72	176.78
0.176	168.65	168.67	168.70
0.157	162.46	162.42	162.44
0.141	157.62	157.58	157.59
0.129	153.67	153.70	153.72

APPENDIX 2 : Data for viscosity experiment of polystyrene standards.

Table 1 : Flow times for different concentrations of polystyrene standard having M_p = 1080000 (Experiment 1)

Concentration % w/v	Flow times (seconds)		
	1	2	3
0	115.99	116.02	115.98
0.107	149.84	149.80	149.80
0.097	146.48	146.49	146.51
0.085	142.55	142.47	142.50
0.075	139.43	139.40	139.42
0.068	136.99	137.02	137.08
0.062	135.07	135.09	134.99
0.056	133.43	133.37	133.39
0.052	130.80	130.77	130.78

Table 2 : Flow times for different concentrations of polystyrene standard having M_p = 1080000 (Experiment 2)

Concentration % w/v	Flow times (seconds)		
	1	2	3
0	116.00	115.98	115.97
0.168	171.45	171.39	171.42
0.140	161.68	161.59	161.61
0.124	156.32	156.31	156.25
0.108	150.64	150.67	150.64
0.096	146.46	146.38	146.45
0.088	143.88	143.85	143.87
0.078	140.37	140.39	140.36

Table 3 : Flow times for different concentrations of polystyrene standard having M_p = 490000 (Experiment 1)

Concentration % w/v	Flow times (seconds)		
	1	2	3
0	116.03	116.06	116.00
0.233	160.02	160.10	160.06
0.186	150.55	150.59	150.54
0.166	146.58	146.60	146.58
0.150	143.40	143.46	146.43
0.137	140.83	140.86	140.83
0.116	136.93	136.96	136.90

Table 4 : Flow times for different concentrations of polystyrene standard having M_p = 490000 (Experiment 2)

Concentration % w/v	Flow times (seconds)		
	1	2	3
0	116.07	115.99	116.03
0.267	167.14	167.10	167.14
0.232	159.82	159.80	159.87
0.191	151.34	151.35	151.39
0.167	146.68	146.60	146.62
0.144	142.24	142.25	142.23
0.133	140.16	140.08	140.24
0.121	137.86	137.83	137.89

Table 5 : Flow times for different concentrations of polystyrene standard having M_p = 195000 (Experiment 1)

Concentration % w/v	Flow times (seconds)		
	1	2	3
0	115.91	115.91	115.87
0.338	148.95	148.91	148.91
0.302	145.23	145.13	145.17
0.273	142.23	142.17	142.17
0.249	139.81	139.76	139.82
0.217	136.48	136.46	136.50
0.201	134.94	134.96	134.97
0.188	133.63	133.63	133.62
0.176	132.47	132.46	132.48

Table 6 : Flow times for different concentrations of polystyrene standard having M_p = 195000 (Experiment 2)

Concentration % w/v	Flow times (seconds)		
	1	2	3
0	116.14	116.12	116.14
0.375	151.90	151.98	152.02
0.326	147.10	147.08	147.05
0.268	141.34	141.38	141.35
0.227	137.40	137.36	137.37
0.208	135.59	135.54	135.62
0.192	133.99	134.10	134.05
0.171	131.89	131.98	131.92

Table 7 : Flow times for different concentrations of polystyrene standard having M_p = 68000 (Experiment 1)

Concentration % w/v	Flow times (seconds)		
	1	2	3
0	116.04	116.03	115.98
1.006	161.07	160.97	161.10
0.869	154.43	154.42	154.47
0.708	146.60	146.65	146.61
0.637	143.33	143.42	143.38
0.579	140.79	140.71	140.79
0.503	137.26	137.37	137.26

Table 8 : Flow times for different concentrations of polystyrene standard having M_p = 68000 (Experiment 2)

Concentration % w/v	Flow times (seconds)		
	1	2	3
0	116.16	116.12	116.09
1.071	164.78	164.81	164.79
0.925	157.63	157.62	157.63
0.754	149.36	149.28	149.22
0.636	143.52	143.58	143.65
0.582	141.11	141.09	141.12
0.509	137.75	137.80	137.70

Table 9 : Flow times for different concentrations of polystyrene standard having M_p = 28000 (Experiment 1)

Concentration % w/v	Flow times (seconds)		
	1	2	3
0	115.90	115.94	115.97
1.847	159.94	159.95	160.05
1.595	153.48	153.46	153.42
1.350	147.22	147.19	147.22
1.210	143.81	143.73	143.79
1.097	141.03	141.05	141.04
1.003	138.82	138.79	138.73
0.877	135.71	135.76	135.73

Table 10 : Flow times for different concentrations of polystyrene standard having M_p = 28000 (Experiment 2)

Concentration % w/v	Flow times (seconds)		
	1	2	3
0	116.10	116.10	116.11
1.963	162.86	162.81	162.89
1.554	152.10	152.15	152.15
1.381	147.85	147.86	147.83
1.166	142.43	142.49	142.46
1.008	138.65	138.70	138.74
0.888	135.75	135.83	135.78

APPENDIX 3

Derivation of modified Higuchi's equation.

According to Higuchi (1961) , the following assumptions were made:

- A region with depleted drug is penetrating into the matrix.
- The rate of diffusion of drug per unit area (the mass flux) throughout this depleted region is independent of this position on the surface.

If C(x) be the concentration of dissolved drug at the parallel surface (at a distance x from the boundary of the matrix),then Fick's first law is given by:

$$\phi = DA(x)\frac{\delta C(x)}{\delta x} \quad \cdots \quad (1)$$

and

$$\phi = \frac{dM(t)}{dt}$$

where

A is the total area of the depleted region of drug.

D is the diffusion coefficient.

Since ϕ is not dependent upon x, equation (1) may be integrated as follows:

$$\int_0^x dC(x) = \frac{\phi}{D}\int_0^x \frac{dx}{A(x)}$$

$$C(x) - C(0) = \frac{\phi}{D}\int_0^x \frac{dx}{A(x)}$$

Assuming at sink condition, then C(0)= 0

$$C(x) = \frac{\phi}{D}\int_0^x \frac{dx}{A(x)} \quad \cdots \quad \text{for } 0 < x < x' \quad \cdots \quad (2)$$

For short time t, x' (and x) should be small and using $A(x) \simeq A-cx$

$$\frac{1}{A(x)} \approx \frac{1}{(A-cx)} \approx \frac{1}{A\left[1-\frac{cx}{A}\right]}$$

$$= \frac{1}{A}\left[1-\frac{cx}{A}\right]^{-1}$$

using

$$\left[1-a\right]^{-1} = 1+a+\frac{a^2}{2!}+\cdots$$

then

$$\frac{1}{A}\left[1-\frac{cx}{A}\right]^{-1} = \frac{1}{A}\left[1+\frac{cx}{A}+\left[\frac{cx}{A}\right]^2+\cdots\right]$$

$$\approx \frac{1}{A}+\frac{cx}{A^2} \quad \cdots \quad (3)$$

Substituting equation (3) into equation (2)

$$C(x) = \frac{\phi}{D}\int_0^x \left[\frac{1}{A}+\frac{cx}{A^2}\right]dx$$

$$= \frac{\phi}{(AD)}\int_0^x \left[1+\frac{cx}{A}\right]dx$$

$$= \frac{\phi}{(AD)}\left[x+c\frac{x^2}{2A}\right] \quad \cdots \quad (4)$$

At the diffusion front,

$$C_s = C(x') \approx \frac{\phi}{(AD)}\left[x'+c\frac{x'^2}{2A}\right] \quad \cdots \quad (5)$$

Eliminating ϕ by dividing (4) by (5),

$$\frac{C(x)}{C_s} \approx \frac{\left[x+c\frac{x^2}{2A}\right]}{\left[x'+c\frac{x'^2}{2A}\right]}$$

$$\approx \frac{x}{x'}\frac{\left[1+\frac{cx}{2A}\right]}{\left[1+\frac{cx'}{2A}\right]}$$

$$\approx \frac{x}{x'}\left[1+\frac{cx}{2A}\right]\left[1+\frac{cx'}{2A}\right]^{-1}$$

$$\approx \frac{x}{x'}\left[1+\frac{cx}{2A}\right]\left[1-\frac{cx'}{2A}+\left[\frac{cx'}{2A}\right]^2+\cdots\right]$$

$$= \frac{x}{x'}\left[1+\frac{cx}{2A}-\frac{cx'}{2A}\right] \quad \cdots \quad (6)$$

The total amount of dissolved drug remaining in the depleted region is

$$= \int_0^{x'} C(x)A(x)dx$$

$$\approx C_s \int_0^{x'} \frac{x}{x'}\left(1+\frac{cx}{2A}-\frac{cx'}{2A}\right)(A-cx)dx$$

$$\approx C_s \int_0^{x'} \left[\frac{Ax}{x'}-\frac{cx^2}{2x'}-\frac{cx}{2}-\frac{c^2x^3}{(2Ax')}+\frac{c^2x^2}{2A}\right]dx$$

$$\approx C_s \left[\frac{Ax^2}{2x'}-\frac{cx^3}{6x'}-\frac{cx^2}{4}-\frac{c^2x^4}{8Ax'}+\frac{c^2x^3}{6A}\right]^{x'}$$

$$\approx C_s \left[\frac{Ax'}{2}-\frac{5}{12}cx'^2\right] \quad \cdots \quad (7)$$

The amount of dissolved drug remaining between 2 parallel surfaces at a distances x' and $x' + dx$

$$= \left[\text{amount at } (x'+dx) \right] - \left[\text{amount at } x' \right]$$

$$= C_s \left[\frac{A}{2} \left(x'+dx' \right) - \frac{5}{12} c \left(x'+dx' \right)^2 \right] - C_s \left[\frac{A}{2} x' - \frac{5}{12} c x'^2 \right]$$

$$= C_s \left[\frac{A}{2} dx' - \frac{5}{12} c \left(2x'dx' + (dx')^2 \right) \right]$$

$$= C_s \left(\frac{A}{2} - \frac{5}{6} cx' \right) dx' \quad \cdots \quad (8)$$

The mass balance (for the region between the two parallel surfaces) becomes

$$\phi dt \approx C_o A(x')dx' - C_s \left(\frac{A}{2} - \frac{5}{6} cx' \right) dx'$$

$$\approx C_o \left(A - cx' \right) dx' - C_s \left(\frac{A}{2} - \frac{5}{6} cx' \right) dx'$$

$$\approx \left(C_o - \frac{C_s}{2} \right) A \, dx' + \left(\frac{5}{6} cC_s - cC_o \right) x'dx' \quad \cdots \quad (9)$$

Also from (5)

$$\phi = \frac{C_s AD}{\left(x' + c\frac{x'^2}{2A} \right)} \quad \cdots \quad (10)$$

Putting (10) into (9)

$$\frac{DC_s A}{\left(x' + c\frac{x'^2}{2A} \right)} dt = \left(C_o - \frac{C_s}{2} \right) A \, dx' + \left(\frac{5}{6} cC_s - cC_o \right) x'dx'$$

$$DC_s A dt = \left[\left(C_o - \frac{C_s}{2} \right) A dx' + \left(\frac{5}{6} cC_s - cC_o \right) x'dx' \right] \left(x' + c\frac{x'^2}{2A} \right)$$

$$= \left[C_o - \frac{C_s}{2}\right] Ax'dx' + \left[\frac{5}{6}cC_s - cC_o\right] x'^2 dx' + \left[C_o - \frac{C_s}{2}\right] \frac{Acx'^2}{2A} dx' + \left[\frac{5}{6}cC_s - cC_o\right] \frac{cx'^3}{2A} dx'$$

$$= A\left[C_o - \frac{C_s}{2}\right] x'dx' + \left[\frac{5}{6}cC_s - cC_o + \frac{cC_o}{2} - \frac{cC_s}{4}\right] x'^2 dx'$$

$$= A\left[C_o - \frac{C_s}{2}\right] x'dx' - c\left[\frac{C_o}{2} - \frac{7}{12}C_s\right] x'^2 dx' \quad \cdots \quad (11)$$

Integrating (11) by using x'=0 when t=0

$$\int_0^t DC_s A dt = \int_0^{x'} \left| A\left[C_o - \frac{C_s}{2}\right] x' - c\left[\frac{C_o}{2} - \frac{7}{12}C_s\right] x'^2 \right| dx'$$

Hence

$$DC_s At = \frac{A}{2}\left[C_o - \frac{C_s}{2}\right] x'^2 - \frac{c}{3}\left[\frac{C_o}{2} - \frac{7}{12}C_s\right] x'^3$$

$$= \frac{A}{2}\left[C_o - \frac{C_s}{2}\right] x'^2 - \frac{c}{6}\left[C_o - \frac{7}{6}C_s\right] x'^3 \quad \cdots \quad (12)$$

From (5) again , ϕ as a function of x' was obtained as follows:

$$\phi = \frac{ADC_s}{x'\left[1 + \frac{cx'}{2A}\right]} = \frac{ADC_s}{x'}\left[1 + \frac{cx'}{2A}\right]^{-1}$$

$$= \frac{ADC_s}{x'}\left[1 - \frac{cx'}{2A} + \cdots\right]$$

$$\approx \frac{ADC_s}{x'} - \frac{cDC_s}{2} \quad \cdots \quad (13)$$

Looking at equation (12) again and putting x' = 1/q , then

$$DC_s At = \frac{A}{2q^2}\left[C_o - \frac{C_s}{2}\right] - \frac{c}{6q^3}\left[C_o - \frac{7}{6}C_s\right]$$

Hence

$$\frac{2DC_s tq^3}{C_o-\frac{C_s}{2}}=q-\frac{c}{3A}\left[C_o-\frac{7}{6}C_s\right]\left[C_o-\frac{C_s}{2}\right]^{-1} \quad \cdots \quad (14)$$

Equation (14) is in the form of the equation as shown below where:

$$aty^3=y-\alpha \quad \cdots \quad (15)$$

To solve equation (15) in terms of y , the following root can be used where :

$$y=\frac{1}{\sqrt{at}}+\delta$$

Hence

$$y^3=\left[\frac{1}{\sqrt{at}}+\delta\right]^3$$

$$=\left[\frac{1}{\sqrt{at}}\right]^3+3\left[\frac{1}{\sqrt{at}}\right]^2\delta+3\left[\frac{1}{\sqrt{at}}\right]\delta^2+\delta^3$$

$$=\frac{1}{at\sqrt{at}}+3\frac{\delta}{at}+3\frac{\delta^2}{\sqrt{at}}+\delta^3 \quad \cdots \quad (16)$$

Putting equation (16) into (15):

$$at\left[\frac{1}{at\sqrt{at}}+3\frac{\delta}{at}+3\frac{\delta^2}{\sqrt{at}}+\delta^3\right]=\frac{1}{\sqrt{at}}+\delta-\alpha$$

$$\frac{1}{\sqrt{at}}+3\delta+3\left[\sqrt{at}\right]\delta^2+at\delta^3=\frac{1}{\sqrt{at}}+\delta-\alpha$$

$$2\delta=-\alpha$$

$$\delta=-\frac{\alpha}{2}=-\frac{c}{6A}\left[C_o-\frac{7}{6}C_s\right]\left[C_o-\frac{C_s}{2}\right]^{-1} \quad \cdots \quad (17)$$

From (14) and (15), we can observed that:

$$q = y$$

$$= \left[\frac{2DC_s t}{C_o - \frac{C_s}{2}} \right]^{-0.5} + \delta$$

Putting δ from (17) into the above equation :

$$q = \left[\frac{2DC_s t}{C_o - \frac{C_s}{2}} \right]^{-0.5} - \frac{c}{6A} \left[C_o - \frac{7}{6} C_s \right] \left[C_o - \frac{C_s}{2} \right]^{-1} \quad \cdots \quad (18)$$

Substituting (18) into (13) and remembering that $x' = 1/q$, then

$$\phi = ADC_s q - \frac{cDC_s}{2}$$

$$= ADC_s \left[\left[\frac{2DC_s t}{C_o - \frac{C_s}{2}} \right]^{-0.5} - \frac{c}{6A} \left[C_o - \frac{7}{6} C_s \right] \left[C_o - \frac{C_s}{2} \right]^{-1} \right] - \frac{cDC_s}{2}$$

$$= ADC_s \left[\frac{C_o - \frac{C_s}{2}}{2DC_s t} \right]^{1/2} - \frac{ADC_s c}{18A} \left[\frac{6C_o - 7C_s}{2C_o - C_s} \right] - \frac{cDC_s}{2}$$

$$= A\sqrt{DC_s} \left[\frac{C_o - \frac{C_s}{2}}{2t} \right]^{1/2} - \frac{cDC_s}{18} \left[\frac{\left[6C_o - 7C_s \right] + 9 \left[2C_o - C_s \right]}{\left[2C_o - C_s \right]} \right]$$

$$= A \left[\frac{DC_s}{2t} \left[C_o - \frac{C_s}{2} \right] \right]^{1/2} - \frac{cDC_s}{18} \left[\left[24C_o - 16C_s \right] \left[2C_o - C_s \right]^{-1} \right]$$

$$= A \left[DC_s \left[\frac{C_o - \frac{C_s}{2}}{2t} \right] \right]^{1/2} - \frac{4}{9} cDC_s \left[\frac{3C_o - 2C_s}{2C_o - C_s} \right] \quad \cdots \quad (19)$$

Integrating (19) (Remember : ϕ = dM/dt and using M=0 when t=0)

$$\int_0^t dM(t) = \int_0^t \left[B'_1 t^{-\frac{1}{2}} - B_2 \right] dt$$

$$M(t)-M(0)=\left[B'_1\frac{2t^{1/2}}{\sqrt{2}}-B_2t\right]^t$$

$$=\sqrt{2}B'_1t^{1/2}-B_2t$$

$$M(t)=\sqrt{2}A\left[\frac{DC_s}{2}\left(2C_o-C_s\right)\right]^{1/2}t^{1/2}-B_2t$$

$$=A\left[DC_s\left(2C_o-C_s\right)t\right]^{1/2}-B_2t \quad \cdots \quad (20)$$

Equation (20) can be represented by a general equation as shown below :

$$M(t)=B_1t^{1/2}-B_2t$$

where

$$B'_1=A\left[DC_s\left(C_o-\frac{C_s}{2}\right)\right]^{1/2}$$

$$B_1=A\left[DC_s\left(2C_o-C_s\right)\right]^{1/2}$$

$$B_2=\frac{4}{9}cDC_s\left(\frac{3C_o-2C_s}{2C_o-C_s}\right)$$

APPENDIX 4 : LISTINGS OF COMPUTER PROGRAM IN BBC BASIC
USED FOR SIZE EXCLUSION CHROMATOGRAPHY

PROGRAM 1

```
  10 REM PROGRAM FOR SAVING DATA FROM IR DETECTOR ON DISC
  20 CLS
  30 DIM DS(1000)
  40 VDU 15
  50 DT=100
  60 PRINT "WHAT NAME DO YOU WANT TO GIVE TO "
  70 INPUT "YOUR DATA FILE",FILE$
  80 INPUT "ENTER TIME OVER WHICH DATA IS TO BE COLLECTED(min)"  DT
  90 ST%=DT*6000/1000
 100 PRINT"PRESS G TO START A CHROMATOGRAPHIC RUN"
 110 *FX15,1
 120 START$=GET$
 130 IF START$="G" THEN 140 ELSE 110
 140 X=OPENOUT(FILE$)
 150 PROCDATCOL
 160 STOP
 170 END
 180 :
 190 DEF PROCDATCOL
 200 FOR I%=1 TO 1000
 210 CT%=TIME
 220 AV=0
 230 FOR J%=1 TO 100
 240 AV=AV+ADVAL(1)
 250 NEXT
 260 AV%=AV/100
 270 DS(I%)=AV%/34900
 280 PRINT I%;"         ";DS(I%)
 290 PRINT£X,I%,DS(I%)
 300 IF TIME<(CT%+ST%) THEN 300
 310 NEXT
 320 CLOSE£X
 330 ENDPROC
```

```
PROGRAM 2
     10  REM ANALYSIS PROGRAM FOR MOLECULAR WEIGHT DETERMINATION
     20  *FX5,4
     30  DIM DS(1000),STY(20),STX(20),F(10)
     40  VDU15
     50  WL=2500
     60  SLW=3
     70  SP=2000
     80  SP%=500:EP%=800
     90  P=50
    100  MODE 131
    110  PROCISA
    120  DT=100
    130  ST%=DT*6000/1000
    140  PROCRETRIEVE
    150  CLS
    160  MODE4
    170  PROCPLOT
    180  PROCALTER
    190  PROCMW
    200  PROCPRINT
    210  *FX15,1
    220  PRINT "DO YOU WISH TO RUN THE SAME DATA AGAIN?Y/N";:INPUT Y$
    230  IF Y$="Y" OR Y$="y" THEN 150 ELSE 240
    240  PRINT"HAVE YOU FINISHED ? Y/N"
    250  IF GET<>78 THEN 260 ELSE 110
    260  STOP
    270  END
    280  :
    290  DEF PROCPLOT
    300  PLOT4,100,850
    310  PLOT5,100,100
    320  PLOT5,1100,100
    330  FOR I%=1 TO 1000
    340    PLOT4,100,100
    350    PLOT65,I%,DS(I%)*1000
    360  NEXT
    370  PROCX(SP%+100,(DS(SP%)*1000)+100)
    380  PROCX(EP%+100,(DS(EP%)*1000)+100)
    390  ENDPROC
    400  :
    410  DEF PROCALTER
    420  VDU28,0,3,39,0
    430  PRINT"A - INC.PEAK START    Z - DEC.PEAK START"
    440  PRINT": - INC.PEAK END      / - DEC.PEAK END"
    450  PRINT"SPACE  -  NO FURTHER CHANGE"
    460  *FX15,1
    470  PROCKEY3
    480  IF F%<>1 THEN 460
    490  PROCBASE
    500  ENDPROC
    510  :
```

```
 520  DEF PROCKEY3
 530  *FX15,1
 540  F%=0
 550  IF INKEY(-99)=-1 THEN F%=1
 560  IF INKEY(-66)=-1 THEN F%=2
 570  IF INKEY(-98)=-1 THEN F%=3
 580  IF INKEY(-73)=-1 THEN F%=4
 590  IF INKEY(-105)=-1 THEN F%=5
 600  IF F%=0 THEN 710
 610  PROCX(SP%+100,(DS(SP%)*1000)+100)
 620  PROCX(EP%+100,(DS(EP%)*1000)+100)
 630  IF F%=2 THENSP%=SP%+1
 640  IF F%=3 THENSP%=SP%-1
 650  IF F%=4 THENEP%=EP%+1
 660  IF F%=5 THENEP%=EP%-1
 670  IF SP%<1 THEN SP%=1
 680  IF EP%>1000 THEN EP%=1000
 690  PROCX(SP%+100,(DS(SP%)*1000)+100)
 700  PROCX(EP%+100,(DS(EP%)*1000)+100)
 710  ENDPROC
 720  :
 730  DEF PROCX(X%,Y%)
 740  PLOT4,X%+25,Y%
 750  PLOT6,X%-25,Y%
 760  PLOT4,X%,Y%+25
 770  PLOT6,X%,Y%-25
 780  ENDPROC
 790  :
 800  DEF PROCBASE
 810  PROCX(SP%+100,(DS(SP%)*1000)+100)
 820  PROCX(EP%+100,(DS(EP%)*1000)+100)
 830  PLOT4,SP%+100,(DS(SP%)*1000)+100
 840  PLOT6,EP%+100,(DS(EP%)*1000)+100
 850  ENDPROC
 860  :
 870  DEF PROCMW
 880  FOR I%=0TO 10
 890    F(I%)=0
 900  NEXT
 910  FOR I%=SP%+1 TO EP%
 920    F(0)=10^(((LOG(KCAL/KTEST))/(1+ATEST))+
(((1+ACAL)/(1+ATEST))*((A*((((ST%*I%)/6000)-TN)/TS))+B)))
 930    CEXP=DS(I%)-DS(SP%)
 940    CEXP=CEXP-(((DS(EP%)-DS(SP%))/(EP%-SP%))*(I%-SP%))
 950    F(1)=F(1)+CEXP
 960    F(2)=F(2)+CEXP*F(0)
 970    F(3)=F(3)+CEXP*(F(0)^2)
 980    F(4)=F(4)+CEXP*(F(0)^3)
 990    F(5)=F(5)+CEXP/F(0)
1000    F(6)=F(6)+CEXP/(F(0)^2)
1010    F(7)=F(7)+CEXP*(F(0)^ATEST)
1020  NEXT
1030  ENDPROC
```

```
1040  DEF PROCPRINT
1050  VDU2
1060  PRINT "DATE OF EXPT:-  "DATE$
1070  PRINT"SAMPLE:-  "D$
1080 PRINT"EXPTL.CODE:-  "EC$
1090  PRINT"STD.POLYMER:-  "PCAL$
1100  PRINT"TEST POLYMER:-  "PTEST$
1110  PRINT"MOBILE PHASE:-  "PHS$
1120  PRINT"TEMP.:-  "TMP$
1130  PRINT"FLOW:- "SP
1140  PRINT"K-STD:-  "KCAL
1150  PRINT"K-TEST:-  "KTEST
1160  PRINT"a-STD:-  "ACAL
1170  PRINT"a-TEST:-  "ATEST
1180  PRINT"DATA COLL TIME:-  "DT" min"
1190  PRINT"NUM. AV. MOL. WT.:- "F(1)/F(5)
1200  PRINT"WT. AV. MOL. WT.:- "F(2)/F(1)
1210  PRINT"VISC. AV. MOL. WT.:- "(F(7)/F(1))^(1/ATEST)
1220  PRINT"Z-AV. MOL. WT.:- "F(3)/F(2)
1230  PRINT"(Z+1)-AV. MOL. WT.:- "F(4)/F(3)
1240  PRINT"(n-1)-AV. MOL. WT.:- "F(5)/F(6)
1250  PRINT"Mw/Mn:- "(F(2)*F(5))/(F(1)^2)
1260  VDU3
1270  ENDPROC
1280  :
1290  DEF PROCCH
1300  *FX229,1
1310  PRINT ADVAL(1)
1320  IF INKEY(-113)=-1 THEN 1340
1330  GOTO 1310
1340  *FX229,0
1350  *FX21,0
1360  *FX21,0
1370  *FX21,0
1380  ENDPROC
1390  :
1400  DEF PROCRETRIEVE
1410  INPUT "TIME OVER WHICH DATA WAS COLLECTED(min)  " DT
1420  ST%=DT*6000/1000
1430  INPUT "FILENAME",FILE$
1440  X%=OPENIN FILE$
1450  FOR I%=1 TO 1000
1460    INPUT£X%,I%,DS(I%)
1470    PRINT I%;"      ";DS(I%)
1480  NEXT
1490  CLOSE£X%
1500  ENDPROC
```

```
1510  :
1520  DEF PROCISA
1530  INPUT "DATE OF EXPT. "DATE$
1540  PRINT "ENTER MARK HOUWINK DATA "
1550  INPUT "K OF STD. POLYMER "KCAL
1560  INPUT "K OF TEST POLYMER "KTEST
1570  INPUT "a OF STD POLYMER "ACAL
1580  INPUT "a OF TEST POLYMER "ATEST
1590  INPUT "STD. POLYMER " PCAL$
1600  INPUT "TEST POLYMER "PTEST$
1610  INPUT "MOBILE PHASE "PHS$
1620  PRINT "FLOW RATE=  "SP
1630  INPUT "TEMP. "TMP$
1640  INPUT "VOID VOLUME TIME(min) "TN
1650  INPUT "STAT. PHASE VOL. TIME(min) "TS
1660  INPUT "SLOPE OF CALIBRATION "A
1670  INPUT "Y INTERCEPT "B
1680  ENDPROC
```